Design and Synthesis of Novel N10 Protected Pyrrolobenzodiazepines for Use in ADEPT and GDEPT

Christina Von Bulow

A thesis submitted in partial fulfilment of the requirements for the degree of Doctor of Philosophy

The School of Pharmacy

University of London

2009

Supervisors:

Dr. Philip W. Howard

Prof. David E. Thurston

This thesis describes research conducted in the School of Pharmacy, University of London between May 2004 and December 2008 under the supervision of Dr. Philip W. Howard and Prof. David E. Thurston. I certify that the research described is original and that any parts of the work that have been conducted by collaboration are clearly indicated. I also certify that I have written all the text herein and have clearly indicated by suitable citation any part of this dissertation that has already appeared in publication.

C von Bulow — 19/03/09

Signature — Date

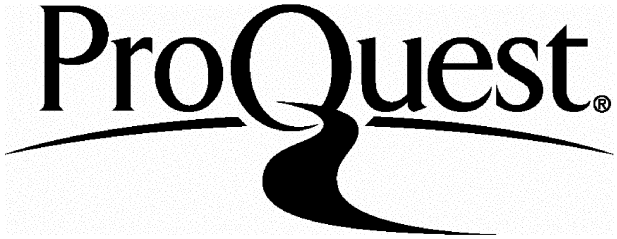

I. *Abstract*

The PBDs are a family of naturally occurring antitumor antibiotics that bind in a sequence selective manner in the minor groove of DNA, interrupting processes such as transcription and replication. A PBD dimer, SJG-136, is currently undergoing Phase I clinical trials. The mechanism of action of the PBDs requires that the N10-position remains unsubstituted in order to maintain antitumor activity. This makes the PBDs excellent candidates for prodrug therapies, as potentiating groups can be introduced at other positions in the molecule while labile substituents at the N10-position can block DNA interaction and act as an "on/off" switch.

The aim of this project was to significantly increase the cytotoxic differential between prodrug and released parent PBD. In particular, SAR data suggest that the cytotoxicity of both PBD monomers and dimers can be greatly enhanced by the introduction of unsaturation between the C2 and C3 positions of the C-ring and inclusion of an aryl moiety at C2. Therefore, an initial objective was to design and synthesize novel prodrugs for use in ADEPT therapy with enhanced differential and potency. A 4-methoxyphenyl C2-substituted PBD was selected as the initial prodrug target, as the Suzuki coupling reaction is known to proceed smoothly and the products can be readily characterised by NMR.

A robust 13-step synthesis has been developed to provide a C2-ketone N10-protected PBD intermediate (**225**). However, the critical triflation reaction, a prerequisite for the Suzuki coupling of the C2-aryl group, produced a mixture of C1-C2 and C2-C3 unsaturated isomers (**255** and **222**) which could only be separated by preparative LC-MS affording only low yields of products. An alternative strategy of installing the N10-progroup at a later stage of the synthesis was explored. This was potentially highly advantageous as the progroup could be introduced in a variety of substituted PBD structures. Unfortunately, the complex glutamate protecting group required for ADEPT was unstable to the conditions required to introduce it to the N10 position of the N10-C11 imine moiety of a PBD.

Both prodrug isomers were evaluated *in vitro* but were found to be inherently unstable and thus cytotoxic (i.e. **255**, IC_{50} = 2.5 μM and 0.19 μM after 1 hour exposure or continuous exposure, respectively; **222**, IC_{50} = 0.17 μM and 0.015 μM for 1 hour exposure or continuous exposure, respectively) in LS174T, K562 and SW1222 cells.

As it was not possible to synthesize stable prodrugs for use in ADEPT, attention turned to a new family of prodrugs suitable for nitroreductase-based GDEPT therapies. A range of N10-protected molecules sensitive to nitroreductase were synthesized. Four N10-carbamates (the benzyl carbamate **263,** *p*-nitrobenzyl carbamate **265,** *p*-methoxy benzyl carbamate **288** and the *p*-nitrophenyl carbamate **287**) were evaluated in LS174T, K562, SW1222, A2780, A549, C33a and 5637 cell lines. It was found that *p*-nitrobenzyl carbamate **265** had up to a 18.4-fold greater potency in a nitroreductase-expressing CMV NRT A2780 cell line compared to the parent A2870 cell line, and this prodrug has been progressed to further *in vitro* and *in vivo* studies.

II. Acknowledgements

This thesis is based on four years research funded by Cancer Research UK. Over this time I have benefited from the assistance and teaching of a number of individuals to whom I owe a debt of gratitude.

First and foremost I would like to thank my supervisors. Professor David Thurston for his enthusiasm and inspirational input, and Dr Philip Howard for his unending patience, valuable advice and guidance. I am grateful to both for their support and for giving me the opportunity to work in such an exciting, and challenging field.

A special thank you to Dr Luke Masterson for his assistance and previous work and to the biologists, Dr Victoria Spanswick, Professor John Hartley, Dr Surinder Sharma, Dr Hassan Shahbakhti, Professor Nicol Keith, and Katrina Stevenson for evaluating my compounds.

Thanks are also due to the services of the analytical department, as well as to Kersti Karu, Dr Min Fang and Marek Domin. Furthermore, to Dr Dyeison Antonow and Dr Gong-Dong Kang for the gift of the parent compounds used in the initial biological evaluation.

Finally, I would like to thank Dr Emma Sharp for helping me in the molecule and figure referencing process, colleagues in Lab G7 and my friends and family for their support and encouragement over the last four years. I must also express my gratitude to Cancer Research UK without which this project would not have taken place.

'I can no other answer make, but, thanks, and thanks'

~William Shakespeare

III. Contents

IV. Abbreviations and Acronyms

5-FC 5-fluorocytosine
5-FU 5-fluorouracil
AcOH .....acetic acid
ADAPT .....antibody-directed abzyme prodrug therapy
ADC.....antibody-drug conjugates
ADEPT .....antibody-directed enzyme prodrug therapy
Alloc .....allyloxycarbonyl
AP .....alkaline phosphatase
AQ4N ..... 1,4-bis-[2-(dimethylamino-*N*oxide)
BBB .....blood-brain barrier
Boc .....*tert*-butoxycarbonyl
Bn .....benzyl
BDEPT .....bacterial-directed enzyme prodrug therapy
CAMs .....cell-to-cell adhesion molecules
CB 1954 .....5-(aziridin-1-yl)-2,4-dinitrobenzamide
CBz .....benzyloxycarbonyl
CEA .....carcinoembryonic antigen
CMDA ....4-[*N*-(2-chloroethyl)-*N*-[2-(mesyloxy)ethyl]amino]benzoyl-L-glutamic acid
COSY .....correlated spectroscopy
CP .....carboxypeptidase
CSA .....camphorsulphonic acid
CyA .....cyclosporin A
DAIB .....iodobenzene diacetate
DABCO .....1,4-diazabicyclo[2.2.2]octane
DAVLBHYD 4-desacetylvinblastine-3-carboxhydrazide
DBU .....1,8-Diazobicyclo[5.4.0]undec-7-ene
DCM .....dichloromethane
DEPT .....directed enzyme prodrug therapy
DIBAL-H .....diisobutylaluminium hydride
DMAP 4-dimethylaminopyridine
DMF .....*N*,*N*-dimethylformamide

DMSO ..... dimethylsulphoxide

DNA..... deoxyribonucleic acid

DTIC ..... 5-(3,3-dimethyl-1-triazeno)imidazole-4carboxamide

EP-0152R 1-carbamoylmethyl-3-carbamoyl-1,4-dihydropyridine

EPR .....enhanced permeability and retention effect

FMN .....flavin mononucleotide

FMPA .....fusion protein-mediated prodrug activation

EtOAc .....ethyl acetate

ESI .....electrospray ionization

GDEPT .....gene-directed enzyme prodrug therapy

GFs ..... growth signals

HAMA .....human anti-mouse antibodies

HACA .....human anti-chimeric antibodies

HCl .....hydrochloric acid

HIV .....human immunodeficiency virus

HPLC .....high performance liquid chromatography

HPV .....human papilloma virus

Hr.....hours

HRMS .....high resolution mass spectrometry

HSV-TK .....herpes simplex virus type 1 thymidine kinase

IgG .....immunoglobulins

IR ..... infrared spectroscopy

LDA .....lithium diisopropylamide

LHMDS .....lithium bis(trimethylsilyl)amide

LTTs .....ligand targeted therapies

PCC .....pyridinium chlorochromate

PD .....pharmacodynamic

PK.....pharmacokinetic

mAb .....monoclonal antibody

MeOH .....methanol

MDEPT .....macromolecular-directed enzyme prodrug therapy

MOM .....methoxymethyl

MS .....mass spectrometry

Ms.....mesyl (methanesulphonyl)

MTD .....maximum tolerated dose

MTIC .....5-(3-methyltriazen-1-yl)imidazole-4-carboxamide

NADH .....nicotinamide adenine dinucleotide

NADPH .....nicotinamide adenine dinucleotide phosphate

NMR .....nuclear magnetic resonance

NTR .....nitroreductase

NQO1 .....NADPH-quinone oxidoreductase-1

NQO2 .....NADPH-quinone oxidoreductase-2

PBD .....pyrrolo[2,1-*c*][1,4]benzodiazepine

PDEPT .....polymer-directed enzyme prodrug therapy

PEP .....prolyl endopeptidase

Py .....pyridine

Pu .....purine nucleotides

Progroup.....enzymatically cleavable PBD N10-carbamate

Red-Al .....sodium *bis*(2-methoxyethoxy) aluminum hydride

RILG .....radioimmunolumiography

RT .....room temperature

SAR .....structure activity relationship

s.e .....standard error

SEM .....trimethylsilylethoxymethyl

TBAF .....tetrabutylammonium fluoride

TBDMS .....*tert*-butyl-dimethylsilyl

TEA .....triethylamine

TEMPO.....2,2,6,6-tetramethyl-1-piperidinyloxy (free radical)

TI..... therapeutic index

TLC .....thin layer chromatography

Tf_2O .....triflic anhydride

TFA .....trifluoroacetic acid

THF .....tetrahydrofuran

TPP .....triphenylphosphine

TsOH .....tosic acid

VDEPT .....virus-directed enzyme prodrug therapy

Chapter 1

Cancer

1. Introduction

1.1 Cancer

Cancer has a long history; the first descriptions were made by the Egyptians, recorded on papyri dated to 1600 B.C. Evidence of ancient tumours was found in the remains of mummies, the oldest specimen being discovered in a female skull dated to the Bronze Age (1900-1600 B.C).[1, 2]

Cancer is a leading cause of death. In 2007, 59 million people died worldwide, 7.9 million (13%) of them from cancer. The greatest number of deaths stemmed from lung cancer (1.4 million deaths/year), followed by stomach (866,00 deaths/year), liver (663,000 deaths/year), colon (677,000 deaths/year), and breast cancers (548,000 deaths/year). [3]

Today, average life span has increased due to better health care, control of infectious diseases, decline in cardiovascular disease and overall improved lifestyle. The fact that people are living longer combined with environmental factors (increased carcinogenic chemicals in the environment and diet, ultraviolet radiation, (UV) ionizing radiation, chronic infections and inherited genetic factors) has paradoxically lead to the proportion and the number of people dying from cancer increasing.

The risk of cancer can be decreased by 40% through a healthy diet, physical activity and by not using tobacco; tobacco being the single largest preventable cause. One-fifth of cancers are caused by chronic infections like Hepatitis B Virus (liver cancer), Human Papilloma Virus HPV (cervix), Helicobacter Pylori (stomach), Liver Fluke (bile duct) and Human Immunodeficiency Virus HIV (Karposi sarcoma and lymphomas).

In the UK, 70% of new cases of cancer occur in those who are over the age of 60. One in three people in the UK will suffer from cancer in their lifetime and one in four will die from the disease. [4]

Cancer is the name given to a group of more than 200 diseases that can affect any part of the body. They are characterised by the uncontrolled growth and spread of abnormal cells. The most common type of cancer involves a rapid proliferation of cells leading to a solid mass called a tumour (or neoplasm) as illustrated in **Figures 1** below. [5]

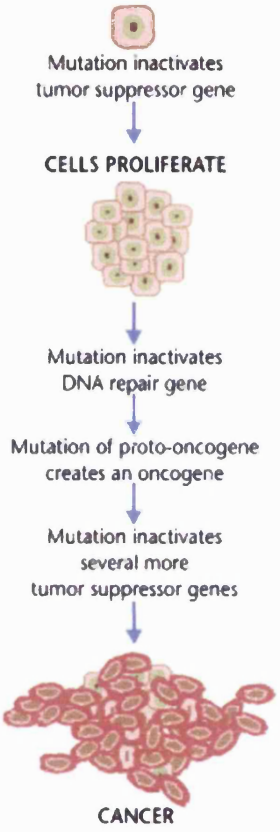

Figure 1: The stepwise nature of tumour progression (Adapted from World Health Organisation, cancer fact sheet, 2007).

The tumour can be either benign (not cancerous) or malignant (cancerous). Benign tumours do not spread to other parts of the body or tissues and rarely cause death. They can become life threatening by growing beyond their usual boundaries and by obstructing vessels and/or organs. Malignant tumours spread to many organs and parts of the body (metastasis), thus making surgical intervention impossible and ultimately leading to death.

1.2 Features of Cancer

Rapid advances in cancer research have lead to a more developed understanding of cancer, revealing it to be a disease involving dynamic changes to the genome through a series of mutations that lead to the production of oncogenes for dominant gain of function and the disabling of tumour suppressor genes to give recessive loss of function. It is now possible to understand some of the rules that govern the transformation of normal cells into malignant cells. Certain traits, molecular, biochemical and cellular are shared by most cancers giving acquired capabilities. As a result, cancer cells are no longer subjected to normal regulation of proliferation, differentiation and death.

In 1994 Pratt *et al.* listed a number of physical characteristics observed in neoplastic tissue, illustrated in diagrammatic form below (**Figure 2**).[6]

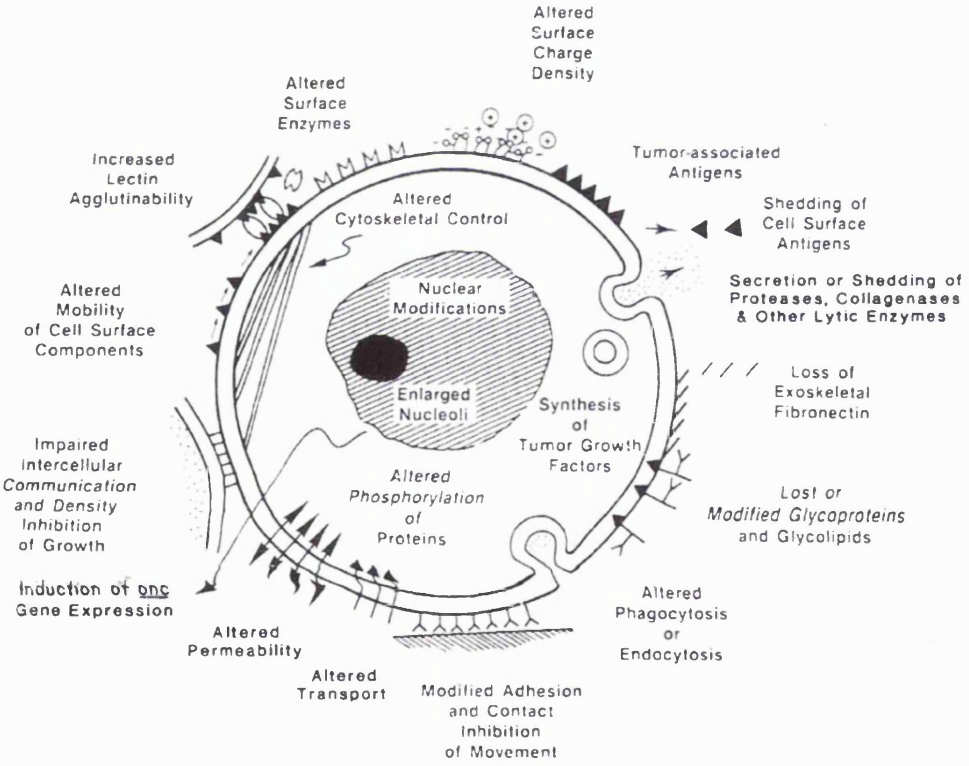

Figure 2: Illustration of a number of observed neoplastic transformations by Pratt *et al.* (Reported from The Anticancer Drugs, 1994)

1.3 Pratt's Observed Physical Characteristics of Neoplastic Tissue

The observed physical and biological characteristics listed below give some insight into the behaviour of tumour cells.

1. An unusual number of mitotic cells in a tissue field.
2. Evidence of cells breaking tissue barriers (e.g., the basal lamina of epithelial tissues).
3. Presence of incompletely differentiated or undifferentiated cells.
4. Cells with large nuclei and prominent nucleoli, altered cell-surface glycoproteins and glycolipids.
5. Over expression of tumour specific antigens in most cancers.
6. Cell secreted tissue digesting enzymes, such as proteases, collagenases and glycosidases.
7. Altered extracellular matrix (laminin, fibronectin).
8. Secretion of a variety of growth factors to stimulate growth.
9. High rates of nucleic acid biosynthesis and associated enzymes in some biosynthetic pathways.
10. A variety of genetic alterations indicating activated or mutated cellular oncogenes or loss of tumour suppressor genes.

1.4 Hanahan and Weinberg's 'Hallmarks' of cancer

More recently, Hanahan and Weinberg enumerated the well-known six 'Hallmarks' of cancer (**Figure 3**) corresponding to alterations in cell physiology, which collectively cause malignant growth. The recognition of the "hallmarks" of cancer is important because it focused attention on critical tumour signalling pathways and helps to identify new therapeutic targets.[7]

The hallmarks of cancer enumerate the most common characteristics shared by most if not all human tumours:

1. Self-sufficiency in growth signals
2. Insensitivity to growth-inhibitory (anti-growth) signals
3. Evasion of programmed cell death (apoptosis)
4. Limitless replication potential
5. Sustained angiogenesis
6. Tissue invasion and metastasis

1.4.1 Self-Sufficiency in Growth Signals (GFs)

Normal cells require mitogenic growth signals before they move from a quiescent state into an active proliferative state. By producing their own growth signals, cancer cells become less dependant on growth signal stimulation from other cells within the tissue. Thus, self-sufficiency in growth signalling subverts the mechanisms that normally operate to ensure normal behaviour of cell types in tissue. Growth factor receptors are over-expressed in some malignant cells causing hyper-responsive activity.[8, 9] Other tumour cells produce their own GFs, establishing autocrine signalling loops[10]. Finally, cancer cells can express mutated GF receptors that are constitutively active and free the tumour cell of the requirement for GF's.[11]

1.4.2 Insensitivity to Growth-Inhibitory (anti-growth) Signals

Within normal tissue, antiproliferative signals maintain cellular quiescence and tissue homeostasis. They include soluble growth inhibitors and immobilized inhibitors found in the extracellular matrix and on the surface of nearby cells. Cancer cells prosper by evading these antiproliferative signals. Normal cells monitor their external environment for the antiproliferative signals which are relayed to the retinoblastoma protein (pRb) and its relatives' p107 and p130. When pRb is hypophosphorylated it blocks proliferation by sequestering E2F transcription factors. Cancer cells avoid this by disrupting the pRb pathway and liberating E2Fs to allow proliferation.[12]

1.4.3 Evasion of Apoptosis (The "Death" Pathway)

Cancer cells have the ability to avoid programmed cell death (apoptosis). All cells possess the ability to use the apoptosis program, once triggered, via a variety of physiological signals. During apoptosis, in chronological order: cellular membranes are disrupted, the cytoplasmic and nuclear skeletons are broken down, the cytosol is extruded, the chromosomes are degraded and the nucleolus is fragmented. The cell's remains are then engulfed by neighbouring cells. Intracellular sensors monitor the cell's well-being and activate the death pathway in response to detected abnormalities, including DNA damage, signalling imbalance provoked by oncogene action, survival factor insufficiency, or hypoxia. Resistance can be acquired in cancer cells by loss of pro-apoptotic regulation through mutations involving the p53 tumour suppressor gene, resulting in loss of function of p53 protein.[13]

1.4.4 Limitless Replication Potential

It is known that once normal cells have progressed through a set number of doublings they stop growing, a phenomenon known as senescence.[14] Senescence can be overcome by the disruption of pRb and p53 tumour suppressor proteins, enabling cancerous cells to continue multiplying for generations until they enter a second state termed crisis. The "crisis" state is typified by karyotypic disarray (e.g. end-to-end fusion of chromosomes causing massive cell death).[15] However, on occasion, 1 in 10^7 cells can acquire the ability to multiply without limit (immortalisation).[16] The mechanism used to regulate cell generation makes use of telomeres, which are composed of several thousand repeats of the same 6 base pair sequence and are located at the ends of chromosomes. After each round of replication there is loss of telomeric DNA from the ends of chromosomes (approx 50-100 base pairs). This shortening is due to the inability of DNA polymerases to completely replicate the 3'-ends of chromosomal DNA. This progressive erosion eventually yields unprotected chromosomal DNA, enabling karyotypic end-to-end fusion of chromosomes to occur. Malignant cells maintain telomeres by up-regulating expression of the telomerase enzyme which adds hexanucleotide repeats on to the ends of telomeric DNA and halts telomere erosion.[17]

1.4.5 Sustained Angiogenesis

The delivery of oxygen and nutrition through the vasculature is essential for cell survival and function. Cells need to be within 100 μm of a capillary blood vessel for survival. The process of growing blood vessels is called angiogenesis and is carefully regulated.[18] As tumours grow in size they outstrip their blood supply and become hypoxic. This triggers the angiogenesis pathways present in all types of cells. In addition, oncogenic mutations present in tumour cells are known to promote angiogenesis.[19-21]

1.4.6 Tissue Invasion and Metastasis

In the development of most types of human cancers, the primary tumour mass will undergo "spawning", where by cells break new ground by moving out to invade neighbouring tissues. They travel to sites around the body where there are more nutrients and space, thus establishing new colonies. This process is called metastasis. Metastases are the main cause of human cancer deaths (>90%).[22] Successful invasion and metastasis depend upon all of the other five required hallmark capabilities and additional cellular changes. Both invasion and metastasis have a similar strategy, involving changes in the physical coupling of cells to their environment and the activation of extracellular proteases.

Invasion and metastasis is a complex process and is a major cancer research area. The cancer cell needs to acquire the ability to leave the tumour, enter a transport system (e.g the blood stream), leave the circulation system and invade a new location to begin growing a new tumour. Important proteins in metastasis are those involved in tethering cells to their surroundings, cell-to-cell adhesion molecules (CAMs) (members of the immunoglobulin and calcium-dependant family) and integrins which link cells to the extracellular matrix substrates.[23] Extracellular proteases are also important during metastasis.[24, 25] Protease genes become unregulated, protease inhibitor genes are downregulated and the inactive zymogen forms of proteases are converted into active enzymes. Proteases on the cell surface can facilitate migration by cancer cells into nearby stroma, across blood vessels walls and through normal epithelial cell layers.[11]

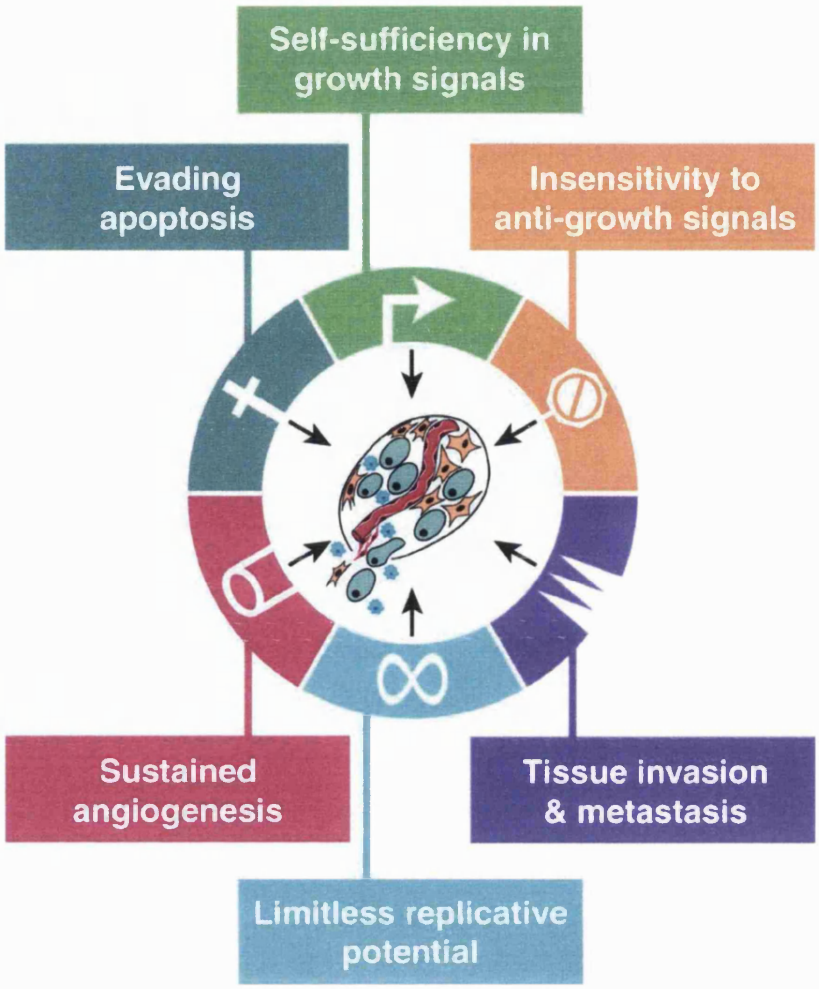

Figure 3: Acquired Capabilities of Cancer. Most if not all cancers acquire the same set of functional capabilities during their development, albeit through various mechanistic strategies.[7] (Diagram adapted from Hanahan and Weinberg, 2000)

1.5 The Therapeutic Rational for Anticancer Agents

The therapeutic effects of many first-line anticancer drugs are dependant on cytokinetic differences between cancer and normal cells. The selectivity of the agents is based, in part, on the greater sensitivity of cancer cells compared to normal cells. Therefore the maximum tolerated dose of any anti-cancer drug is limited by its toxic effects, on healthy cells.

The majority of chemotherapy regimens use antiproliferative agents (cytotoxics) that preferentially kill dividing cells, by attacking DNA processes such as replication, synthesis or processing. Examples of chemotherapeutics commonly used today include doxorubicin, vincristine, cyclophosphamide, topotecan and paclitaxel. Their

therapeutic efficiency is limited by the damage that they cause to normal proliferating cells such as those in the bone marrow and gut epithelia. They are also limited in their ability to treat solid tumours, as many solid tumour cells tend not to proliferate rapidly. Subsequently, patients with tumour burdens treated with cytotoxics usually enjoy remissions of only limited duration, followed by regrowth and spread of more-malignant and multi-drug resistant disease. Part of the reason for resistance is the presence of hypoxic cells in the centre of tumours. These cells become dormant and are much less susceptible to traditional cancer drugs which depend on cell division for their activity. In addition, they tend to be in a temporarily growth-arrested state and allow only limited drug penetration, which induces cellular resistance mechanisms.[26]

Novel, recently developed, therapeutic agents interfere with pathways which are specifically activated in cancer cells. Examples include imatinib (Glivec), which targets the BCR-ABL protein that causes chronic myelogenous leukaemia, and trastuzumab (Herceptin), which targets the ErbB2 (HER2/neu) receptor and is used to treat breast cancer.

Another strategy is to use prodrug and ligand-targeted therapies (LTTs) for the delivery of anticancer drugs to cancer cells by associating the drugs with molecules that bind to antigens or receptors which are either uniquely expressed or over expressed by the target cancer cells.

1.6 Prodrugs

A prodrug is a molecule which is chemically altered after administration to afford a therapeutically-active drug. [27]

Generally:

- they have a structure that improves solubility, permeability, or targeting to a tissue in order to improve pharmacokinetics.
- the progroup is cleaved *in vivo* to release the active structure
- prodrugs can improve physicochemical properties when no other structural modification is sufficient.

World wide, 5% of clinically-used drugs are prodrugs, mainly activated by hydrolysis or biotransformation. Typically, prodrugs have been developed to overcome pharmaceutical, pharmacokinetic (PK), and pharmacodynamic (PD) barriers. However, many discoveries have occurred by accident rather than design.

Barriers	Issues
Permeability	Not absorbed from the GI tract because of polarity
	Low brain permeation
	Poor Skin penetration
Solubility	Poor absorption and low oral bioavailability
	IV formulation cannot be developed
Metabolism	Vulnerable drug metabolized at absorption site
	Half-life is too short
	Sustained release is desired
Stability	Better Shelf life is needed
Transporter	Lack of specificity
	Selective delivery is desired
Safety	Intolerance/irritation
Pharmaceutics	Poor patient/doctor/nurse acceptance
	Bad taste or odour problems
	Painful injection
	Incompatibility (tablet desired but liquid is active)

Table 1: Drug Development Barriers and Issues that can be Overcome by Prodrug Strategies.[27]

Prodrugs can be used to:-

- Increase permeability of compounds by masking polar functional groups and hydrogen bonds with ester or amide linkers and by increasing lipophilicity.
- Improve solubility by using a non-ionizable progroup (e.g, glycol, polyethylene glycol and sugars). This can improve solubility by two- or three-fold. Prodrugs with ionisable prodrugs (e.g. phosphates) can increase solubility by orders of magnitude. There are two types, amino acid types, attached to hydroxyls (e.g. glucocorticoids) and phosphate types, attached to hydroxyls or amines (e.g. fosphenytoin).

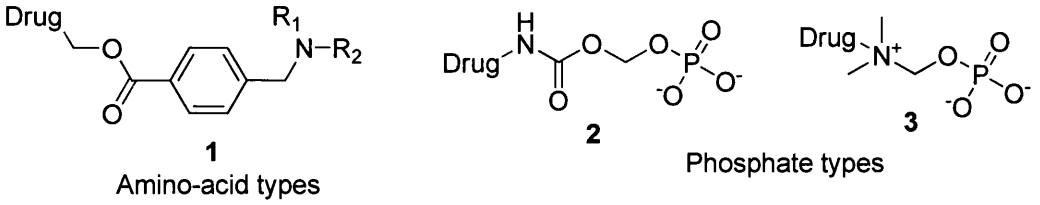

Figure 4: Amino-acid type and phosphate type prodrugs used to increase solubility

- Increase passive diffusion permeability; alkyl esters are preferred over carboxylic acid prodrugs. Other prodrugs used include the aryl groups, double esters with diols, cyclic carbonates, lactones and, most commonly, ethyl esters.
- Increase the lipophilicity of alcohols and phenols by preparing ester prodrugs using carboxylic acids. These prodrugs show an increase, for example, in corneal permeability, brain penetration and oral absorption.
- Increase the lipophilicity of nitrogen-bearing functional groups. Effective prodrug functionalities for amines include imines and enamines which can be stabilised by hydrogen bonds and small peptide derivatives. Carbamates can be used as prodrugs for amidines. Compounds which contain acidic NH functional groups, such as sulphonamides, carboxamides and carbamates, can be also effective prodrugs.
- Enhance intestinal absorption by taking advantage of transporter-mediated processes. Different types of prodrug transporters include peptide transporters, amino acid transporters, nucleoside transporters, bile acid transporters and monocarboxylic acid transporters.
- Reduce metabolism; the half-life of a parent drug can be improved by masking labile functional groups such as phenolic alcohols which are susceptible to phase II metabolism.

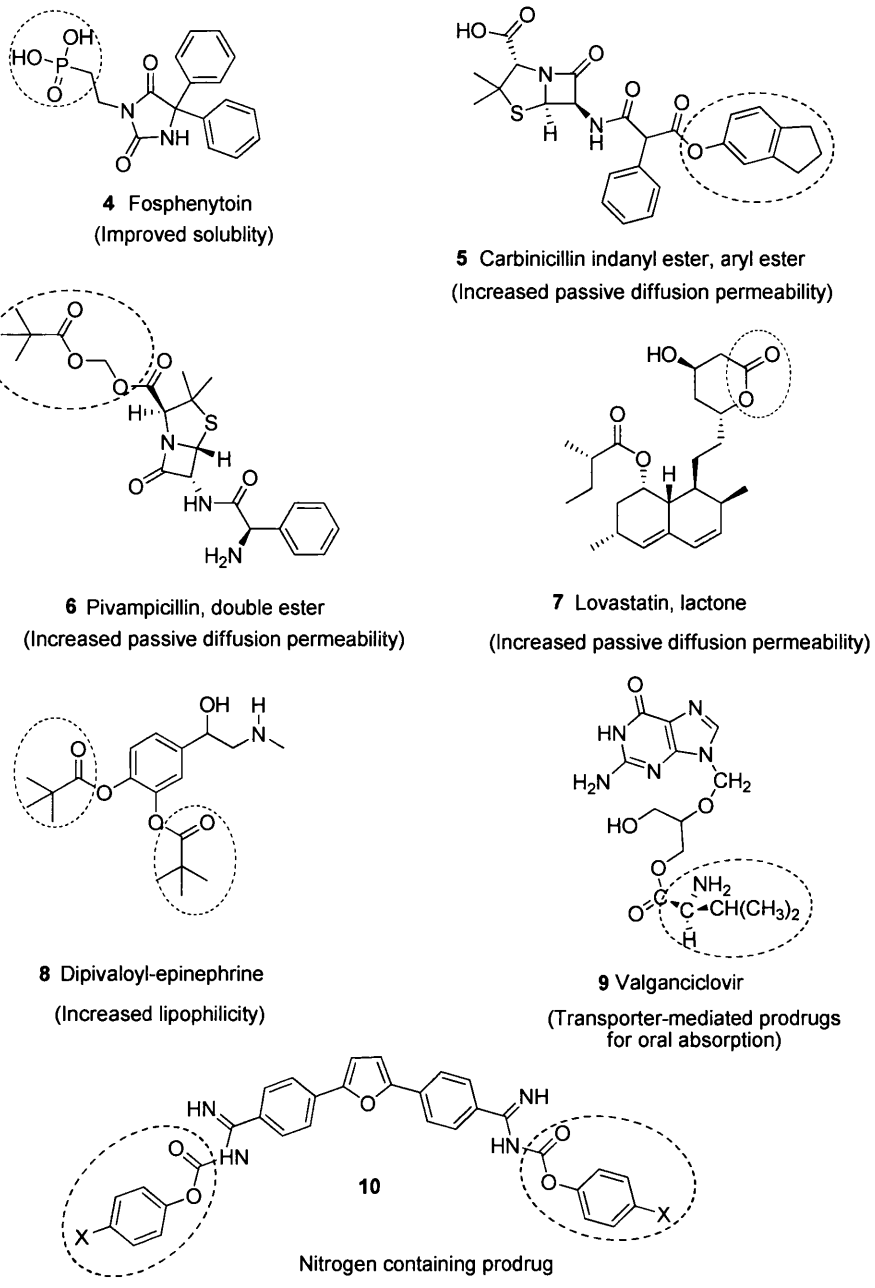

Figure 5: Structures of Prodrugs showing examples of chemical strategies to improve physicochemical properties.

1.7 The Uses of Prodrugs in Cancer Chemotherapy

Prodrugs have been used in a number of ways in cancer chemotherapy. Their uses range from providing a better formulation profile to selective activation at the tumour site. **Table 2** shows the range of uses that prodrugs have been put to in Chemotherapy.[28]

Improve solubility
Assist formulation
Improve pharmacokinetics/tissue distribution
Prevent unfavourable metabolism
Overcome tissue barriers, e.g. blood-brain
Overcome resistance
Provide selective organ effects
Provide specific tumour toxicity

Table 2: The Uses of Prodrugs in Cancer Chemotherapy

The prodrug form of a cytotoxic anticancer drug should be selectively activated at the tumour site. This can be achieved in a numbers of ways. For example, some methods exploit the unique aspects of tumour physiology such as selective enzyme expression or hypoxia. Others involve tumour-specific delivery techniques, for example the activation of prodrugs by exogenous enzymes delivered to tumour cells by monoclonal antibodies (ADEPT) or generated in the tumour cells by DNA constructs containing the corresponding gene (GDEPT). An effective prodrug needs to be substantially less toxic than the active drug. The greater the differential between prodrug and drug (the less toxic the prodrug and the more cytotoxic the drug), the better the efficacy system.[29]

1.7.1 Prodrugs Based on Taxol

Taxol (paclitaxel) has become one of the most effective drugs used against breast and ovarian cancers. It is isolated from the bark of the yew tree and works by stabilizing rather that disassembling the microtubules required for successful mitosis. The clinical success of taxol and related taxanes, combined with the insolubility of the parent compound have led to the synthesis of many analogues. [30] In early clinical trials of taxol, a hydroxypropylmethacrylamide polymer bearing an aminoacidic chain was linked through an esteric bond at the 2'-position of taxol. This resulted in a slow release form of taxol, thus targeting tumours and extending its permeability and retention.[31]

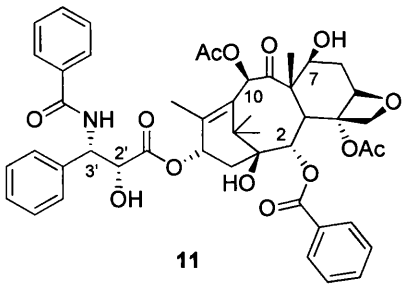

Figure 6 Taxol

1.7.2 Prodrugs Based on DTIC

DTIC (dimethylaminotrizene imidazole carboxamide) is used in the treatment of melanoma and some sarcomas. DTIC is an example of a prodrug being used to bypass the problem of the active drug being unstable to light. The active drug requires special storage and administration procedures because its photolysis products have no antitumour activity and are toxic. An additional problem is that DTIC is activated by demethylation in the liver. These issues have been overcome by the development of the prodrug temozolomide, which is stable to light and releases the same active metabolite as DTIC. This is achieved through a spontaneous ring opening as shown in **Scheme 1**. An added advantage of temozolomide is that it is readily bioavailable when administrated orally, allowing doses be given on an outpatient basis.

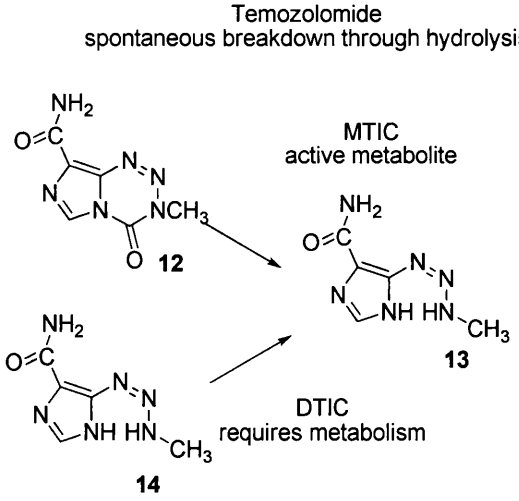

Scheme 1: Comparison of the activation of DTIC and temozolomide to the active drug MTIC

Other applications of prodrugs in the area of cancer include:

1. Increasing the intracellular concentrations of therapeutic agents and penetration of tissue areas inaccessible to parent drugs.

2. Improving bioavailability, e.g. the monophosphate of etoposide for the treatment of lung cancer

3. Improving tissue distribution, e.g. esterification of a parent drug can reduce or abolish charge (e.g., of a carboxylic acid) and improve the partition coefficient at physiological pH.

1.7.3 Penetration of the Blood-Brain Barrier

Many potential drugs for treating cerebral neoplasms are unable to enter the brain due to the impermeability of the blood-brain barrier (BBB). Rapoport *et al.*[32] reported that the BBB arises from the close joining of cells forming the cerebral capillaries, thus eliminating intracellular transport of most substances. Only the most lipophilic of compounds are able to enter. Bodor *et.al* [33] found that by esterifying the carboxylic acid group of chlorambucil, the lipophilicity of the drug could be improved and higher brain concentrations could be obtained. The prodrug was converted by tissue oxidoreductases to form methylpyridinium derivatives. In extracerebral tissue the charged metabolite is rapidly excreated, but in the brain the BBB prevents rapid excretion of the prodrug and so esterases are able to release the active parent drug.

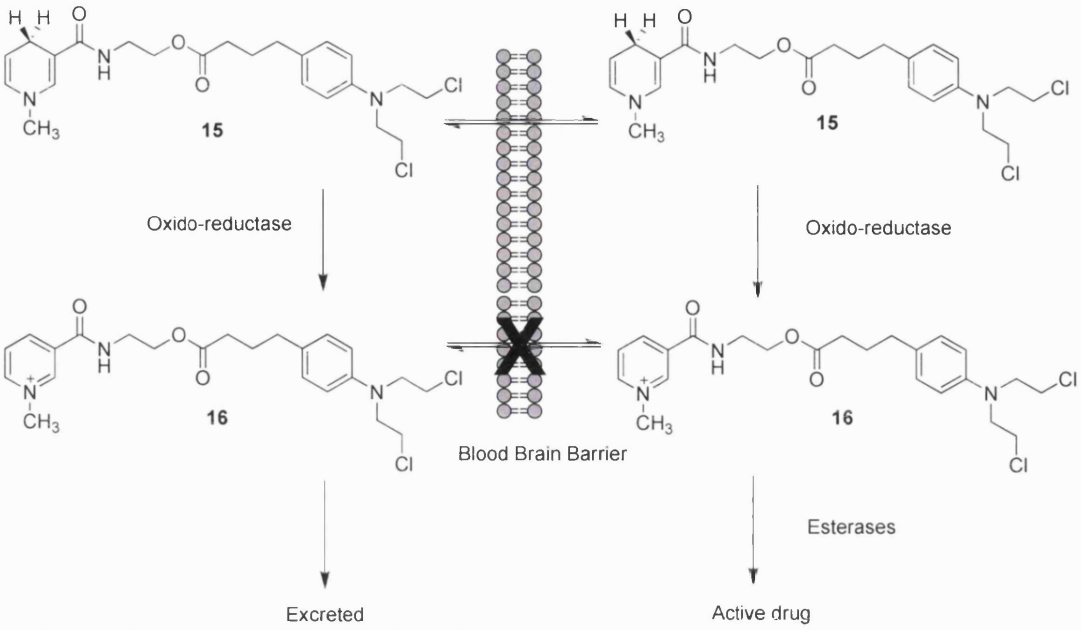

Figure 7: Penetration of the blood-brain barrier by prodrugs made by derivatization of drugs with a 1-substituted acid moiety.

Prodrug strategies have also been used to directly target tumour cells. The use of directed enzyme therapies will be discussed in the following section.

1.8 Directed Prodrug Therapy

1.8.1 Introduction

Classic chemotherapy targets not just cancer cells but all rapidly dividing cells such as those in the intestinal tract, stomach lining, hair follicles, bladder, nails, blood, and bone marrow. The resulting collateral cytotoxicity leads to common side effects such as nausea and vomiting, hair loss, tiredness, pain, mouth sores and myelosuppression (bone marrow suppression).

Paul Ehrlich, the 1908 Nobel Laureate, coined the term "chemotherapy" and popularized the concept of a "magic bullet", a term to describe drugs or therapies which are selectively active at their site of action with minimal effect on the rest of the body. A number of prodrug therapies have been developed for the treatment of cancer with the aim of realising Ehrlich's vision.[34, 35]

As discussed earlier, prodrugs are pharmacologically inactive compounds that undergo an *in vivo* conversion to the active drug molecule in order to produce a therapeutic effect.[36] Central to the idea of prodrug therapy is selective activation of the prodrug at the tumour site. This can be achieved in a number of ways. Some methods exploit unique aspects of tumour physiology such as selective enzyme expression or hypoxia. Others employ tumour-specific delivery techniques, for example the activation of prodrugs by exogenous enzymes delivered to tumour cells by monoclonal antibodies (ADEPT) or generated in the tumour cells from DNA constructs containing the corresponding gene (GDEPT).

In general, prodrugs designed for tumour-activated prodrug therapy must fulfil several requirements. The most important requirements are:- [37]

i) The tumour-associated biomolecule must be present in significantly elevated levels in tumour tissue compared to normal tissue. Concentration must be high enough to generate cytotoxic levels of free drug in the tumour.

ii) Prodrug activation at sites distant from tumour tissue must be minimal.

iii) The prodrug must be a good substrate and/or possess high binding affinity for the tumour-associated biomolecule.

iv) Ideally, the prodrug should be significantly less toxic than the parent drug.

v) The prodrug must not be rapidly excreted from the body and must not enter cells randomly.

Most significantly, the prodrug needs to be substantially less toxic than the active drug. When the cytotoxicity differential between prodrug and active drug increases (the less toxic the prodrug and the more cytotoxic the drug) the more efficacious the system becomes.[29]

1.8.2 Directed Prodrug Strategies

Mono-therapy with prodrugs is passively directed to exploit the intrinsic properties of tumour cells such as hypoxic conditions, change of pH, or over-expression of enzymes or specific receptors.

Directed prodrug strategies normally involve specific antibodies. Antibody-drug conjugates (ADCs), involve cytotoxic drug molecules covalently linked to a monoclonal antibody (via a chemical linker) that binds to an antigen expressed on the surface of targeted cancer cells (**Figure 8**). ADCs are prodrugs requiring drug release for activation, commonly after ADC internalization into the target cell. Examples of cytotoxic agents that have been conjugated to antibodies are doxorubicin, vinblastine, calicheamicin, maytansine and duocarmycin.[38, 39]

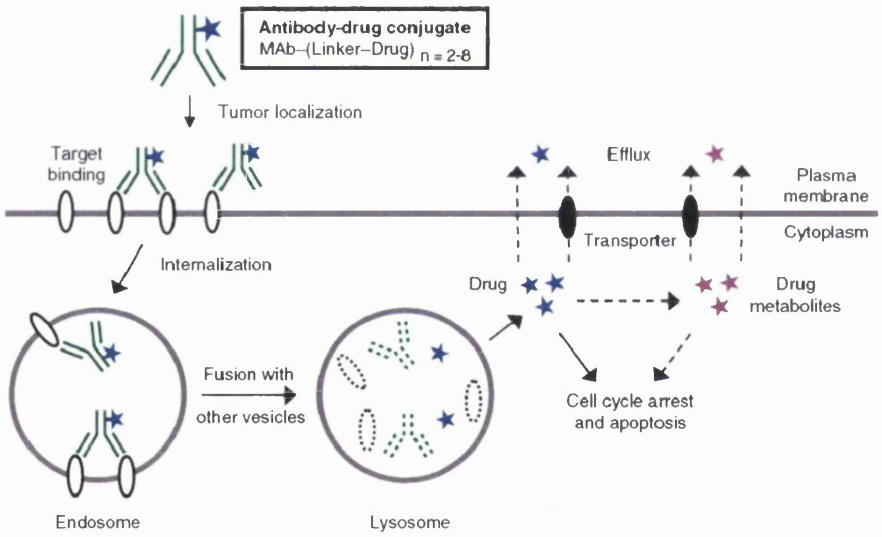

Figure 8: An ADC comprises an antibody conjugated via a linker to a cytotoxic drug. ADCs are commonly in IgG format with 2–8 drugs/antibody. ADCs are delivered intravenously and then localize to a tumour and bind to a target antigen on the surface of the tumour cell. Internalization of the ADC commonly proceeds via a clathrin-coated pit mechanism. Proteases in the acidic environment of the endosomes then digest the antibody, and potentially also the linker, thus releasing free drug. The drug then enters the cytoplasm where it binds to its molecular target, commonly leading to cell cycle arrest and apoptosis. A portion of the drug is effluxed from the cell by passive diffusion or active transport. It may also leave the cells after cellular fragmentation through apoptosis or necrosis (Reproduced from Chari *et al.*, 2007).

1.8.3 Types of DEPT (Directed-Enzyme Prodrug Therapy)

Alternatively, an enzyme can be directed to a tumour and the prodrug administered systematically (DEPT). These approaches tend to be more complicated,

involving distinct tumour targeting and prodrug delivery stages. In step 1 the enzyme-antibody conjugate is administered and allowed to localise at the tumour site. In step 2 the prodrug is administered systemically, but is only activated at the tumour site by the antibody enzyme conjugate.

Currently, delivery methods for an enzyme/prodrug strategy can be divided into two major classes: (a) delivery of active enzyme to tumour tissue (e.g., ADEPT) and (b) delivery of genes that encode prodrug-activating enzymes to tumour cells (e.g., GDEPT/VDEPT) as shown in **Figure 9**. [40]

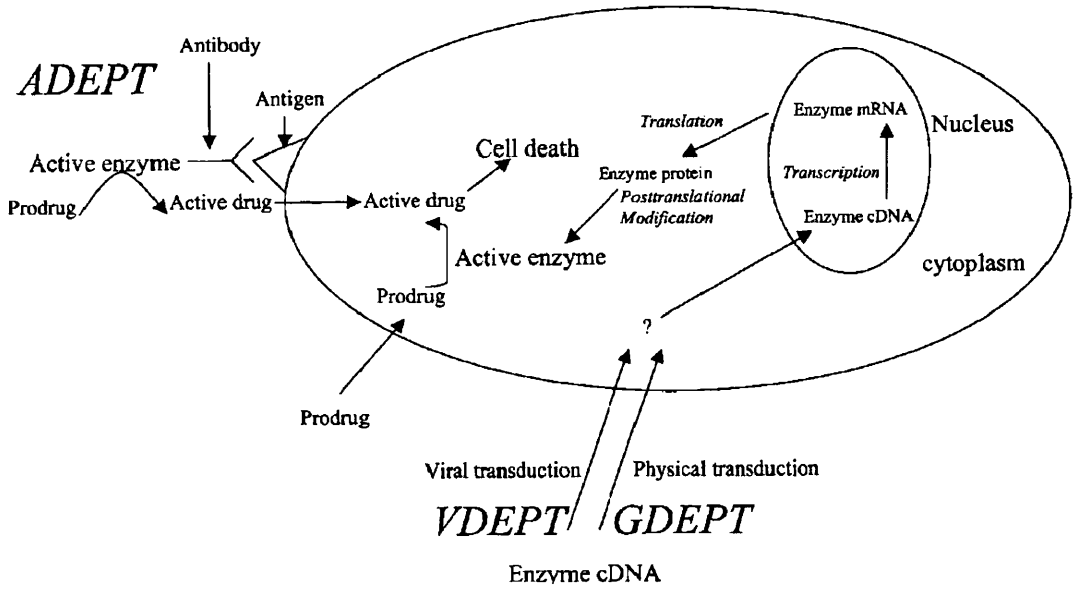

Figure 9: Summary of approaches for enzyme/prodrug cancer therapy (reproduced from Huber *et al.*, 1991)

A listing and brief description of the various targeting strategies is given below. In all these, the prodrug is administered after prior localization of a specific enzyme.[41, 42]

1. Antibody-directed enzyme prodrug therapy (ADEPT)[43-45]. A specific enzyme can be localized in the first step using an antibody-enzyme conjugate. The monoclonal antibody (mAb) must specifically bind a tumour-associated antigen on the cell surface (see **Section 1.9**)
2. Gene-directed enzyme prodrug therapy (GDEPT). This involves delivery of a gene encoding the activating enzyme to tumour cells in the first step.[46]
3. Virus-directed enzyme prodrug therapy (VDEPT). A retrovirus is used to deliver the gene to the tumour cell.[47]

4. Bacterial-directed enzyme prodrug therapy (BDEPT). Spores of genetically modified anaerobic bacteria, which can germinate only in hypoxic regions of the tumour, are employed.[48] The bacterium then produces the programmed enzyme selectively at the tumour site.
5. Polymer- or macromolecular-directed enzyme prodrug therapy (PDEPT/MDEPT). This makes use of the enhanced permeability and retention effect (EPR)[49] in tumour tissue, which leads to accumulation of a polymer-conjugated activating enzyme.[28]
6. Antibody-directed abzyme prodrug therapy (ADAPT), a humanized catalytic antibody (abzyme) is used to activate the prodrug.[50, 51]
7. Fusion protein-mediated prodrug activation (FMPA). This uses DNA recombinant technology to prepare fusion proteins that contain both the antibody and the enzyme.[52] Bispecific antibodies that bind to both the tumor cell antigen and the enzyme can also be employed for prodrug activation.

The most important examples of ADEPT, GDEPT and VDEPT enzyme-prodrug approaches are shown in **Table 3**.

Enzyme	Prodrug	Drug
Nitroreductase	CB 1954	5-(Aziridin-1-yl)-4-hydroxyl-amino-2-nitro-benzamide
Cytochrome P450	4-Ipomeanol	Unidentified (furan epoxide is speculated)
Cytochrome P450	Ifosfamide	Isophosphoramide mustard
Cytochrome P450	Cyclophosphamide	Phosphoramide mustard
Purine-nucleoside phosphorylase	Fludarabine	2-Fluoroadenine
Purine-nucleoside phosphorylase	MeP-dR	MeP
Thymidine kinase	Ganciclovir	Ganciclovir-triphosphate nucleotide
Alkaline phosphatase	Etoposide phosphate	Etoposide
Alkaline phosphatase	Mitomycin C phosphate	Mitomycin C
Alkaline phosphatase	POMP	POM
Alkaline phosphatase	*N*-(4-phosphonooxy)-phenylacetyl)doxorubicin	Doxorubicin
β-Glucuronidase	Glucuronidated Nor-nitrogen mustard	Oxazolidinone
β-Glucuronidase	Glucuronidated 9-amino-camptothecin	9-Aminocamptothecin
β-Glucuronidase	Glucuronide mustard	Mustard
Carboxypeptidase	Methotrexate-amino acids	Methotrexate

Carboxypeptidase	CMDA	Benzoic acid mustard
Penicillin amidase	DPO	Doxorubicin
Penicillin amidase	MelPO	Melphalan
Penicillin amidase	NHPAP	Palytoxin
Penicillin amidase	N-(phenylacetyl) doxorubicin	Doxorubicin
Penicillin amidase	N-(phenylacetyl) melphalan	Melphalan
β-Lactamase	LY 266070	DAVLBHYD
β-Lactamase	C-DOX	Doxorubicin
β-Lactamase	PRODOX	Doxorubicin
β-Lactamase	CM	Phenylenediamine mustard
β-Lactamase	CCM	Phenylenediamine mustard
β-Lactamase	Cephalosporin-DACCP	DACCP
β-Lactamase	PROTAX	Taxol
β-Lactamase	Cephalosporin mitomycin C	Mitomycin C
β-Lactamase	C-Mel	Melphalan
Cytosine deaminase	5-Fluorocytosine	5-Fluorouracil
Methionine γ-lyase	Selenomethionine	Methylselenol
Methionine γ-lyase	Trifluoromethionine	CSF_2

Table 3: Bioactivating enzymes and prodrugs used in ADEPT, GDEPT and VDEPT strategies. [53](MeP, 6-methylpurine; POMP, p-*N,N*-bis(2-chloroethyl)amino_phenyl phosphate; POM, p-*N,N*-bis(2-chloroethyl)amino_phenol; DAVLBHYD, 4-desacetylvinblastine-3-carboxylic acid hydrazide; DACCP, 4-carboxyphthalato(1,2-cyclohexanediamine) platinum; CSF2, carbonothionic difluoride.)

1.8.4 Cleavable Linkers

Generally prodrugs are made up of three parts: a trigger, linker (or spacer) and an effector unit, (**Figure 10**). These types of prodrugs release the active agents through a two step process:- Step 1, enzymatic or chemical activation of the trigger; Step 2, spontaneous chemical breakdown of the linker, thus allowing expulsion of the active agent.

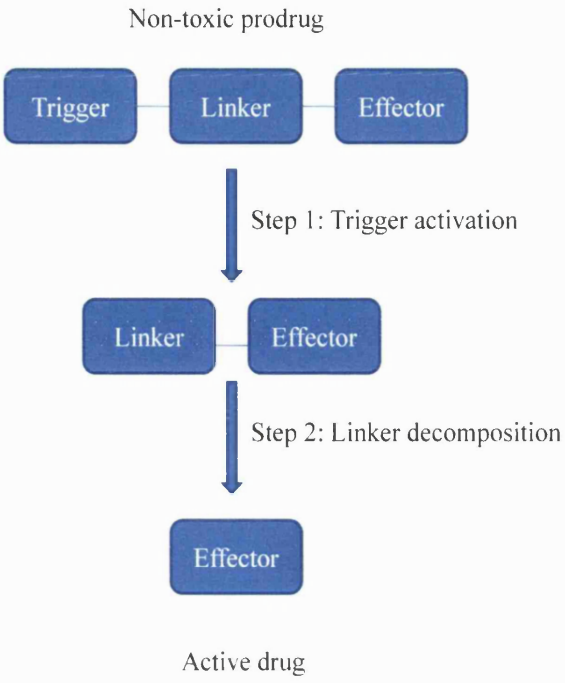

Figure 10: Trigger, linker and effectors components of a prodrug.

The linker or spacer can be used in a number of ways in different tumour targeting systems. Prodrugs using self-immolative linker types have been developed for antibody-drug conjugates (ADCs) and for directed-enzyme prodrug therapy (DEPT). ADCs are usually composed of between 1-8 molecules of a cytotoxic drug covalently linked to a monoclonal antibody which binds to an antigen expressed on the surface of targeted cancer cells.[38, 39]

Schemes 2 and 3 show some of the mechanisms of self-decomposition of the linker units through elimination and cyclization processes. **Scheme 4** shows more complex systems such as extended self-immolative linkers and self-immolative dendrimers.

A cleavable (self-immolative) linker (or spacer), once incorporated, can be fragmented enzymatically to release the parent drug. A number of factors need to be considered when designing a prodrug for enzymic activation. Firstly, steric factors need to be considered. For example, a hindered linker or a bulky parent drug (or both), may block efficient enzymatic cleavage. Generally, there are two types of self-immolative linkers (**Scheme 2**). The first contains a self-immolative linker that

eliminates via a cascade of electron movements, ultimately leading to expulsion of a leaving group, i.e. the drug. The second type involves a cyclisation linker (**Scheme 3**). which releases the drug moiety after activation has provoked an intramolecular cyclization.[41]

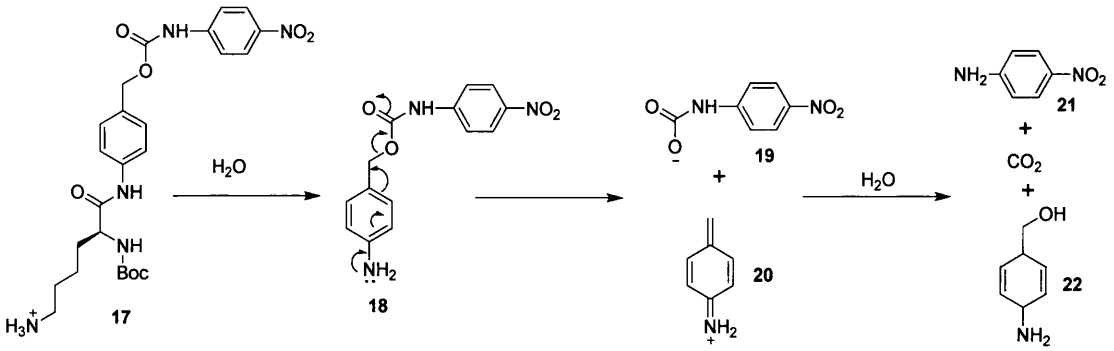

Scheme 2: Prodrug activation via (1) hydrolysis, (2) 1,6-elimination and (3) drug release

In the early 1980s, Carl *et.al* [54] reported one of the first examples of an electronic cascade spacer involving an 1,6-elimination linker as shown in **Scheme 2**. Enzymatic hydrolysis of the lysine amide group by trypsin unmasks a strongly electron-donating 4-aminobenzyl group which undergoes a 1,6-elimination to release 4-nitroaniline (i.e., the surrogate drug). This 1,6-elimination linker can be considered as one of the most versatile self-immolative connectors.[55] An example of a cyclization linker is the ethylene diamine linker that, after removal of the trigger R1, cyclises to yield a cyclic urea derivative and the liberated parent drug HOR^2 (**Scheme 3**).[56]

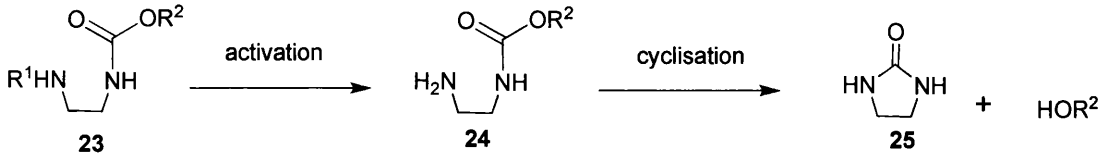

Scheme 3: Prodrug activation via intramolecular spacer cyclization and drug release

Dendritic self-immolative linkers can also be used in targeted drug delivery. They have the advantage of being able to liberate more than one drug molecule, through a domino-like mechanism, in response to a simple triggering stimulus. Cascade release dendrimers are constructed from two or more generations of branched self-immolative linkers, each of which releases leaving groups (i.e. drug) after a single activation as shown in **Scheme 4.**[57-59]

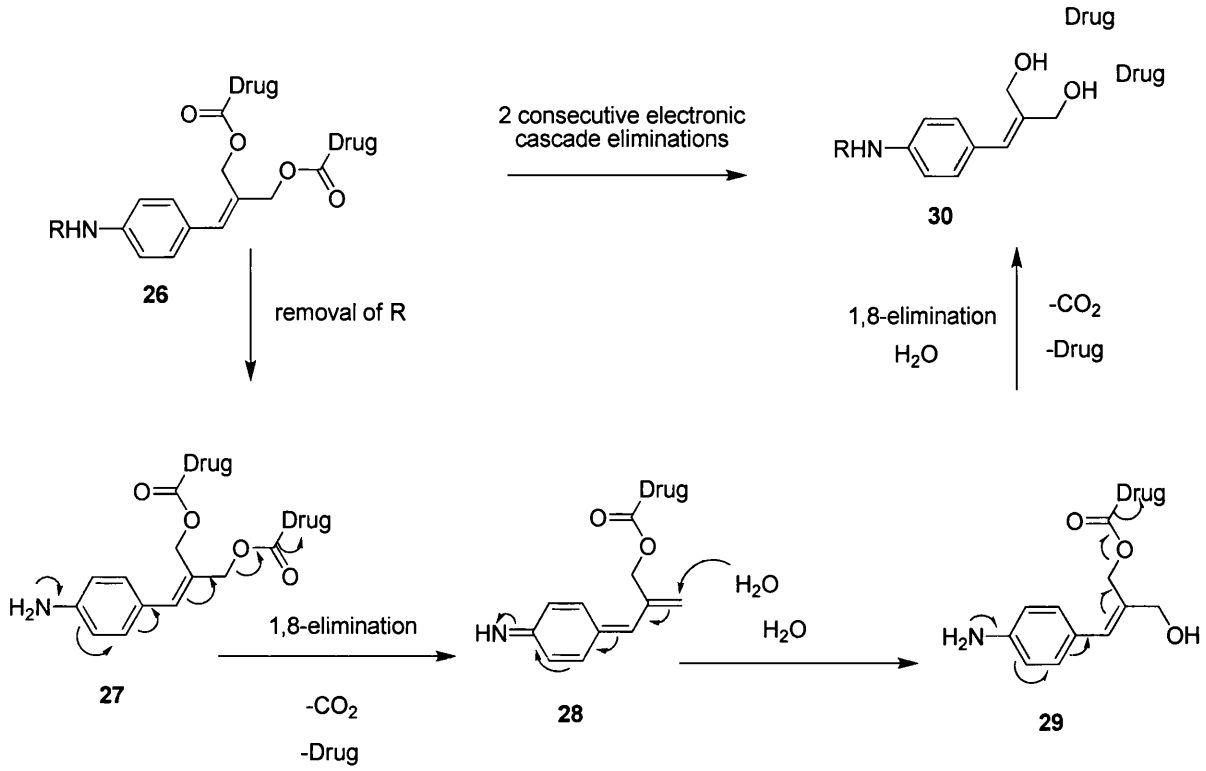

Scheme 4: Self-immolative dendrimers

1.9 ADEPT (Antibody-Directed Enzyme Prodrug Therapy)

1.9.1 Introduction

ADEPT (antibody-directed enzyme prodrug therapy) is a technique used for the selective targeting of tumour cells. It was introduced by Bagshawe [60] in 1988, in an attempt to reduce the side effects exhibited by other chemotherapy treatments. [61, 62]

ADEPT is based on the observation that tumour cells express different antigens to normal cells. As a result, tumour selectivity can be achieved by using compatible antibodies to target the tumour. The therapy works in two stages and is illustrated in **Figures 11.** [63-65]

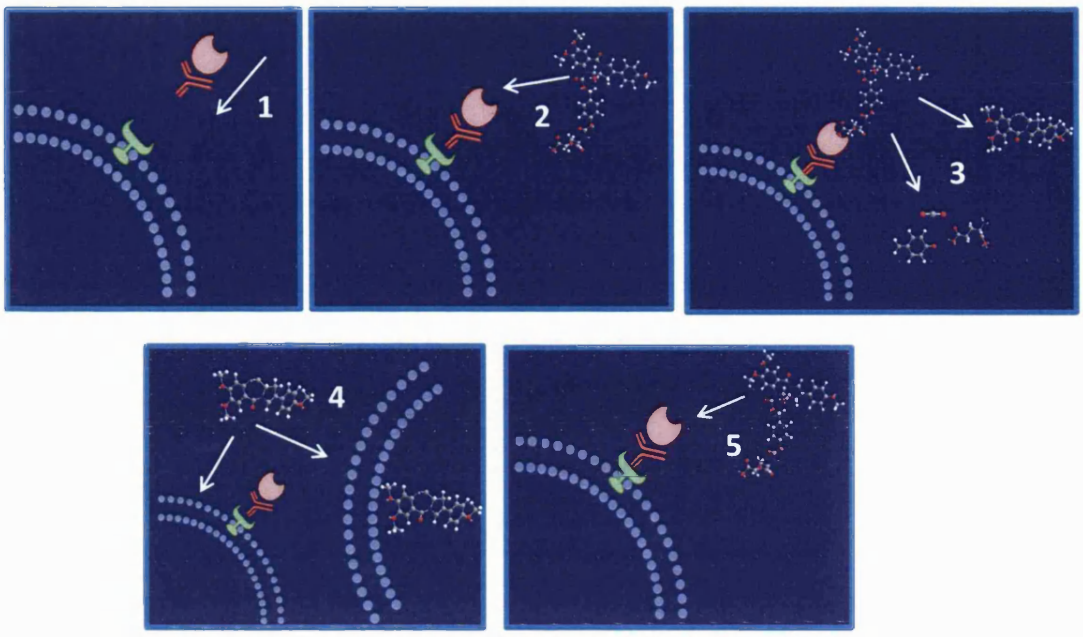

Figure 11: An illustration of antibody-directed enzyme prodrug therapy (ADEPT). (1) The mAb-enzyme conjugate is administered. It binds to tumour cell-surface antigens, and time is allowed for unbound mAb-enzyme to actively or passively be cleared from the circulation. (2) Administration of an inactive prodrug which is then selectively interacts with the mAb-enzyme conjugate at the tumour cell surface. (3) Cleavage of the progroup (the inactivating moiety from the prodrug), (4) release of the active drug in the tumour microenvironment allowing it to enter cells which exhibit the antigen and also neighbouring cells which do not. (5) One molecule of the antibody enzyme conjugate is able to activate more than one prodrug molecule in a "catalytic" sense.

An antibody (Ab) is chemically attached to an enzyme, allowing the conjugate to bind to its corresponding antigen on the tumour cell surface. The Ab-enzyme conjugate is administered to the patient intravenously and time is allowed for it to attach to tumour cells and for the excess conjugate to clear from the blood and normal tissues, thus allowing the tumour to be selectively targeted. The second step involves the administration of the prodrug which is selectively converted by the Ab-enzyme conjugate at the tumour site into a low molecular weight cytotoxic drug which enters the cancer cells.

Advantages of ADEPT are:

- Only tumour cells are targeted.
- multiple prodrug molecules can be converted to the toxic agent by the enzyme conjugate.

- The bystander effect allows the killing of surrounding antigen-negative cells and those that have no Ab-enzyme conjugate attached.

Disadvantages of ADEPT are:

- Some active drug diffuses back into the blood stream from tumour sites or other sites where enzyme activity persists and thus has some access to normal cells. This can lead to dose-limiting toxicity [64].

- The potential immunogenicity of the non-human Ab-conjugate may contraindicate repeated treatments.

- The process is more complicated than administering a simple tablet/capsule or injection.

1.9.2 Exploitation of Antigens in ADEPT

The principle of ADEPT relies on the over-expression of specific cell surface antigens in tumour cells. Tumour pathophysiology enables the production of tumour specific antigens and these can be exploited as targets in antibody delivery systems. The target antigen should ideally be absent from normal tissue, but this is seldom, if ever, achieved. Tumour-associated antigens are commonly selected and utilised on the basis of their higher expression levels in tumours and limited expression in normal tissues.

Patients with a particular tumour type normally express a specific target antigen. This antigen expression can also become a diagnostic test that may aid the choice of therapy for a patient. For example: - profiling HER2 expression can lead to treatment with trastuzumab, and EGFR profiling may lead to treatment with cetuximab or panitumumab.

Another problem to be considered when targeting tumours is the potential shedding of target antigen from the surface of tumour cells into the circulation. This can increase the risk of toxicity due to immune complex formation and subsequent deposition in the kidneys. This would also lead to accelerated clearance of antibody-directed conjugate (ADC) and impaired tumour localization. However, a phase I study

with an anti-HER2 ADC, trastuzumab-DM1, in metastatic breast cancer has demonstrated that shedding of antigen can be tolerated.[66]

1.9.3 Carcinoembryonic Antigen

The carcinoembryonic antigen is expressed by some cancers, especially colon cancers, and by the developing foetus. However, in the foetus production stops before birth. CEA is a glycoprotein involved in cell adhesion (**Figure 12** and **13**).[67] Testing for CEA levels in the blood can be used to establish how widespread a cancer is in the body.

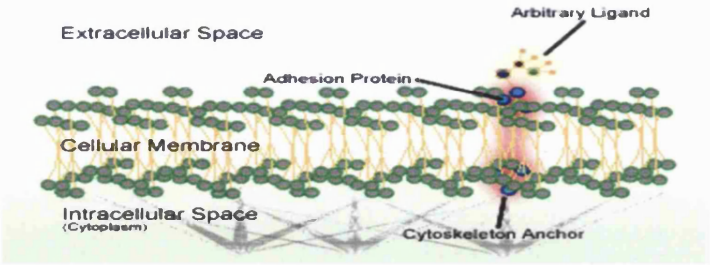

Figure 12: Location of CEA antigen (adhesion protein) on cell surfaces.

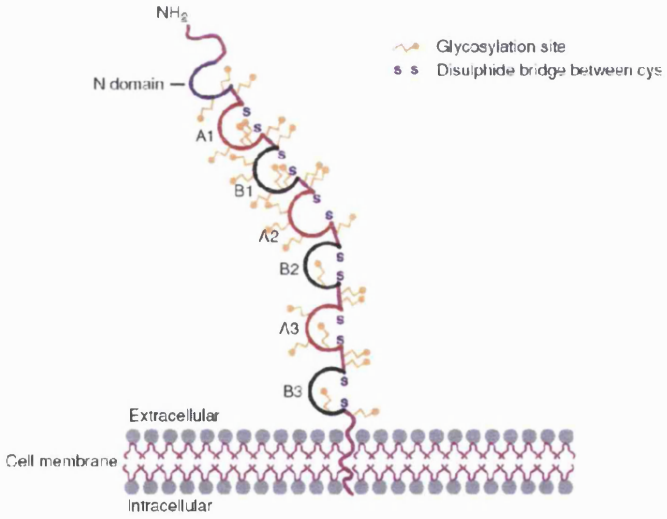

Figure 13: Schematic representation of the human carcinoembryonic antigen (CEA) protein (the 70-kD protein becomes 180 kD when glycosylated).

As mentioned previously, target antigens are heterogeneously distributed and not limited to expression in a tumour. **Figure 14** illustrates the potential for discrimination between tumour and normal tissue using antibody specific to carcinoembryonic antigen (CEA). [68] In this case, some expression of CEA occurs in

normal tissue. However, expression is much stronger in tumours cells, than in the normal bowel mucosa adjacent to the colon carcinoma. Quantitative measurement of the concentration of CEA found in the tumour area had a value of 2μg g^{-1} while the concentration in the normal mucosa was normally below 30 ng g^{-1}.

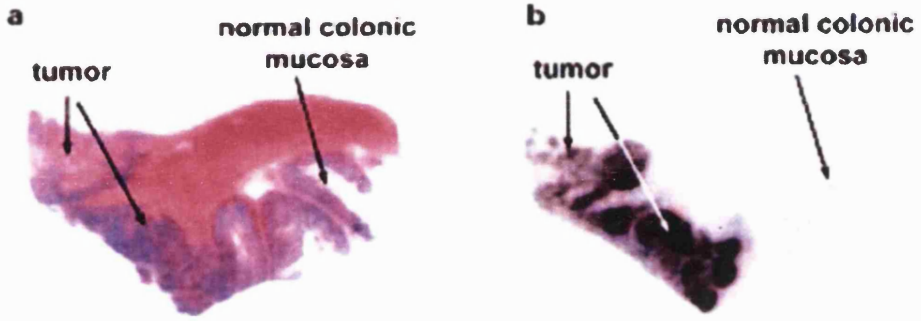

Figure 14: Quantitative mapping of CEA antigen concentration within preserved tissue architecture; a. H&E immunostaining reveals the morphological appearance of a colorectal adenocarcinoma arising in the large bowel and infiltrating through the muscle wall. b. Radioimmunolumiography (RILG) is used to quantify CEA concentration. Both techniques are performed in serial section and this allows quantification of the concentration of CEA antigen within histological sections whilst preserving tissue architecture. CEA concentration in colorectal cancer as determined by RILG assay ranges from 22 to 212 ng g-1 (in paraffin sections) and between 40 and 594 ng g-1 in cryostat sections, with local concentrations of up to 2μg g-1

The diagrams in **Figure 15** demonstrate that it is possible to target enzymes to tumour cell with antibodies by exploiting tumour specific cell-surface antigens. Three biopsies are shown: biopsy **A** shows a general antigen stain, **B** shows an anti-CEA antibody stain revealing tumour selectivity; and **C** shows an anti-CPG2 antibody stain indicating that it is possible to locate enzyme-antibody conjugates to the tumour site.

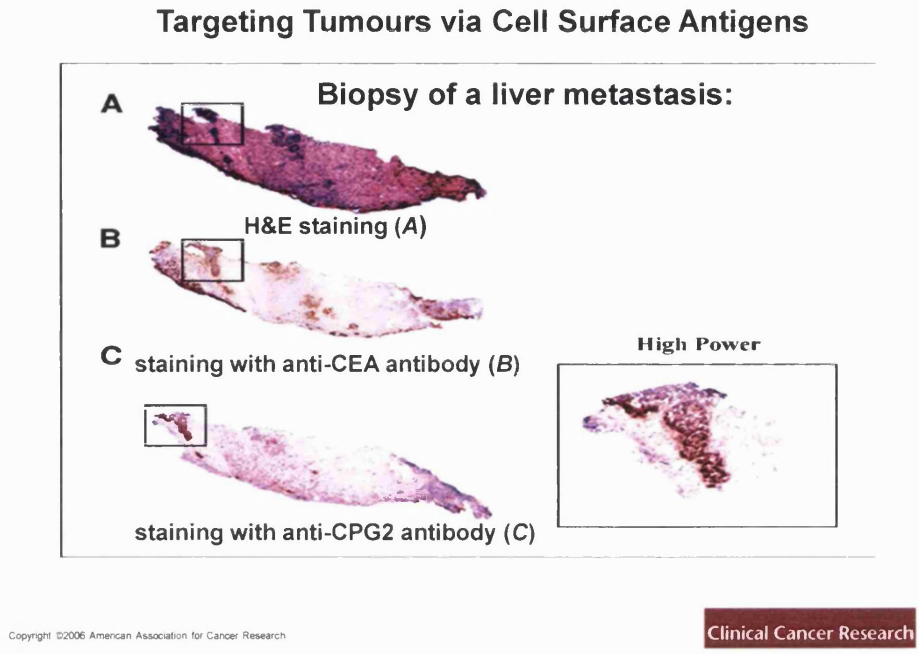

Figure 15: Targeting tumours via cell surface antigens. Biopsy of a liver metastasis: H&E staining; (A), Staining with anti-CEA antibody, (B) Staining with anti-CPG2 antibody, (C) The H&E-stained section confirms the presence of tumour in the biopsy. Staining with anti-CEA antibody confirms CEA expression in tumour, and staining with anti-CPG2 antibody provides further contrimitory evidence (From Mayer, A. *et al.* [69]).

1.9.4 Monoclonal Antibodies

One challenge for the ADEPT approach[70] is to reduce or abolish the immunogenicity of the antibodies. Recent advances in antibody engineering have led to the production of chimeric, humanised and fully-human mAbs.[71] These advances have helped to address the immunological problems associated with ADEPT.

Most of the mAbs used are in the IgG class (IgG_1, IgG_{2a}, IgG_{2b}) of immunoglobulins, (**Figure 16**). A whole antibody has a higher binding avidity due the presence of two binding sites. It also contains the Fc domain which can bind to normal tissue through Fc receptors, particularly in the case of macrophages, leading to higher liver and spleen uptake which can cause increased immunogenicity. As a result, antibody fragments are more commonly used for targeting drug carriers. The $F(ab')_2$, Fab' and scF_v single chain fragments lack the Fc domain therefore reducing immunogenicity (**Figure 17**). The $F(ab')_2$ fragments still contain two binding regions bound together by disulphide bonds which can be broken to give a free thiol (-SH)

group, thus allowing the ligand targeted therapeutics to be attached to the antibody. Fab' and scF_v have only one binding site, thus reducing their binding avidity with respect to $F(ab')_2$ or whole antibodies. However, an advantage of a scF_v fragment is that it can be easily produced via *Escherichia coli* fermentation.

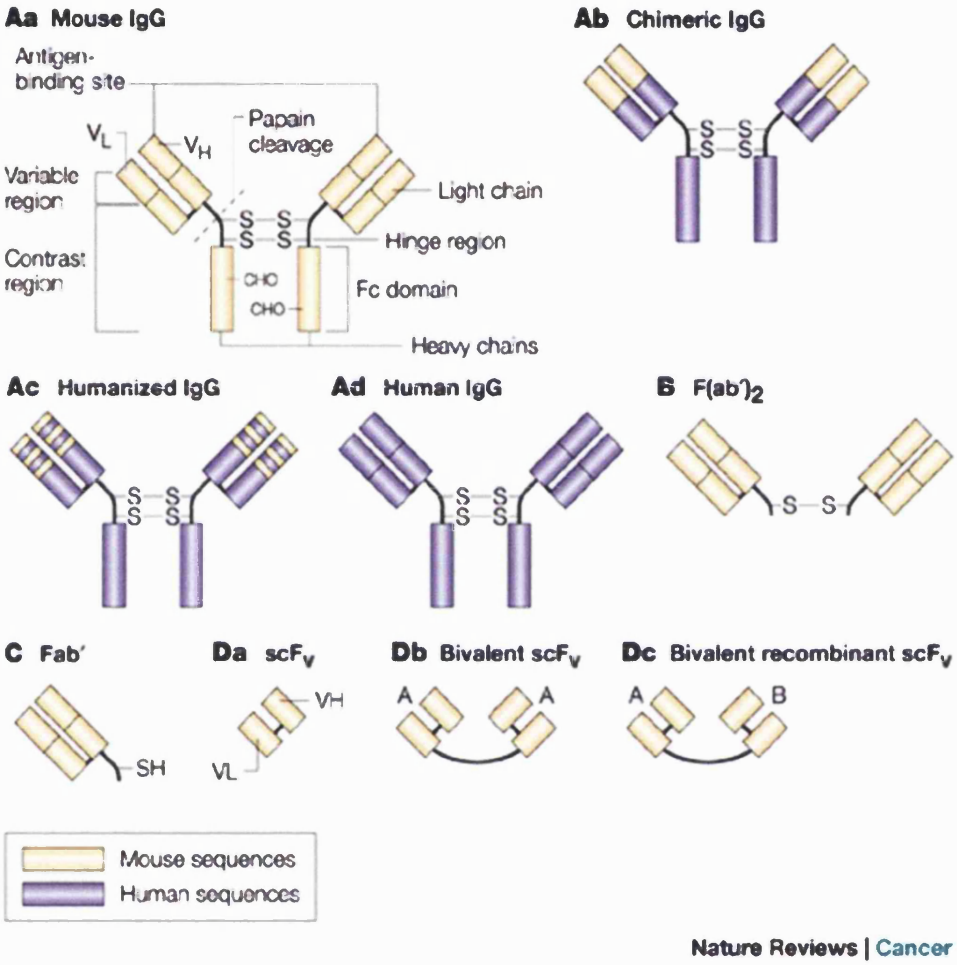

Figure 16: Antibodies and antibody fragments. Targeting antibodies are normally monoclonal immunoglobulin G (IgG) (Aa) or IgG fragments (B–D)/ F(ab')2 (B) or Fab' (C) fragments can be made by enzymatic cleavage of the whole monoclonal antibody (mAb) (Aa) or by molecular biology techniques — for example, Fab' (C), scFV (Da), bivalent (Db) or recombinant fragments (Dc). mAbs that are made by traditional hybridoma techniques are murine in origin. Recent developments have led to improved techniques for the production of chimeric, humanized or fully human antibodies or fragments (Ab–d) (VH, variable heavy chain; VL, variable light chain).[71]

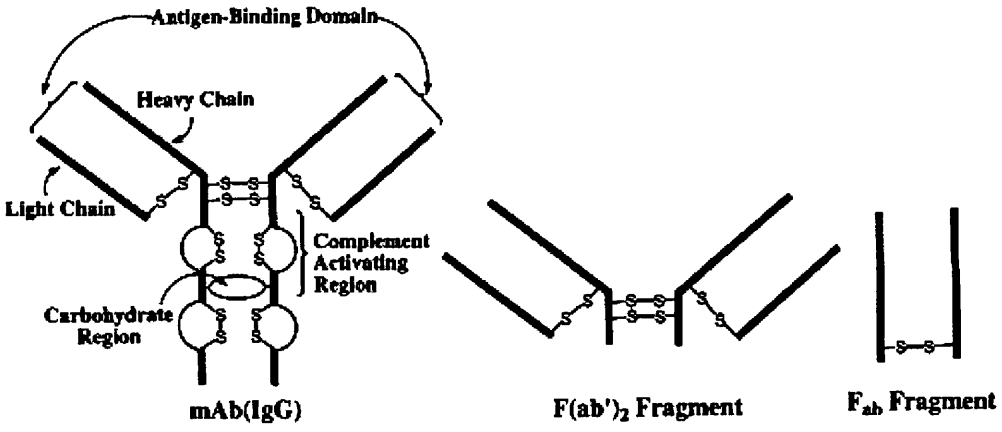

Figure 17: Schematic representations of the structures of mAbs and smaller Ab-binding fragments derived from selective proteolytic cleavage [26]

1.9.5 Immunogenicity of Antibody-Enzyme Conjugates

Early clinical studies indicated that patients treated with ADEPT therapy using a benzoic mustard prodrug CMDA, showed an immune response[64] towards the antibody-enzyme conjugate. Each patient received murine monoclonal anti-CEA antibody fragments (A5B7-F(ab')2 conjugated to the bacterial enzyme G2(CPG2), followed 36-48 hours later by a galactosylated monoclonal anti-CPG2 antibody (SB43). All patients developed human anti-mouse (HAMA) and anti-CPG2 antibodies within 10 days of receiving a single course of treatment, with one patient still testing positive 10 months after treatment. Clearly, immune responses are undesirable as they can result in an allergic reaction and also decrease the effectiveness of therapy by removing the antibody from circulation before it reaches its target. Furthermore, the immunogenicity problem means that repeat treatments are not possible.[72]

One potential way investigated to overcome the host immune response was to co-administer an immunosuppressive agent such as cyclosporin A (CyA), to allow more than one cycle of therapy. CyA was given to two patients orally. Unfortunately, this caused massive hepatomegaly and poor liver function, with both patients dying after one cycle of therapy from hepatorenal failure. As a result, CyA was given to another four patients intravenously. This successfully delayed the appearance of host antibodies to the murine antibodies-bacterial enzyme conjugate in plasma, thus allowing two patients to receive three cycles of therapy over a 21 day period. Two patients received two cycles due to treatment being halted as there was a significant

increase in nausea and vomiting. HAMA and anti-CPG2 antibodies appeared as soon as cyclosporine A treatment was stopped. [73]

Attempts have also been made to overcome the immunogenicity of ADEPT by using human enzymes such as β-glucuronidase or mutant carboxypeptidase A1. However, these enzymes were not sufficiently active *in vivo* because the activity of human β-glucuronidase is low at physiological pH, and carboxypeptidase A1 is not sufficiently stable [74].

Heinis *et al.* (2004) elected to use human prolyl endopeptidase (PEP; EC 3.4.21.26) as a candidate enzyme for ADEPT. Cytosolic serine endopeptidase was highly active and cleaved peptide bonds on the carboxyl side of proline in peptides. The enzyme had a low activity in blood, which should have prevented non-specific activation of the prodrug. Furthermore, the human origin of the peptidase should lower the risk of immunogenic reactions in humans and allow administration of multiple doses of antibody-enzyme conjugate. However, their results showed that PEP was thermally inactive in human serum at 37°C. They overcame this problem by producing a PEP mutant with a single amino acid change that had a 4-fold longer half-life in human serum at 37°C. Two prodrugs containing a proline-containing dipeptide linked to the primary amides of the chemotherapeutic drugs doxorubicin and melphalan were synthesised and investigated. However, only the melphalan prodrug was efficiently hydrolyzed by PEP in conjuction with their own human antibody L19. This retention of both antigen binding and enzyme activity of SIP(L19)-PEP was encouraging in terms of the possible use of this immunoconjugate in ADEPT.

1.10 ADEPT Enzymes

A range of non-human enzymes have been investigated in ADEPT for the activation of produgs. For example, alkaline phosphatase, carboxypeptidase (G2, A and A1), cytosine deaminase, β-glucoronidase, β-lactamase, nitroreductase, penicillin-V amidase and penicillin-G amidase have all been studied. [74] The utility of some of the enzymes cited above was limited by inhibition due to endogenous inhibitors and in some cases inefficient conversion of prodrug to drug. Ideally, the following

requirements need to be fulfilled by candidate enzymes: first, the ability to convert inactive prodrug to active drug efficiently, with the enzyme's optimum pK similar to the pH of the extracellular fluid at the tumour site. Second, in order to minimise the amount of enzyme required, the enzyme-substrate interaction should have a high k_{Cat} but low K_m.[64]

1.10.1 Alkaline Phosphatase

Alkaline phosphatase (AP) is a mammalian enzyme which catalyses the cleavage of phosphate groups from phosphorylated prodrugs. The prodrug is usually more soluble than the parent due to the presence of the phosphate group(s), but less active than the parent compound partially due to decreased cellular uptake[26]. Senter *et al.*[45] used a mammalian AP (a dimeric protein isolated from calf intestine), conjugated to two IgG2a monoclonal antibodies, L6 (anti-lung adenocarcinoma) and IF5 (anti-β lymphoma), which were CD30 antigen specific.[75] The prodrug etoposide phosphate was found to be 100-fold less active than its parent *in vitro*, in the human colon carcinoma cell line (H3347) in the absence of enzyme. However, a potential disadvantage of the use of this enzyme is the possibility of non-specific conversion of the prodrugs due to endogenous alkaline phosphatases found in normal tissue throughout the body.[76]

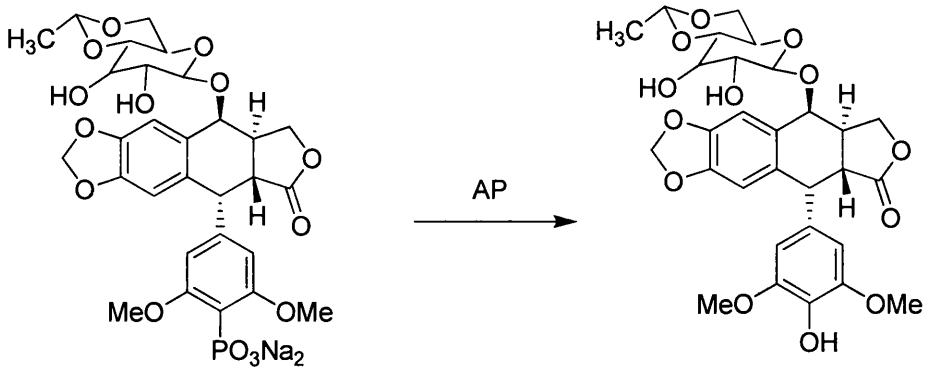

31 Etoposide phosphate prodrug

32 Etoposide

Scheme 5: Generation of etoposide (32) from etoposide phosphate (31) by alkaline phosphatise.

1.10.2 Glycosidase

Roffler *et al.* [77] used a β-glucuronidase isolated from *Escherichia coli* to remove glucuronide from a hydroxyaniline mustard. The prodrug **33** was found to be significantly less cytotoxic than the parent mustard (**34**) when tested in a range of human cancer cell lines but in the presence of enzyme it was as cytotoxic as the parent drug. The hydroxyaniline mustard was activated in certain animal tumours by elevated levels of endogenous β-glucuronidase to give site-specific cytotoxicity, but this was not found to occur in humans.

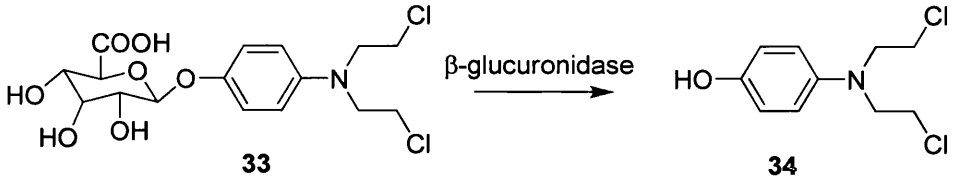

33 **34**

Scheme 6: Hydroxyaniline glucuronide mustard prodrugs (33) and its parent, hydroxyaniline mustard (34).

1.10.3 β-Lactamase

The β-lactamases are widely distributed in gram negative bacteria and are classified by their ability to hydrolyse various β-lactam rings. Alexander *et al.* and Svensson *et al.* (**Figure 18**) synthesised cephalosporin-based prodrugs for use in an ADEPT system (**Scheme 7**)[78]. The prodrugs were good substrates for β-lactamase and rapidly released the parent active drug, the phenylenediamine mustard. Prodrugs based on doxorubicin were evaluated by Vrudhula *et al.*[79] using a F(ab')-β-lactamase conjugate to activate a cephalosporin derivative of the vinca alkaloid, 4-desacetylvinblastine-3-carboxhydrazide (DAVLBHYD). Xenograft studies with the human H2981 lung adenocarcinoma showed pronounced growth delays with a single injection of conjugate (1 mg per kilogram), followed 96 hours later by three separate injections of 63 mg/kg prodrug at four hour intervals.[76]

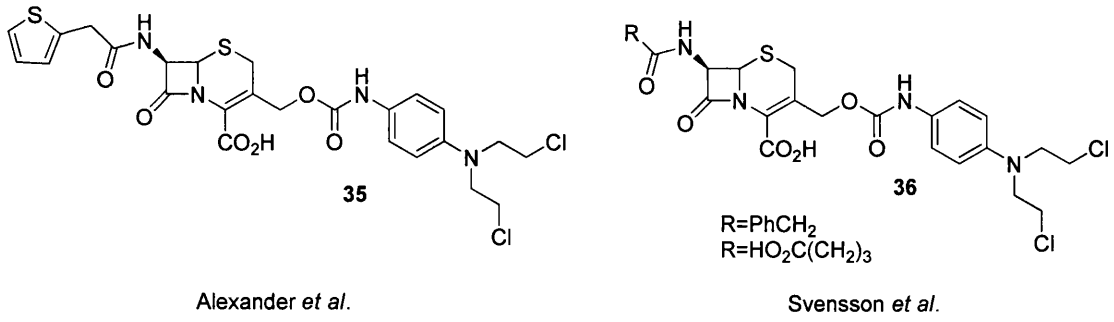

Figure 18: Cephalosporin-based mustard prodrugs

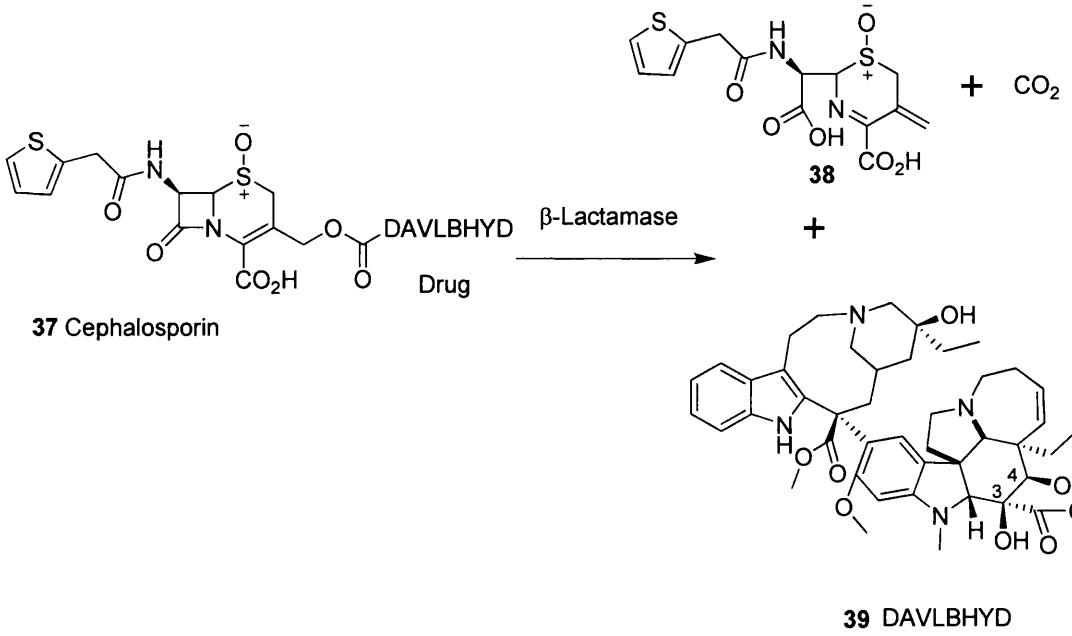

Scheme 7: The activation of 4-desacetylvinblastine-3-carboxhydrazide (DAVLBHYD) by β-lactamases.

1.10.4 Penicillin V/G Amidase

Kerr *et al.* investigated doxorubicin phenoxyacetamide and melphalan phenoxyacetamide as potential prodrugs **(Scheme 8)**. The phenoxyacetamides were substrates for penicillin-V amidase isolated from *Fusarium oxysporum*. The doxorubicin phenoxyacetamide prodrug was evaluated in a range of cell lines to providing differential cytotoxicity values of 20-80 fold on conversion to the parent doxorubicin. However, in the presence of antibody-enzyme conjugate, the differential for activation of the doxorubicin phenoxyacetamide prodrug was only 7.5-12.5 fold, indicating that the penicillin amidase enzymes were too slow to generate the active

doxorubicin efficiently. The melphalan phenoxyacetamide prodrug exhibited a greater differential of 100-1000 fold, however unfortunately this differential was not maintained when cells were treated with prodrug in the presence of antibody enzyme conjugate.

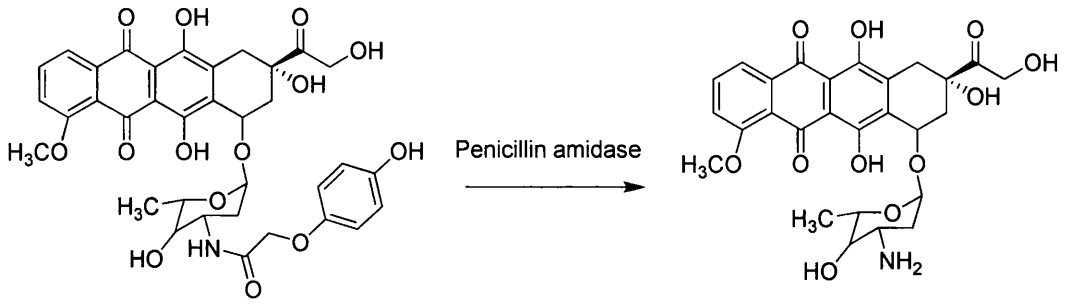

40 Doxorubicin phenoxyacetamide

41 Doxorubicin

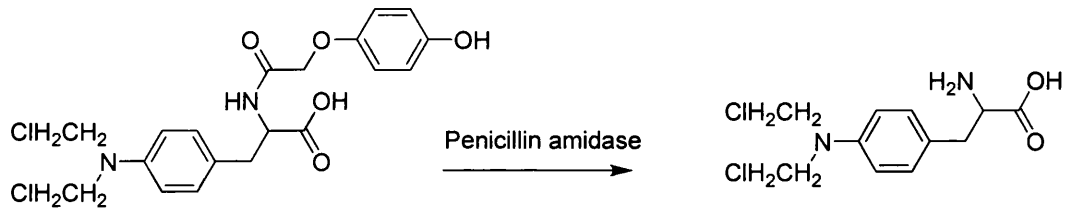

42 Melphalan phenoxyacetamide

43 Melphalan

Scheme 8: Phenoxyacetamide-modified prodrugs that are substrates for penicillin amidases

1.10.5 Cytosine Deaminase

Cytosine deaminase is found in many fungi and bacteria but not in mammalian cells. It catalyzes the conversion of cytosine into uracil. Cytosine deaminase converts the antifungal agent 5-fluorocytosine (5-FC) into the known anticancer drug 5-fluorouracil (5-FU). It has been extensively studied for GDEPT (see GDEPT section) but has also been evaluated in ADEPT. Senter *et al.* have chemically conjugated cytosine deaminase to an antibody. *In vivo* studies measured the amount of 5-FU was formed in the tumour demonstrating a 17-fold differential compared to conventional administration of 5-FU.

1.10.6 Carboxpeptidase

The first ADEPT system was proposed by Bagshawe in 1987[43] based on carboxypeptidase G2, a bacterial enzyme isolated from *pseudomonas* species.[63, 80] This system stood out from the others, by demonstrating good results in animal

models. CPG2 has no mammalian counterpart and catalyses the conversion of reduced and non-reduced folates into pteroates and L-glutamic acid. The enzyme belongs to the group of bacterial calcium-binding zinc-endopeptidases which contain thermolysin and other neutral peptidases from *Bacillus subtilis* and *Aeromonas proteolytica.*[81]

A number of aromatic nitrogen mustard prodrugs were shown to be activated by CPG2 into their corresponding active parent drugs as shown in **Scheme 9 and Figure 19.**[82]

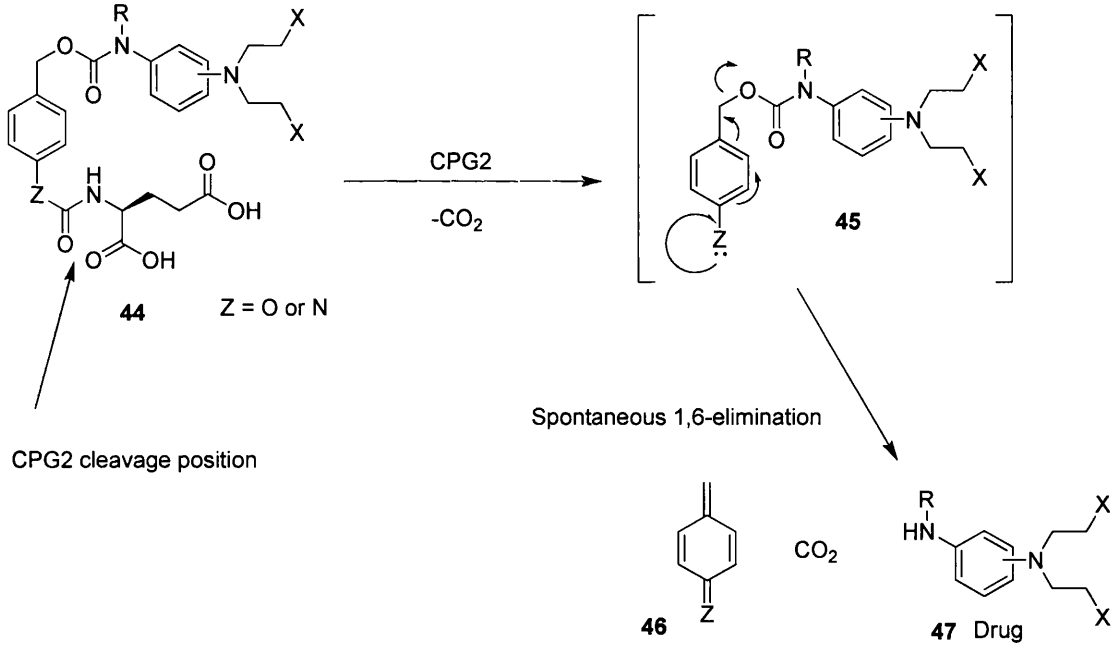

Scheme 9: Mechanism of drug release for self-immolative mustard prodrugs

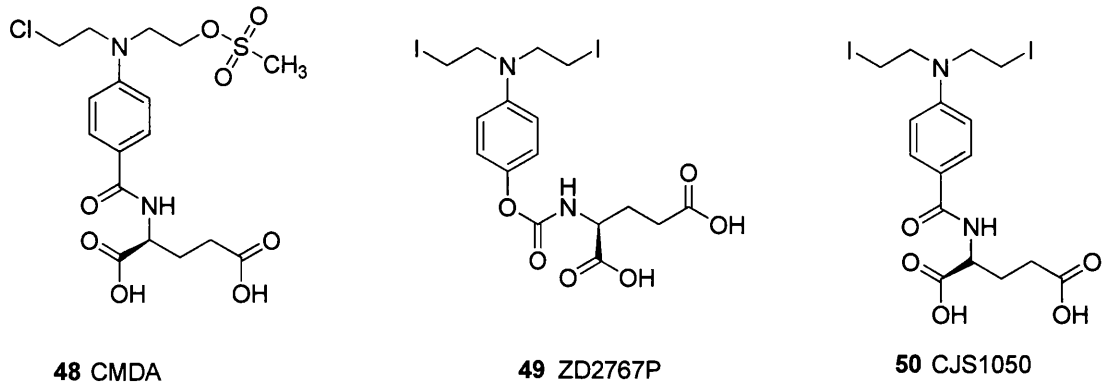

Figure 19: Examples of mustard prodrugs for use in ADEPT therapy.[83]

In 2005 Sharma and co-workes carried out an ADEPT study in human colorectal cancer xenografts using a multifunctional mannosylated fusion protein. This pivotal study led to a phase 1 clinical trial in 2006 by Mayer and *et al.* using a *bis*-iodo phenol glutamate mustard ZD2767P (**Figure 19)** with the MFECP1 antibody-enzyme fusion protein. [69, 84, 85] MFECP1 was the first mannosylated fusion protein to be used in ADEPT. [86] It is a recombinant fusion protein of carboxypeptidase G2 (CPG2), an enzyme derived from *Pseudomonas aeruginosa.* The carboxypeptidase was directly linked to the NH_2 terminus of the anti-CEA single-chain Fv antibody, MFE-23. Results indicated that MFECP1 was safe and well tolerated, and was rapidly eliminated from plasma and other normal tissues via the liver but selectively retained within tumours. It was also less immunogenic than previously used antibody-enzyme conjugates. Previous studies had shown that the development of an immune response to anti-CEA antibody fragments (A5B7-F(ab')2 conjugated to bacterial enzyme G2(CPG2) had produced human anti-mouse antibodies HAMA and HACA, which prevented repeat treatments. Without immunosuppressant treatment, 100% of patients who received chemical conjugate A5CP developed HAMAs. Similarly, 97% of patients who received A5B7 mAb developed HACAs. In the Mayer study, using the same assay, none of the patients treated with MFECP1 developed HAMAs, and only 36% of patients developed HACAs on treatment with MFECP1.

Four patients received ^{123}I-labelled MFECP1 (**Figure 20**), It was found to be rapidly cleared through the liver with prominent hepatic tracer activity seen at 1 hour and with no uptake of tracer in unexpected areas.[69]

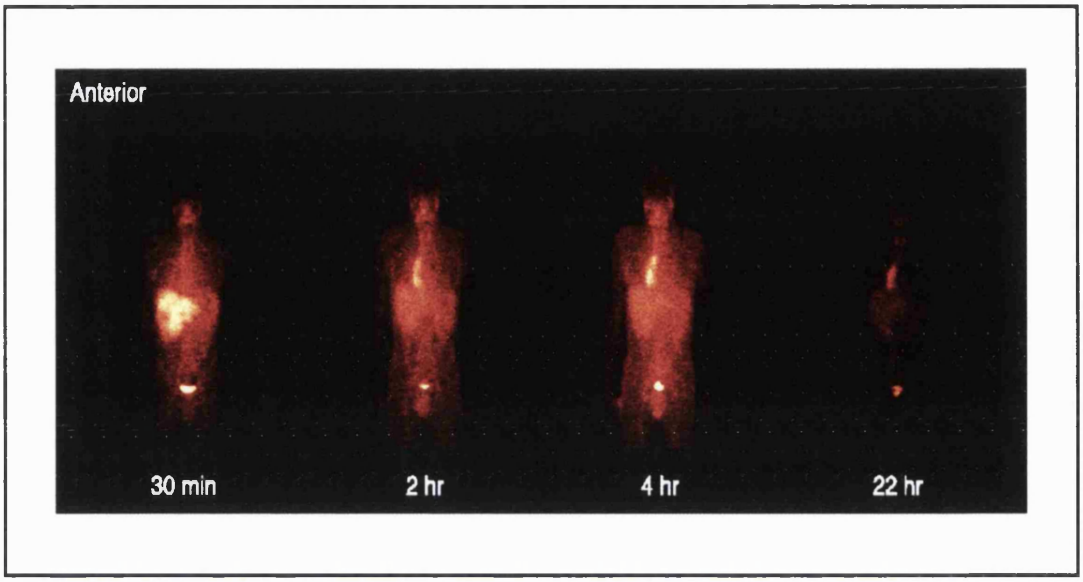

Figure 20: The liver is the main organ for elimination of MFECP1. Radiolabeled MFECP1 is taken up by the liver 30 minutes after administration followed by rapid elimination. The uptake in the thorax of this patient is due to the gastric "pull-up" following partial esophagectomy. (From Mayer, A. *et al.*)[69]

Of the thirty-one patients in the ADEPT trial with the antibody-enzyme fusion protein MFECP1[86] and a bis-iodophenol mustard prodrug, 28 patients tolerated treatment for 8 weeks. The best observed response was a 10% reduction in tumour diameter in one patient. Eleven patients had stable disease after 8 weeks and 17 had progressive disease. From these results it was concluded that although MFECP1 was a good enzyme conjugate for use in ADEPT there was a requirement for development of a more potent prodrug system. Examples of current prodrugs for use with ADEPT are not effective enough to kill tumours due to the lesions formed being readily repaired by cancer cells. The development of novel cytotoxic agents that form lesions which are more repair-resistant is discussed in the next chapter.

1.10.7 Nitroreductase

A phenol mustard and some phenylenediamine mustard prodrugs were designed to be activated by nitroreductase. This exploited the enzymic reduction of the 4-nitrobenzyloxycarbonyl derivative of the phenol mustard to generate the parent agent through self-immolation. Unfortunately, cytotoxicity studies in Chinese Hamster V79 cells revealed that the prodrug **51** was more cytotoxic than the parent compound. However, the phenylenediamine mustard prodrug **52** (**Figure 21**) was 5-10 fold less

toxic than the parent mustard.[78] Studies with CB 1954 [5-(aziridin-1-yl)-2,4-dinitrobenzamide] stimulated further interest in the use of nitroreductase enzymes in prodrug therapy, and this is discussed in more detail in the GDEPT section below.

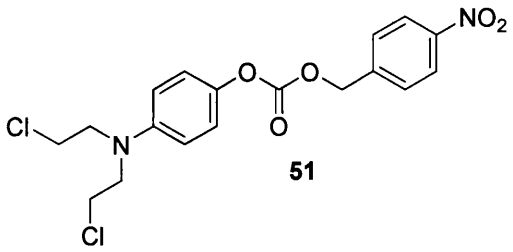

51

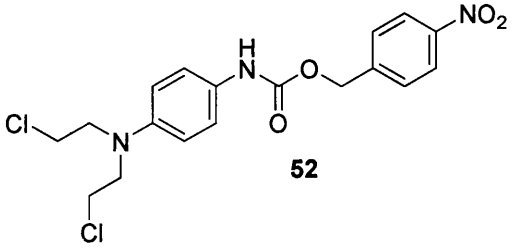

52

Figure 21: A phenol mustard prodrug and phenylenediamine mustard prodrug

1.11 GDEPT (Gene-Directed Enzyme Prodrug Therapy)

1.11.1 Introduction

Gene directed enzyme prodrug therapy (GDEPT), also known as "suicide gene therapy", [28] [87] is an approach related to ADEPT but relying on the selective delivery of a gene coding for the enzyme to the tumour cells rather than the protein itself. GDEPT systems that use viral vectors are sometimes referred to as VDEPT (virus directed enzyme prodrug therapy).[47] GDEPT is made up of three components, the prodrug to be activated, the activating enzyme and the delivery system for the corresponding gene. The first step involves delivery of a gene encoding a foreign enzyme for selective expression in the tumour cells and capable of catalysing the activation of the prodrug to its cytotoxic form. The enzyme itself is non-toxic, and cytotoxcity results only after administration of the prodrug, in the second step.[88] Schepelmann *et al.* demonstrated that it was possible to achieve very high enzyme concentrations in the tumour, exceeding the levels obtained in ADEPT.

One limitation of gene therapy is that the delivery vector usually cannot target all malignant cells within a tumour mass. However, the bystander effect plays a role whereby the active drug, once produced, can migrate into non-transduced cells (i.e killing of non-expressing, neighbouring cells), mitigating this limitation. Another potential advantage of GDEPT is that expression of foreign enzymes in the tumour and the resultant death of tumour cells can induce an immune response that can enhance the overall therapeutic effect.[89]

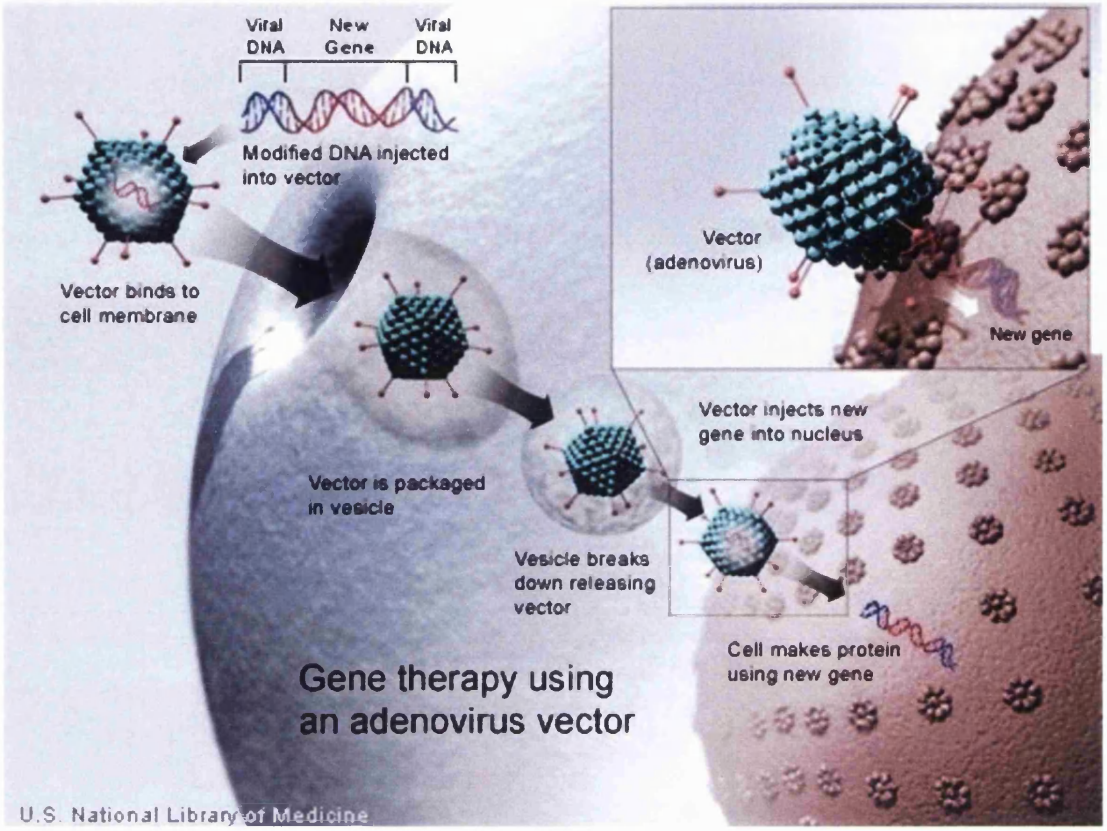

Figure 22: Gene therapy using an Adenovirus vector [[PD-USGov-HHS-NIH]][90]

1.11.2 Retroviral and adenoviral vectors

A number of viral and non-viral gene delivery systems have been developed for GDEPT. The non-viral GDEPT vectors include naked DNA, liposomes, peptides and polymers. These are advantageous due to their safety record following administration in humans. However, viruses are more effective at delivering genes into human cells. Hence, the majority of current gene therapy programs in clinical trials today exploit viral gene therapy vectors.[89]

Retroviral-based vectors can only infect replicating target cells, but robust integration occurs leading to stable expression of the transduced gene so that enzyme synthesis can be sustained. Adenoviral vectors that can infect both dividing and non-dividing cells are more efficient at transduction but usually do not integrate into the host DNA thus minimising the risk of insertional mutagenesis. However, adenovirus-mediated gene expression is relatively short term lasting up to several weeks, and it can be difficult to regulate gene expression (**Figure 22**).

1.11.3 Enzymes for GDEPT and VDEPT

Many of the enzyme/prodrug systems used in GDEPT act intracellularly by converting prodrugs into active drugs within cells. **Tables 4** and **5** show a range of systems used in GDEPT/VDEPT[40]. Strategies using nitroreductase enzyme are of special interest.

Viral vectors	Enzymes delivered	Prodrugs	Model systems
Adenovirus	Herpes simplex virus thymidine kinase	GCV	Mouse prostate cancer cell line
	Human carboxylesterase	Irinotecan	Human lung adenocarcinoma cell lines and nude mice tumor model
	E. coli nitroreductase	CB 1954	Ovarian tumor cells and animal model of disseminated intraperitoneal carcinoma
Retrovirus	*E. coli* nitroreductase	CB 1954	Colorectal, pancreatic, ovarian cancer cells and xenografts of human ovarian & pancreatic cancer
	Yeast cytosine deaminase	5-FC	SCC VII murine squamous carcinoma cells and YCD-expressing tumors
	Human CYP and p450 reductase	Cyclophosph mide and IFA	Gliosarcoma cells and in vivo tumor model
EBV	Nitroreductase	CB 1954	EBV-positive B-cell lines

Table 4: Examples of VDEPT Systems.[40]

Enzymes	Prodrug	Model systems
Human β-glucuronidase	HMR 1826	Tumor cells and xenograft model in nude mice
Bacterial nitroreductase	CB 1954	Chinese hamster and 3T3 cells
Carboxypeptidase	MTX-α-peptide	Cos-1 cells
CYP2B1 and p450 reductase	Cyclophosphamide	Rat 9L gliosarcoma cells
Rabbit CYP4B1	2-AA or 4-IM[a]	Human, rat glioma cells and in nude mice tumor model
Thymidine phosphorylase	5-FU or 5'-DFUR[a]	LS 174T human colon carcinoma cells
Rabbit and human carboxylesterase	Irinotecan	Glioblastoma and rhabdomyosarcoma cells and preclinical mouse xenograft model
***E. coli* β-galactosidase**	Anthracycline	Human melanoma cells
Cytosine deaminase	5-FC	Murine fibroblast cells
Thymidine kinase	GCV	Cisplatin-resistant human ovarian carcinoma cells

Table 5: Examples of GDEPT [a] 2-AA, aminoanthracene; 4-IM, 4-ipomennol; D'FUR, 5'-deoxy-5-fluorouridine[40].

1.11.4 Thymidine Kinase

Herpes simplex virus thymidine kinase (HSV-Tk) is a non-mammalian enzyme that phosphorylates known antiviral agents such as acyclovir and ganciclovir (GCV) (**Scheme 10**). Endogenous cellular kinases then convert GCV monophosphate (**53**) into the triphosphate (**54**), with competes with normal nucleotides in the DNA replication process in mammalian cells leading to inhibition of cell growth and eventually cell death.

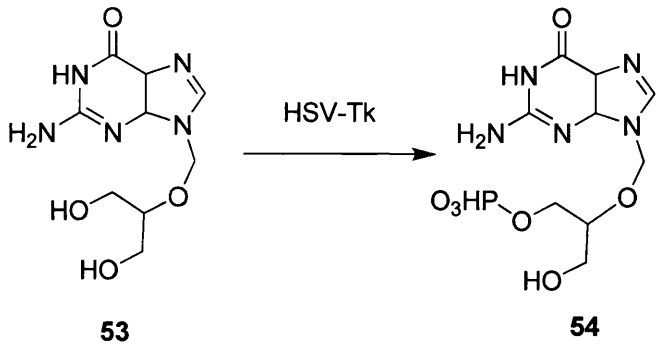

Scheme 10: Activation of ganciclovir (GCV) by HSV-Tk

1.11.5 Cytosine deaminase

As discussed previously in the ADEPT section, cytosine deaminase is found in many fungi and bacteria, but not in mammalian cells. It catalyzes the conversion of cytosine into uracil, and also converts the antifungal agent 5-fluorocytosine (5-FC) into the known anticancer drug 5-fluorouracil (5-FU). 5-FC is further metabolised into 5-fluorouridine 5'-triphosphate, 5-fluoro-2'-deoxyuridine 5'-triphosphate and 5-fluoro-2'-deoxyuridine 5'-monophosphate. The first two compounds inhibit RNA and DNA synthesis, respectively and the last inhibits thymidylate synthase, an important enzyme involved in DNA biosynthesis[28]. *In vitro*, murine sarcoma and colon adenocarconoma tumour cell lines transduced with the cytosine deaminase gene exhibit sensitivity to 5-FC, completely suppressing the growth of cytosine deaminase expressing tumour cell lines[26].

1.11.6 Cytochrome P450

Cyclophosphamide (**55**) is a clinically useful anticancer prodrug activated in the liver by microsomal cytochrome P450 mixed function oxidases to form a nitrogen mustard via a 4-hydroxy intermediate (**Scheme 11**). The poor penetration of the active drug through the blood brain barrier and the lack of cytochrome P450 activity in the brain have prevented successful application to brain tumours. However, strategies using transfected rat C6 glioma cells with a PA317 packing cell line and an adenoviral vector Ad.CMVp450 have demonstrated sensitivity to cyclophosphamide. Studies in human breast cancer cells (MCF7) with p450-encoding plasmids and adenoviral vector, Ad.CMV-2B1, have also provided encouraging results.[26]

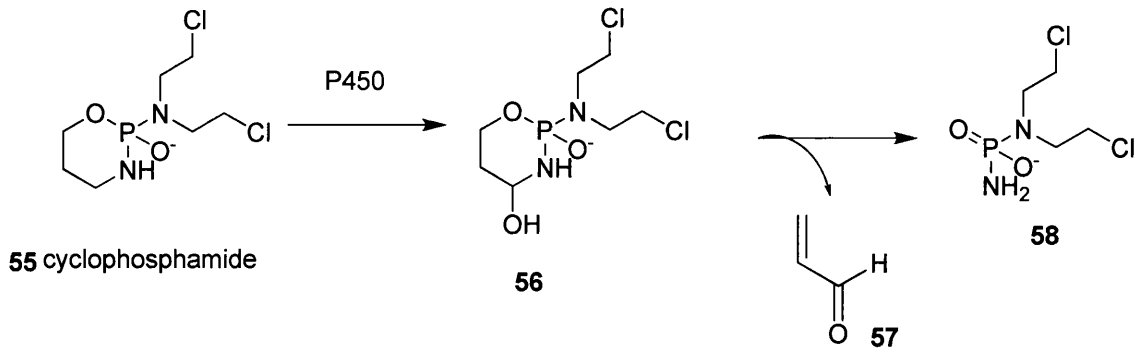

Scheme 11: Cytochrome P450 metabolism of cyclophosphamide to an active mustard moiety.

1.11.7 Carboxypeptidase

Carboxypeptidase has been extensively studies in ADEPT, as discussed previously. Schepelmann *el al.* first demonstrated the GDEPT strategy using the enzyme carboxypeptidase G2 (CPG2) which converts mustard prodrugs such as ZD2767P (**Figure 19**) into potent alkylating cytotoxic agents. An oncolytic adenovirus was used to deliver the prodrug-activating enzyme carboxypeptidase G2 (CPG2) to tumours in a single systemic administration. The adenovirus replicated and produced high levels of CPG2 in two different hepatocellular carcinoma xenografts (Hep3B and HepG2). Growth was inhibited and prolonged the survival of the animals.[82, 91]

1.11.8 Nitroreductase Enzyme

Nitroreductase is an enzyme used in both ADEPT and GDEPT that requires either NADH or NADPH to reduce aromatic nitro groups to hydroxylamines. Enzymes which metabolize aromatic nitro groups to amines can be used to trigger self immolation and can be exploited in both ADEPT and GDEPT systems. Nearly all GDEPT studies with nitroreductases have been performed with the *nfs* gene product of *E. Coli*, an oxygen-insensitive flavin mononucleotide (FMN) containing nitroreductase (NTR). The crystal structure of NTR has revealed it to be a homodimer with one FMN per monomer and two channels leading to the active site.[92] Nitroreductase can efficiently reduce aromatic nitro groups to hydroxylamines by two steps. Nitroreductase studies have been carried out on classes of prodrugs, including the dinitrobenzamide mustards, the 4-nitrobenzylcarbamates, the dinitroaziridinyl benzamide CB 1954, and the mustard-based DNA minor-groove alkylating agent tallimustine (**60**) (**Scheme 12**).[93] For example, the latter exhibited differential cytotoxicity towards cell lines in culture when co-treated with NRT plus cofactor NADH, but studies have not been reported with NTR-transfected cell lines.

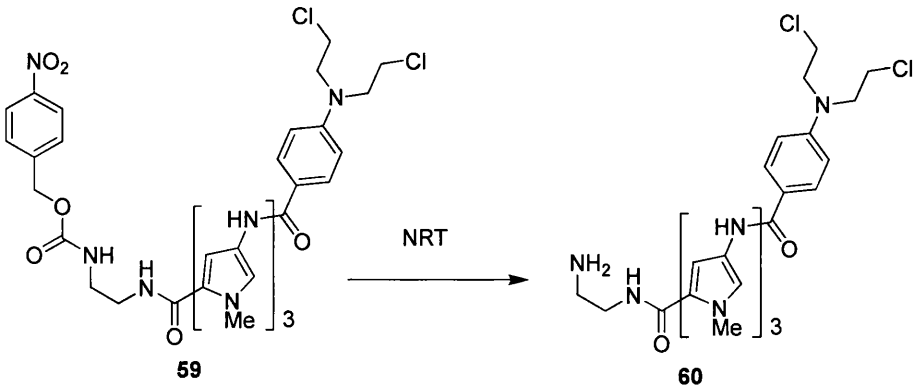

Scheme 12: The tallimustine mustard prodrug and its conversion to the active agent.

The enediynes are very potent cytotoxic agents with IC_{50} values in the low pM region. The nitrobenzylcarbamate moiety is able to stabilise the enediyne by engaging the lone pair of electrons on the phenanthridine nitrogen (**Scheme 13**). After reduction there is liberation of the corresponding parent amine **(62),** which is able to promote opening of the epoxide ring. Ring opening leads to a change in conformation of the macrocyclic ring allowing Bergman cyclisation to occur. The resulting diradical can cause DNA damage via radical reactions and leads to the formation of double strand breaks. The enediyne prodrug **61** showed a moderate 135-fold selectivity in the NRT-transfected WiDr human colon carcinoma cell line. Similarly, addition of extracellular NRT enzyme and NADH to UV4 cells led to a 90-fold differential. However, the activation of enediyne prodrugs against hypoxic cells may be limited due to their requirement for oxygen. [94]

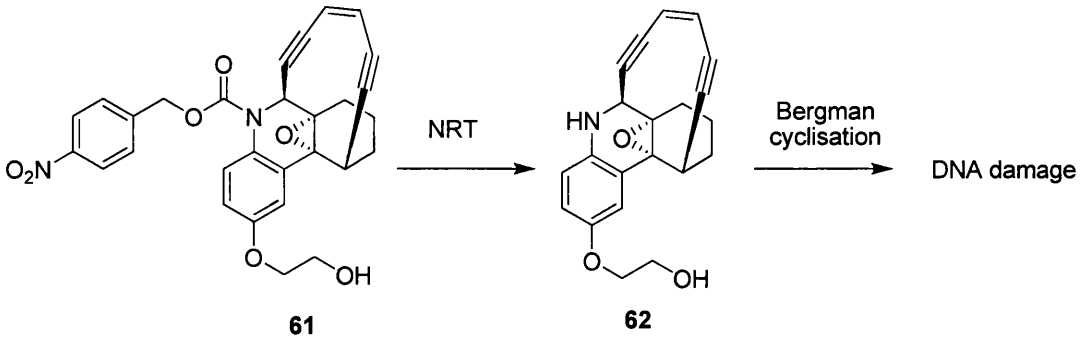

Scheme: 13 Activation of an enediyne prodrug.

CC 1065 is a potent naturally-occurring DNA minor-groove binding antibiotic whose structure has also been used as a basis for ADEPT prodrugs.[95] For example, the nitropyrrole carbamate **63** was found to be 20-fold more cytotoxic towards SKOV-3 cells transfected with NRT than wild cell types. Reduction of the pyrrole nitro group

triggers self-immolation of the carbamate leading to formation of free amine (**64**), which in turn promotes cyclisation to afford the DNA-reactive cyclopropyl species **65**.

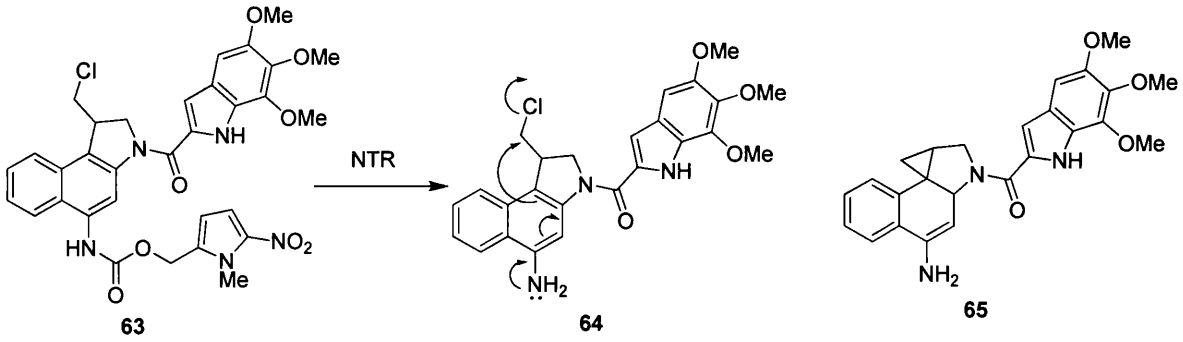

Scheme 14: 2-Nitroimidiazole carbamate prodrug 63 and the released active agent 65.

1.11.8.1 CB 1954

CB 1954 [5-(aziridin-1-yl)-2,4-dinitrobenzamide] (**Scheme 15**), was first synthesized in the 1960s, and exhibited highly selective activity towards the rat Walker 256 tumour, leading to complete cures.[96] Unfortunately, CB 1954 (**66**) appeared to be only effective against rat tumours and had little activity against a range of murine and human tumours *in vivo*. Even when administered at the maximum tolerated dose, it failed to exhibit anti-tumour activity in a range of xenografts.[97, 98]

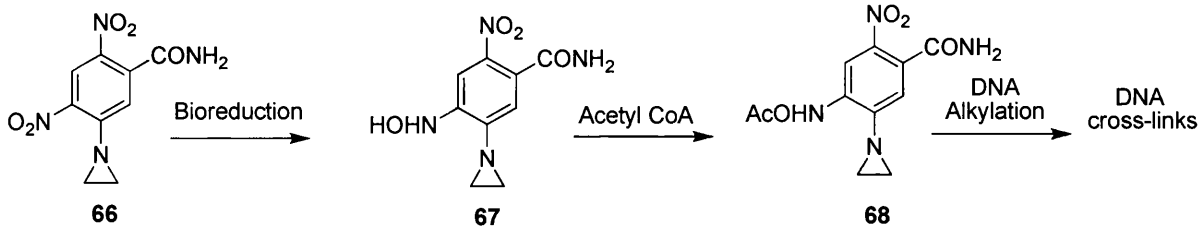

Scheme 15: The prdrug CB 1954 (66) and its bioreductive conversion into the DNA-reactive agent 71.

CB 1954 is a relatively lipophilic (log P = +1.54) prodrug, with a low molecular weight, it can be enzymatically activated (i.e., reduced by nitroreductase) to generate a difunctional agent, which forms DNA-DNA interstrand crosslinks. The high frequency of DNA lesions (up to 70% of total DNA interactions)[99] is significant especially when compared to the level of interstrand crosslinks observed with Cisplatin or Carboplatin (i.e., less than 2% of the total DNA reactions)[100]. Also the cross-links are poorly repaired which may cause them to be even more intrinsically cytotoxic. After bioactivation of CB 1954 in rat Walker 256 tumour cells, there is a

10-fold increase in the amount of DNA-bound drug, as compared to cells which cannot bioreduce it.[99] The active agent, **68** was modified with various substituents, and it was found that slight alterations in the structure often led to complete loss of activity. In particular, it was established that the 4-nitro group of CB 1954 was essential for activity. Interestingly, CB 1954 was also found to be cytotoxic in hypoxic mammalian cells. Under hypoxic conditions, CB 1954 appears to act on these normally resistant cells in a similar manner to Walker cells under normal conditions.

Although CB 1954 had excellent activity in Rat carcinomas, unfortunately this was not reproduced in non-hypoxic human tumours due to the intrinsic inability of human NQO1 (a gene commonly found in human tumour cells) to efficiently reduce CB 9154. However, CB 1954 is a good substrate for *E. Coli* nitroreductase suggesting its potential use in GDEPT and VDEPT strategies. In addition, CB 1954 can also be reduced by NQO2, another endogenous human enzyme expressed in tumours. This reduction can be enhanced by the co-administration of EP-0152R (1-carbamoylmethyl-3-carbamoyl-1,4-dihydropyridine).[101]

In another approach, Keith *et al.*[102] have investigated the use of adenovirus vectors harbouring the bacterial NTR gene the under control of hTR or hTERT promoters to sensitise cancer cells to CB 1954.[103] The aim was to exploit the prevalence of telomerase expression in human cancers. Telomerase is a ribonucleoprotein reverse transcriptase that extends human telomeres by a terminal transferase activity. Human telomerase activity is present during embryonic development but is repressed in most adult somatic tissue. This concept was based on the original demonstration by Bilsland *et al.*[104] of NTR expression in both normal and cancer cells infected with adenoviral vectors expressing telomerase. Using seven different cancer cell lines they achieved up to an 18-fold sensitisation to the prodrug CB 1954. No sensitisation was observed with either promoter in any of the four normal cell strains.

1.12 PBD Prodrugs for ADEPT and GDEPT

Sagnou and *et al.* [105] first demonstrated that nitroreductase-sensitive pyrrolobenzodiazepine (PBD) prodrugs have no DNA-binding activity or cytotoxicity until the N10-protecting group (which blocks DNA interaction) is removed (**Scheme**

16). The aromatic nitro group of the N10-(*p*-nitrobenzyl carbamate) protecting group can be reduced by the nitroreductase enzyme to a hydroxylamine which induces self-immolation leading to formation of the parent drug DNA-interaction.

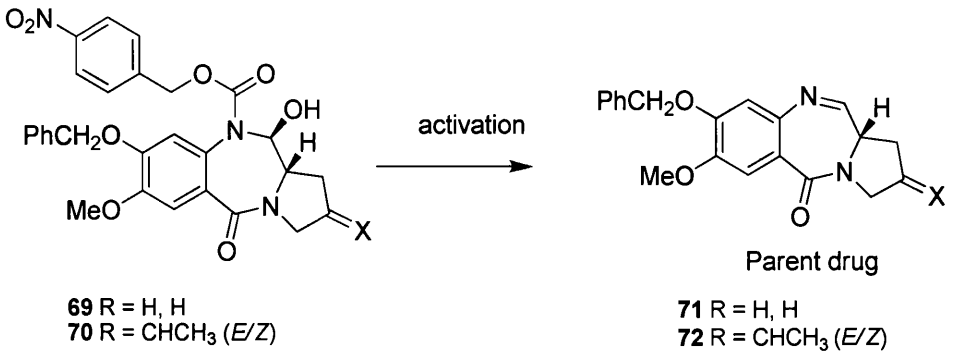

69 R = H, H
70 R = $CHCH_3$ (*E/Z*)

71 R = H, H
72 R = $CHCH_3$ (*E/Z*)

Scheme 16: Pyrrolobenzodiazepine (PBD) prodrug (69 and 70) and their conversion to the active DNA binding agents (71 and 72).

Sagnou *et al.* found prodrug **69** to be essentially non-cytotoxic in a human adenocarcinoma cell-line LS174T (IC50 = >500 μM) (**Table 6**). However, in the presence of the nitroreductase enzyme and NADPH the IC_{50} was ~5 μM. These results suggested a ~100-fold differential in activity between prodrug and parent. This is a significant differential, but the IC_{50} value of its parent **71** was 0.008 μM in the same cell line. Suggesting that incomplete release of the progroup had occurred. Similarly, a 13.5-fold differential was observed for the benzyl tomaymycin prodrug *E/Z* mixture **70** (IC_{50} value 86.2 μM alone, 6.4 μM with enzyme) in LS174T cells, which also suggesting incomplete activation given that the parent drug **72** had an IC_{50} value between 0.001-0.01 μM.

Prodrug Structure	IC_{50} (μM) of prodrug in LS174T cells	IC_{50} (μM) in presence of enzyme and NADH	Released (Parent) drug structure	IC_{50} (μM) of parent PBD	Activation factor
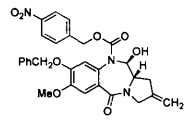 **69**	>500	5.0-6.0	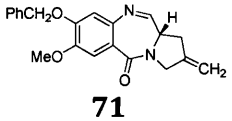 **71**	0.008	100 (or >)
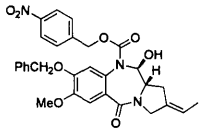 **70**	86.2	6.4	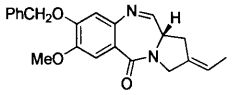 **72**	0.001-0.01	13.5
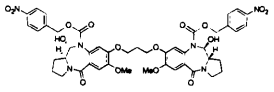 **73**	215.3	13.7	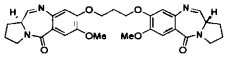 **74**	0.0005	15.7

Table 6: Cytotoxcity of PBD prodrugs before and after activation with nirtoreductase/NADH in the LS174T cell line: 72 is a mixture of *E/Z* isomers.

A similar result was observed for the PBD dimer prodrug **73** which was relatively non-toxic towards LS174T cell lines with an IC_{50} value of 215.3 μM decreasing to 13.7 μM after addition of enzyme, (i.e., activation differential of 15.7-fold). The corresponding parent PBD dimer **74** had an IC_{50} value of 0.0005 μM (**Scheme 17**), again suggesting that activation was even less efficient than for the monomeric PBD prodrugs.

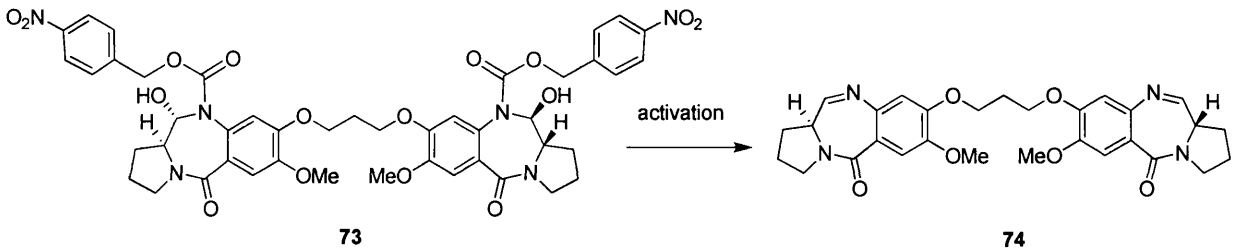

73 **74**

Scheme 17: Ppyrrolobenzodiazepine prodrug dimer

Taken together, these results provided good evidence that N10-protected analogues of PBD monomers and dimers have potential as prodrugs for use in ADEPT and GDEPT-type therapies, although further optimisation of prodrug conversion was clearly required.

Chapter 2

Pyrrolo[2,1-*c*][1,4]benzodiazepines

2. Pyrrolo[2,1-c][1,4]benzodiazepines

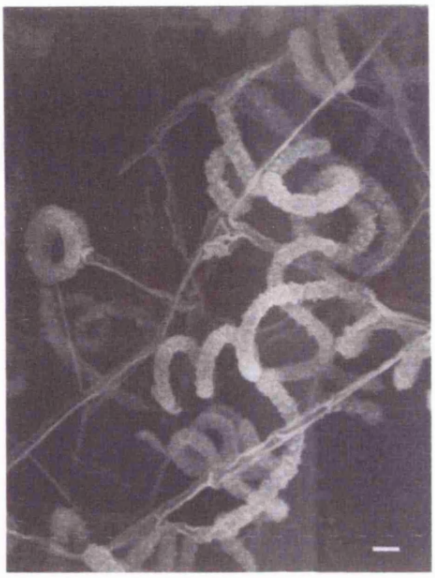

Streptomyces species strain An-2604 (Omura 1986)

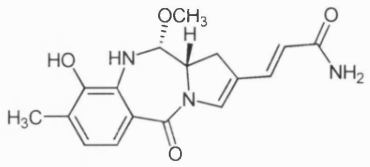

75 Anthramycin

Figure 23: Streptomyces species strain An-2604 and structure of anthramycin

2.1 Background to PBDs

The *Streptomycetes* are bacteria which physically resemble fungi due to their branching filamentous structure. They are found in soil and play an important role in soil ecology. Over 50 different antibiotics have been isolated from *Streptomycetes* species.[106] The most widely accepted theory to explain antibiotic production is that antibiotics help the organism compete with other organisms in the relatively nutrient-depleted environment of the soil by reducing competition

Tendler and Korman were amongst the first scientists to observe the antibiotic and anti-tumour properties of the fermentation broth produced by the *Streptomycetes refuines* variant. [107] Leimgruber isolated the antibiotic, determined its structure analytically, gave it the name anthramycin and then confirmed its structure by total synthesis [108-110]. Later, further anti-tumour antibiotics made by related *streptomycetes* species, were isolated, these members were linked by a common pyrrolobenzodiazepine core structure. More than 12 naturally occurring PBDs have been discovered and many synthetic routes to these molecules have been reported.

Family members include abbeymycin, anthramycin, chicamycin, DC-81, mazethramycin, neothramycins A and neothramycin, prothracarcin, sibanomycin (DC-102), sibiromycin and tomaymycin (**Figure 24**) [111].

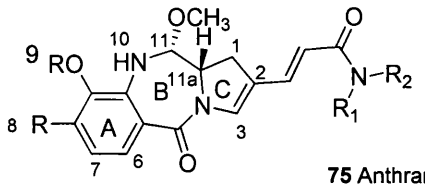

75 Anthramycin: $R_8 = CH_3$; R_9, R_1, R_2 = H
76 Mazethramycin: R_8, $R_1 = CH_3$; R_9, R_2 = H
77 Porothramycin B: R_8 = H; R_9, R_1, $R_2 = CH_3$

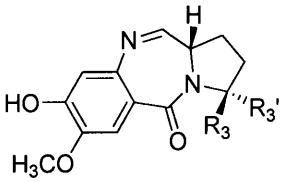

78 Neothramycin A: R_3 = H; $R_{3'}$ = OH
79 Neothramycin B: R_3 = OH; $R_{3'}$ = H
80 DC-81: R_3, $R_{3'}$ = H

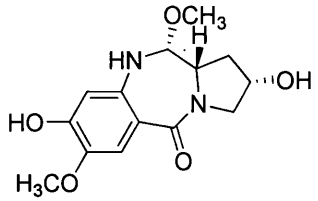

81 Chicamycin A

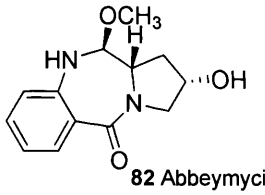

82 Abbeymycin

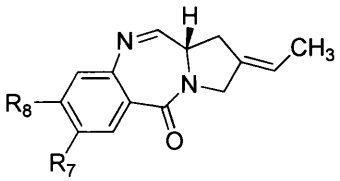

83 Tomaymycin: $R_7 = CH_3O$; R_8 = OH
84 Prothracarcin: R_7, R_8 = H

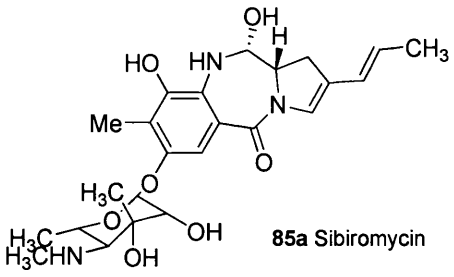

85a Sibiromycin

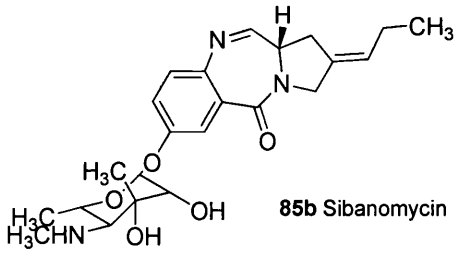

85b Sibanomycin

Figure 24: Structures of known members of the pyrrolo[2,1-*c*][1,4] benzodiazepine family of antitumour antibiotics.

2.2 Structure of PBDs

PBD's are made up of 3 rings, a benzene A ring, diazepine B ring and pyrrolo C ring and they all share (*S*)-stereochemistry at the chiral C11a position. (**Figure 25**)

The structures of the individual PBDs differ in the location and type of substituents around the basic pharmacophore, degree of saturation of the C-ring and the presence of an imine carbinolamine or carbinolamine methyl ether at the N10-C11 position. [112]

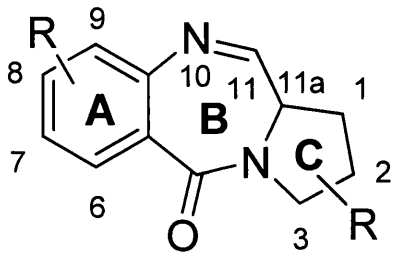

Figure 25: PBD core structure

During the isolation of anthramycin, Leimgruber found that different solvents could readily convert anthramycin to the anthramycin methyl ether and to anhydroanthramycin (imine form), the interconvertable species are generally know as the carbinolamine, carbinolamine methyl ether and imine forms **Figure 26.**[110]

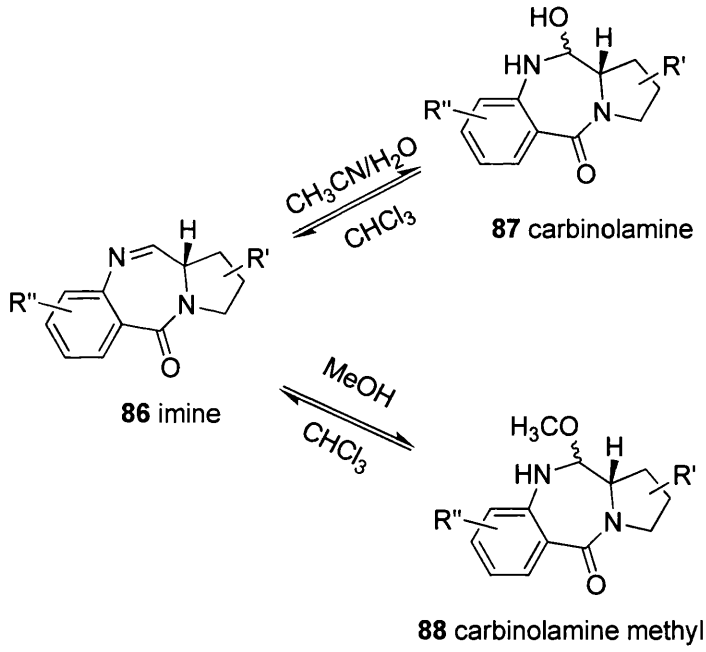

Figure 26: Carbinolamine, carbinolamine methyl ether and imine PBD forms

In 1986 Hertzberg *et al.* demonstrated through DNA footprinting studies that PBDs bind to DNA in a sequence selective manner with preference for PuGPu base sequences. In 1988 Hurley *et al.* reported an exonuclease III stop assay, which

supported the earlier SAR predictions showing a correlation between DNA-binding affinity and biological potency [111].

A number of studies with anthramycin revealed evidence of the formation of adducts with DNA. Later NMR studies and molecular modelling established the orientation of the molecules in the minor grove of DNA. These studies confirmed the (*S*) stereochemistry at the C11 position and adducts of anthramycin are formed exclusively at C11(*S*) with various fragments of DNA. The aromatic A-ring points in the direction of the 3' end of the strand to which the drug is bonded, with (*S*)-stereochemistry at C11. Orientation towards the 5' end of the bonded strand is energetically unfavourable compared with the 3' orientation. The (*R*)-configuration is least favoured [113].

2.3 Biological activity of PBDs

PBD's bind covalently in the minor grove of DNA (**Figure 27**) to the exocyclic N2 of a guanine base through their N10-C11 imine functionality resulting in a number of biological effects, such as inhibition of transcription and binding of nuclear proteins and enzymes. (*S*)-stereochemistry at the chiral C11a position imparts a right handed twist and allows them to follow the curvature of the minor groove of B-form double-stranded DNA spanning three base pairs. Footprinting studies demonstrated that the preferred order of sequence was 5`-Pu-**G**-Pu > 5`-Pu-**G**-Py or 5`-Py-**G**-Pu > 5`-Py-**G**-Py. [114]

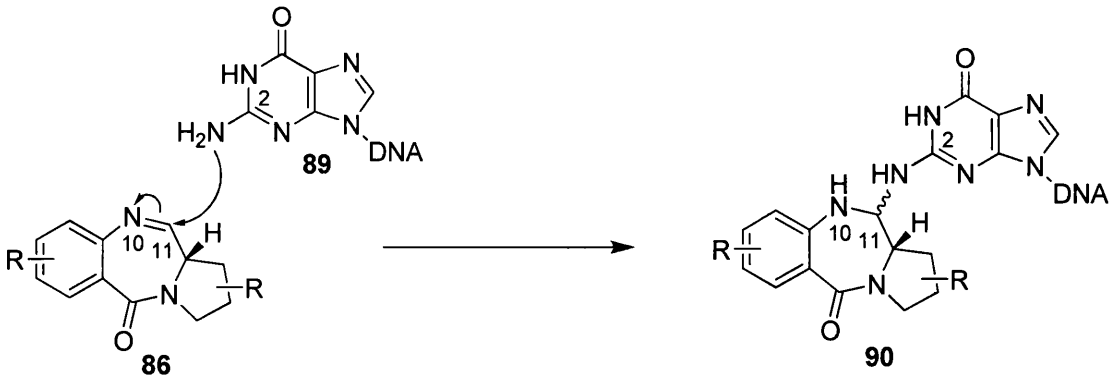

Figure 27: Proposed mechanism of action of PBD's. The formation of an aminal bond between the C11 position of the PBD and of a guanine base.

2.4 Synthesis of PBDs

Since the first total synthesis of anthramycin a number of alternative synthetic routes to naturally occurring PBDs and novel PBD analogues, have been published. Some of the more influential strategies are reviewed below.

2.5 Leimgruber

Leimgruber's synthesis of pyrrolobenzodiazepines was based on his realisation that the PBD carbinolamine could be obtained by the reduction of suitably protected PBD dilactams.

2.5.1 The First Synthesis of Anthramycin

Leimgruber began his synthesis with the acylation of the commercially available amino acid derivative (**Scheme 18**); L-hydroxyproline methyl ester **92**, which was coupled to 3-benzyloxy-4-methyl-2-nitrobenzoyl chloride **91** in the presence of TEA to give the A and C-ring amide **93**. Reduction of the amide with sodium dithionite in THF/H_2O afforded the amine **94**, which was treated with aqueous HCl and cyclised to form the dilactam **95**. Oxidation of the C2 secondary alcohol with Jones' reagent gave the ketone **96**. The ketone was converted to the β,γ-unsaturated ester **97** through a Horner-Wadsworth-Emmons olefination reaction with triethyl phosphonoacetate in THF at 0°C. Treatment with diisobutylaluminum hydride in toluene at -60°C, provided the conjugated aldehyde **98**. The aldehyde was converted to the epimeric cyanohydrins **99** with potassium cyanide and sodium bisulphite. Subsequent treatment with methanesulphonyl chloride in pyridine at 0°C yielded the corresponding epimeric mesylates **100**. The mesylates were eliminated with triethylamine to afford a separable mixture of *cis-trans* conjugated nitriles **101**, in a 1:4 ratio. The benzyl group was then removed with trifluoroacetic acid and boron trifluoride etherate at room temperature to give a mixture of phenolic *trans*- and *cis*-nitriles. The mixture could be separated or heated at reflux in aqueous TFA to afford the major *trans*-amide product **102**. Condensation of **102** with benzaldehyde dimethyl acetal at 200°C provided the benzal derivative **103**, which was converted to the amide **104** with polyphosphoric acid at 95°C. Amide **104** was reduced to the protected carbinolamine **105** with

lithium aluminium hydride in THF at -60°C. Hydrolysis of the carbinolamine with aq HCl in MeOH afforded anthramycin **75**.

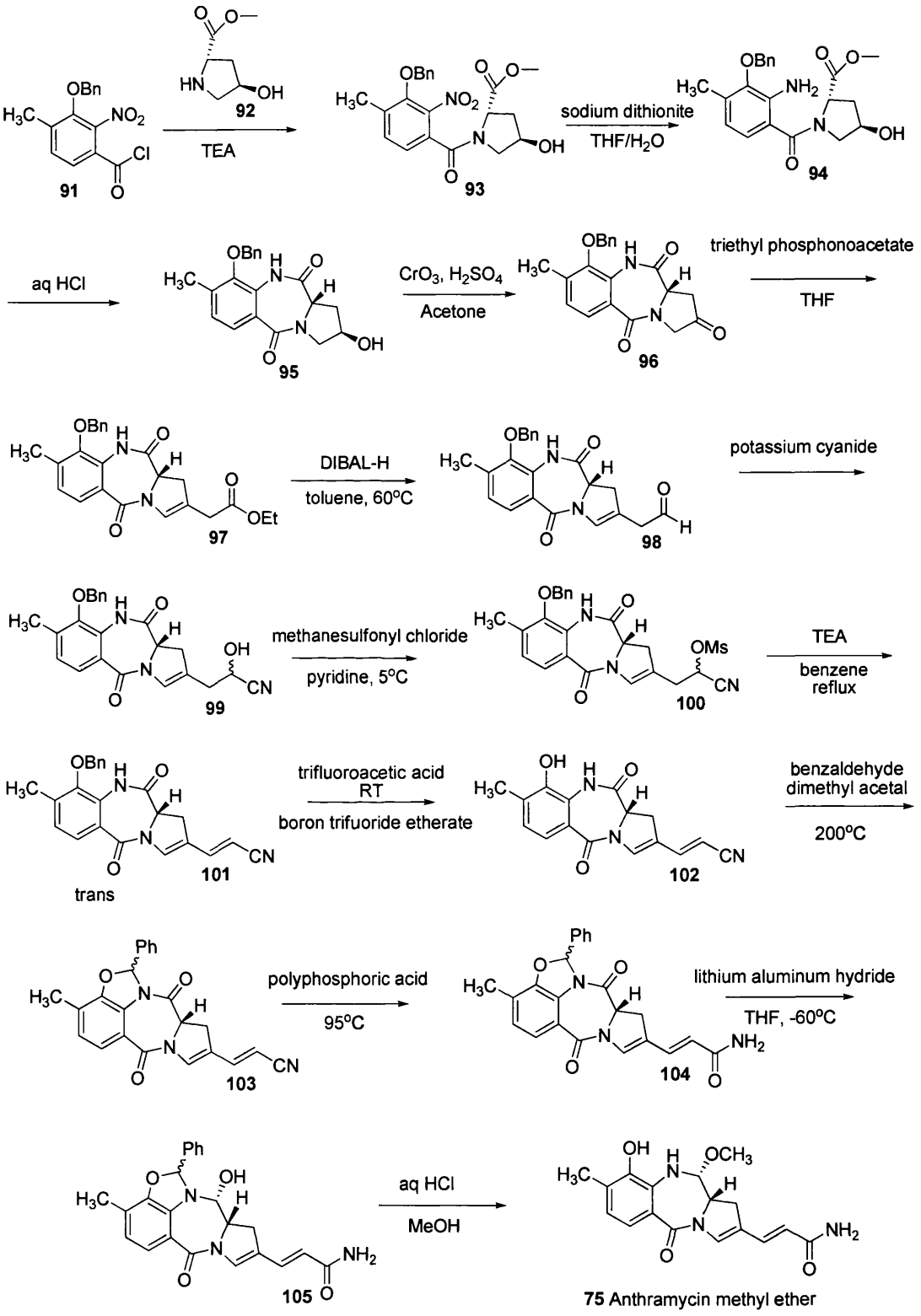

Scheme 18: Leimgruber Synthesis of Anthramycin

2.6 Mori

Mori *et al.* reported the total synthesis of prothracarcin, pretomaymycin and *E*/*Z* tomaymycin in 1986 [115]. The synthesis of tomaymycin and prothracarcin were almost identical, but varied in the need to incorporate different A-ring substituents. Mori's original contribution to PBD synthesis lies in the closure of the B-ring by palladium catalysed carbonylation and the application of the more versatile MOM protecting group. This allowed the dilactam reduction strategy to be applied to PBDs lacking the 9-hydroxy group.

2.6.1 Mori Synthesis of Tomaymycin via Palladium Catalysed Carbonylation

The acid chloride **108** was coupled with *o*-bromoaniline to give the A and C-ring coupled amide **109** (**Scheme 19**) the amide and hydroxyl group were protected as the MOM hemiaminal and acetal respectively, the latter with MOMCl, diisopropylethylamide, and the former with MOMCl and sodium hydride to give **111**. Treatment with NH_3-MeOH cleaved the *N*-trifluoroacetyl group giving to give the free amine **112**. The PBD B-ring was formed by a carbon monoxide insertion in the presence of $Pd(PPh_3)_4$ catalyst, a small amount of quinoxaline side product **114** was also obtained. The *O*-methoxymethyl group of dilactam **113** was cleaved with HCl-MeOH to give the free alcohol **115** in 65% yield, some loss of the N10 MOM group was also observed (30%), but this could be replaced by treatment with MOMCl and sodium hydride. Alcohol **115** was oxidised with PCC to the ketone **117**, which underwent a Wittig reaction at 0°C to give the *Z*-ethylidene **118**, as the major product, in 93% yield. The tosyl group was removed with aqueous KOH to give phenol **119**. Finally, **119** was reduced with $LiAlH_4$ and treated with silica gel to give pretomaymycin **120**; Pretomaymycin was converted to tomaymycin on treatment with methanol, however the optical rotation did not match that of authentic material, and NMR analysis indicated that the *Z*-isomer had been formed instead.

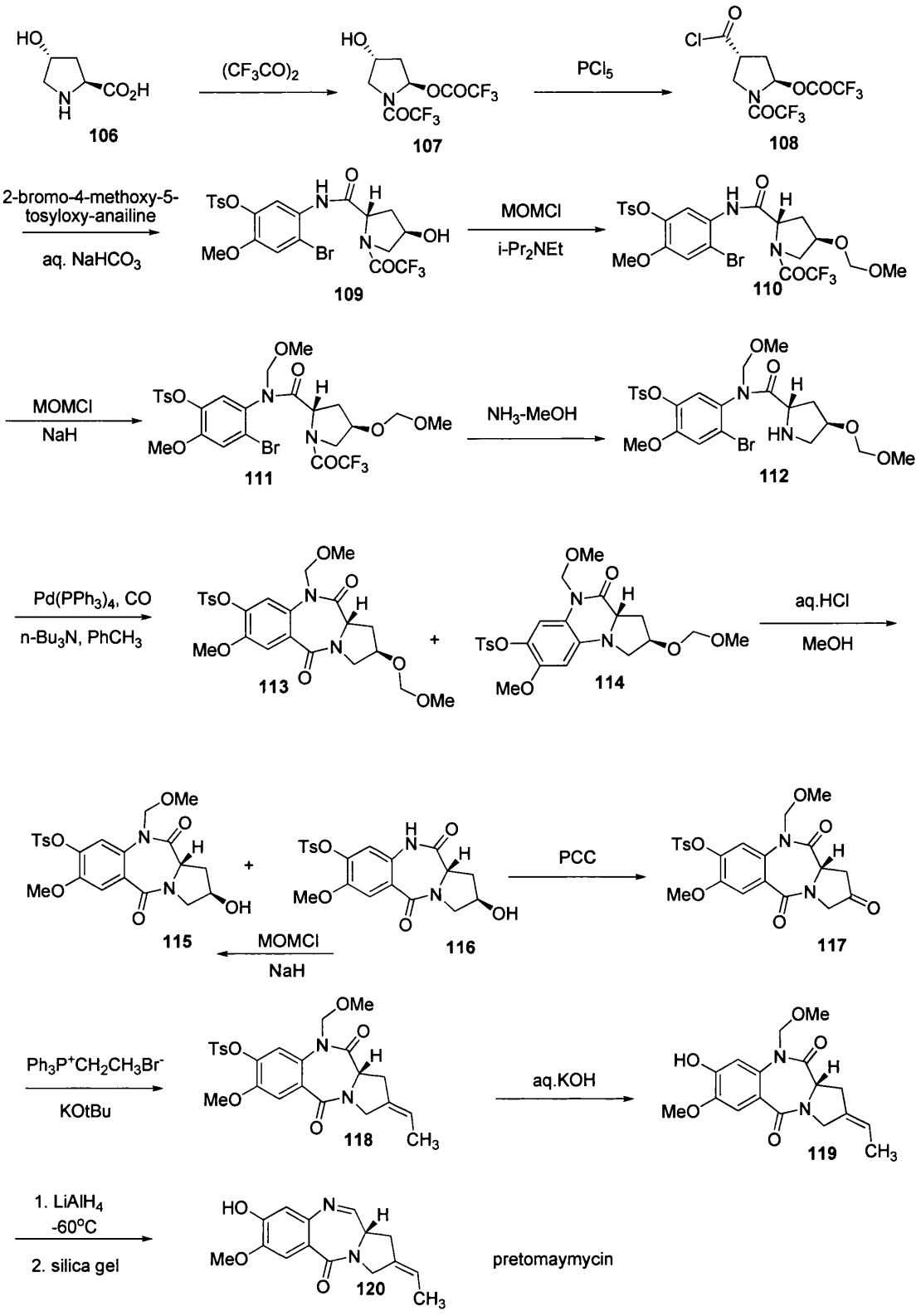

Scheme 19: Mori Synthesis of Pretomaymycin

2.6.2 Conversion of Z-tomaymycin Derivative

The *E*-tomaymycin isomer is the naturally occurring form of tomaymycin. In **Scheme 20** the N10 MOM derivative of *Z*-tomaymycin **118** formed in the Wittig reaction, was converted into *E*-tomaymycin. This was acheived by the conversion of **118** to the diols **121** and **122** with *N*-methylmorpholine *N*-oxide and OsO_4. Treatment with MsCl and NEt_3 gave **123** and **124**. The isomers were separated and treated with KOH to give the corresponding epoxides **125** and **126**. Deoxygenation of the separated epoxides with P_2I_4 and pyridine gave the desired *E*-tomaymycin derivative **127**, which was then reduced with $NaBH_4$ and treated with silica gel to give **128** *E*-pretomaymycin **128**. The imine was converted to *E*-tomaymycin on treatment with methanol on this occasion ^{1}H-NMR and IR spectra matched naturally occurring tomaymycin **83**.

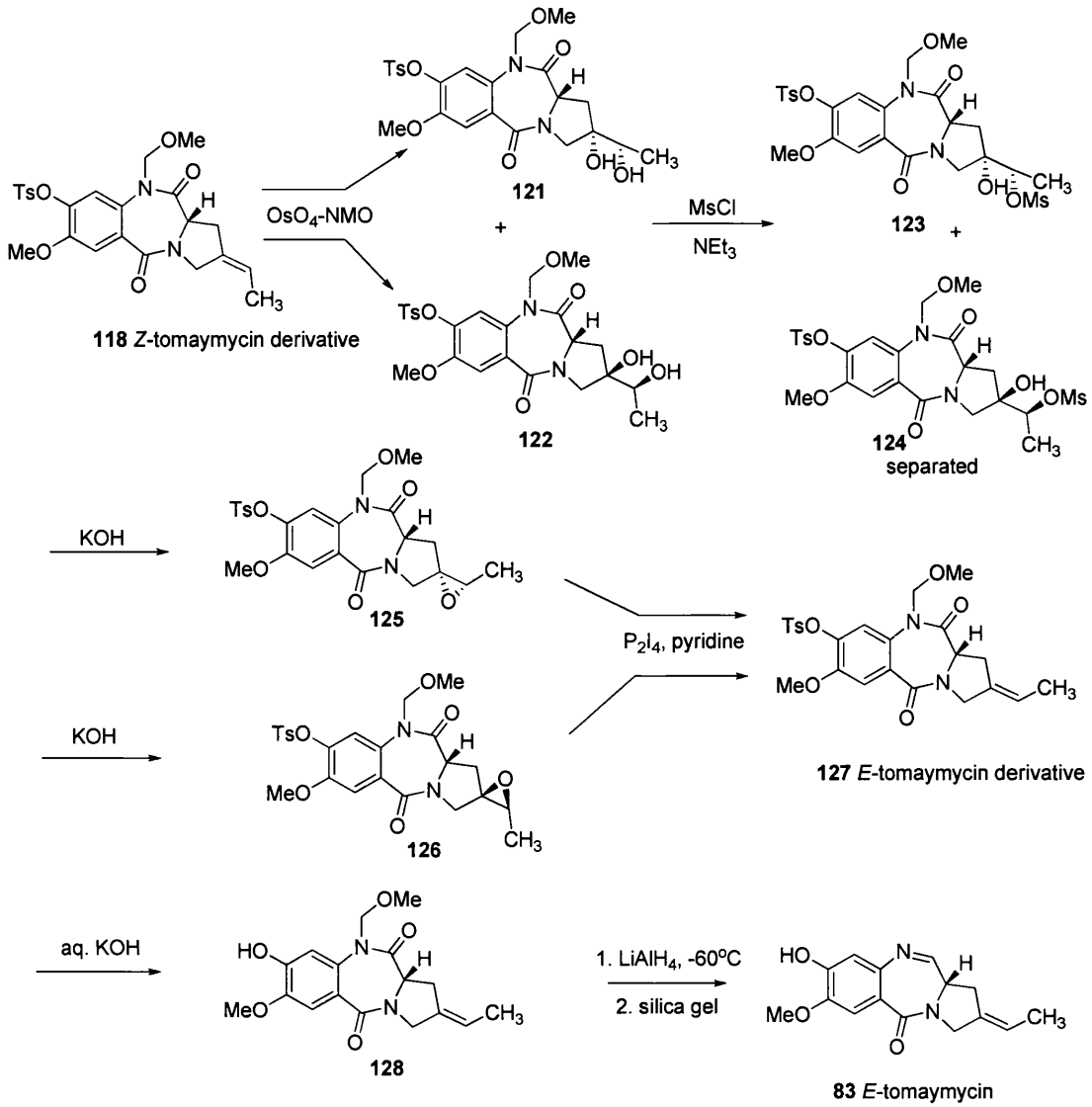

Scheme 20: Conversion of Z-tomaymycin Dervitive

2.7 Peña and Stille

Peña and Stille in 1989 published a new total synthesis of anthramycin [116]. They introduced a palladium-catalyzed coupling reaction to attach the acrylic side chain via a vinyl triflate, reducing the number of steps needed to synthesise anthramycin. The formation of the enol triflate from the ketone precursor was regiospecific and installed the double bond in the pyrrolo (C-ring) at the 2,3 position. Construction of the acrylamide side chain previously required 8 steps from the dilactam (illustrated in **Scheme 21**), whereas Peña and Stille's route (**Scheme 22**) takes two steps starting from the dilactam. Another advantage of the palladium-catalyzed coupling strategy is it can be utilized to form synthetic anthramycin analogues.

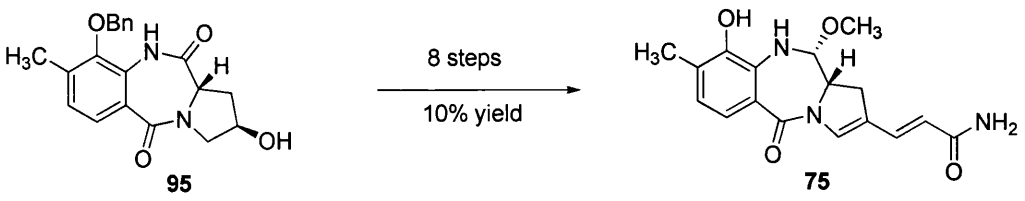

Scheme 21: From the dilactam (95), it takes 8 steps to form the acrylamide side chain.

2.7.1 Peña and Stille Synthesis of Anthramycin

The first 6 steps of the synthesis are almost identical to those employed by Leimgruber (**Scheme 22**). The route will, therefore be discussed from the benzyl intermediate **95**.

Hydrogenolysis of the benzyl group of **95** followed by reaction of the free phenol with benzaldehyde dimethyl acetal protected both the phenol and amide to give **130**. The alcohol was oxidised to form the ketone **131** by Swern oxidation. The ketone was converted to the vinyl triflate **132** with 2 eq of pyridine and 2 eq of triflic anhydride. The acrylamide side chain was attached by the Heck coupling reaction with DABCO, MeOH, and $(CH_3CN)_2PdCl_2$.

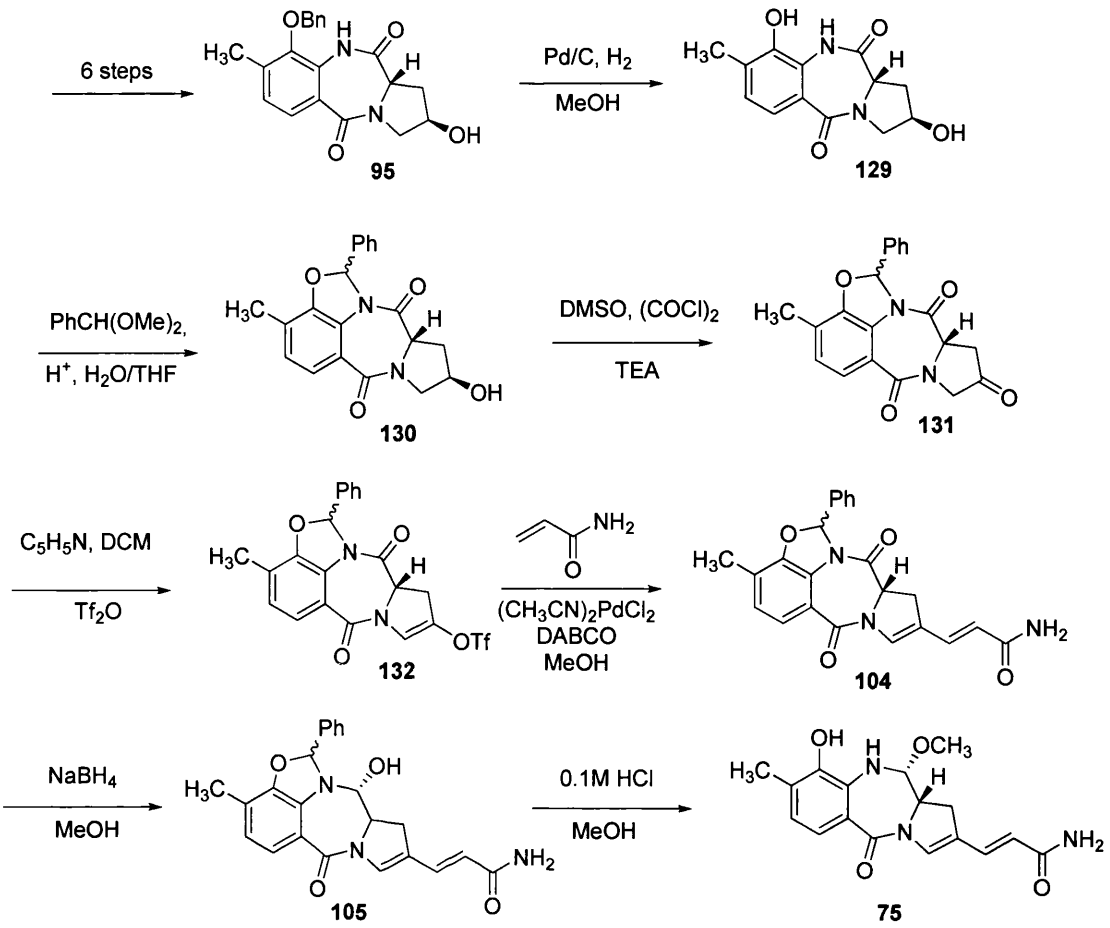

Scheme 22: Peña and Stille Total Synthesis of Anthramycin

2.8 Cooper

Howard, Cooper and Thurston combined features of pre-existing PBD strategies in order to develop a flexible route to C2-substituted PBDs [117]. Leimgruber had demonstrated that *endo-exo* unsaturated PBD dilactams could be successfully reduced in the presence of a benzal group to the PBD carbinolamine (or equivalents). Mori had shown that the benzal protecting group could be replaced with the simpler MOM-group thereby avoiding the requirement for a 9-hydroxy group. Peña and Stille were able to perform palladium coupling reactions on MOM and benzal protected PBD ketones, but interestingly failed to report the reduction of many model C2-substituted PBD dilactams.

2.8.1 The Synthesis of Novel C2-aryl Pyrrolobenzodiazepines

Commercially available 6-nitroveratric acid **133** (A-Ring) was coupled to the previously prepared tosyl salt of methyl prolinate (C-ring) **134** (**Scheme 23**) to give the A/C-ring amide **135**. Catalytic hydrogenation with 10% Pd/C in EtOH reduced the nitro group to yield the amine. Interestingly, on a greater than 1 g scale, a spontaneous cyclisation to the dilactam **136** was observed. The cyclisation did not occur when using other reduction methods. The alcohol group was protected with TBDMS-Cl and imidazole in DMF to give **137**. The dilactam **137** was then treated with SEM-Cl and NaH in DMF at 0°C to yield **138**. The C2-OTBDMS ether was selectively cleaved with TBAF at room temperature to afford the free alcohol **139**. The Swern oxidation furnished the ketone **140**, which was then converted to the C2-C3 enol triflate **141** with trifluoromethanesulfonic anhydride and pyridine. The enol triflate underwent a Suzuki coupling reaction with three different boronic acids in benzene to give three different C2-aryl derivatives **145, 146** and **147**. Reduction of the dilactams **145**, **146** and **147** was achieved with sodium borohydride in EtOH/THF and the N10-SEM protecting group was cleaved in the presence of wet silica to provide three novel C2-aryl substituted PBDs **148, 149** and **150**.

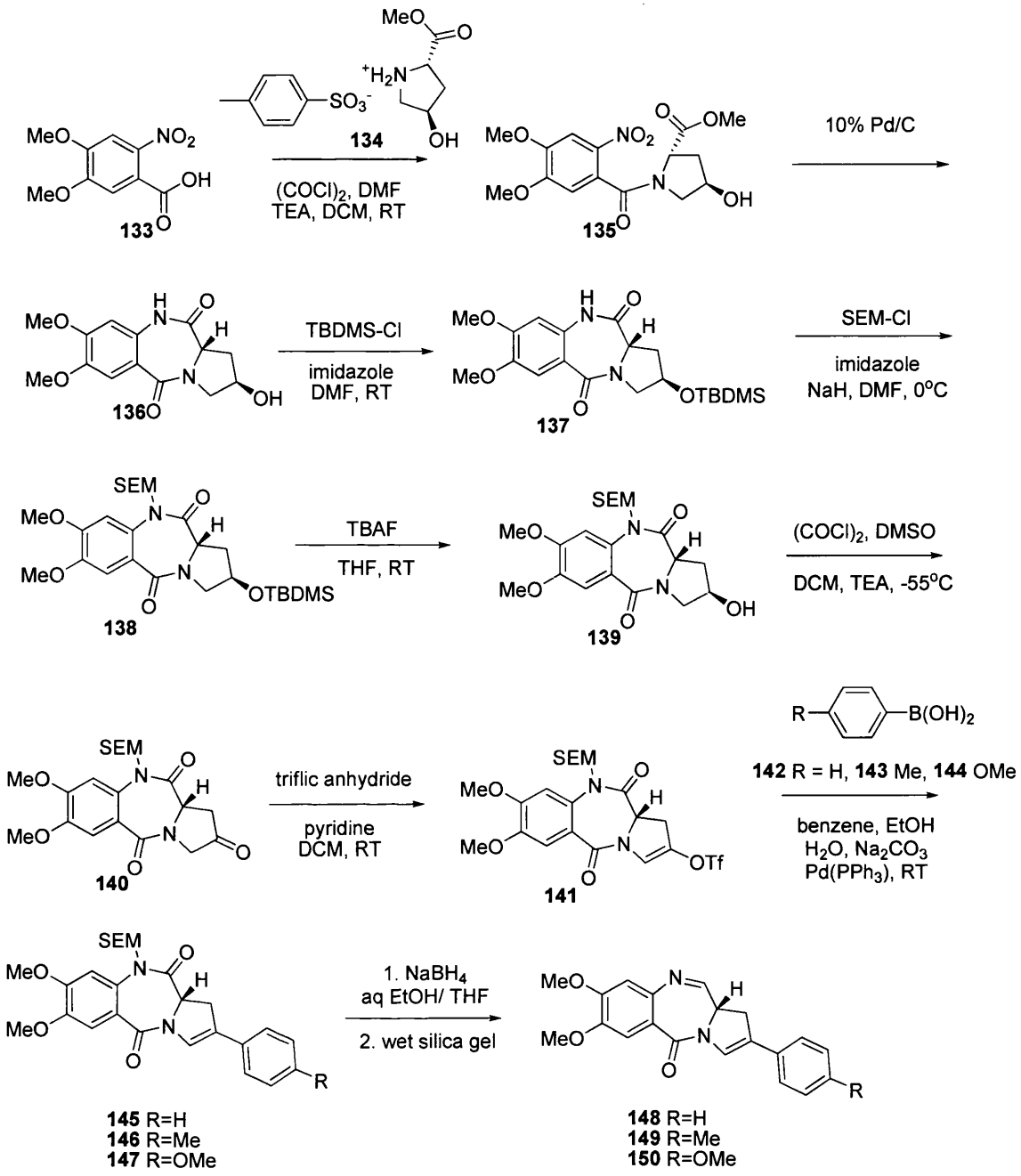

Scheme 23: The Synthesis of C2-Aryl PBDs.

2.9 Fukuyama

Tohru Fukuyama and *et al.* reported the total synthesis of neothramycin A methyl ether in 1990 [118] and the total synthesis of porothramycin B in 1993 [119].

In their synthesis of neothramycin A, Fukuyama *et al.* applied an interesting approach to PBD synthesis. The usual proline-derived C-ring building block was

replaced with a *bis* thioester derived from glutamic acid. The thioesters were ultimately reduced to aldehydes simultaneously closing both B and C rings.

In the synthesis of porothramycin, Fukuyama *et al.* cyclised the B-ring separately and then continued to elaborate the C2-substituent through a 5 step sequence. Perhaps the most influential aspect of the synthesis was the protection of the N10 position with allyl chloroformate before performing an oxidation/cyclisation reaction to close the B-ring.

2.9.1 Fukuyama Synthesis of Neothramycin A Methyl Ether

Commercially available *N*-Boc-L-glutamic dithiol ester **151** was deprotected with borontrifluoride etherate and coupled to the aryl chloride **153** to give the amide **154** (**Scheme 24**). The nitro group was reduced to the amine **155** with zinc and acetic acid in ether. The double cyclisation was preformed with 10% palladium on carbon and triethylsilane in DCM. The epimeric mixture of neothramycin C-3 alcohols **156** and **157** were converted to the more stable methyl ethers **158** and **159**. The **159** dimethylthexylsilyl ether group was deprotected with TBAF, AcOH to afford neothramycin A methyl ether **78**.

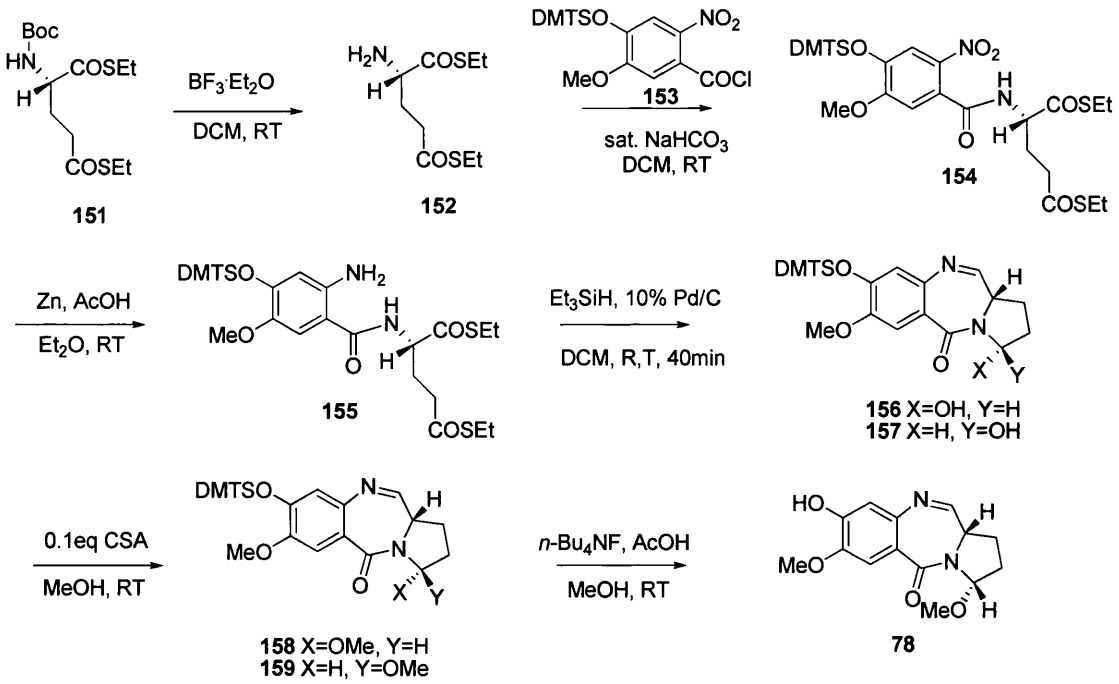

Scheme 24: Synthesis of Neothramycin A Methyl Ether

2.9.2 Synthesis of Porothramycin B

L-glutamic acid **160** was treated with benzyloxycarbonyl chloride, followed by *para*-formaldehyde in the presence of *p*-toluenesulfonic acid, in refluxing benzene to give the oxazolidinone **161** (**Scheme 25**). The carboxylic acid group was converted to the ethyl thiolester **162** with ethanethiol, dicyclohexylcarbodiimide, *N,N*-4-dimethylaminopyridine in acetonitrile. Subsequent treatment with triethylsilane and 10% palladium on carbon gave the aldehyde **163**. The aldehyde **163** was protected to afford the dimethyl acetal **164**, and the oxazolidinone opened with sodium methoxide to give benzyloxy carbonyl amino ester **165**. The benzyloxy carbonyl protecting group was removed by hydrogenolysis to afford the C-ring precursor **1** as the free amine.

Acylation of the amide **165** with 3-methoxy-2-nitrobenzoyl chloride (A-ring) yielded amide **167**. Reduction of the methyl ester **167** with lithium borohydride and a catalytic amount of lithium triethylborohydride in THF gave the primary alcohol **168**. The alcohol **168** was protected as an acetyl group, using acetic anhydride in pyridine at room temperature to yield **169**. The amidoacetate **169** was treated with quinolinium camphorsulphonate, provoking cyclisation and elimination to give the enamide **170** (C-ring). Vilsmeier-Haack formylation with $POCl_3$ in DMF at 100°C afforded the aldehyde **171**, which was converted to the acrylamide **173** under Wittig conditions. The nitro group was reduced to the amine **174** with zinc and acetic acid. Hydrolysis of the acetate gave **175** and *N*-protection with allyl chloroformate provided the allyl carbamate **177**. Swern oxidation provoked spontaneous cyclisation, forming the B-ring as a single stereoisomer of the protected porothramycin A **178**. Deprotection of the allyl carbamate **178** under the Deziel's conditions and crystallisation with MeOH/EtOAc yielded pure porothramycin A **77**.

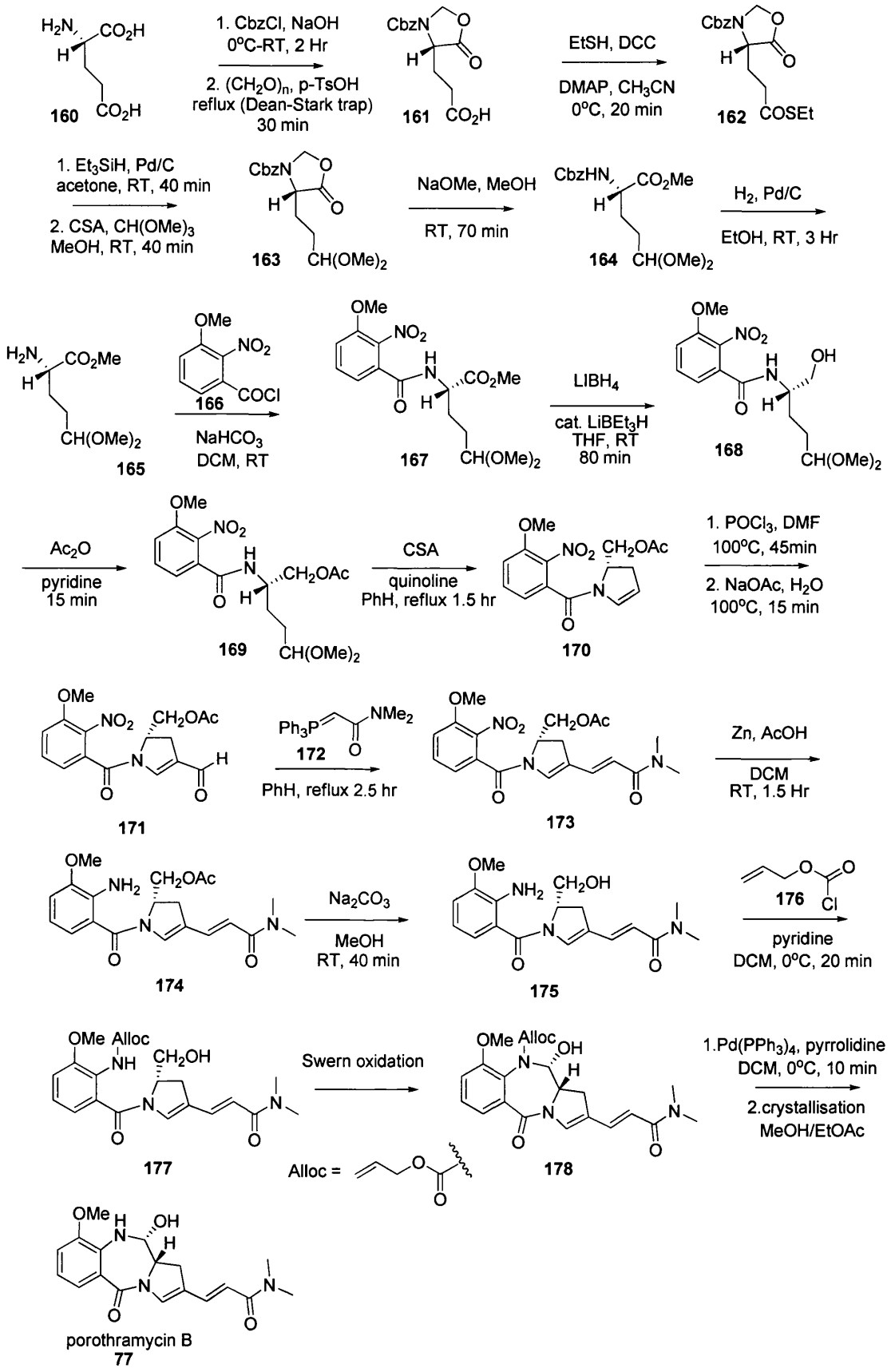

Scheme 25: Synthesis of Porothramycin B.

2.10 Langlois

2.10.1 Synthesis of Porothramycin B derivatives

PBDs with phenolic hydroxyl groups at the C7 and C9 positions exhibit cardiotoxicity, in order to avoid such side effects Langlois *et al.* synthesised porothramycin B without the hydroxyl or alkoxy groups on the aromatic ring. The synthesis involved a final stage reductive cyclisation of the *N*-(2-nitrobenzoyl) pyrrolidine carboxaldehyde **179** to yield the imine **180** with Raney nickel. Using a reduction to make a PBD from a nitroaldehyde is one of the earliest and most obvious approaches to PBD synthesis. Unfortunately this approach can also produce secondary amine side products (e.g. 3) as demonstrated in the Langlois synthesis. Imine **180** was treated with anhydrous methanol with small amounts of trifluoroacetic acid to give **182** in **Scheme 26.**[120]

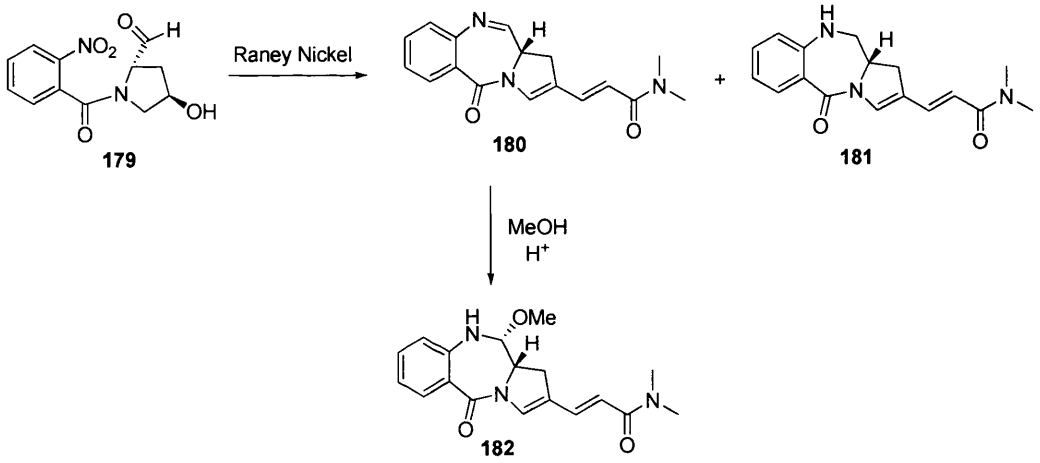

Scheme 26: Synthesis of porothramycin B derivative

2.4.6 Thurston's Thioacetal Approach

2.5.6.1 Synthesis of DC-81

In 1990 Thurston *et al.* reported the synthesis of DC-81 using a thioacetal based strategy (**Scheme 27**). [121] The thioacetal masks the aldehyde moiety and allows the nitro group to be reduced without fear of the secondary amine formation. The benzyl protected A-ring was coupled to the C-ring, and subsequent unmasking of the aldehyde resulted in B-ring cyclisation to afford the 8-benzyl ether of DC-81.

Selective removal of the benzyl group, without affecting the N10-C11 imine, was achieved under mild catalytic transfer hydrogenation conditions.

Vanillic acid **183** was benzylated with benzyl chloride in the presence of aqueous sodium hydroxide as base, to give 4-benzyloxy-3-methoxybenzoic acid **184,** in 76% yield (**Scheme 27**). Nitration with a tin (IV) chloride-nitric acid complex in DCM afforded 4-benzyloxy-3-methoxy-2-nitrobenzoic acid **185**, in 83% yield. Under these conditions, the partial or complete simultaneous nitration of the benzyl group, referred to by other workers was not observed. Pyrrolidine-2-carboxaldehyde diethyl thioacetal **186** was coupled to the acid chloride **185** to provide the amide **187**, in 68% yield. Reduction of the nitro group with stannous chloride formed the amine **188**, in 87% yield. The thioacetal **188** was deprotected with mercury chloride, in the presence of calcium carbonate to yield the cyclised, benzyl protected imine **189**. Finally, debenzylation with 10% palladium on carbon and 1,4-cyclohexadiene gave DC-81 (**80**) in 89% yield. NMR, MS and IR revealed the final product to be identical to a sample of the natural material. However, there was a difference in optical rotation; the synthetic product recording a higher value than the natural product. This was thought to be due to racemization during isolation of natural product (DC-81) from the culture broth. The same phenomenon had been previously observed with synthetic prothracarcin.

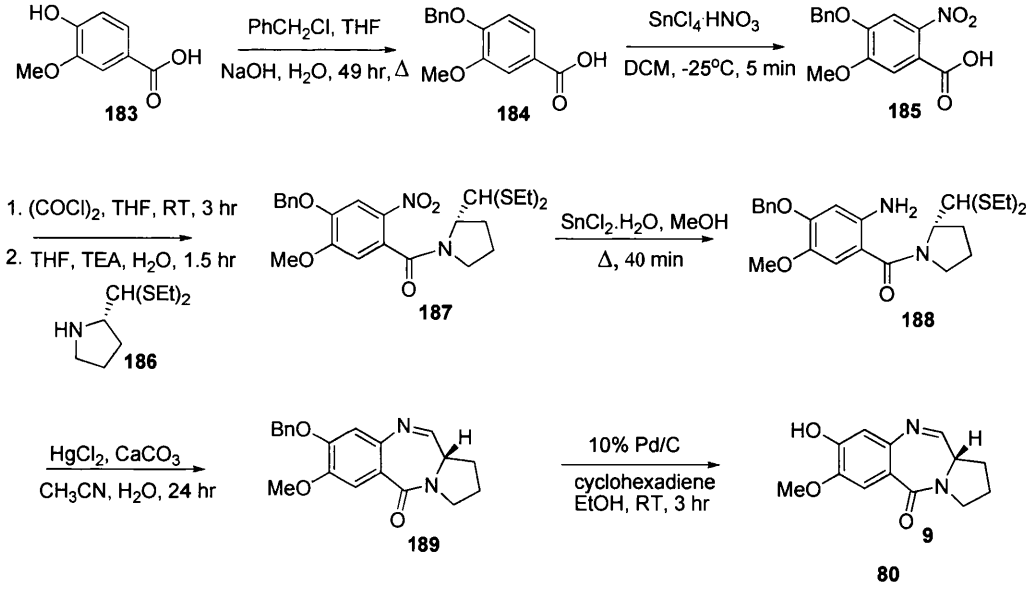

Scheme 27: The Thurston Approach: Synthesis of DC-81

2.11 Aza-Wittig reaction

In 1995, Molina and Eguchi's groups independently reported a new synthetic approach to PBD synthesis. The two groups employed an intramolecular aza-Wittig reaction to achieve B-ring cyclisation and obtain the PBD in the imine form. [122, 123]

2.11.1 Molina's Synthesis of DC-81

4-benzyloxy-5-methoxy-2-nitrobenzoic acid **190** was converted to the *o*-aminobenzoic acid derivative **191** with iron in HCl, in 93% yield (**Scheme 28**). The azidobenzoic acid **192** was formed by diazotisation of **191** in 84% yield, which was coupled to L-prolinol **193** via an acid chloride intermediate to give the A/C ring coupled alcohol **194** in 68% yield. The alcohol **194** was oxidised to the aldehyde **195** with PCC in DCM. The aza-Wittig reaction and cyclisation with triphenylphosphine in DCM at room temperature furnished DC-81 **80** in 79% yield.

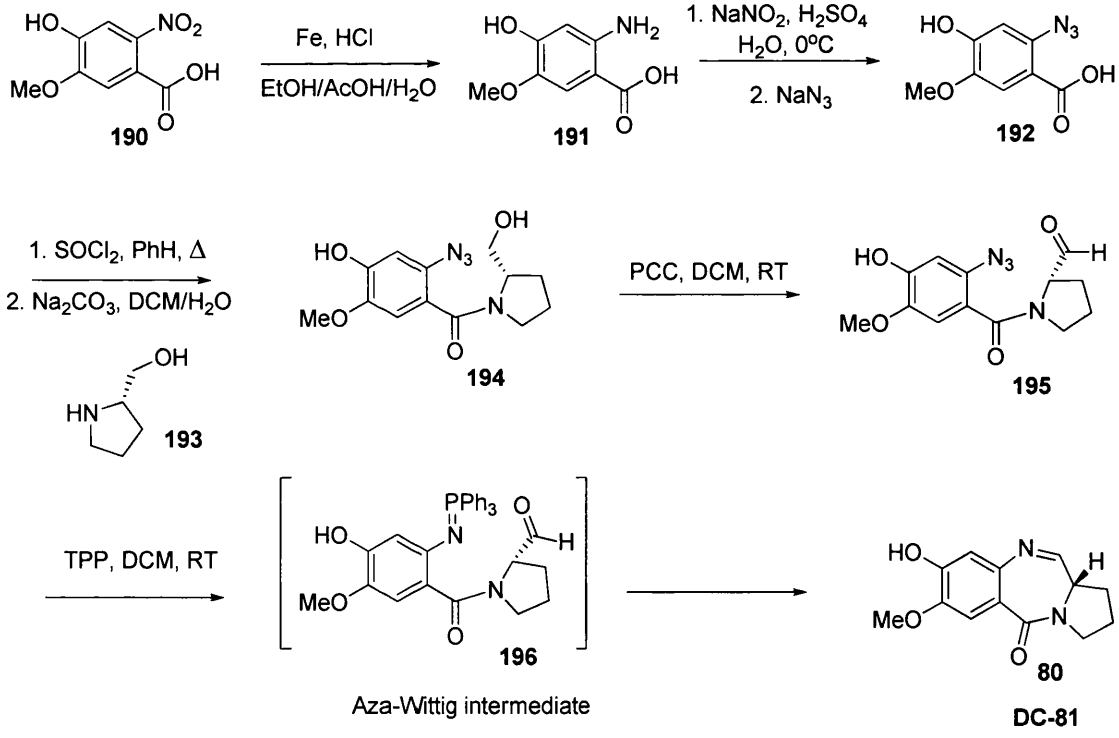

Scheme 28: Molina's synthesis of DC-81

2.12 Eguchi's Synthesis of DC-81

Eguchi *et al.* also employed the aza-Wittig reaction to synthesise the benzyl ether of DC-81 and converted it to DC-81 via catalytic transfer hydrogenation, following Thurston's approach

Reduction of 4-benzyloxy-5-methoxy-2-nitrobenzoic acid **185** (**Scheme 29**) with tin(II) chloride in methanol at reflux for 1.2 hr gave the anthranilic acid **197** in 62% yield. An alternative reduction with sodium borohydride-nickel(II) chloride afforded **197** in 53% yield. Diazotization of **197** with sodium azide furnised the azido carboxylic acid **198**, in 64% yield. Treatment of **198** with thionyl chloride gave the acid chloride, which was coupled to L-proline methyl ester in the presence of TEA and DMAP in THF at reflux for 1 hr, to afford **200** in 69% yield. Reduction of **200** with DIBAL-H at -78°C over 25 min gave **201**, in 76% yield. The alcohol **201** underwent the Staudinger reaction and intramolecular aza-Wittig reaction with TPP in toluene at room temperature over 2.5 hr to afford **189,** the benzyl ether of DC-81 in 98% yield.

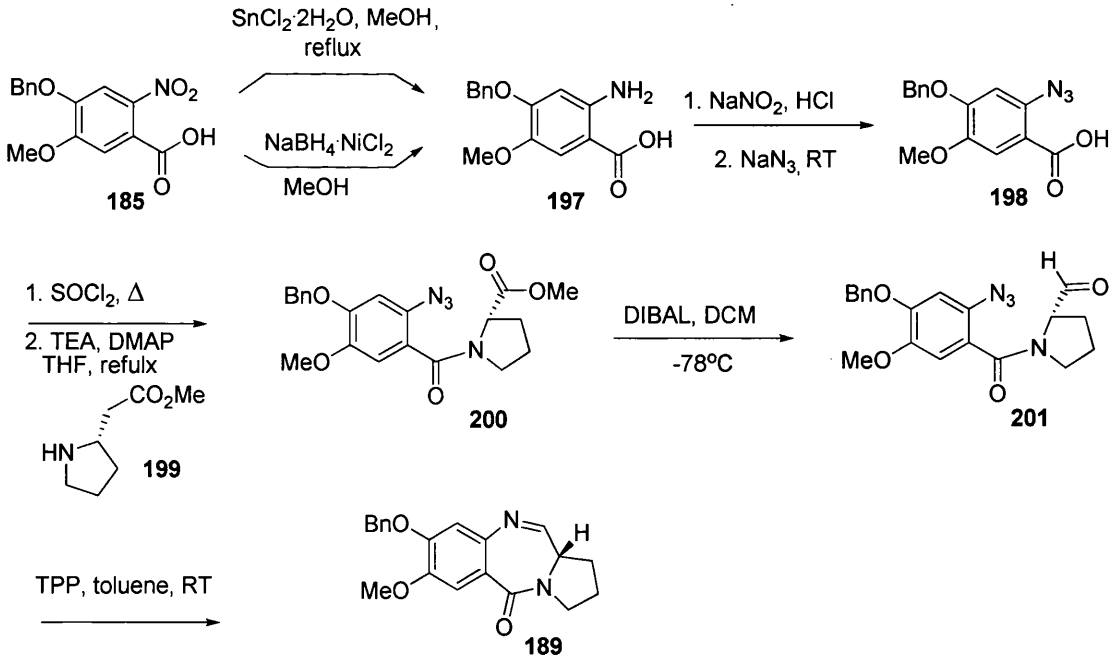

8-benzyl DC-81

Scheme 29: Eguchi's Synthesis of DC-81

2.13 O'Neil's Synthesis of Functionalised PBDs via an aza-Wittig reaction

O'Neil *et al.* were interested in making PDBs with novel functionality about the aromatic A-ring [124]. Their synthesis differed from that of Molina and Eguchi in the conditions used; especially the oxidation of the alcohol to form the aldehyde with Dess-Martin periodinane.

The treatment of anthranilic acid (A-ring) **202** with sodium nitrite and conc. HCl followed by the addition of sodium azide gave the 2-azidobenzoic acid **203**, in 53% yield (**Scheme 30**). Treatment with oxalyl chloride and catalytic DMF provided to the 2-azidobenzoylchloride which was coupled to prolinol **193** to give the tertiary amide **204**, in 89% yield. This approach gave a superior yield when compared to Molina's 68% yield with thionyl chloride. Oxidation with Dess-Martin periodinane furnished the aldehyde and a subsequent Staudinger reaction generated the phosphoroimine and allowed ring closure under aza-Wittig conditions to give the B-ring.

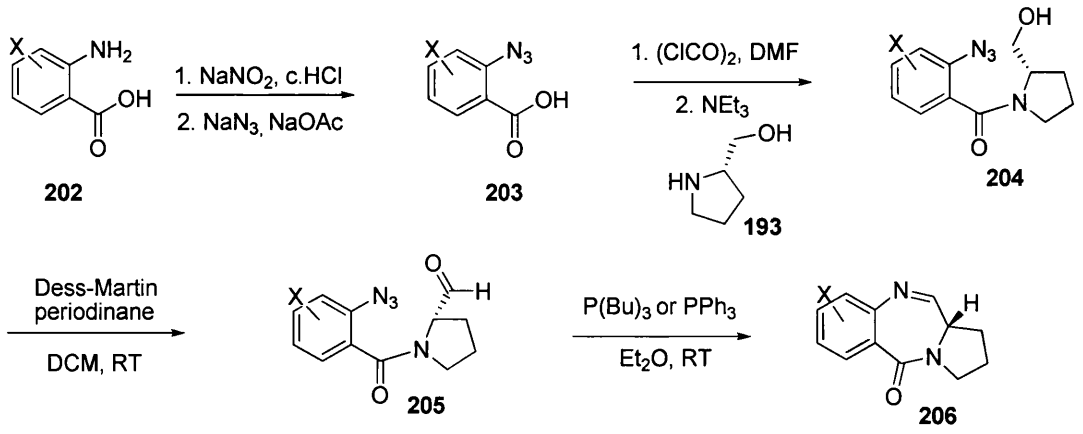

202 203 193 204 205 206

Scheme 30: O'Neil's Synthesis of Functionalised PBDs at the A-ring

2.14 Structure Activity Relationship (SARs)

Application of the strategies discussed in the preceding section has allowed the preparation of many natural and synthetic PBDs, making it possible to elucidate the SAR of this family of antitumour antibiotics (Scheme 28).[125] An imine, carbinolamine or carbinolamine methyl ether is an essential requirement for biological activity, for example groups such as the secondary amine (-NH-CH_2-) are generally not active.

However, dilactams are known to bind non-covalently to DNA and have limited anti-tumour activity and biological activity in their own right.

Bulky substituents at the N10 position inhibit DNA binding and abolish biological activity. An N10 protected PBD with a bulky group should have no biological activity, significantly the subsequent removal of the protecting group with a suitable enzyme restores activity. This offers the possibility of using N10 protected PBDs as potential prodrugs.

The (*S*)-stereochemistry at C11a is a common feature for all PBDs. It gives the PBD the correct three-dimensional shape to fit the minor grove of DNA. DC-81 analogues with the C11a (*R*) stereochemistry fail to bind to DNA and were found to be non-cytotoxic in a B16 melanoma cell line when compared to the C11a (*S*) isomer (which had a high DNA binding efficiency and an IC_{50} value of 0.06 μM in the same cell line).

An sp^2 carbon at the 2-position combined with an exocyclic double bond or saturation between C2-C3 enhanced DNA-binding affinity, cytotoxicity and *in vivo* anti-tumour activity when compared to a C2 sp^3 carbon, with or without substituents. Complete unsaturation of the C-ring leads to inactivity due to stabilization of the N10-C11 imine through conjugation to the aromatic pyrrole, reducing electrophilicity.

Small substituents at the C3 position such as –OH maintain DNA-binding affinity, cytotoxicity and *in vivo* activity.

The sugar moiety at C7, as in sibiromycin, enhances DNA-binding affinity and cytotoxicity in some cell lines (i.e. PC6)

An important feature required for enhancing biological activity is in the presence of electron-donating substituents on the aromatic A-ring. PBD's with electron-withdrawing groups e.g. such as 7-nitro groups are not considered cytotoxic [113].

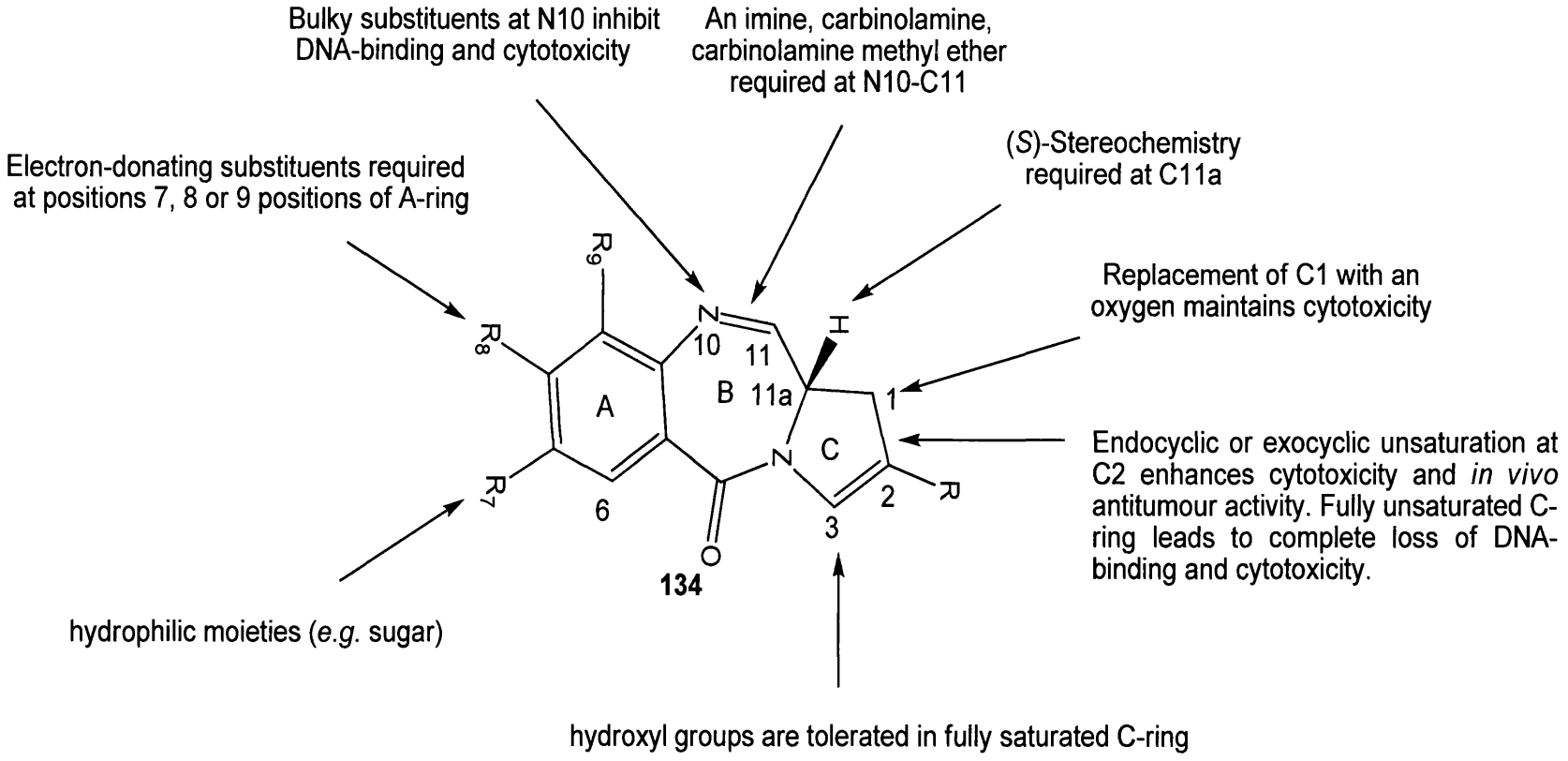

Figure 28: Significant structure-activity relationships for naturally occurring and synthetic PBDs.

Chapter 3

Background and Aims

3. Background and Aims

3.1 Antibody-directed enzyme prodrug therapy using PBDs

The presence of a N10 protecting group in the PBD structure blocks its cytotoxicity. Sagnou *et al.* demonstrated that nitroreductase-sensitive prodrug forms of the pyrrolobenzodiazepines (PBDs) have no DNA-binding activity or cytotoxicity until the N10-protecting group (which blocks DNA interaction) is removed (**Figure 29**). For example, prodrug **207** was found to be essentially non-cytotoxic in a human adenocarcinoma cell-line LS174T (IC_{50} = >500 μM). However, in the presence of a nitroreductase enzyme and NADPH, the IC_{50} was found to be ~5 μM. These results indicated a ~100-fold differential in activity between prodrug and parent.[105]

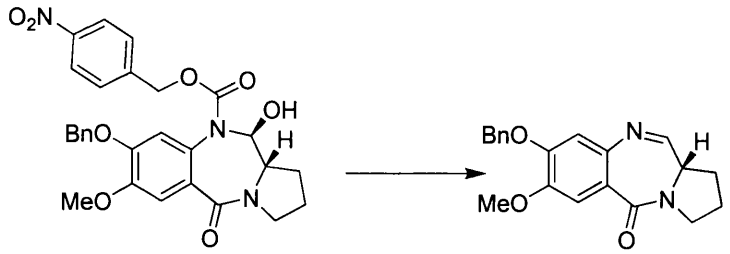

207 189

Figure 29: Prodrug 207 and its conversion to parent PBD 189

Masterson *et al.* synthesised four novel pyrrolo[2,1-*c*][1,4]benzodiazepine (PBD) prodrugs for use in ADEPT therapy (**214, 215, 216** and **217**). The N10-C11 functionality, which is essential for biological activity was masked by an L-glutamic acid based CPG2 substrate attached through either a carbamate or ureidic linkage (X = O or NH, respectively) to the 4'-position of the N10-benzyloxycarbonyl substituted PBD.[126]

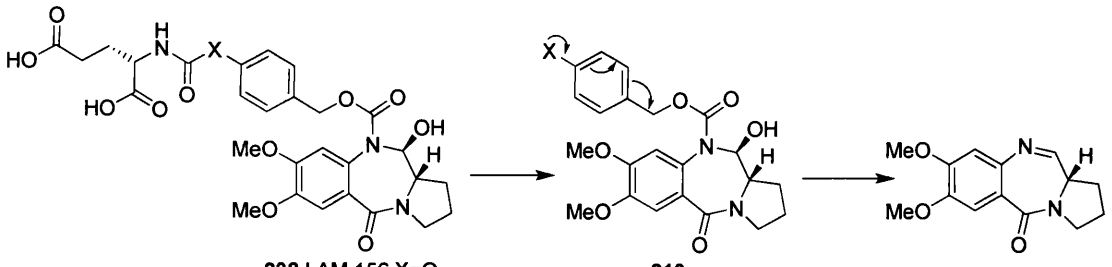

208 LAM 156 X=O
209 LAM 187 X=NH
210
211

Figure 30: ADEPT Concept

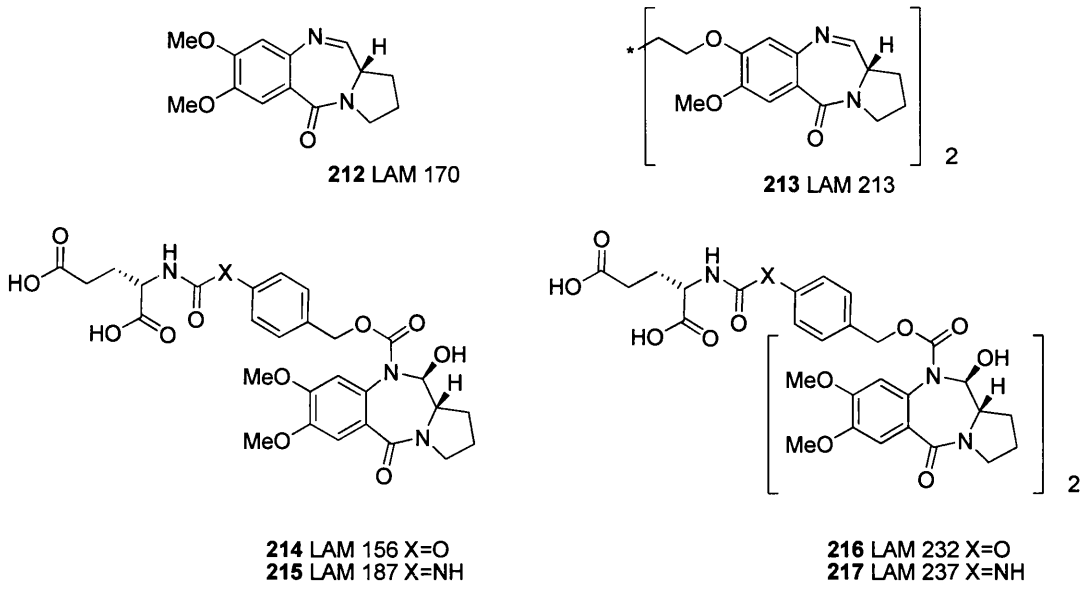

Figure 31: Previous PBD (Pyrrolo[2,1-*c*][1,4] benzodiazepines) Monomer and Dimer Prodrugs.

These molecules were able to provide proof of concept for use of PBD prodrugs in an ADEPT system [A5B7 F(ab')(2)/G2 (CPG2) antibody-enzyme conjugate] in colorectal carcinoma cells expressing carcinoembryonic antigen (CEA). The carbamate monomer and dimer compounds both appeared to be good CPG2 substrates. The monomer **214** was completely converted into the parent PBD within 50 minutes and the dimer **216** to parent PBD **213** within 75 minutes of exposure to enzyme.

Compound	1h Exposure (μM)	Continuous Exposure (μM)
212 (Parent PBD Monomer)	14 ± 1.5	1.4 ± 0.1
214 (Carbamate)	> 100	20 ± 1.2
215 (Urea)	28 ± 5.9	1.6 ± 0.2
Compound	**1h Exposure (nM)**	**Continuous Exposure (nM)**
213 (Parent PBD Dimer)	13±2.4	0.47±0.09
216 (Carbamate)	200±15	21±2.3
217 (Urea)	6±1	0.8±0.2

Table 7: *In vitro* cytotoxicity of prodrugs (214, 215 and 216, 217) and parent PBDs (212 and 213) in LS174T cells following 1hr and continuous exposure. Results are expressed as mean IC_{50} (μM) ± standard error for the monomer compounds, and as mean IC_{50} (nM) ± standard error for the dimer compounds.

3.2 Initial aim of project

- The aim of this project was to significantly increase the cytotoxicity differential between prodrug and released parent PBD.
- Available SAR evidence had suggested that the cytotoxicity of PBD monomers and dimers could be greatly enhanced by the introduction of unsaturation between the C2-C3 position of the C-ring and inclusion of an aryl moiety at C2.[117] The C2-aryl PBDs in **Table 8** are considerably more cytotoxic than the C8 methyl ether of DC-81 (**212**).[127]

Compound	K562 IC_{50} (nM)
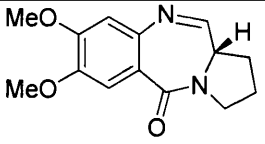 **212**	**288**
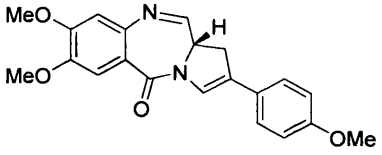 **218**	**0.28**
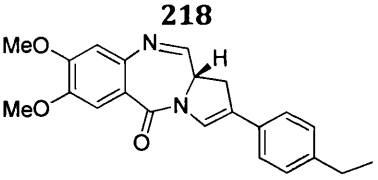 **219**	**79.5**
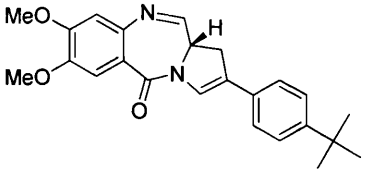 **220**	**47.8**
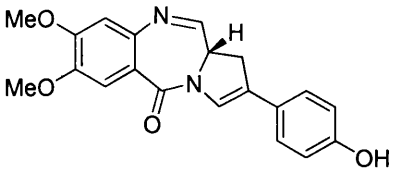 **221**	**10.3**
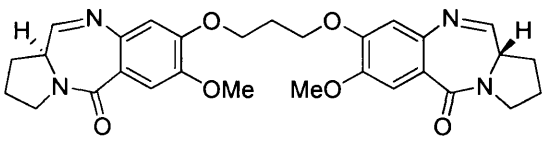 **213**	**30.4**

Table 8: Cytotoxicity of PBD monomers and dimers.

- Developing prodrugs from these intrinsically more cytotoxic PBDs was considered a viable strategy to increase differential activity between prodrug and parent, as N10-substitution blocks activity regardless of other potentiating moieties present in the PBD.
- A 4-methoxyphenyl C2-substituted PBD was selected as the initial prodrug target, as the Suzuki coupling reaction was known to proceed smoothly with this type of compound and the products could be readily characterised by NMR.

Chapter 4

Results and Discussion: Chemistry

4. Results and Discussion: Chemistry

4.1 Retrosynthesis 1

The retrosynthesis (**Scheme 31**) indicates that the favoured disconnection would be at the C2 position, revealing the corresponding triflate. The C2/C3-enol-triflate intermediate would be a starting material for cross-coupling with various boronic acids in order to introduce a range of C2-aryl substituents. A disconnection between the N10 and C11 position would open the B-ring. A further disconnection at the carbamate would give the progroup and A + C ring PBD precursor.

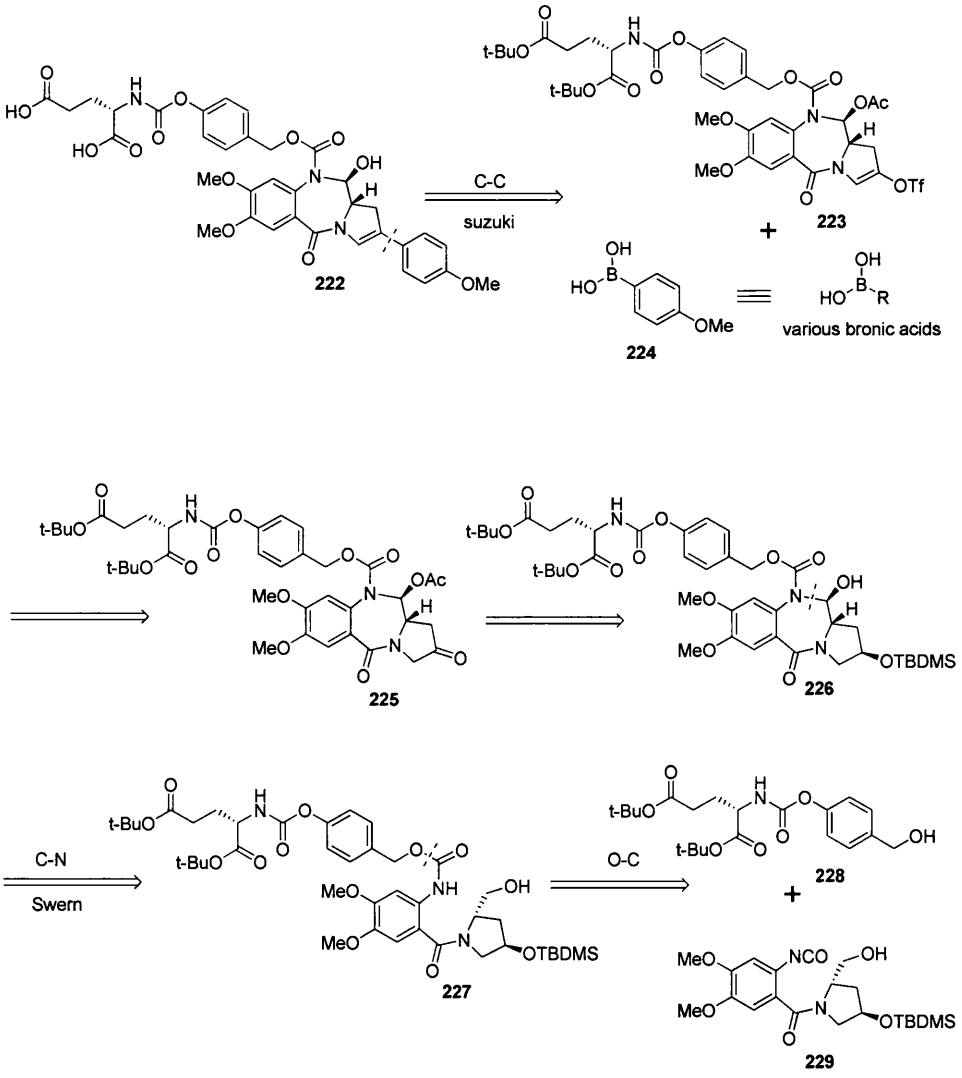

Scheme 31: Retrosynthesis 1

4.2 Proposed Synthesis of C2-Aryl PBD Prodrugs

4.2.1 Constructing the PBD Skeleton, Joining the A + C-Ring PBD Precursor

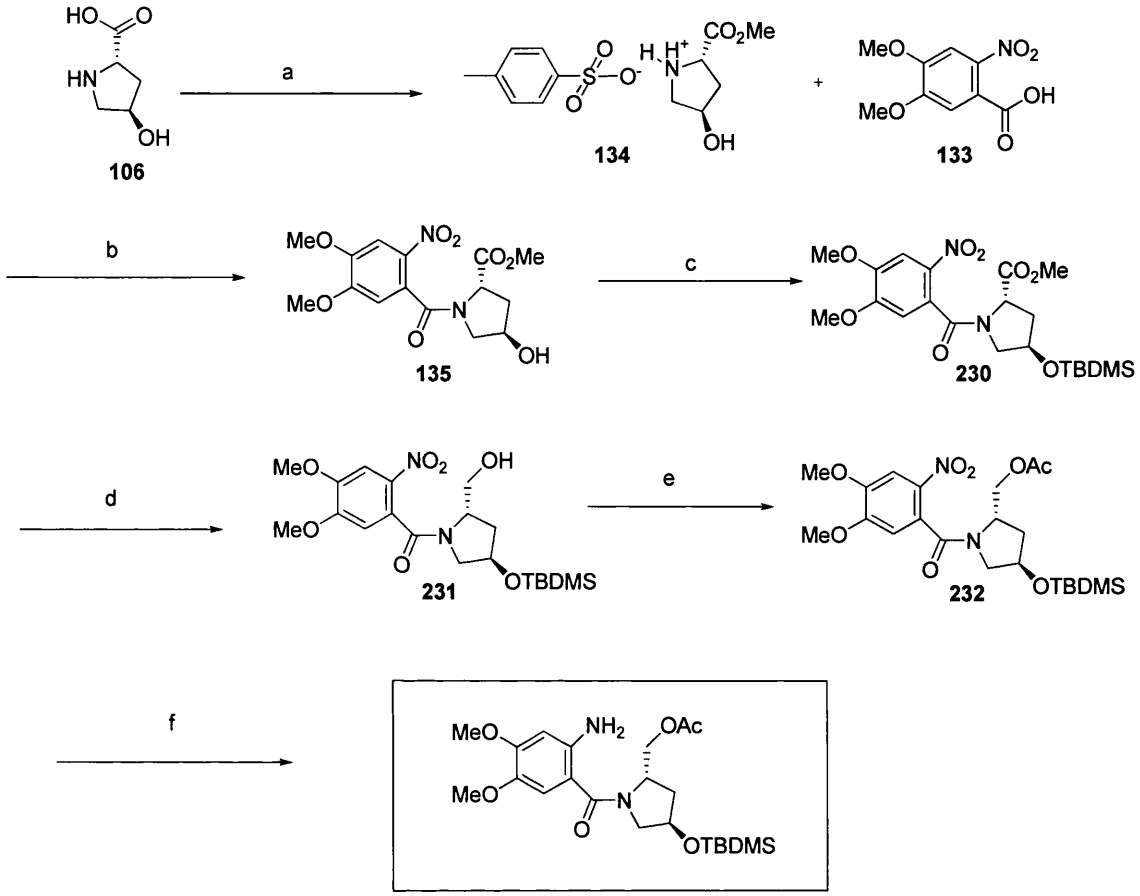

Scheme 32: A + C-Ring Synthesis a) tosic acid, methanol, benzene, reflux, 5 hr, 48%. b) 1. oxalyl chloride, DCM, DMF, RT 16 hr, 2. amine, TEA, DCM, -20°C, RT 16 hr, 96%. c) TBDMSCl, imidazole, DMF, RT, 16 hr, 55%. d) $LiBH_4$, THF, 0°C, 30min, RT, 2 hr, 91%. e) acetyl chloride, TEA, DCM, RT, 16 hr, 91%. f) H_2, Pd catalyst, ethanol, 5 hr, 84%.

The first task was to prepare the PBD A + C ring PBD precursor **233** (**Scheme 32**), in six steps. The route commenced with the preparation of the ester **134** from commercially available *trans*-4-hydroxy-L-proline **106** with tosic acid in methanol and benzene (in 48% yield).[128] Commercially available 2-nitro-4,5-dimethoxybenzoic acid was converted to its acid chloride and coupled to the previously prepared amine salt **134** to afford the nitrobenzamide **135**, in 96% yield. The C2 alcohol (using pro PBD numbering) was then protected with TBDMSCl and imidazole in DMF to provide the silylated nitro derivative **230** in 55% yield.[129]

Attempted reduction of the ester to the alcohol **231** with DIBAL-H in toluene at -50°C produced the desired product as well as some side products (**Table 9**). On using the same reagents at 0°C, LC-MS revealed a trace of the desired alcohol along with unwanted side products. Treatment of the ester with Red-Al in toluene at 0°C gave a similar result. Reduction of the ester with sodium borohydride in toluene at 0°C again afforded a trace of desired alcohol contaminated with an unknown side product.

Finally, the ester was successfully reduced to the alcohol on treatment with lithium borohydride in THF to furnish alcohol **231**, in 91% yield. The success of the reaction was supported by the presence of an OH stretch (2900-3370 cm^{-1}) in the IR spectrum, a new methylene in the ^{13}C NMR spectra (60.37 ppm) and confirmed by high resolution mass spectrometry.

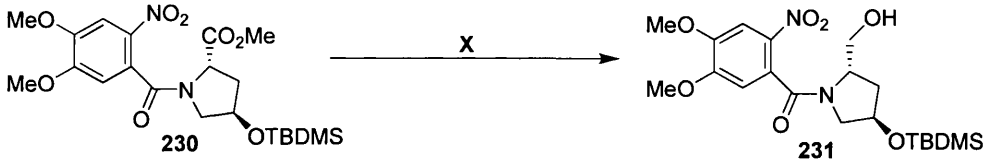

Figure 32: Reduction of the Ester 230.

No.	X (conditions)	Result
1.	DIBAL, toluene, -50°C, N_2	unwanted side products
2.	DIBAL, toluene, 0°C, N_2	trace of desired alcohol and unwanted side products
3.	$NaBH_4$, toluene, 0°C, N_2	trace of desired alcohol and unwanted side products
4.	Red-Al, toluene, 0°C, N_2	desired alcohol and unwanted side product
5.	$LiBH_4$, THF, 0°C, N_2	desired alcohol in 91% yield

Table 9: Reduction of the Ester 230.

Protection of the alcohol **231** with acetyl chloride in the presence of TEA in DCM afforded **232** in 91% yield. Hydrogenation of the nitro group of **232** with 10 % palladium on carbon catalyst in ethanol, using a Parr apparatus, afforded amine **233**, in 84% yield. Interestingly, a marked up field shift of the 9-H signal (from 7.69 to 6.20 ppm) was observed in the NMR spectrum consistent with the formation of the amino product.

With 38 g of the A + C PBD precursor in hand, attention switched to synthesis of the self-immolative progroup.

4.2.2 Progroup Synthesis

A number of approaches to the glutamate derived prodrug have been described in the literature. Initially Niculescu-Duvaz *et al.* reported a five step synthesis commencing with 4-hydroxybenzaldehyde and employing a thioacetal intermediate **Scheme 33**. [130] The same workers later adopted a two step procedure that avoided the use of obnoxious (ethanethiol) and toxic reagents (mercury). The new approach formed the carbamate directly from the 4-hydroxybenzaldehyde, which was reduced with sodium cyanoborohydride to afford the required benzyl alcohol.

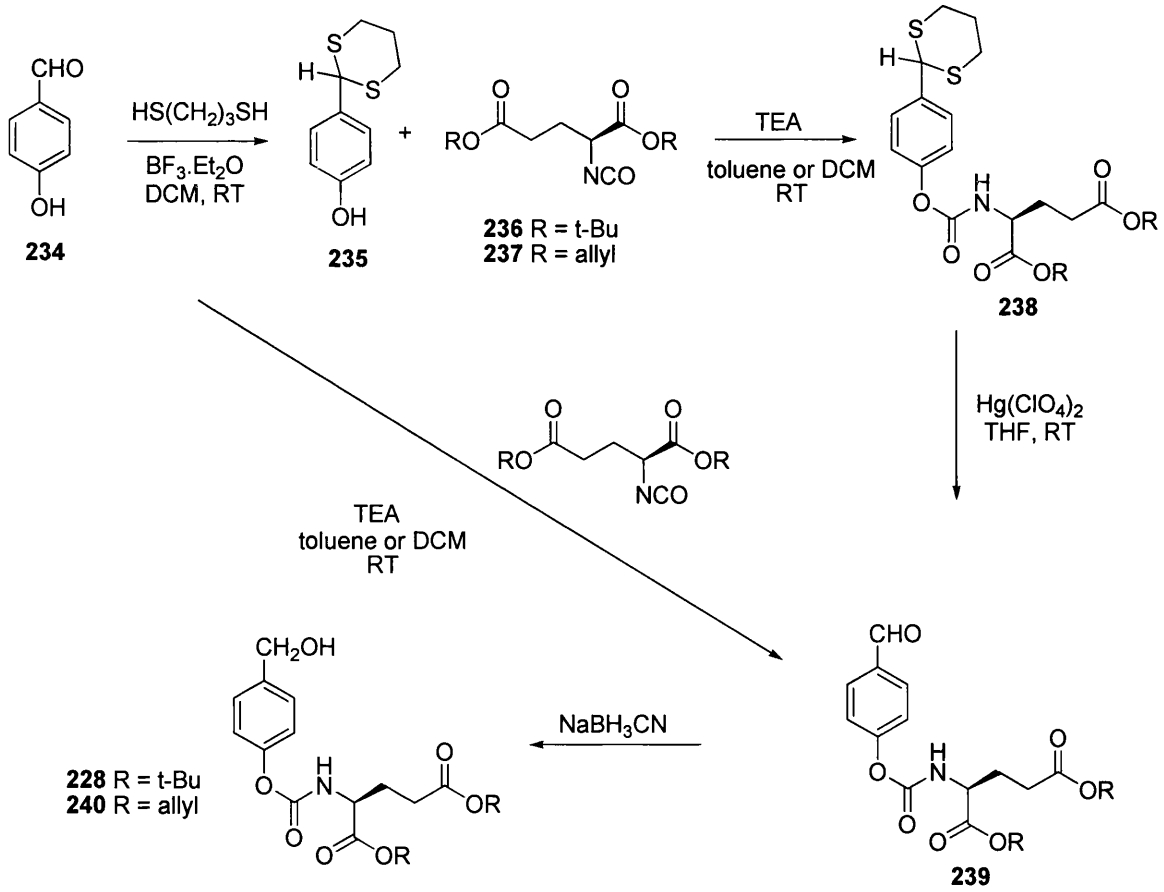

Scheme 33: Background

In an alternative one-pot procedure Jones *et al.* converted the glutamate **236** to the isocyanate by treatment with triphosgene, TEA, DCM at -78°C, followed by 18-crown-6 ether, potassium *tert*-butoxide in THF and finally addition of 4-hydroxybenzaldehyde (**Scheme 33**). Unfortunately, when this procedure was applied to the current synthesis, although the isocyanate was generated (as shown by presence

of IR band at 2248 cm^{-1}), the reaction intermediate precipitated on addition of 18-crown-6 thus preventing the reaction from proceeding (**Table 10**).

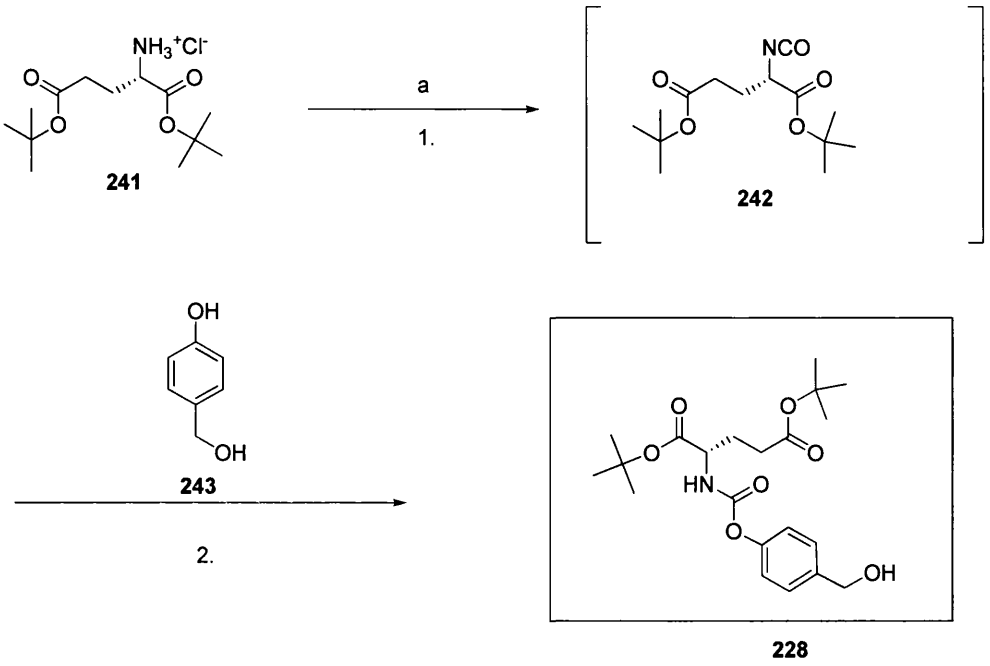

Scheme 34: Progroup Synthesis.

a) 1. triphosgene, TEA, DCM, -78°C. 2. TEA, DCM, 0°C, 2hr, 67%

Repeating the reaction in the absence of 18-crown-6, but still using TEA as base, successfully furnished the required self-immolative progroup. The progroup was somewhat unstable, and could best be isolated by removal of the reaction solvent followed by column chromatography, to yield the prodrug **228** in 67% yield.

No.	X (conditions)	Result
1.	1. Triphosgene, TEA, THF, -78°C to RT 2. 18-crown 6 ether, potassium tert-butoxide in THF at –78°C, N_2	isocyanate formed but no desired product
2.	1. Triphosgene, TEA, DCM, -78°C to RT, N_2 2. 18-crown 6 ether, potassium tert-butoxide in DCM at –78°C, N_2	isocyanate formed but no desired product
3.	1. Triphosgene, TEA, DCM, -78°C to 0°C, N_2 2. TEA, DCM at –78°C, N_2 2 hr	desired prodrug 67% yield

Table 10: Conditions of isocyanate reaction

The ^{1}H NMR of the newly formed carbamate (**Figure 33**) was compared with the NMR of material obtained unambiguously from 4-hydroxybenzaldehyde,[126] confirming that the carbamate had been formed on the phenolic as opposed to the benzyl hydroxyl group. The COSY for the progroup shows the correlation between the H-7, H-9 and H-8 protons (**Figure 34**).

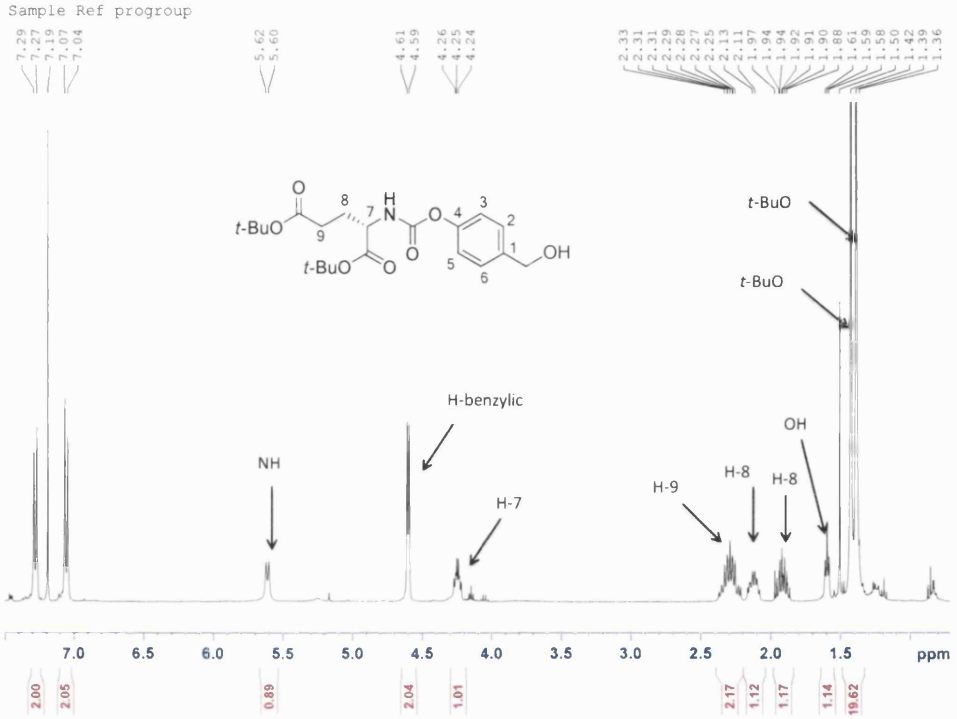

Figure 33: ^{1}H NMR of Progroup (228)

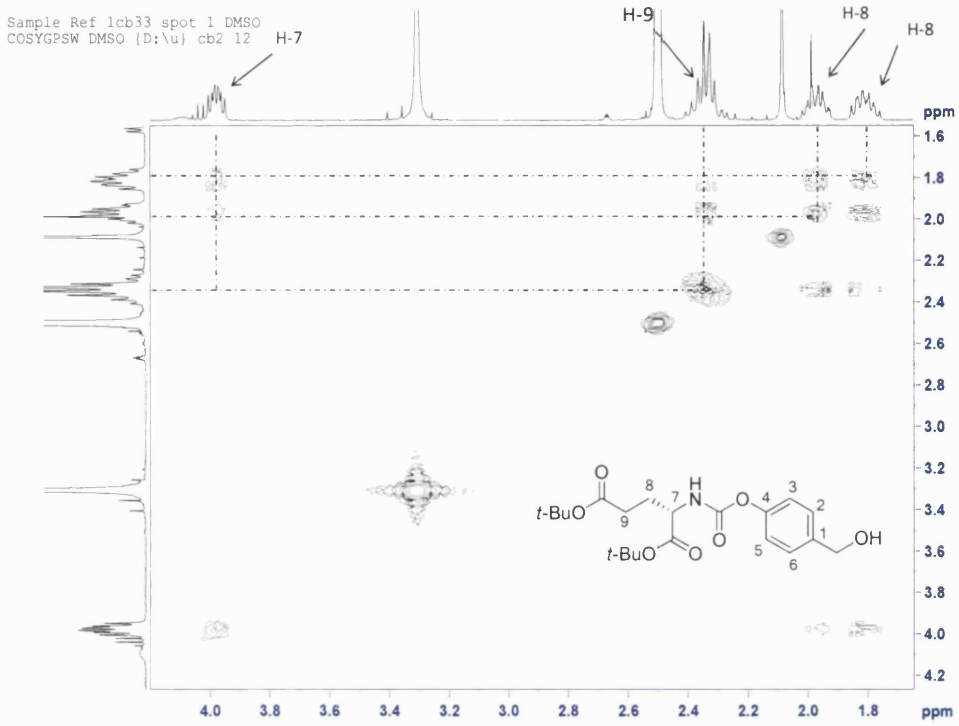

Figure 34: COSY NMR of Progroup (228)

If the carbamate had formed at the benzyl alcohol **244,** one would expect the molecule to be very unstable due to its self-immolative nature (**Scheme 35**).

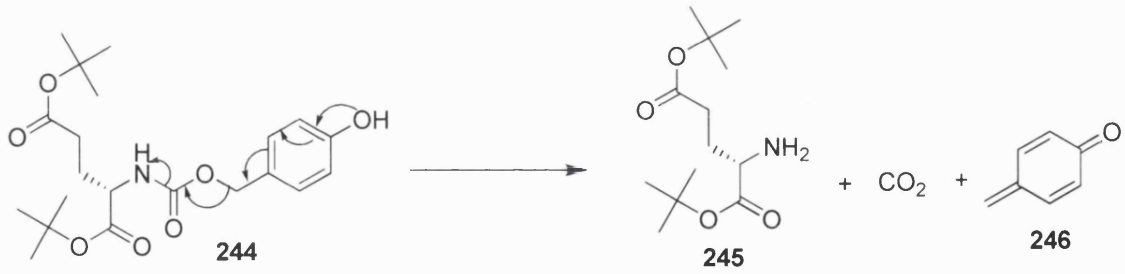

Scheme 35: Self-immolative nature of 244

The progroup could now be attached to the A+C ring PBD precursor using isocyanate chemistry.

4.2.3 Attachment of Progroup and Cyclisation of the PBD B Ring

Initially the A + C ring amine **233 (Scheme 36)** was treated with triphosgene and TEA in toluene. IR analysis of the reaction mixture revealed an isocyanate peak at 2265 cm^{-1}. The isocyanate was then added directly to a solution of progroup **228** to afford the protected N10 A + C ring **248** in 70% yield.

The next strategic objective was closure of the PBD B-ring, which would require removal of the acetate group to provide a primary alcohol for the oxidation/cyclisation reaction. Acetates can usually be removed with aqueous potassium carbonate. However, a series of test reactions on the progroup alone, using potassium carbonate, water, methanol and DCM, revealed the progroup's fragility to the standard conditions. The removal of the acetyl protecting group from the N10-protected amine **227** with 1,8-diazabicyclo[5.4.0]undec-7-ene (DBU) in methanol at room temperature failed to give the expected alcohol.[131] Characterisation of the product obtained by LC-MS and NMR revealed that both the acetyl and butyl protecting groups have been cleaved under these conditions. Repeating the reaction at lower temperature (0°C and –10°C) gave the same result. Performing the reaction in benzene (**Caution!**) afforded a different product, identified as the free amine by NMR and LC-MS. Treatment of the N10-protected amine **227** with guanidine hydrochloride, sodium ethoxide in ethanol/DCM at room temperature and at 0°C also afforded the free amine (A/C Ring), contaminated with other side products.[132] Attempted deprotection with hydrazine in methanol again yielded the free amine (A/C ring).[133]

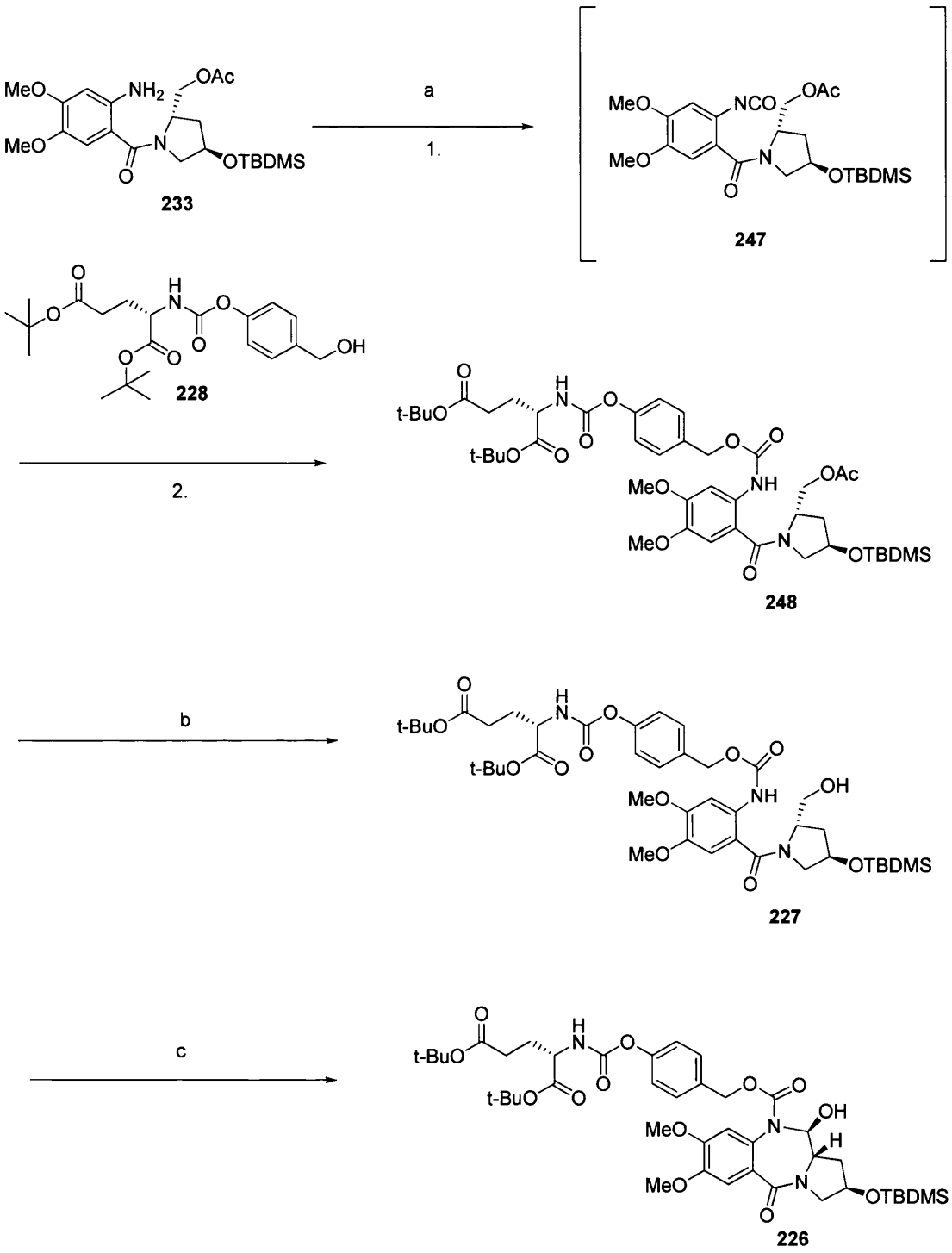

Scheme 36: Attachment of 'progroup' and cyclisation of the PBD B ring.

a) 1. triphosgene, TEA, toluene, RT, 3 hr, 2. TEA, RT, toluene, 70%. b) 'super hydride', ($LiBHEt_3$), -78°C, 2 hr, 76% c) DAIB, TEMPO, DCM, RT, 18 hr, 89%.

Finally, the N10-protected amine **227** was successfully deprotected with lithium triethylborohydride solution (super hydride) in THF at –78°C to furnish alcohol **226,** in 76% yield [134].

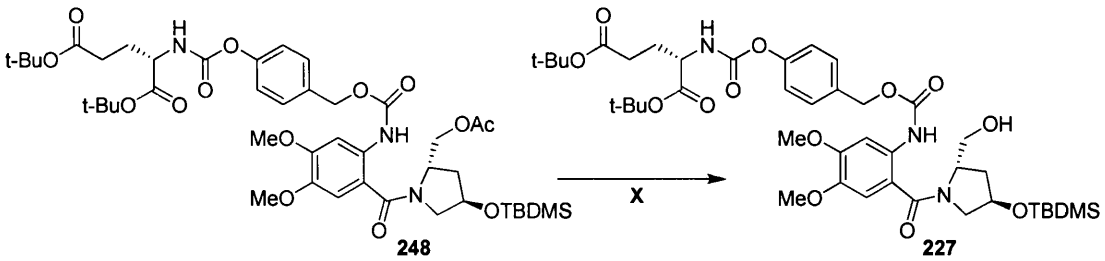

Figure 35: Acetyl deprotection

No	X (conditions)	Result
1	Potassium carbonate, water/methanol/DCM, RT	degradation of starting material
2	DBU, methanol, RT, N_2	removal of acetyl and butyl groups
3	DBU, methanol, 0°C, N_2	removal of acetyl and butyl groups
4	DBU, methanol, -10°C, N_2	removal of acetyl and butyl groups
5	DBU, benzene, -10°C, N_2	removal of acetyl and butyl groups
6	Guanidine hydrochloride, sodium ethoxide, ethanol/ DCM, RT, N_2	unwanted free amine
7	Hydrazine, methanol, N_2	free amine and side products
8	'Super hydride', THF, -78°C, N_2, 2hr	afforded desired alcohol 169

Table 11 Acetyl deprotection conditions

Oxidation of alcohol **227** with TEMPO and DIAB provoked ring closure to give the N10 protected PBD carbinolamine **226** in 89% yield (**Scheme 37**). The potential aldehyde intermediate **249** was not observed and the presence of a 9.7 Hz coupling between 11a-H and the newly formed H-11 methine indicated an *anti* relationship between the protons.

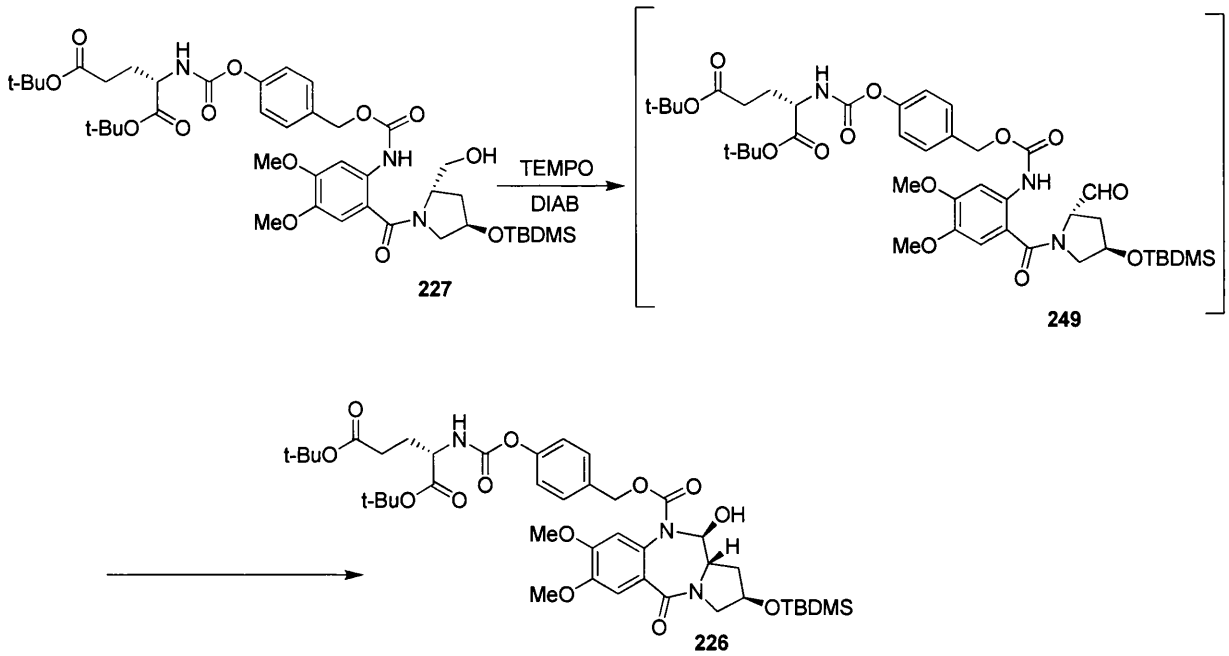

Scheme 37: Ring closure to form N10 protected PBD carbinolamine 226.

The newly formed C11-OH could interfere with the planned triflation reaction and was therefore protected with acetic anhydride and DMAP in DCM to afford **249** in 94% yield. With the B-ring closed and the newly formed C11-OH protected, attention could now focus on elaboration of the PBD C-ring. Removal of the C2 silyl ether, followed by oxidation would furnish the ketone **225** required for the critical triflation reaction.

4.2.4 Synthesis of C2 Ketone

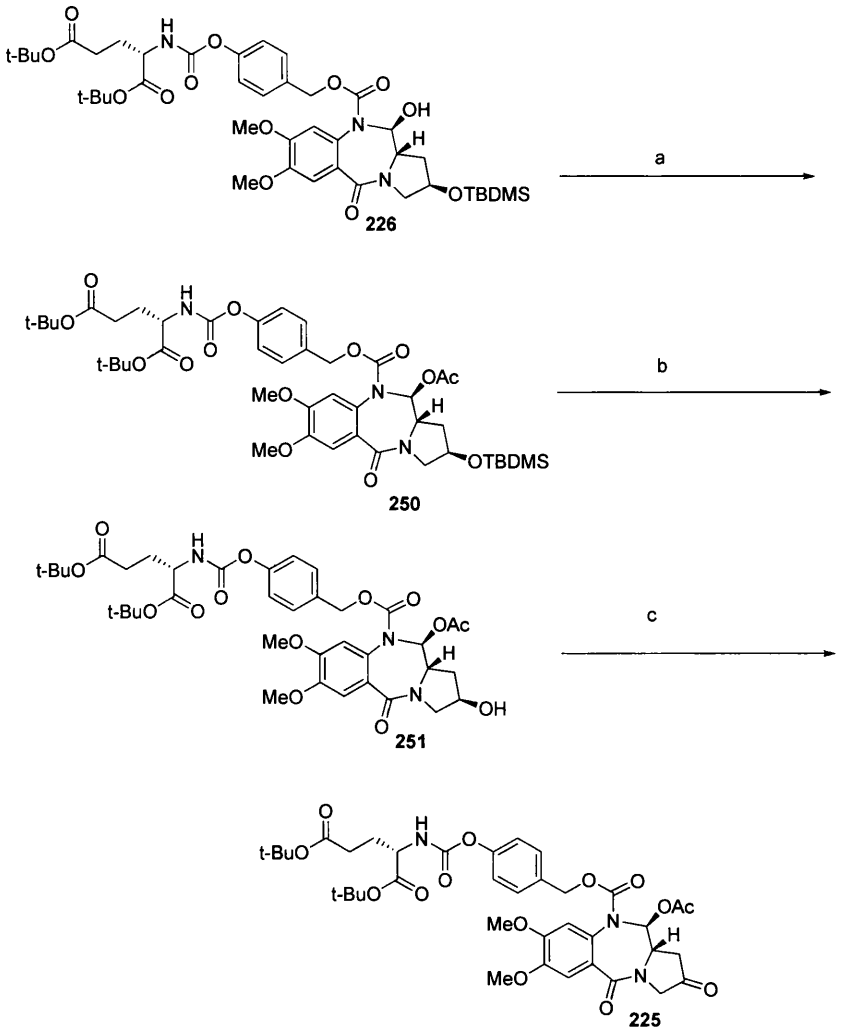

Scheme 38: Synthesis of C2 Ketone.

a) DMAP, acetic anhydride, DCM, 94%, b) HF-pyridine, THF, 0°C 30 min, RT, 1.5 hr, 82%. c) Dess-Martin periodinane 15% Sol. in DCM, acetic anhydride, DCM, RT, 80%.

Silyl ethers are typically cleaved with fluorides or under mild acidic conditions. The attempted desilylation of the N10-protected PBD derivative **250** with tosic acid in aqueous THF or acetic acid in aqueous THF [135] afforded a mixture of the desired product and side products as revealed by LC-MS (**Table 12**). Treatment with tetrabutylammonium fluoride at 0°C-RT for 1 hr gave a single unwanted product. NMR and LC-MS confirmed the side product to be the free PBD with no N10 protecting group. Treatment with lithium chloride, in aqueous DMF under microwave conditions at 120°C (or in a sealed tube at 90°C),[136] or alternatively reaction with $BF_3{\cdot}OEt_2$ in acetonitrile at 0°C,[137] afforded only degradation products. Treatment with

dichloro*bis*(benzonitrile) palladium in acetone at room temperature for 18 hours,[138] gave the C11 alcohol **226** (loss of acetyl protecting group) as revealed by LC-MS. Attempts to deprotect with pyridinium toluene-4-sulphonate, $CuCl_2 \cdot 2H_2O$ in aqueous acetone and iodine in methanol at reflux,[139] gave a range of unidentified products. Treatment with caesium fluoride in aqueous acetonitrile[140] and treatment with potassium fluoride and 18-crown-6 in acetonitrile at room temperature yielded the same unknown product (low molecular mass).[141]

Finally, successful desilylation with hydrogen fluoride-pyridine complex in THF for 1.5 hr furnished the desired N10 protected PBD C2-alcohol **251** (in 82 % yield).[142] High resolution mass spectrometry confirmed the presence of the required product (measured mass: 441.2053 $[M + H]^+$).

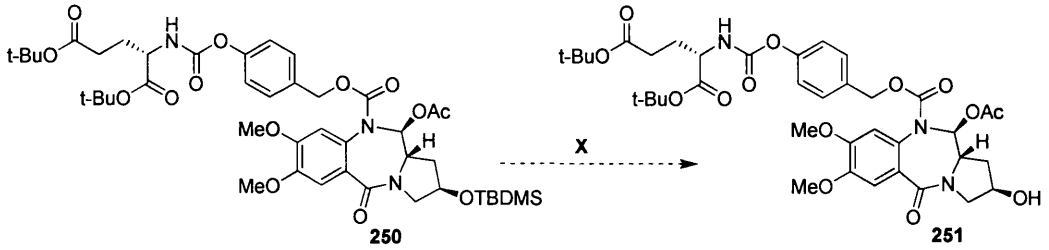

Figure 36: Desilyation

	X (conditions)	Result
1.	AcOH, THF/water, RT, 18 hr	desired product and side products
2.	$Bu_4N^+F^-$, 0°C-RT, N_2, 1 hr	unwanted free PBD
3.	Pd $Cl_2(CH_3CN)_2$, acetone, RT, N_2, 18 hr,	loss of acetyl protecting group
4.	LiCl, water, DMF, microwave 120°C, N_2,	degraded products
5.	LiCl, water, DMF, sealed tube, 90°C, N_2,	degraded products
6.	TsOH, THF/water 20:1, RT	desired product and side products
7.	TsOH.Py, N_2, RT	desired product and side products
8.	I_2, methanol, reflux	unidentified products
9.	CsF, acetronitrile/water 20:1, RT	unidentified products
10.	18-Crown-6, KF, acetronitrile, RT, 2 hr	unidentified products
11.	$BF_3.OEt_2$, acetronitrile, 0°C	degraded products
12.	$CuCl_2.2H_2O$, acetone/water 95:5, 3 hr	loss of acetyl protecting group
13.	HF-pyridine, THF, 0°C, N_2, 1.5 hr	desired free alcohol

Table 12: Desilyation of OTBDMS

Oxidation of N10-protected PBD C2 alcohol **251** on treatment with Dess-Martin periodinane and acetic anhydride in DCM afforded ketone **225**. The deprotected secondary alcohol was oxidised to the corresponding ketone using the Dess-Martin periodinane in 92% yield. Successful oxidation was indicated by the broad band at 1721.7 cm^{-1} in the IR corresponding to the ketone group. The NMR showed a change in the C-ring H-1 and H-3 signals and the loss of the H-2 signal.

4.2.5 Triflation

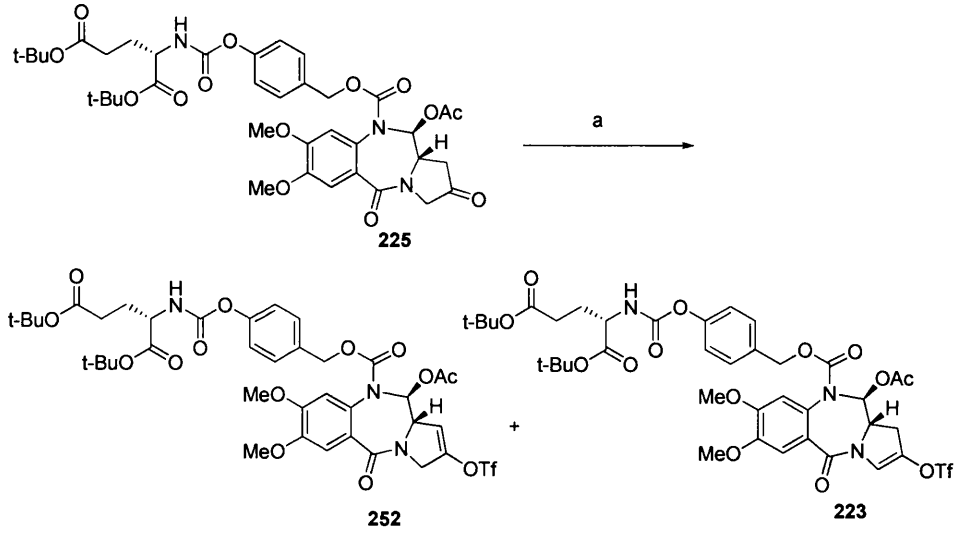

Scheme 39: Triflation. a) 5-chloro-*N,N*-(trifluromethanesulfonyl)aminopyridine, LHMDS, THF, -78°C to RT, 47%.

Synthesis of the C2 ketone allowed formation of the critical enol triflate to be addressed. Peña and Stille had reported the successful triflation of the C2 ketone of a dilactam anthramycin precursor under mild thermodynamic conditions. Later Cooper *et al.* had successfully employed similar conditions in their synthesis of the first C2-aryl substituted PBDs. The approach had also been applied to N10-protected cabinolamine PBDs,[143, 144] although a higher concentration of the triflic anhydride was required. Unfortunately, when these conditions (9 eq. triflic anhydride, 11 eq. pyridine) were applied to the protected carbinolamine (**225**) bearing the sensitive N10 progroup, the reaction failed to afford the required triflate (**Table 13**), furnishing instead a variety of degradation products. Application of the less reactive *N*-phenyltriflimide with pyridine in DCM at room temperature for 20 hr failed to afford the product, even when heated at 60°C for 18 hr. On treatment with *N*-

phenyltriflimide and a stronger base (LHMDS) in THF at –78°C, LC-MS and TLC revealed starting material and one unidentified product.

Finally, successful triflation was achieved with 5-chloro-*N*-*N*-(triflurомethane sulphonylaminopyridine) and LHMDS in THF at –78°C under a nitrogen atmosphere for 2 hours (**Scheme 39**). NMR analysis revealed the presence of the two triflate products. Fortunately, the 1,2 and 2,3-enol triflates (**252** and **223**) had distinctive NMR profiles and their spectra could be interpreted by comparison with earlier, less complex triflates, prepared by. [143-145]

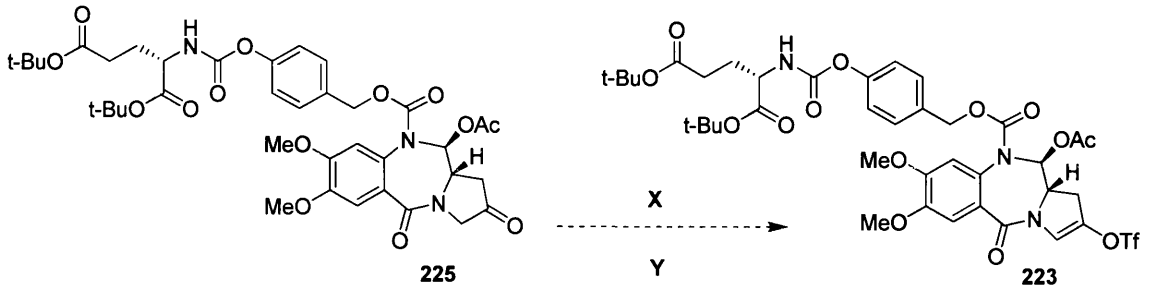

225 223

Figure 37: Triflation

No	Reagents X	Conditions Y	Result
1	9 eq triflic anhydride, 11 eq pyridine	DCM, -78°C, N_2, 30 min	More than five products formed, none corresponding to desired product
2	9 eq Triflic anhydride, 11 eq pyridine	chloroform, -10°C, N_2	More than five products formed, none corresponding to desired product
3	1.1 eq triflic anhydride, 1.2 eq pyridine	chloroform, -10°C, N_2, 30 min	Mainly one product formed, not corresponding to desired product
4	1.1 eq triflic anhydride, 1.2 eq pyridine	chloroform, -10°C, 24hr	Mainly one product formed, not corresponding to SM without acetyl group
5	1.5 eq *N*-phenyltriflimide, 2 eq pyridine	DCM, RT, N_2, 20 hr	No reaction
6	1.5 eq *N*-phenyltriflimide, 2 eq pyridine	DCM, 60°C, N_2, 18 hr	No reaction
7	*N*-phenyltriflimide, LHMDS	THF, -78°C, N_2	Starting material and one side product
8	1.1eq triflic anhydride, 1.2 eq pyridine, DMAP	chloroform, -10°C, N_2, 40 min	Starting material and one side product MW 749
9	1.1 eq trifluoromethane-sulphonyl, 1.2 eq pyridine	chloroform, -10°C, N_2, 40 min	Starting material and one side product

10	1.5 eq *N*-phenyltriflimide, 2 eq pyridine	chloroform, Microwave	No reaction
11	1.1 eq Triflic anhydride, 1.2 eq pyridine, HMPA	DCM, -10°C	Starting material
12	5-chloro-*N*-*N*-(trifluro- methane-sulphonylamino, LHMDS	THF, -78°C, N_2, 1 hr	Mixture of isomers

Table 13: Triflation conditions

4.2.5.1 Separation of Triflate Isomers

Unsurprisingly, the polarities of the two triflate isomers (**Figure 38**) were very similar and attempts to separate the isomers by flash column chromatography were unsuccessful. Initially, TLC of the isomers with conventional TLC methods gave no separation, but attempts with different solvent systems finally separated the two isomers, after eluting with neat chloroform three times.

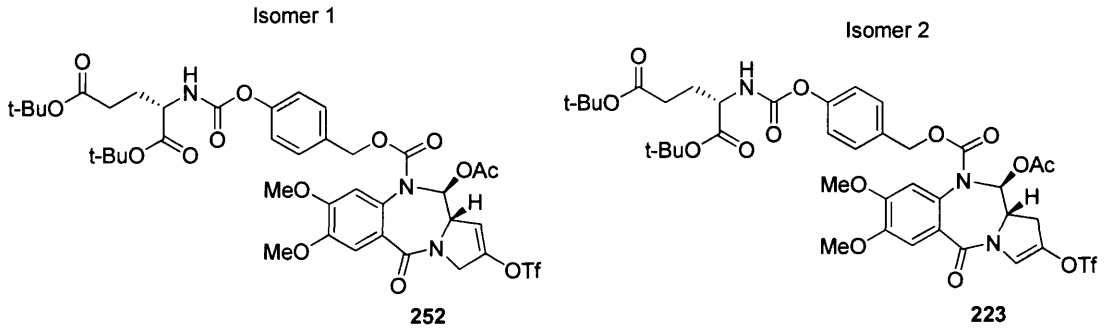

Figure 38: Triflate isomers

The separation was attempted on preparative TLC plates, eluting three times with a 1:4 hexane:chloroform mobile phase, and 4 times with neat chloroform. The TLC plate showed two bands. The top band was thin and bright in colour and the bottom band was thick and dull. The two bands were etched from the Preparative TLC plate, extracted with ethyl acetate and filtered. NMR of the extracts revealed that some separation had been achieved, but ultimately there was still a mixture.

Attempts to Separated Triflate Isomers: Preparative TLC

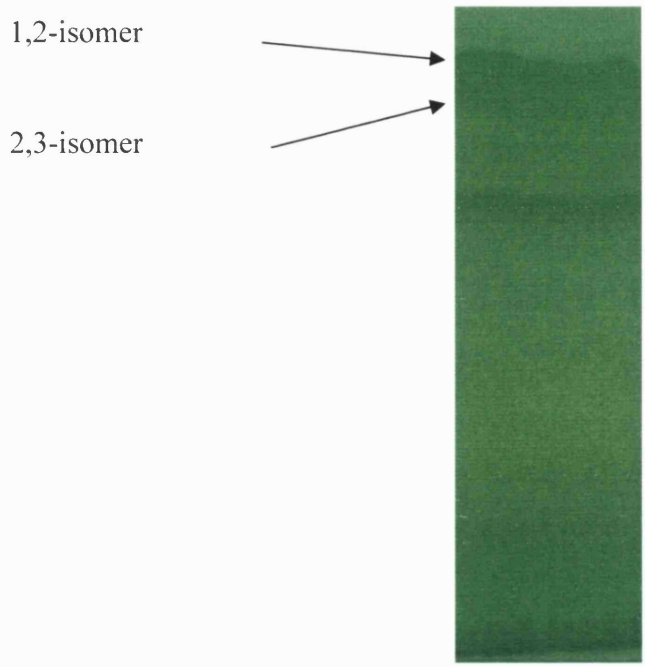

Figure 39: Preparative TLC plate of 1,2- and 2,3- triflate isomers

Eventually, the enol triflate isomers were successfully separated by preparative LC-MS as illustrated in **Figure 41**. The separation was possible on a slow gradient over a 25 minute period (**Figure 40**).

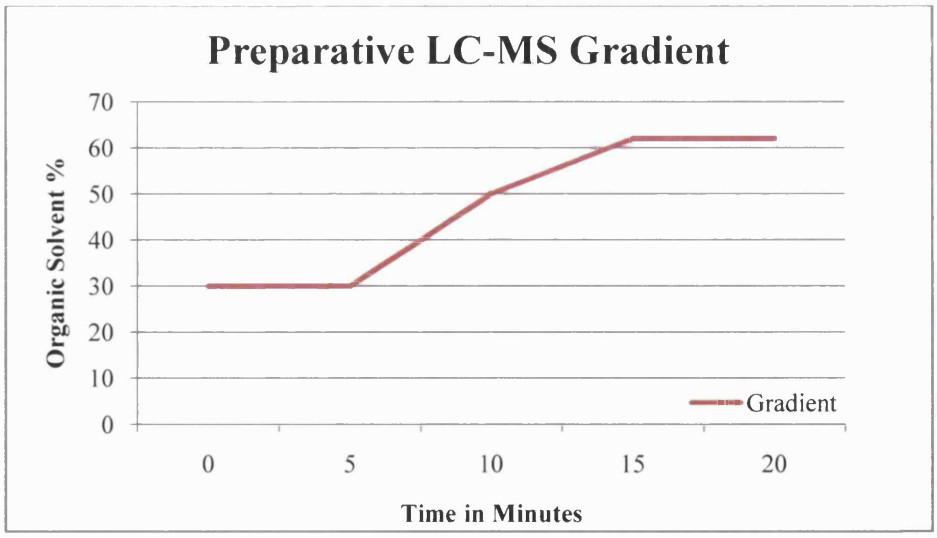

Figure 40: Separation of Triflate Isomers LC-MS Gradient (percentage of organic solvent over time).

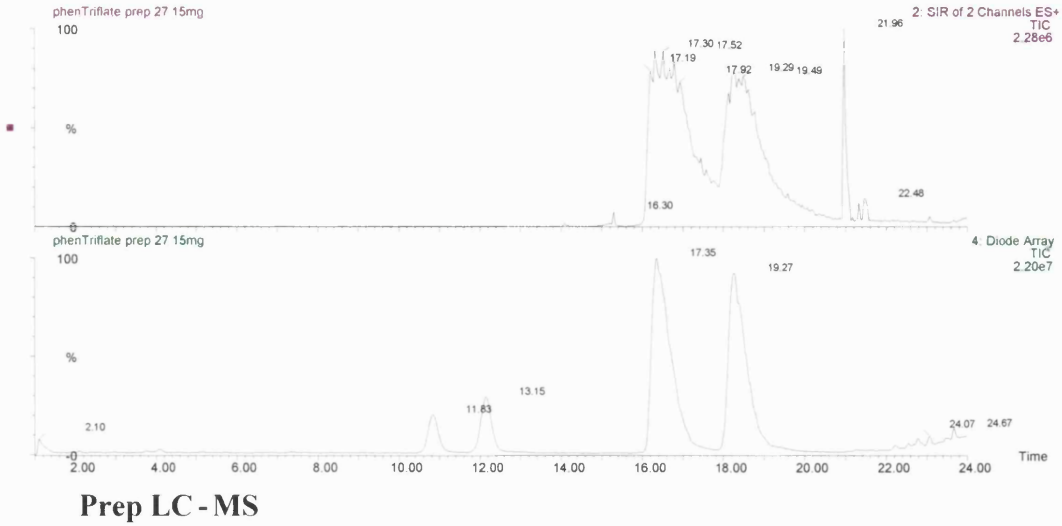

Figure 41: Preparative LC-MS traces for1,2- and 2,3- triflate isomers

The ^{1}H NMR of the 1,2-triflate **252** in CD_3OD exhibited a clear narrow multiplet for H-1 at 5.88 ppm coupled with one of the H-3 protons at 4.32 ppm (**Figure 42**). The presence of the 2,3-triflate was identified by a diagnostic enamine H-3 signal observed at 7.18 ppm, and H-1 signals partially obscured by a solvent peak at 3.21 ppm and a doublet at 2.90 ppm. On changing the NMR solvent to chloroform, the 2,3-triflate H-1 signals became clearly visible at 3.23 ppm (doublet of doublets) and 3.05 ppm (doublet) (**Figure 43**).

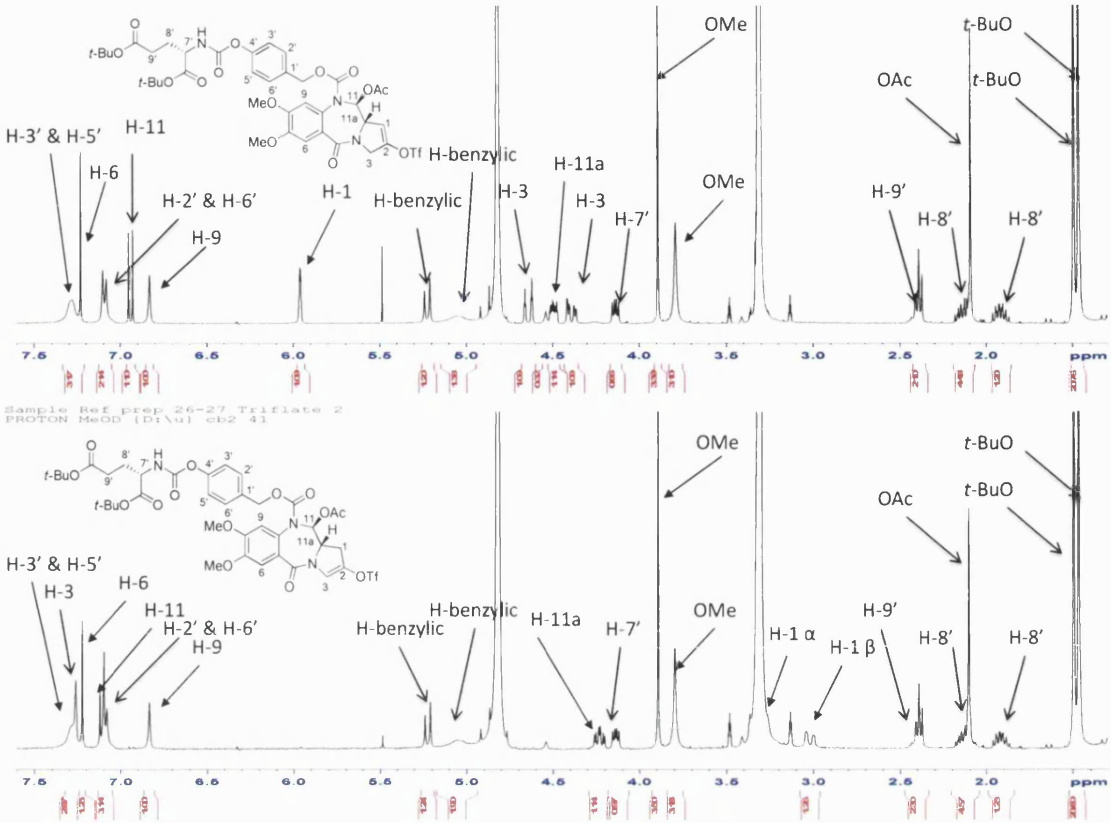

Figure 42: ^{1}H NMR spectra of triflate isomers in CD_3OD, Spectrum 1 corresponds to the 1,2-triflate isomer (252) and spectrum 2 to the 2,3-triflate isomer (223).

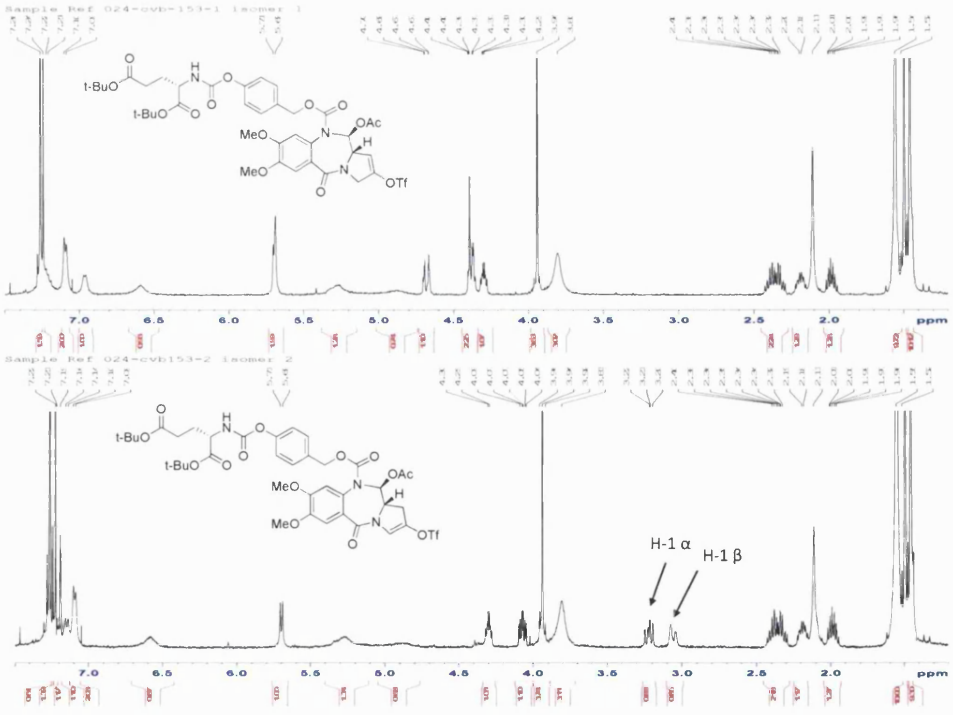

Figure 43: ^{1}H NMR spectra of triflate isomers in $CDCl_3$. Spectrum 1 (above) corresponds to the 1,2-triflate isomer (252) and spectrum 2 (below) to the 2,3-triflate isomer (223).

The COSY spectrum for the 1,2-triflate isomer showed a correlation between the H-11, H-11a, H-1 and H-3 signals (see **Figure 43**). The COSY spectrum for the 2,3-triflate isomer also showed a correlation between the H-11, H-11a, H-3, H-1α and H-1β signals (**Figure 44**).

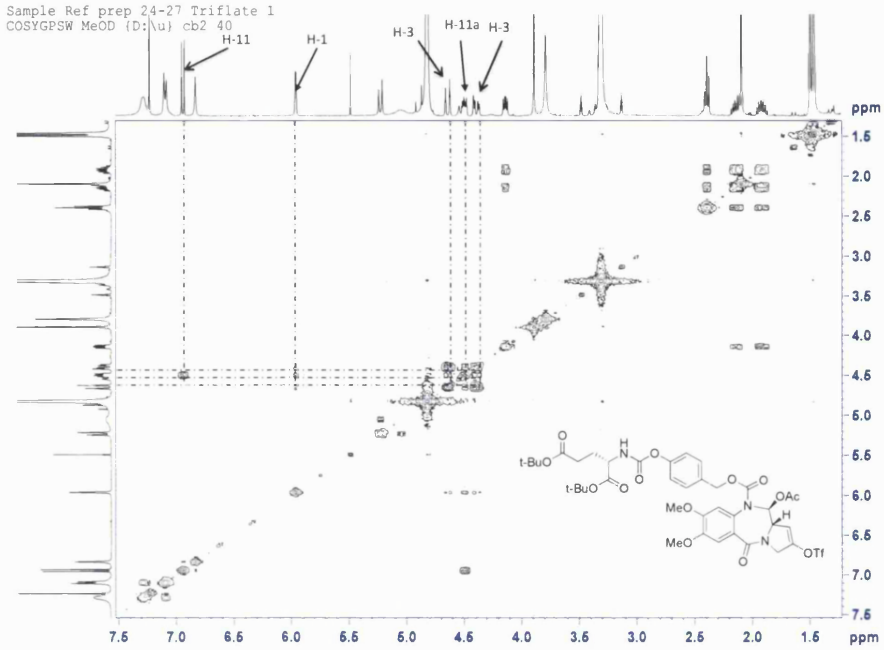

Figure 44: COSY NMR of 1,2-triflate isomer (252) in CD_3OD

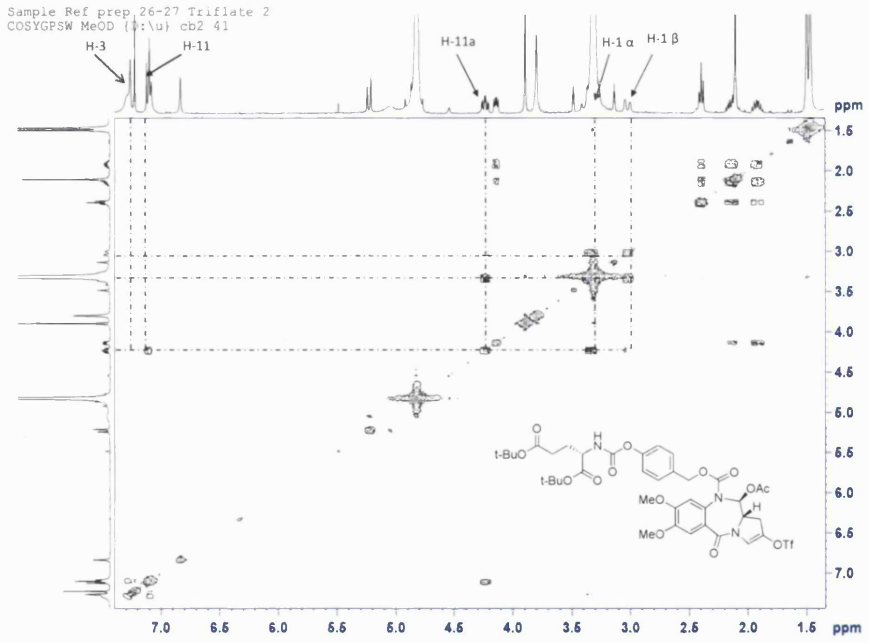

Figure 45: COSY NMR of 2,3-triflate isomer (223) in CD_3OD

4.2.6 Suzuki Coupling

The separated enol triflate isomers both underwent Suzuki coupling reactions with boronic acids to yield the corresponding C2-aryl derivatives. Suzuki coupling with 4-methoxyphenylbronic acid yielded the 1,2- and 2,3-isomer C2-aryl products, **253** and **254**, respectively (**Scheme 40**). The synthesis of both products was confirmed by NMR and MS. For both isomers additional C2-aryl signals were observed at 7.4 and 6.9 ppm (**Figure 46**). There was also a singlet signal corresponding to the C2-aryl methoxy group at 3.9 ppm (for both isomers). The benzylic signals at 5.3 ppm (doublet) and 5.1 ppm (broad signal) are a consistent feature of N-10 protected carbinolamine PBDs.

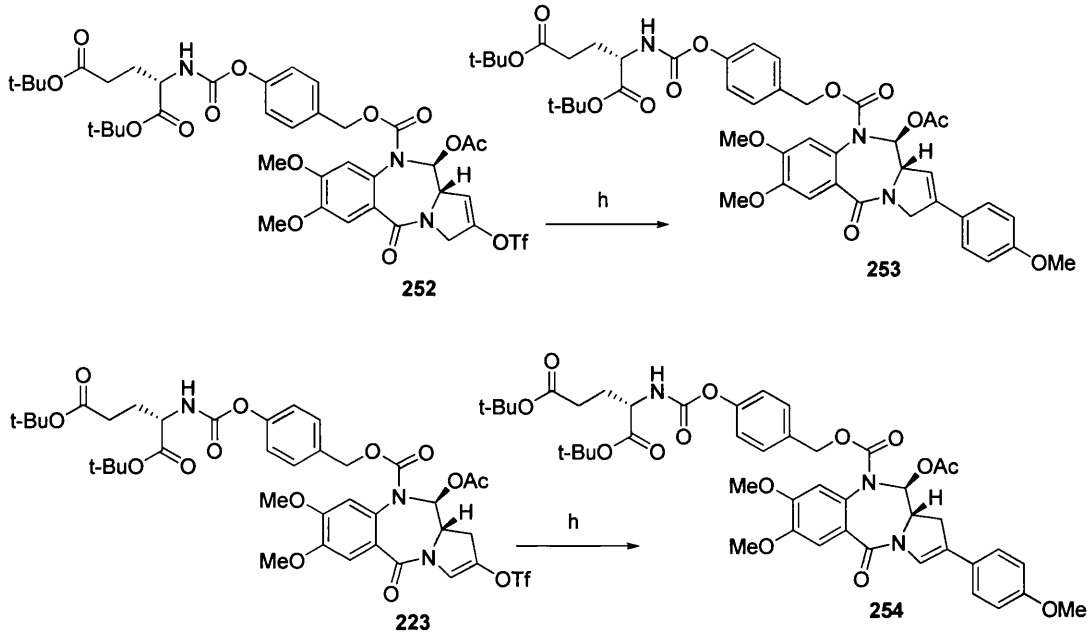

Scheme 40: Suzuki coupling of the C1-C2 (255) and C2-C3 (222) isomers to give the C2-aryl analogues 253 and 254, respectively, h) TEA, water, ethanol, toluene, $Pd(PPh_3)_4$, 4-methoxyphenylboronic acid, RT.

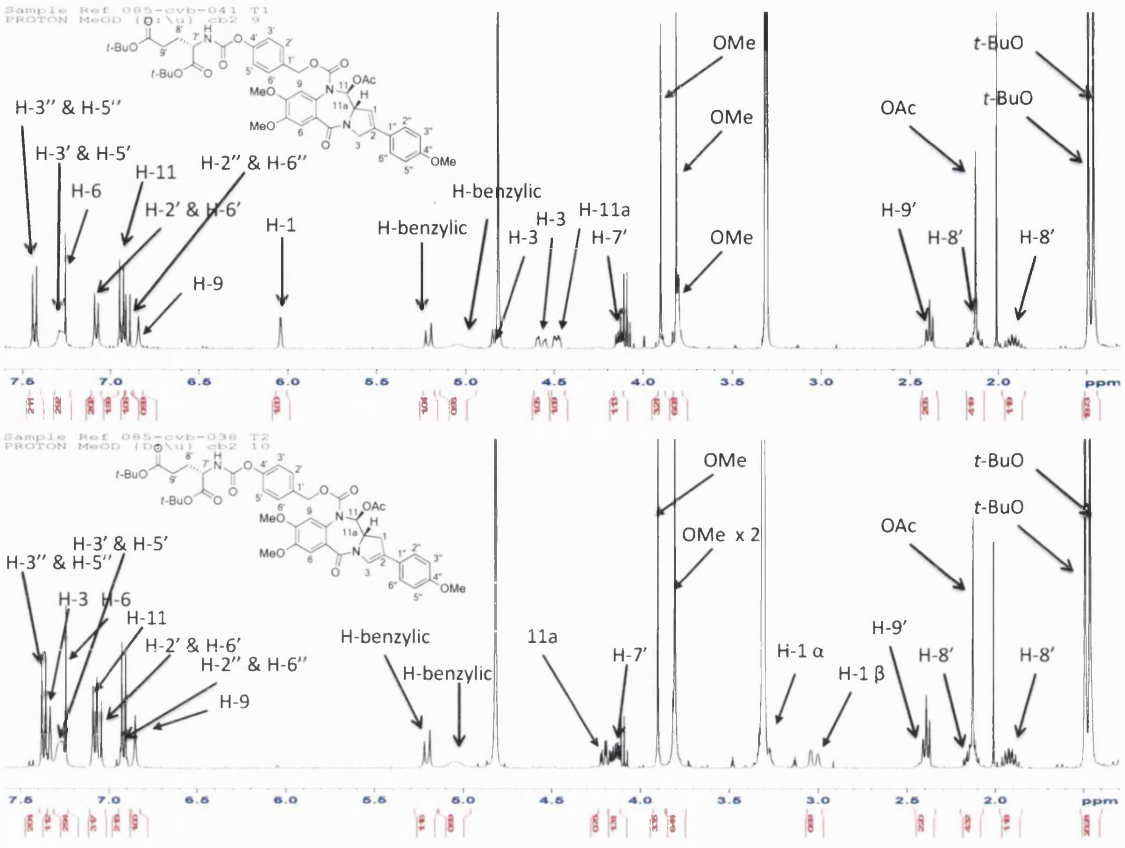

Figure 46: ^{1}NMR spectra of *tert*-butyl protected prodrugs in CD_3OD. Spectrum 1 corresponds to the 1,2-isomer (253) and spectrum 2 to the 2,3-isomer (254)

4.2.7 Final Deprotection and Synthesis of Target Prodrug

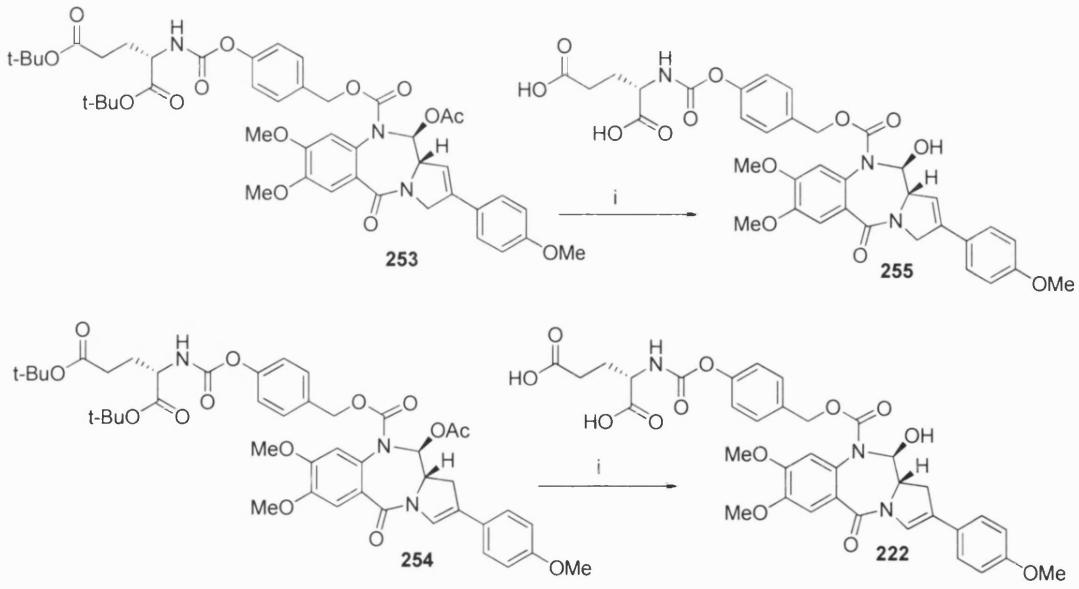

Scheme 41: Final deprotection and synthesis of target prodrugs 255 and 222, i) neat formic acid, RT.

The final step involved the deprotection of the *tert*-butyl groups which was achieved by treatment with formic acid. The 11-acetyl group was also removed under these conditions furnishing the two C2-aryl PBD prodrugs **255** (1,2-isomer) and **222** (2,3-isomer) (**Scheme 41**). Preparative LC/MS was used to purify the final compounds for biological testing. Unfortunately, the quantity of each compound obtained was very low: 6.8 mg of **255** and 4.1 mg of **222**. The ^{1}H NMR confirmed the removal of the protecting groups, revealing the absence of the *tert*-butyl and acetyl signals (**Figure 47**). There was also a change in the benzylic signals at 5.1 ppm (doublet) and 4.9 ppm (partially obscured by a solvent peak).

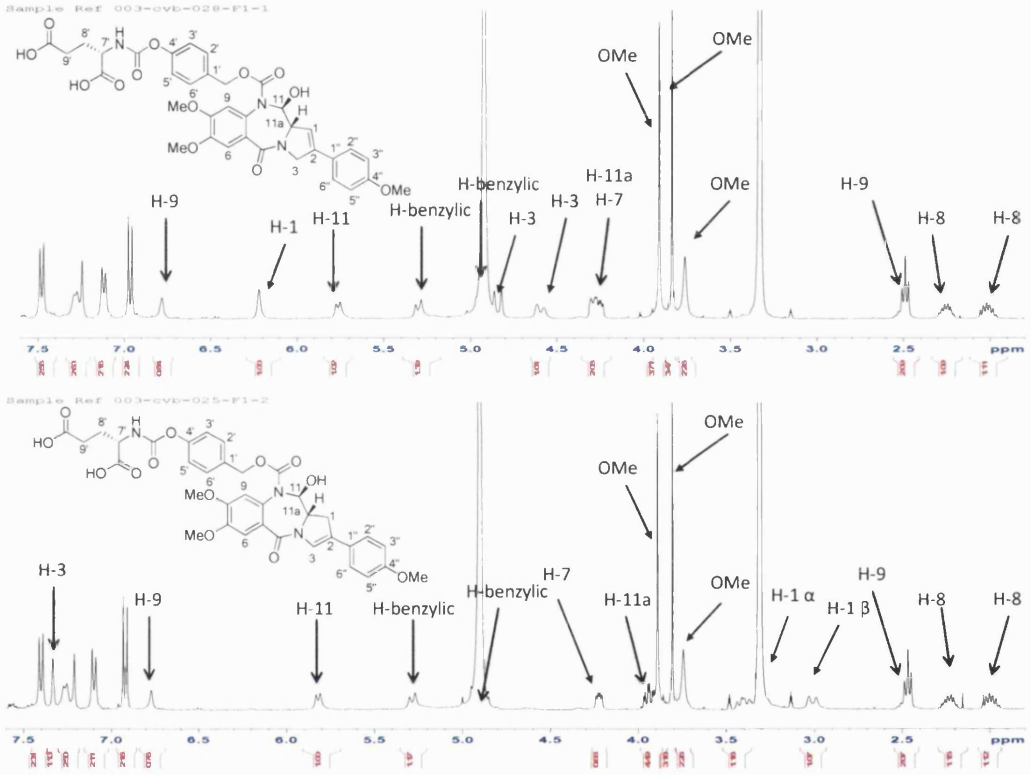

Figure 47: ^{1}H NMR spectra of the C2-aryl PBD prodrugs in CD_3OD; spectrum 1 (above) corresponds to the 1,2-isomer (253) and spectrum 2 (below) to the 2,3-isomer (222).

4.3 Summary of First Synthetic Approach

A robust 13 step synthesis afforded the C2-ketone N10-protected PBD intermediate. The critical triflation reaction, a prerequisite for the Suzuki coupling to introduce the C2-aryl group, produced a mixture of isomers which could only be separated by preparative LC-MS. The separated triflate isomers were subjected to a Suzuki coupling, followed by a final deprotection to remove the butyl and acetate protecting groups. The crude products were purified again by preparative LC/MS to yield the target molecules for biological testing (6.8 mg of 1,2-isomer and 4.1 mg of 2,3-isomer).

Although the initial synthetic campaign was successful, a number of synthetic challenges were identified. For example, the N10-progroup was fragile and not robust enough to survive the conditions required to unambiguously afford the 2,3-enol triflate. It was inefficient to make a mixture of isomers and purify them twice by preparative LC/MS (both at the triflate stage and the final purification of the diacid prodrug), thus producing only small quantities of prodrugs.

It was decided that this problem could be overcome by installing the N10 progroup at the end of the synthesis after the triflation and Suzuki coupling, or by performing triflation and Suzuki coupling on a C-ring ketone prior to joining to an A-ring.

4.4 Retrosynthesis 2

The retrosynthesis indicates that the favoured disconnection would be at the N10-position, revealing the corresponding N10 anionic and carbonyl cationic synthons (**Scheme 42**). Chloroformates and fluoroformates would provide potential equivalents for the carbonyl cation, and the free imine itself is an equivalent of the N10 anion.

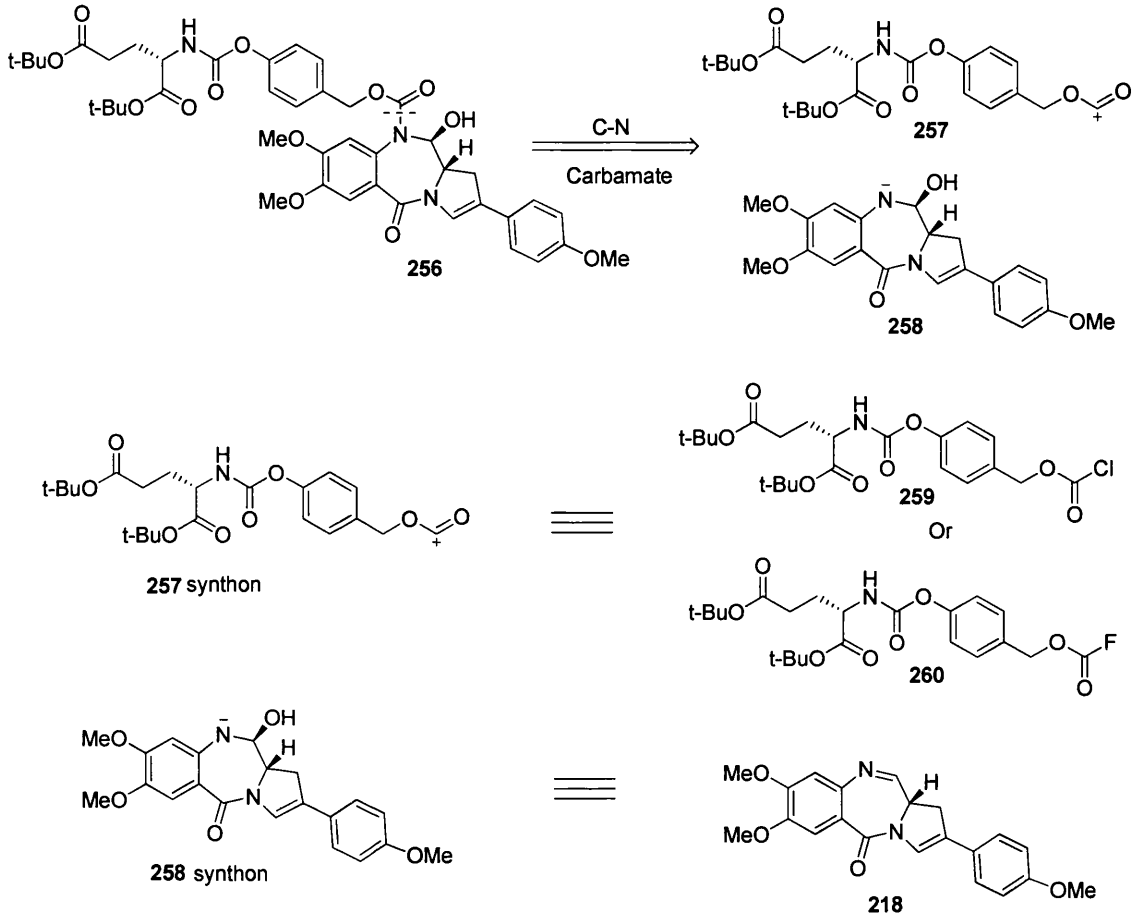

Scheme 42: Retrosynthesis 2 analysis of 256

4.5 Alternative Synthesis of C2-Aryl PBD Prodrugs

4.5.1 Model Study Part 1

The feasibility of the approach was investigated with simple chloroformates (i.e., those lacking an enzyme-labile moiety). The first model study (**Scheme 43**) introduced commercially available benzyl chloroformate to a C-ring unsubstituted imine PBD. A range of conditions was explored as shown in **Table 14**.

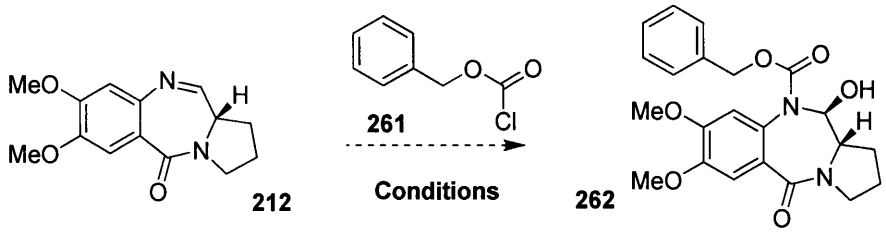

Scheme 43: Model study part 1

No.	X (conditions)	Result
1.	Benzyl chloroformate, pyridine, DCM, RT, N_2, 24 hours.	Unwanted side product [M+H] 247
2.	Benzyl chloroformate, sodium bicarbonate, THF/water, RT, N_2, 24 hours.	No reaction took place
3.	Benzyl chloroformate, sodium bicarbonate, toluene/water, RT, N_2, 5 days.	Desired product.

Table 14: Model study part 1 conditions

Treating the PBD imine with benzyl chloroformate in DCM at room temperature in the presence of pyridine for 24 hours failed to afford the desired N10 carbamate, yielding only an unidentified product with a $[M+H]^+$ ion at m/z 247 (the expected $[M+H]^+$ ion was at m/z 413). Treatment of the imine with benzyl chloroformate in aqueous THF failed to afford any product. However, prolonged exposure to the chloroformate in a two-phase toluene/water system with sodium bicarbonate gave the desired carbamate.

The ^1H NMR of the isolated product **262** (**Figure 48**) was compared with the ^1H NMR of authentic material (personal communication, Luke Masterson) using a Fukuyama approach (**Figure 49**). The ^1H NMR spectra were identical, and the MS/MS mass spectrum revealed the protonated $[M+H]^+$ ion at m/z 413 and a HRMS accurate mass $[M+H]^+$ ion at m/z 413.1703, confirming the success of this direct carbamoylation protocol.

The ^1H NMR spectrum exhibited a number of diagnostic features which could be helpful in the analysis of more complicated prodrugs. Two non-equivalent benzylic doublets were observed at 4.9 ppm and 5.4 ppm, and a multiplet was observed at 5.7 ppm arising from H-11. The complexity of the signal is a result of coupling to both the H-11a and the 11-OH hydroxy protons. This feature is useful, as it can be used to confirm the presence of a free hydroxyl group at the 11-position. Finally, the 9-H

signal was observed at a relatively upfield position (6.5 ppm) consistent with the presence of the electron-donating carbamate group.

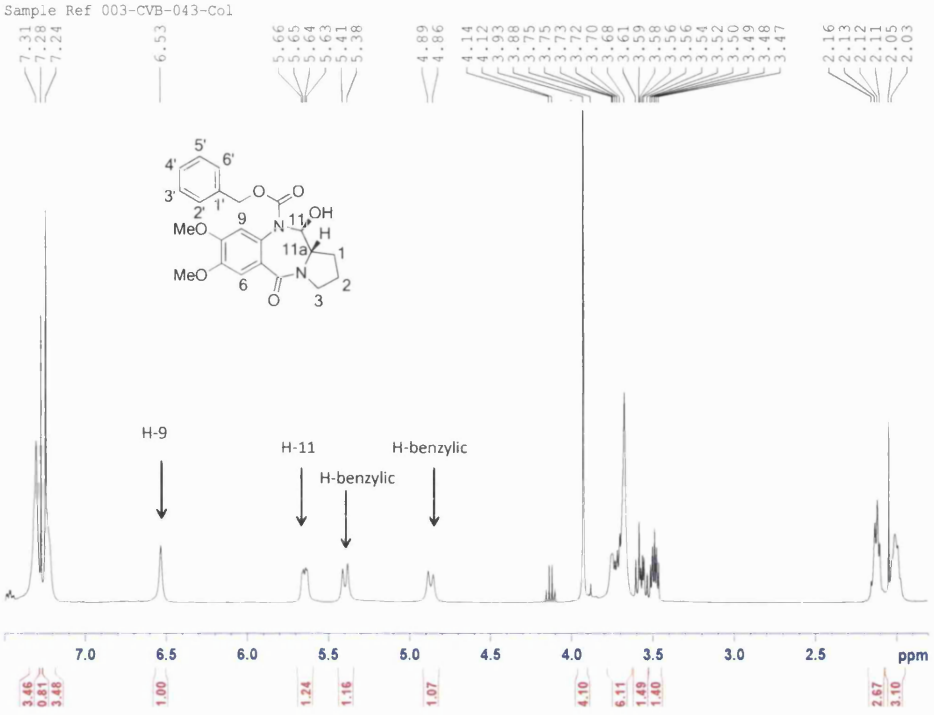

Figure 48: ^{1}H NMR Spectrum of 262 in $CDCl_3$ made via retrosynthesis 2

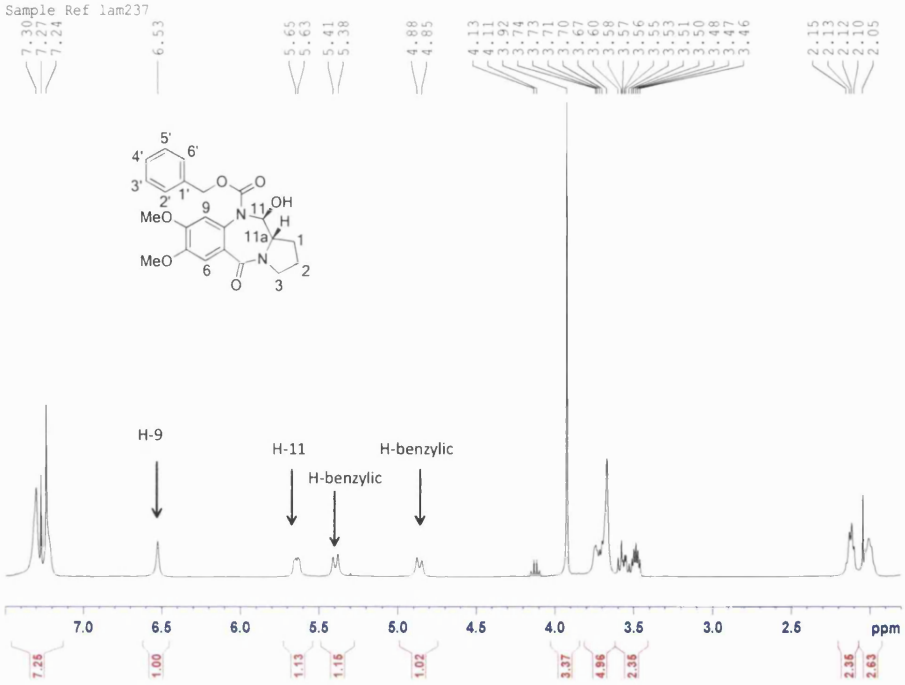

Figure 49: ^{1}H NMR spectrum of 262 made via the Fukuyama synthetic route in $CDCl_3$

4.5.2 Model Study Part 2

The second model study introduced the benzyl carbamate to the N10-position of the C2-aryl imine PBD **263** (synthesised utilising Cooper's route[117]), using the same conditions as applied previously to the simple imine PBD molecule (**Scheme 44**). Unfortunately, prolonged exposure to benzyl chloroformate and aqueous sodium bicarbonate in toluene failed to give the desired product, yielding mainly unreacted starting material. However, substituting DCM for toluene and allowing the reaction mixture to stir at room temperature for 24 hours yielded the desired carbamate in 30% yield. The structure was confirmed by NMR, LC/MS and HRMS.

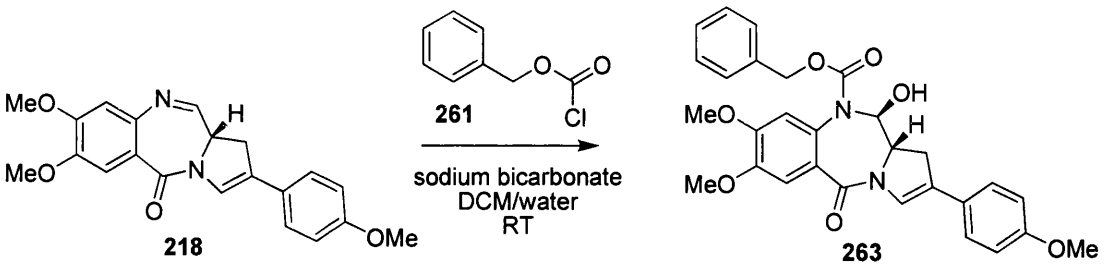

Scheme 44: Model study part 2

The MS/MS mass spectrum revealed the protonated $[M+H]^+$ ion at m/z 517 and a HRMS accurate mass $[M+H]^+$ ion at m/z 517.1962. The diagnostic peaks (*i.e.* benzylic protons) observed in the ^1H NMR spectrum along with mass spectrometric evidence confirmed the success of the direct carbamoylation protocol.

Interestingly, two peaks corresponding to the H1 protons (*i.e.* H-1 α and H-1 β) were recorded at 3.4 ppm and 3.1 ppm. The 0.4 ppm difference indicates that the chemical environment is substantially different on the opposing faces of the PBD ring system of **263** (**Figure 50**).

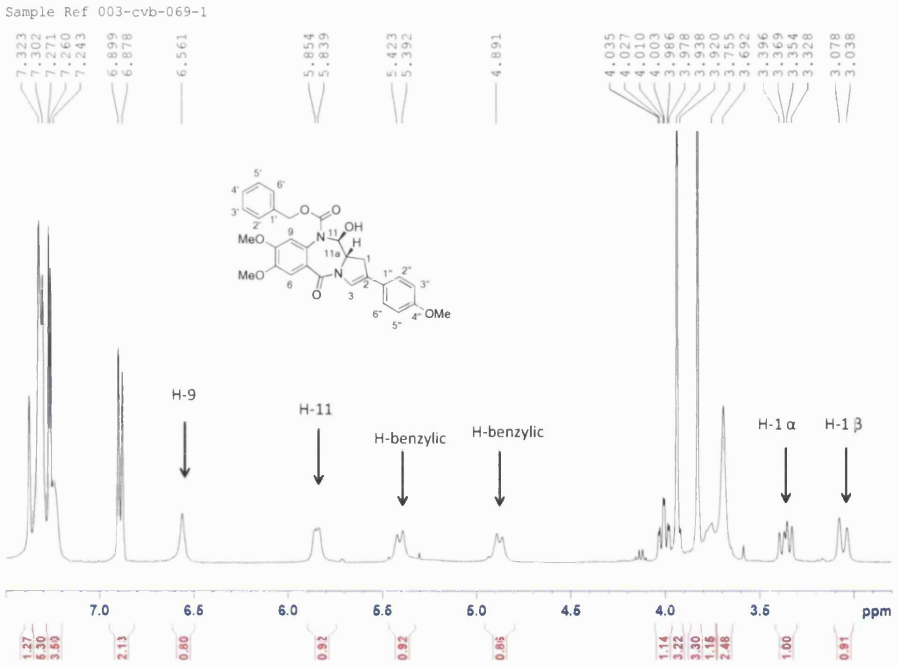

Figure 50: ^{1}H NMR of 263 in $CDCl_3$

A ^{1}H NMR D_2O shake simplified the H-11 signal, revealing a simple doublet. The observed *J*-value (9.52 Hz) was consistent with a large dihedral angle (170°, Karplus) and *(S)*-stereochemistry at the H-11 position (**Figure 51**).

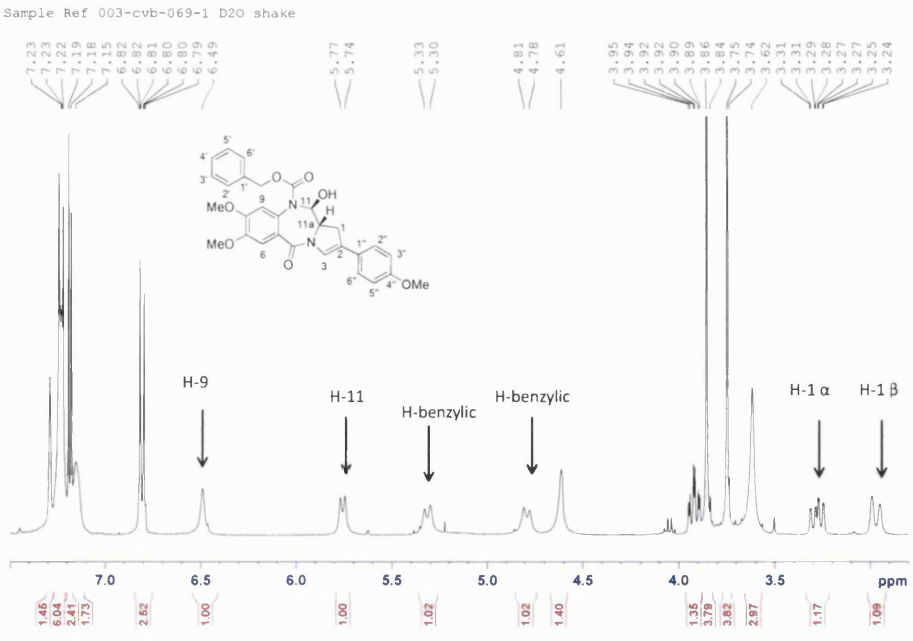

Figure 51: ^{1}H NMR of D_2O shake of 263 in $CDCl_3$

4.5.3 Molecules for Biological Evaluation with Nitroreductase

To investigate the scope of the reaction, benzyl chloroformate was replaced with the *p*-nitrophenyl analogue (**Scheme 45**). If the reaction was successful, the resulting carbamate could be of value to nitroreductase-based ADEPT or GDEPT studies.

The C2-aryl PBD imine (**218**) was treated with *p*-nitrophenylbenzyl chloroformate and aqueous sodium bicarbonate in DCM at room temperature for 3 days (**Scheme 45**).

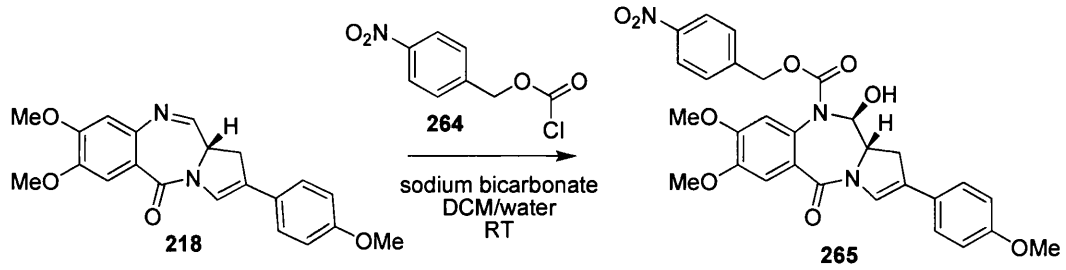

Scheme 45

The MS/MS mass spectrum of the product revealed a protonated $[M+H]^+$ ion at m/z 562.2 and HRMS accurate mass $[M+H]^+$ ion at m/z 562.1818. The ^1H NMR for **265** revealed the characteristic two non-equivalent benzylic doublets at 5.1 ppm and 5.3 ppm. Two peaks corresponding to the H1 protons (*i.e.* H-1 α and H-1 β) were recorded at 3.4 ppm and 3.0 ppm (**Figure 52**). Finally the 9-H signal was observed at a relatively upfield position (6.7 ppm) consistent with the presence of an electron-donating carbamate group.

The application of compound **265** to GDEPT studies will be discussed in **Section 6.4**.

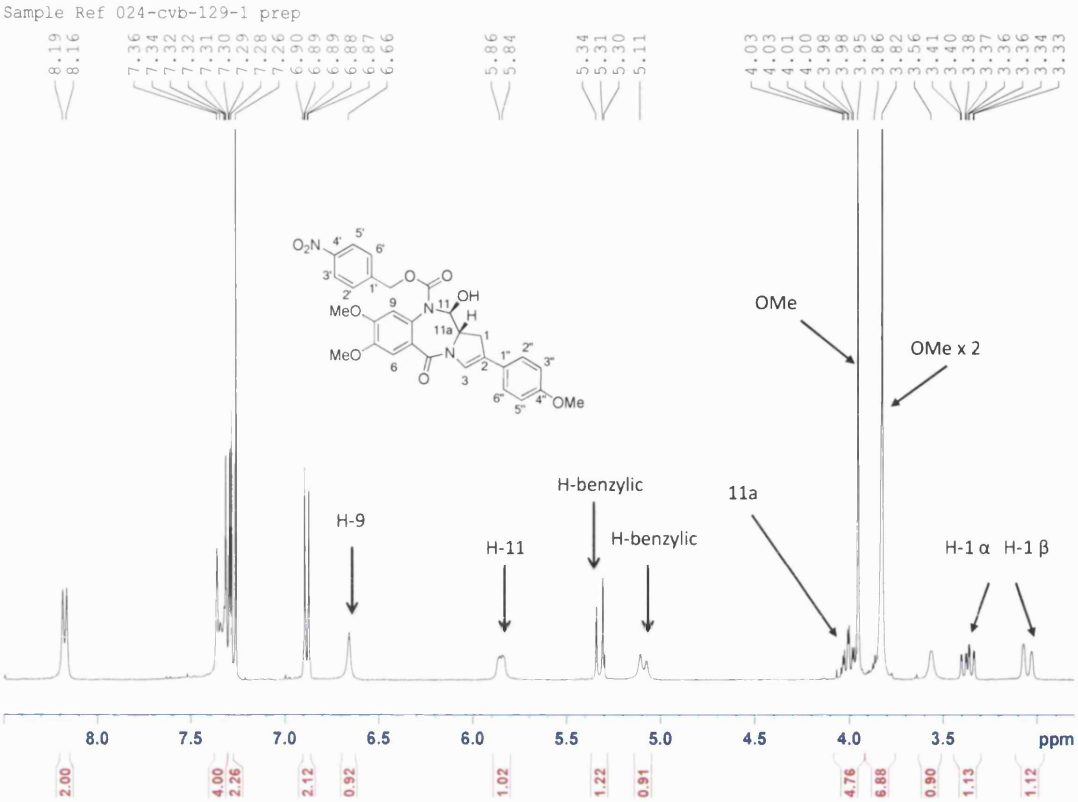

Figure 52: ^{1}H NMR of 265 in $CDCl_3$

4.6 Background to the Fluoroformate/Chloroformate Strategy

The next step was to synthesise the chloroformate or fluoroformate version of the progroup which could be introduced into the PBD in the same manner as for the benzyl carbamates (**Scheme 46**). Niculescu-Duvaz *et al.*[130] attempted to obtain the chloroformate of alcohol **228** using phosgene, diphosgene or triphosgene variety of experimental conditions but were unsuccessful. The chloroformates were reported to be unstable above -40 °C. [146] As a result they converted the progroup alcohol to the corresponding fluoroformate which was believed to be more stable.

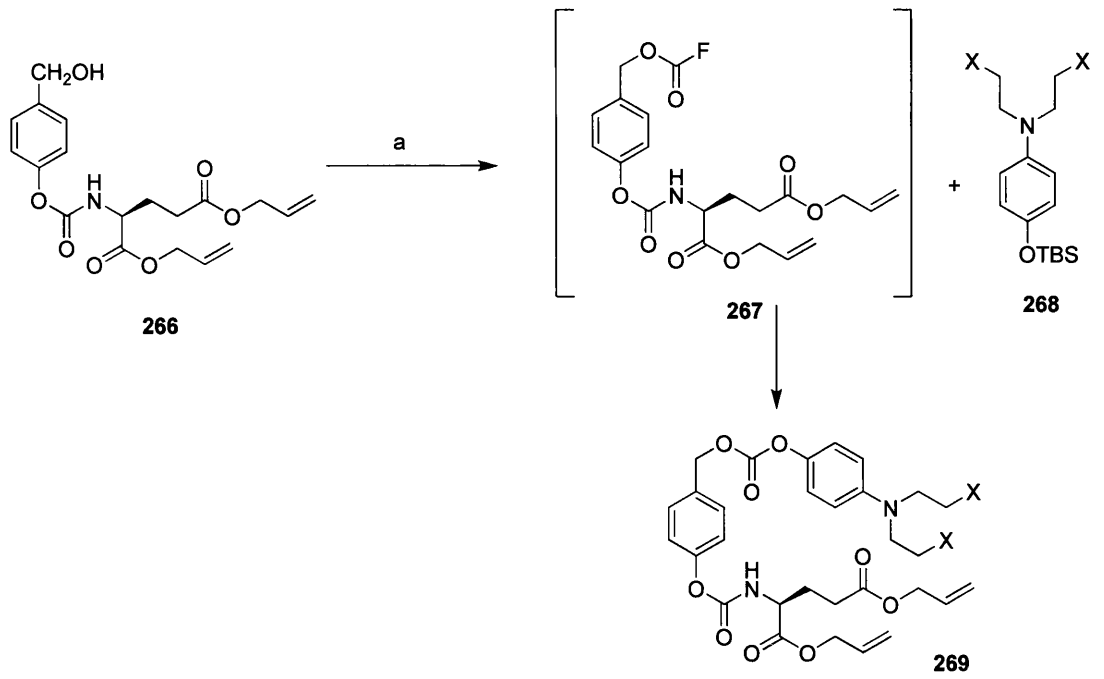

Scheme 46: Fluoroformate/chloroformate Strategy. a) $COCl_2$, KF.HF, 18-crown-6, -78°C

The fluoroformate of **266** was formed with phosgene, KF·HF and 18-crown-6 ether at -78°C in DCM, and then allowed to warm to room temperature and treated with the silylated nitrogen mustard **268** to afford **269**. However, coupling of the fluoroformate and the nitrogen mustard proceeded in a very low yield of only 5%.

4.6.1 Application of the Fluoroformate Approach to PBD N10-prodrug Synthesis

Attempts to apply the fluoroformate approach (**Scheme 47**) to the synthesis of PBD N10-prodrugs proved unsuccessful. The progroup **228** was treated with phosgene and KF·HF in the presence of 18-crown-6 at -78°C, and the mixture was allowed to stir overnight at room temperature. The PBD imine together with aqueous sodium bicarbonate was then added to the reaction mixture. Unfortunately evidence of the desired product could not be found, and LC/MS analysis indicated the presence of unreacted imine. It seems likely that the inherently low reactivity of the PBD imine (compared to a mustard amine) resulted in overlong reaction times, which lead to decomposition of the fluoroformate.

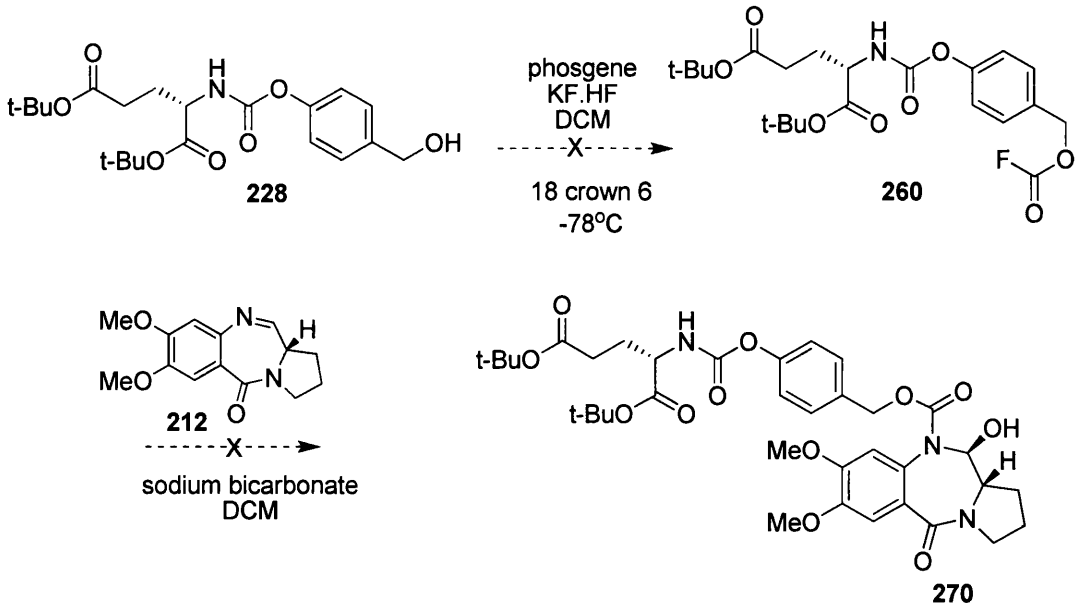

Scheme 47: Fluoroformate approach

4.7 p-Nitrophenyl Carbamate Displacement Strategy

As the fluoroformate strategy proved unsuccessful an alternative approach was required. Model studies had demonstrated that it was possible to introduce simple carbamates to imine PBDs.[147-149] Interestingly, Atwal *et al.*[150] had reacted nitrophenyl chloroformate with a series of pyrimidine compounds and used the resulting nitrophenyl carbamate intermediates to introduce various alcohols and amines (**Scheme 48**). They were then able to displace the nitrophenoxy moiety with ammonia in acetonitrile. The reaction mixture turned yellow instantaneously, indicating the liberation of the nitrophenol by-product and affording the product **273**. They also introduced the more complex *(S)*-1-methyl-2-[methyl(phenylmethyl)amino] ethyl alcohol in acetonitrile at 50°C to give **274** in an analogous fashion.

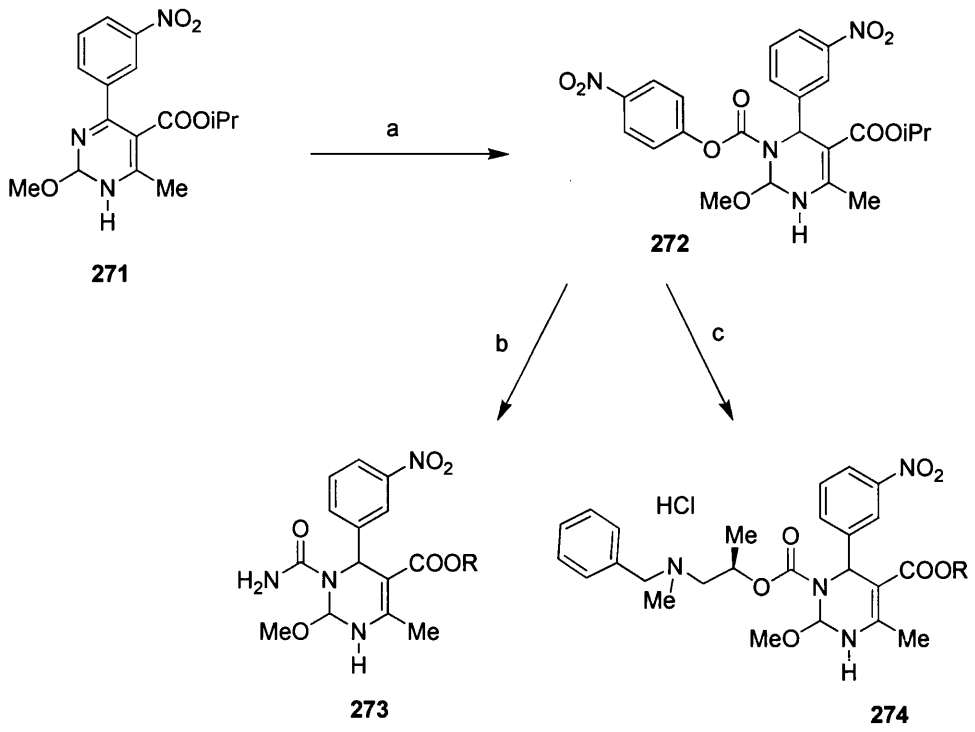

Scheme 48: Atwal *et al.* [150] a) 1. pyridine, *p*-nitrophenyl chloroformate, 2. THF, MeOH, HCl. b) acetonitrile, excess ammonia, RT. c) acetonitrile, excess ammonia, RT.

Alexander *et al.*[151] and Hudson *et al.* independently used nitrophenyl carbamate derivatives as intermediates in the synthesis of cephalosporins. Alexander *et al.* introduced the nitrophenyl carbamate in the presence of pyridine in THF (**Scheme 49**). Various conditions were used to replace the nitrophenyl moiety with amines. The nitrophenyl carbamate intermediate displacement reaction was performed in DMF at -26°C. Successful results were also achieved in DMSO and pyridine. Hudson *et al.* introduced the 4-nitrophenyl chloroformate with TEA in THF, at room temperature for 2 hours, and then also displaced the nitrophenoxy moiety with amines. Together the work of Alexander and Atwal suggests the possibility of using nitrophenyl carbamate as a reactive intermediate to introduce the alcohol progroup.[152]

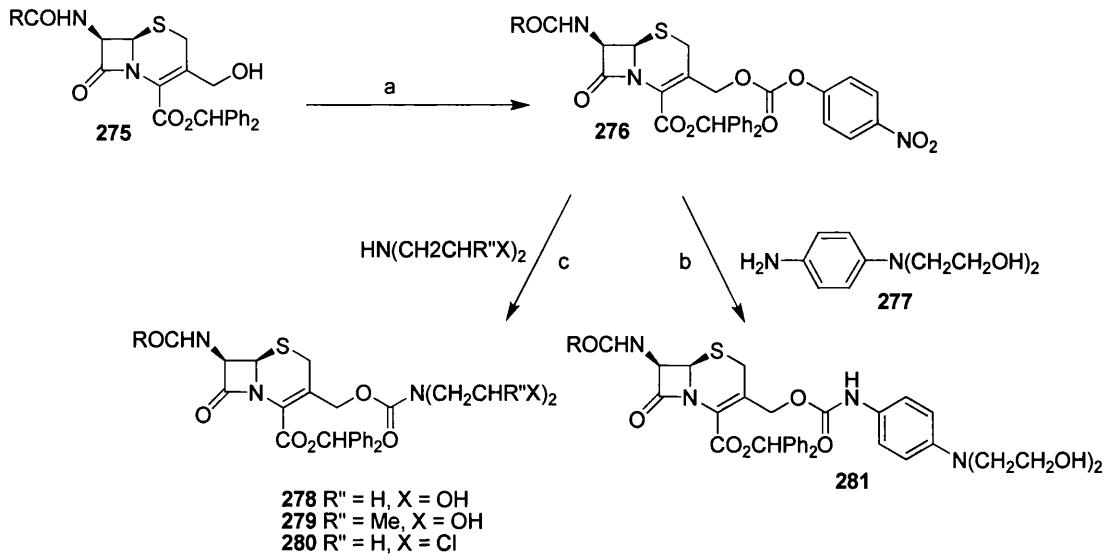

Scheme 49: Alexander *et al.*[151] a) *p*-nitrophenyl chloroformate, pyridine, THF. b) pyridine, 0°C, 2hr, DMSO. c) -26°C-RT, 1hr, DMF.

4.7.1 Model Study

The examples cited above suggest that it should be possible to introduce the progroup carbamate via a 4-nitrophenyl carbamate displacement strategy. The feasibility of this approach was investigated using a simple C-ring unsubstituted PBD imine. Commercially available 4-nitrophenyl chloroformate was introduced in the presence of aqueous sodium bicarbonate in DCM at room temperature (**Scheme 50**). NMR confirmed the desired product had been formed in 77% yield.

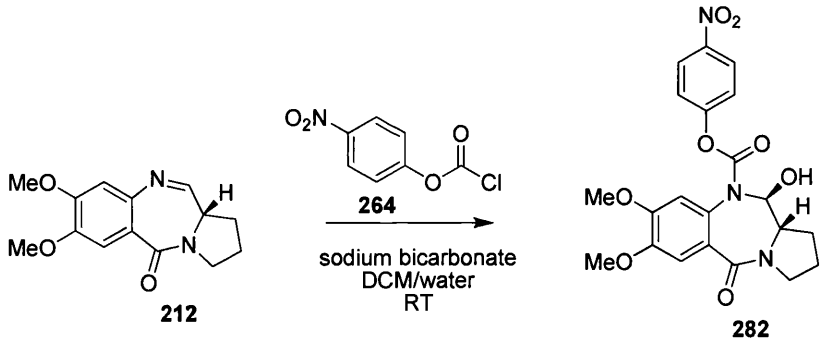

Scheme 50

The ^{1}H NMR spectrum clearly revealed two new sets of aromatic signals arising from the *p*-nitrophenyl group (**Figure 53**). A downfield doublet arising from the H-3'/H-5' protons was observed at 8.2 ppm; this was consistent with their proximity to the electron withdrawing nitro group. The second doublet was observed at 7.2 ppm,

consistent with the H-2'/H-6' protons position ortho to oxygen. The H-11 signal at 5.7 ppm was observed as a doublet of doublets, the complexity which resulted from coupling to both the H-11a proton and the 11-OH hydroxy proton. As with the benzyl carbamate model compounds, a high vicinal coupling constant was observed, consistent with a large dihedral angle and 11-*S* stereochemistry.

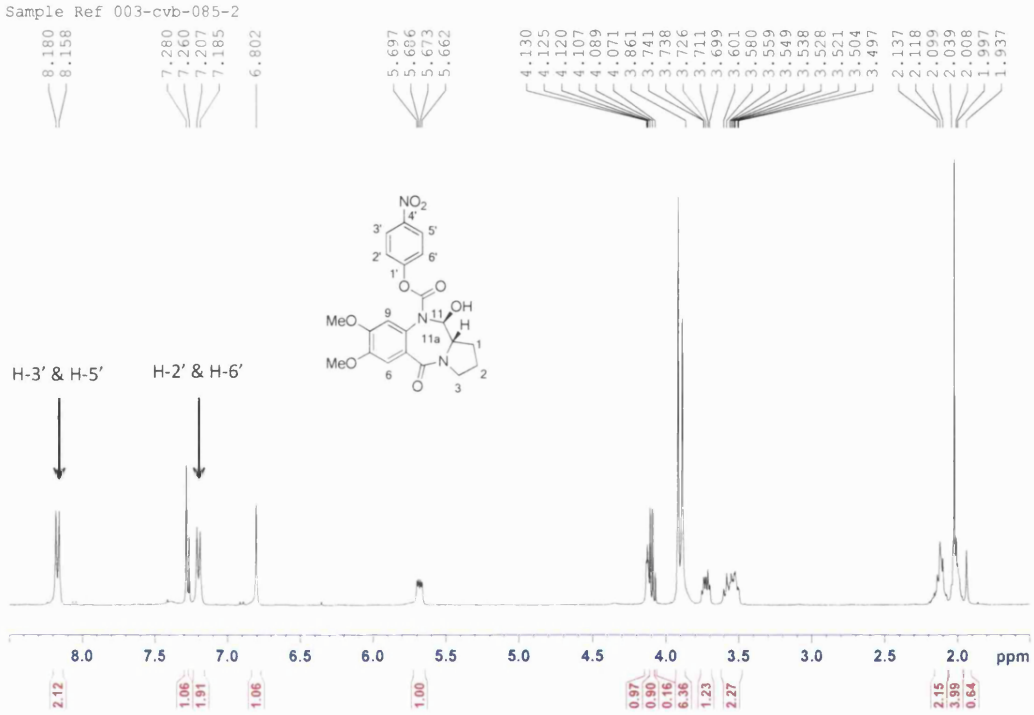

Figure 53: Full ^{1}H NMR spectrum of 282 in $CDCl_3$

4.7.2 Displacement of the Nitrophenyl with a Benzyl Group

The alkoxide of the benzyl alcohol was prepared overnight with potassium *tert*-butoxide. The N10 4-nitrophenyl carbamate was added to the alkoxide, resulting in the formation of a yellow solution, indicating the liberation of the *p*-nitrophenoxy group. LC/MS analysis revealed the formation of two new products: the desired benzyl carbamate and the PBD imine. It seems likely that the parent imine was formed through alkaline hydrolysis of the 4-nitrophenyl carbamate. Comparison with LC/MS data from the earlier model studies confirmed the successful displacement of the *p*-nitrophenoxy group with benzyl alcohol.

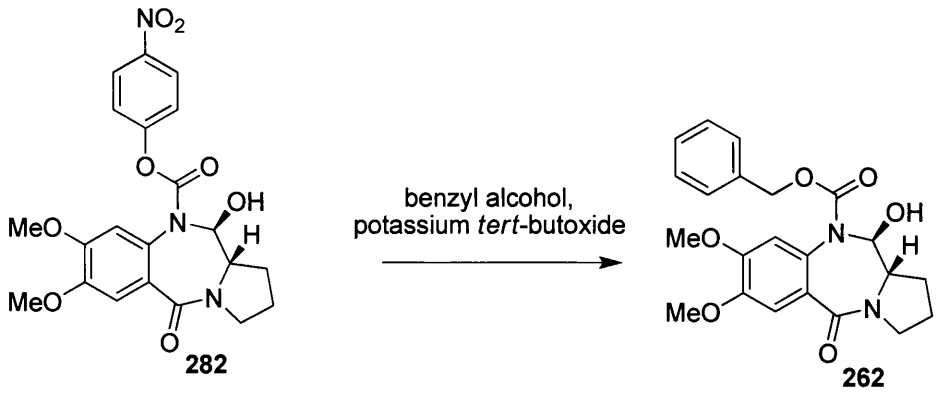

Scheme 51: Displacement of nitrophenyl with benzyl group

4.7.3 Displacement of the Nitrophenyl Group with the Alcohol Progroup

The model reaction conditions were applied to the introduction of the required N10 progroup. Progroup alcohol **228** was deprotonated with potassium *tert*-butoxide in DMF overnight, and the resulting alkoxide was treated with the N10-*p*-nitrophenoxy carbamate **282** in DMF. ^{1}H NMR confirmed that the desired product **270** had been formed in 26% yield; however, the major component isolated from the reaction mixture corresponded to recovered PBD imine **212**.

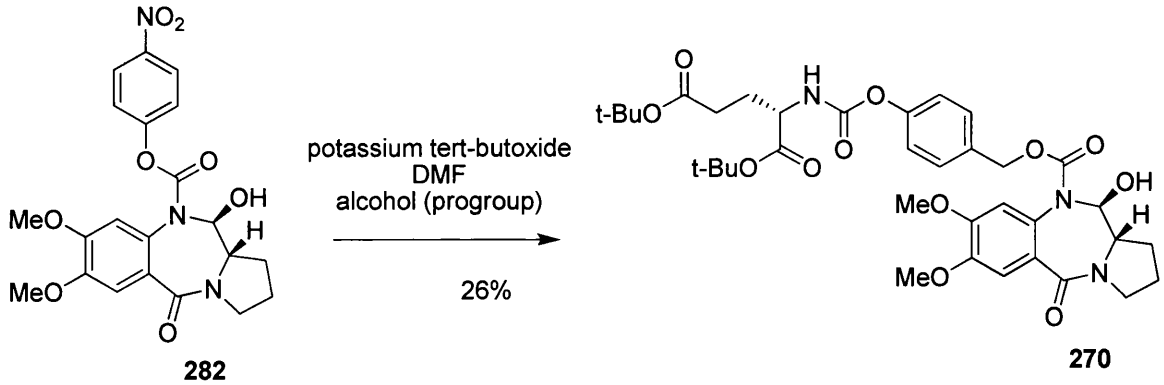

Scheme 52: Displacement of the nitrophenyl group with the alcohol progroup 228

The ^{1}H NMR spectrum revealed signals which appeared to arise from both the PBD and progroup portions of the target molecule (**Figure 54**). However, a molecular ion could not be observed in the mass spectrum (**Figure 55**). Nevertheless, the results were sufficiently encouraging to justify proceeding to the target C2-aryl substrate.

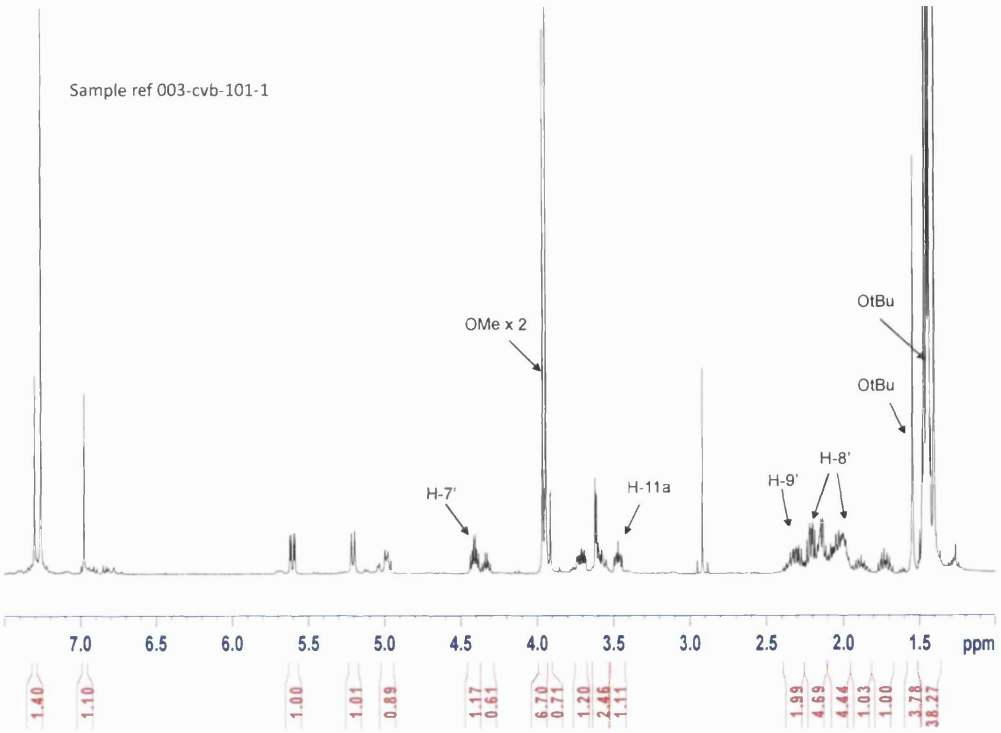

Figure 54: Full ^{1}H NMR spectrum of 270 in $CDCl_3$

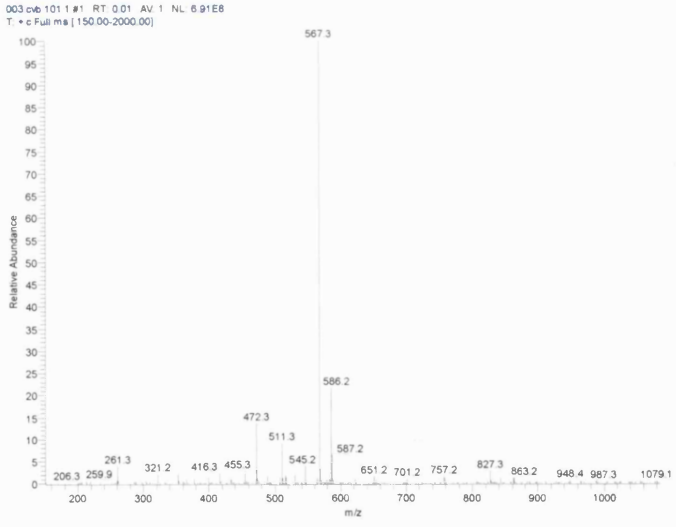

Figure 55: Full mass spectrum of compound 270

4.7.4 p-Nitrophenyl Carbamate Displacement Strategy

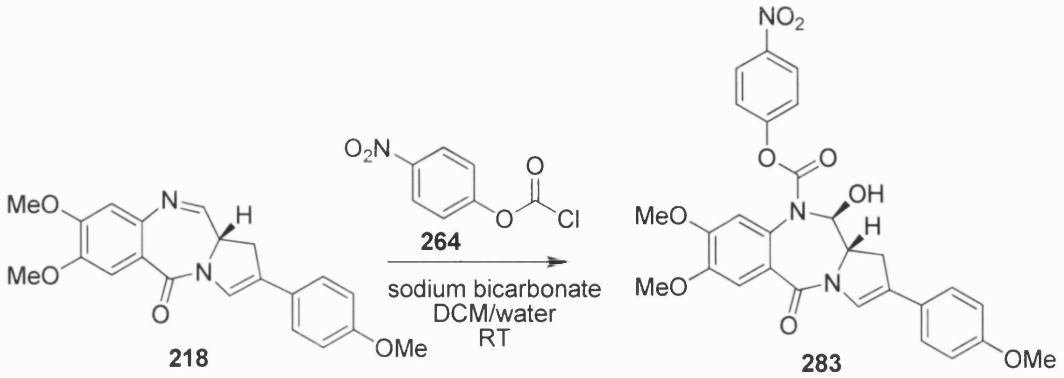

Scheme 53

The first step was to introduce the *p*-nitrophenyl carbamate to the more complicated C2-aryl substituted PBD imine (**Scheme 53**). The C2-aryl PBD imine was treated with *p*-nitrophenyl chloroformate under the conditions described in **Section 4.5**. Although it was difficult to purify the reaction mixture, two products were successfully isolated. The minor product corresponded to the desired N10 PBD carbamate, obtained in 15% yield. However, the major product (49%) required extensive NMR and mass spectrometric analysis for structural determination.

4.7.4.1 NMR Investigation of Major Product 284

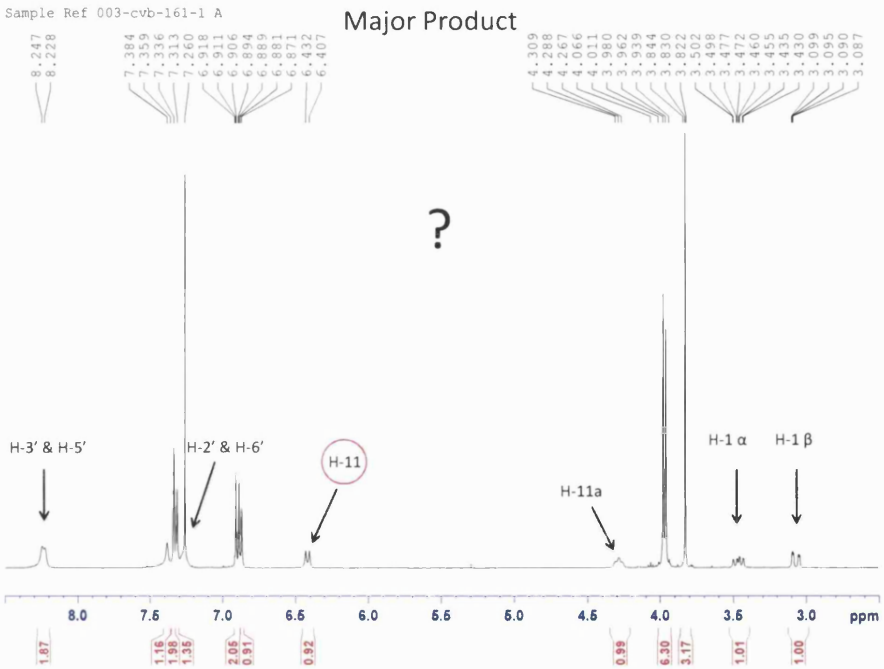

Figure 56: ^{1}H NMR spectrum of 284 in $CDCl_3$

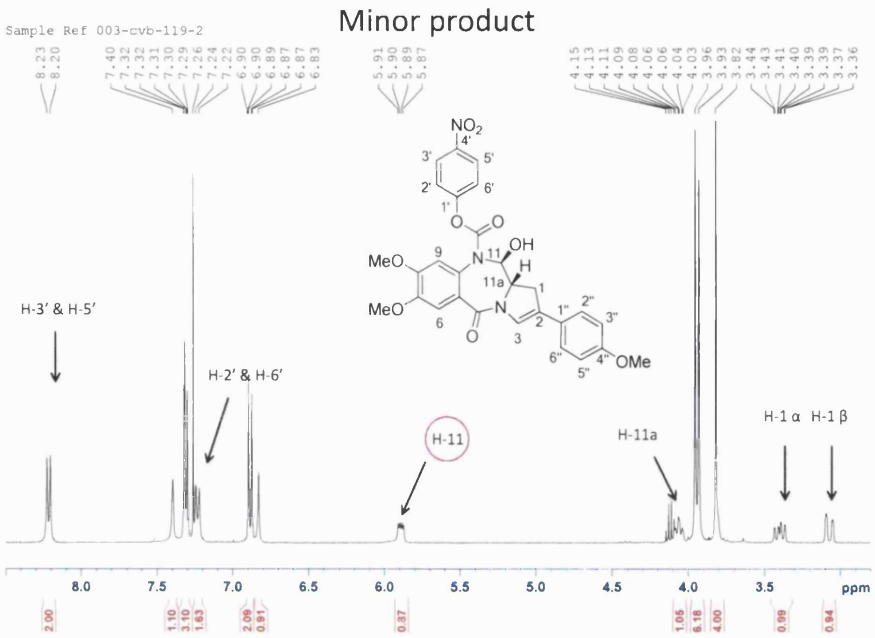

Figure 57: ^{1}H NMR spectrum of 283 in $CDCl_3$

A comparison of the ^{1}H NMR spectra of the major and minor products **(Figures 56 and 57,** respectively or **Figure 58**), clearly showed a downfield shift of the resonance assigned to H11. A doublet of doublets was observed at 5.89 ppm (J = 4.56, 9.56 Hz) in the spectrum of the desired product (minor component) and a doublet was observed at 6.42 ppm (J = 10.16 Hz) in the case of the major component, indicating a change in the chemical environment of the H11 proton, possibly due to the presence of an electronegative group at C11-position.

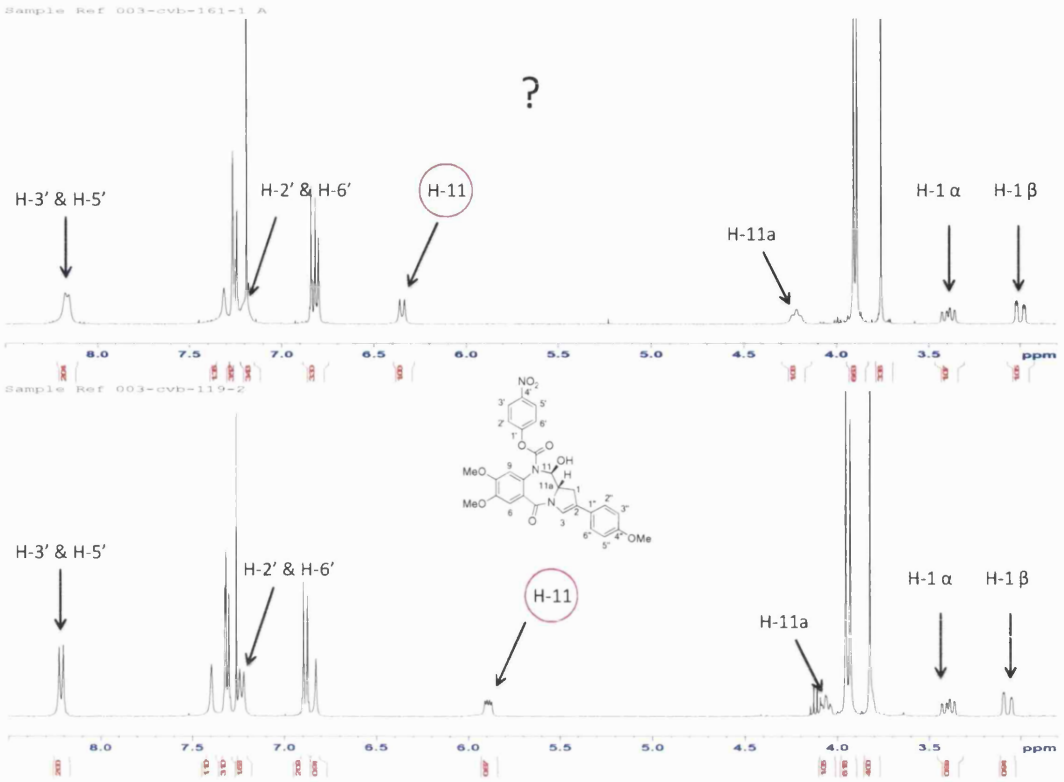

Figure 58: Expanded for comparison ^{1}H NMR spectrum of major product 284 and minor product 283

Comparison of the aromatic regions of the major and minor products revealed a change in the shape of the doublet (H-3' and H-5') at 8.23 ppm (**Figure 59**). In the spectrum of **283,** H-3' and H-5' doublets are well-defined and sharp, whereas for the unknown product (**284**) the H-3' and H-5' signals are broad and rounded. The aromatic H-2'and H-6' doublets have also altered. In the desired product, a doublet can be observed at 7.22-7.24 ppm, whereas in the spectrum of the unknown product, the H-2' signal is obscured by the chloroform signal.

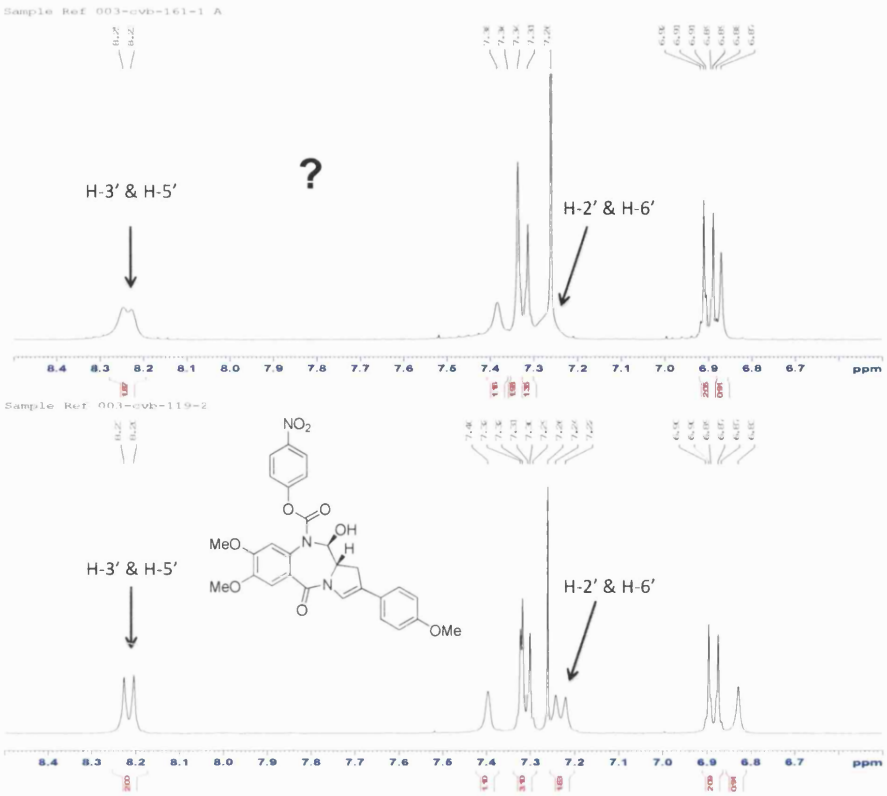

Figure 59: Expansion of the aromatic region of the major product 284 (above) and minor product 283 (below) in $CDCl_3$

The COSY NMR spectra shown in **Figures 60** and **61** reveal a correlatation between the 1α, 1β, 11a and 11 proton signals. The correlation between the doublet at 6.4 ppm and the doublet of doublets at 5.9 ppm and their respective H-11a signals comfirms their identity as H-11 protons. Indeed, the overall similarity of the spectra strongly suggests that the molecules only differ in their subsitution at the 11-position.

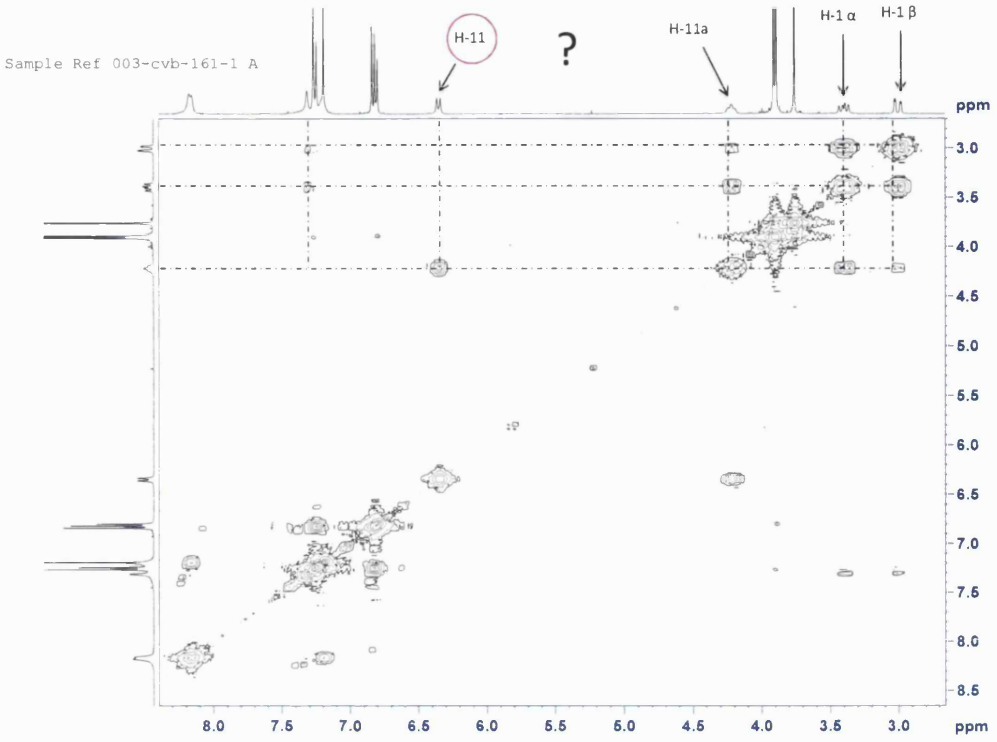

Figure 60: COSY NMR of major product 284 in $CDCl_3$

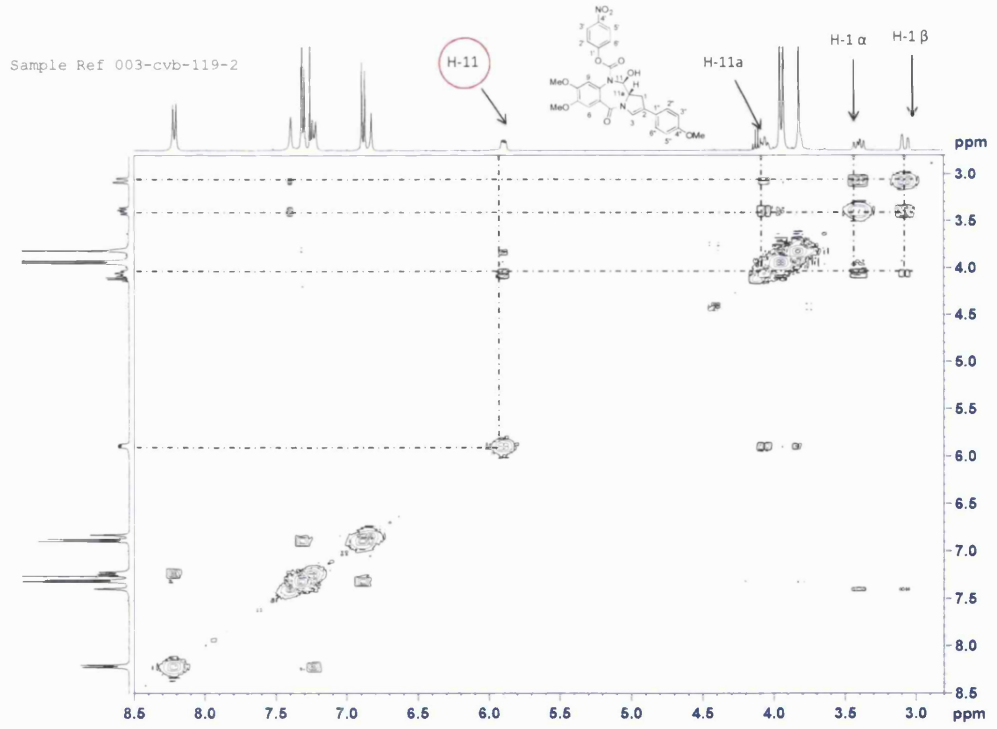

Figure 61: COSY NMR of minor product 283 in $CDCl_3$

4.7.4.2 Mass Spectrometric Evidence

The full mass spectrum of the minor product revealed a protonated $[M+H]^+$ ion at m/z 548, consistent with a molecular weight of 547. The major component revealed a protonated $[M+H]^+$ ion of 566, and further investigation of the m/z 566 and m/z 548 fragments was performed with MS/MS (**Figure 62**).

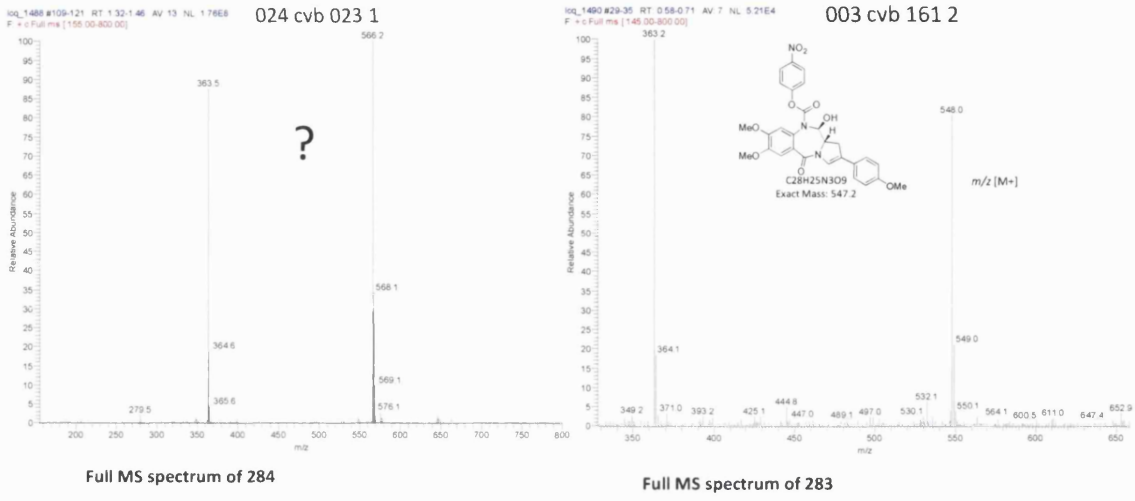

Figure 62: Full mass spectrum of 284 and 283.

4.7.4.3 MS/MS Investigation

The MS/MS instrument (as an ion trap instrument) consists of two mass separating devices (MS_1 and MS_2) arranged in series, in an in-time mode. The product-ion scan is recorded when a precursor-ion is selected by MS_1, fragmented by collision-induced dissociation, and its fragment ions recorded by scanning MS_2.

The $[M+H^+]$ ion of the major product (m/z 566) was subjected to MS/MS, yielding a new fragment ion at m/z 530, a difference of 36 suggesting the presence of a chlorine ion (**Figure 63**) Similar treatment of the desired product also yielded a fragment ion at 530 m/z, in this case consistent with loss of water (18 mass units) confirming the presence of the 11-OH. The mass spectrometric evidence further supports the similarity of the products, indicating only slight differences in structure.

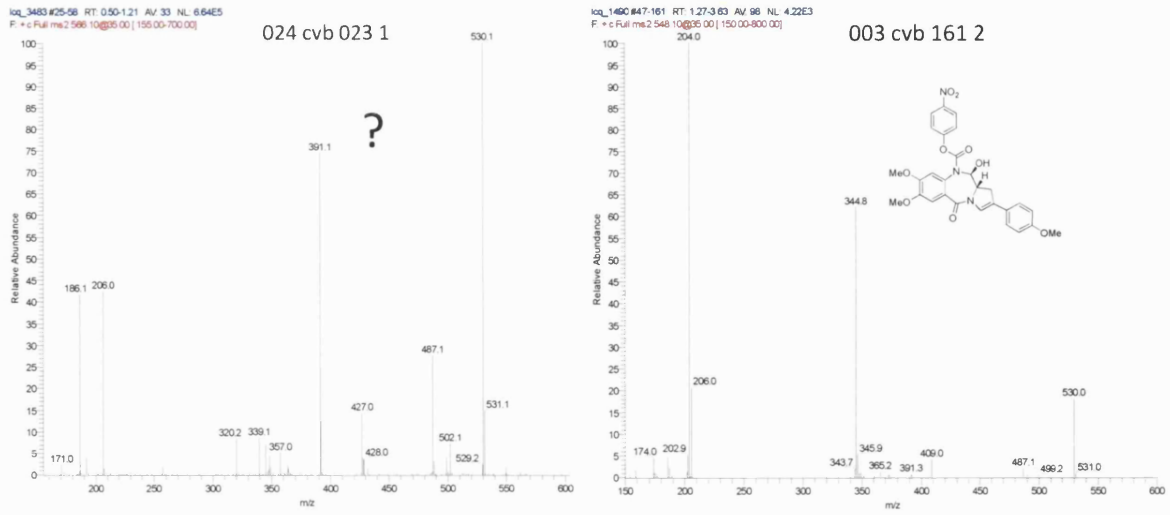

Figure 63: MS/MS of 284 and 283

In an expansion of the **284** spectrum, the $[M+H]^+$ ion around m/z 566 shows an isotopic pattern similar to that expected for a molecule containing a single chlorine atom. When the hydroxyl group of **283** was substituted for chlorine at the C11 position, a theoretical mass spectrum was generated **284** (see **figure 64**).

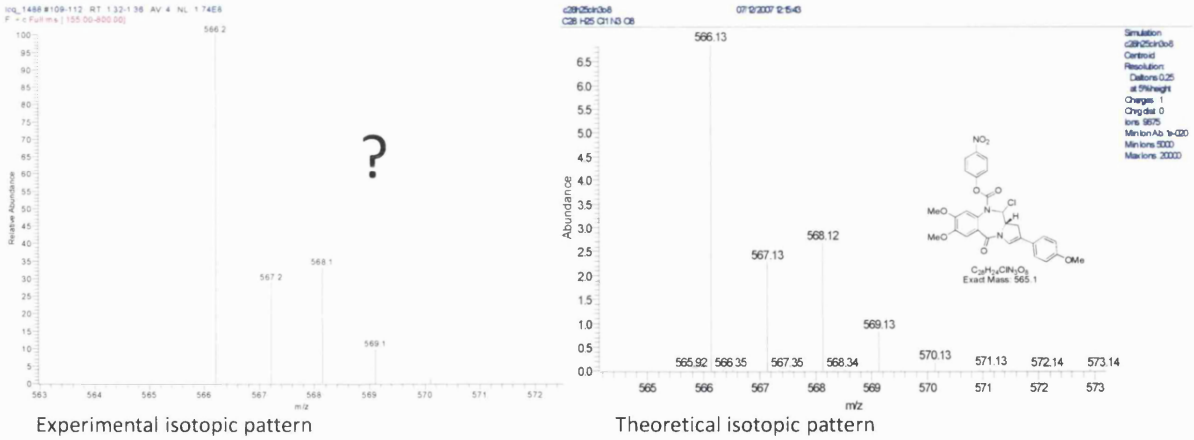

Figure 64: MS/MS isotopic pattern of 284 and theoretical isotopic pattern for $C_{28}H_{25}ClN_3O_8$

A comparison of the theoretical isotopic pattern and experimental isotopic pattern above (**Figure 64**) revealed that they are identical.

An 11-chloro substituent should deshield the 11-H proton and simplify its splitting pattern (with respect to the 11-hydroxy compound) to exhibit as a simple doublet. The evidence for an 11-chloro group in the mass spectrum supported the NMR data, as the presence of an 11-chloro group, would explain the downfield shift of the H-11 signal

and **284** could therefore be confidently indentified as the H-11 chloro compound **(Figure 65).**

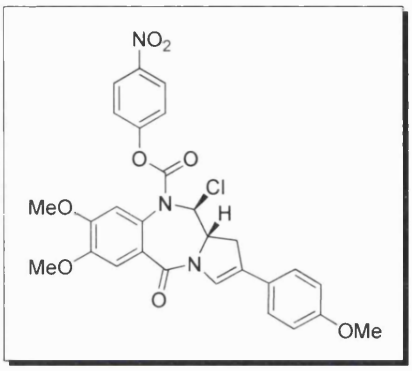

Figure 65: Structure of 284

4.7.4.4 Proposed Mechanism of C-11 Chloride Formation

The proposed mechanism in **Scheme 54** below explains the addition of chlorine to the C11-position. The mechanism suggests that after *p*-nitrophenyl chloroformate addition to the PBD imine, the nitro electron-withdrawing group facilitates the attack of the weakly nucleophlic chloride ion at the C11 position.

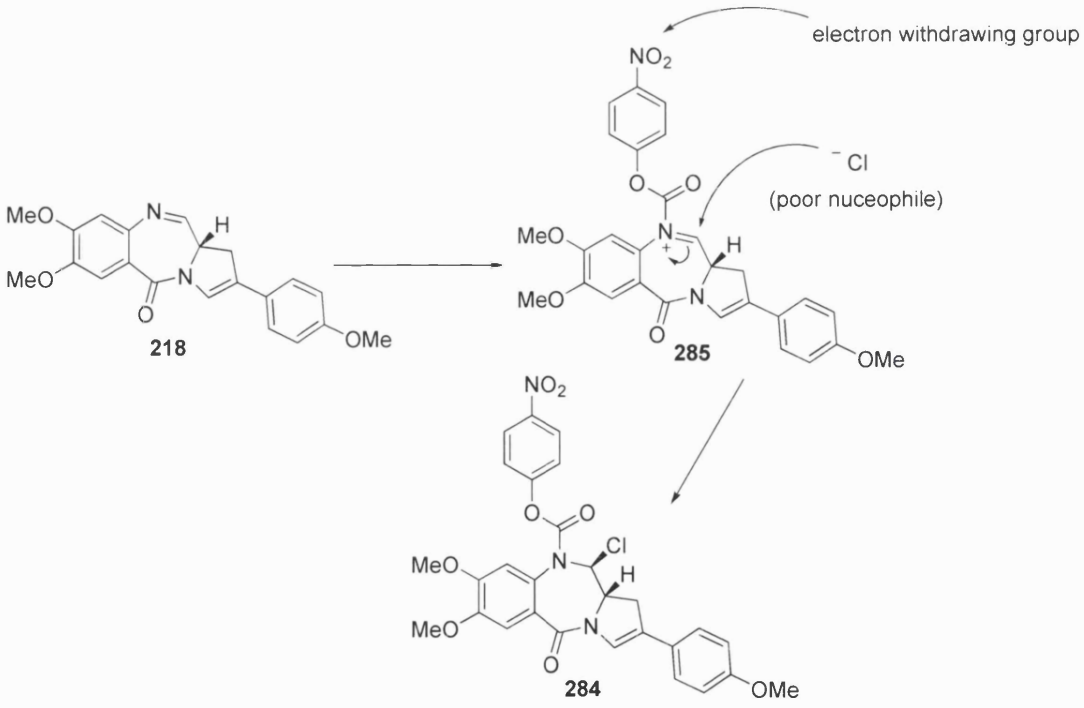

Scheme 54

4.7.5 Displacement of Nitrophenyl with Methoxy Group

The 11-chloro substituted compound **284** was treated with freshly prepared sodium methoxide. As expected, the *p*-nitrophenyl group was replaced by a methoxy group (**Scheme 55**). However, NMR (and MS data) revealed that the 11-chloro group was also displaced affording the MOC-protected carbinolamine methyl ether **286.**

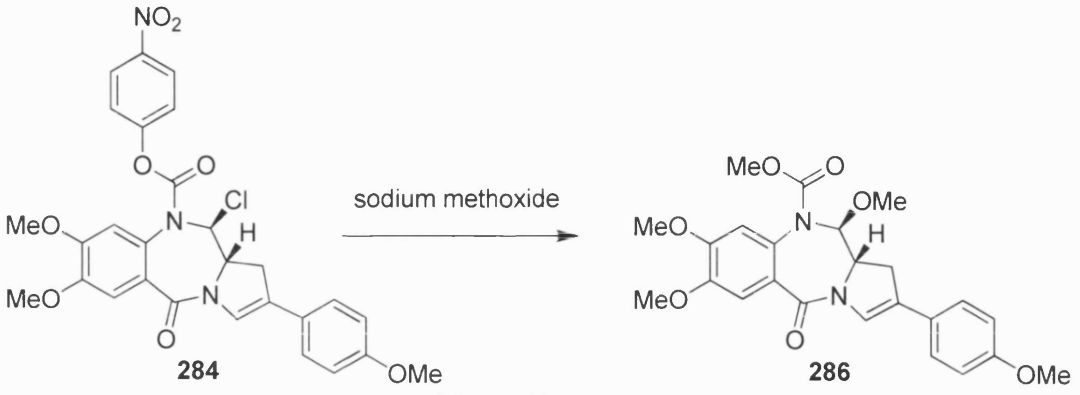

Scheme 55

The ^{1}H NMR spectrum (**Figure 66**) showed the appearance of two singlets at 3.65 ppm and 3.61 ppm corresponding to the two new methoxy groups. The disappearance of the nitrophenyl aromatic signals H-2', H-3', H-5'and H-6' was also evident.

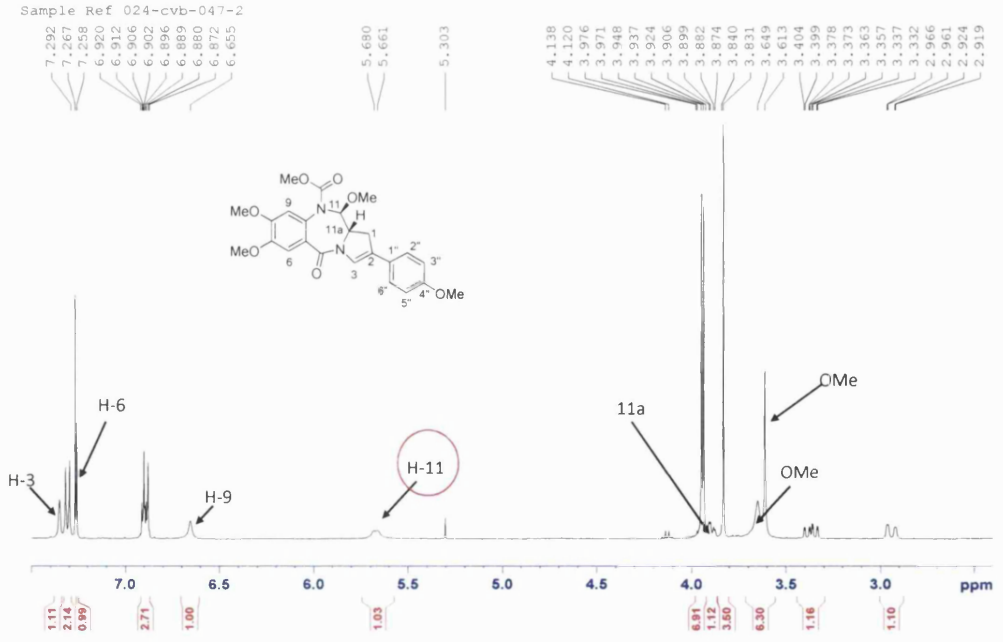

Figure 66: ^{1}H NMR spectrum of 286 in $CDCl_3$

The MS/MS mass spectrum revealed a protonated $[M+H]^+$ ion at m/z 455 indicating a molecular weight of 454, equivalent to **286**. A HRMS accurate mass $[M+H]^+$ ion at m/z 455.1805 was also obtained.

The $[M+H^+]$ ion (m/z 455) of **286** was subjected to MS/MS, yielding a new fragment ion at m/z 423, a difference of 32 suggesting the presence of a methoxy ion. Similarly, MS/MS of the fragment ion m/z 423 revealed a new mass at m/z 391, a difference of 32 suggesting the presence of a second methoxy ion. This evidence supported the presence of two additional methoxy groups, one at the C11 position while the other corresponded to the N10-methoxy carbamate (**Figure 67**).

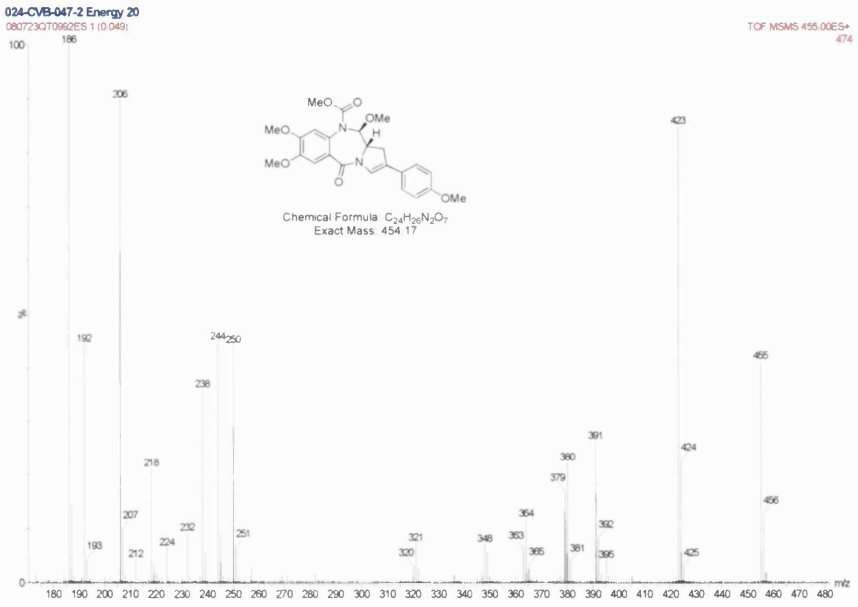

Figure 67: MS/MS fragmentation pattern of 286

4.7.6 Selective Substitution of Chlorine for a Methoxy Group

Chlorination at the C11 position and the subsequent double displacement of the nitrophenoxy and chloro groups by the methoxide ion, raised the possibility spectre of introducing two progroup moieties at the C11 as well as the N10 positions.

Fortunately, the chloro group proved much easier to displace than the *p*-nitrophenoxy group, allowing selective introduction of a methoxy group at C11 without affecting the N10 *p*-nitrophenoxy carbamate. Therefore, selective

displacement of the C11-chloro group was possible on prolonged exposure of **287** to methanol (**Scheme 56**).

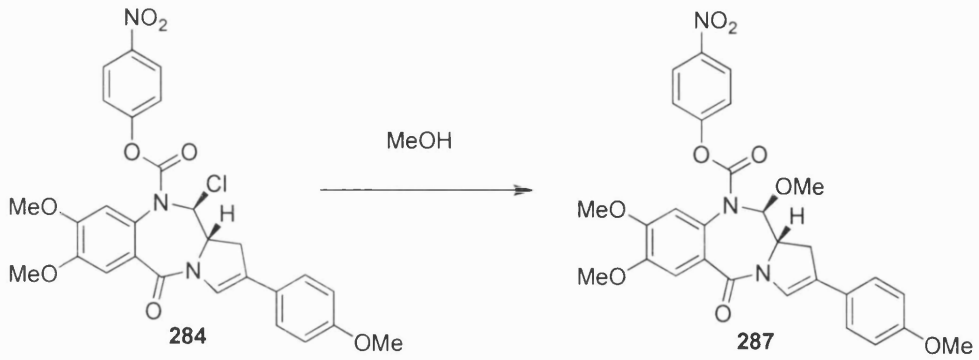

Scheme 56

The ^{1}H NMR (**Figure 68**) revealed a new signal, a singlet corresponding to the additional methoxy group. There was a significant shift in the frequency of the H-11 signal; it had moved upfield due to the presence of a less electronegative methoxy group at the C-11.

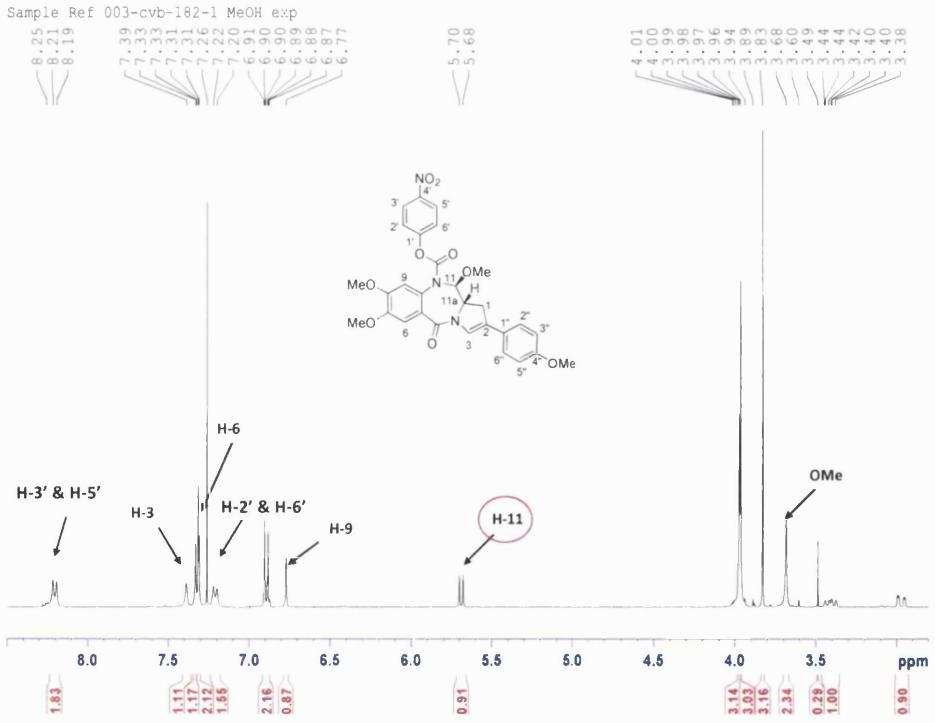

Figure 68: ^{1}H NMR spectrum of 287 in $CDCl_3$

The MS/MS mass spectrum revealed the protonated $[M+H]^+$ ion at m/z 562, indicating a molecular weight of 561, the same molecular mass as **287**. The HRMS accurate mass $[M+H]^+$ ion was found to be m/z 562.1837.

The $[M+H^+]$ ion (m/z 562) of **287** was subjected to MS/MS, yielding a new fragment ion at m/z 530, a difference of 32 suggesting the presence of a methoxy ion (**Figure 69**). The mass spectrometry evidence further supported the similarity of **287** to the products from **Figure 64** indicating only slight differences in structure of the three molecules.

This experiment demonstrated that it was possible to exchange the H-11 chlorine of **284** to a methoxy, to afford the N10-protected carbinolamine methyl ether **287**. It should be remembered that naturally occurring PBDs are often isolated as their C11-carbinolamine methyl ethers.

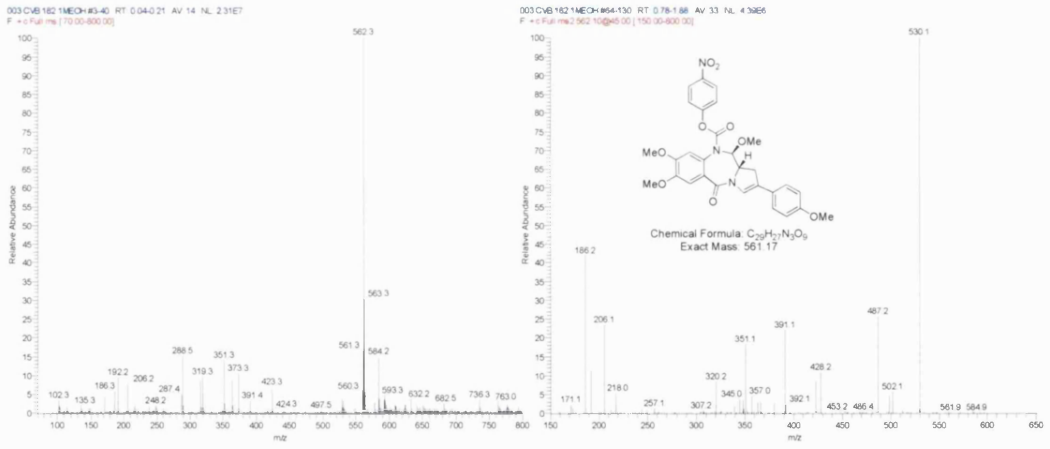

Figure 69: Full mass spectrum of compound 287 and MS/MS of m/z 562 from compound 287.

4.7.8: ^{1}H NMR Comparison of 11-substituent N10 p-nitrophenyl Carbamate

Figure 70 shows the ^{1}H NMR spectra of the 11-hydroxy, 11-chloro and 11-methoxy (**283, 284, 287**) N10-*p*-nitrophenoxy PBD carbamates.

Not, surprisingly, the shift of the H-11 signal is very sensitive to the nature of the C11 substituent. H-11 is further upfield in the 11-methoxy compound and further downfield for the 11-chloro species. As noted previously, the hydroxyl substituted

compound presents a more complex signal (doublets of doublets signal for H-11) due to additional coupling to the hydroxy proton.

Interestingly, the *p*-nitrophenyl aromatic protons are much sharper in the 11-hydroxy compound. This may be the result of hydrogen bonding between the carbamate carbonyl oxygen and the 11-hydroxy group (**Figure 71**). This would lock the molecule into one conformation. The broadness of the aromatic signals in the other spectra may result from a time-averaged effect caused by rotation of the carbamate (whose C11 substituent cannot contribute to H-bonding).

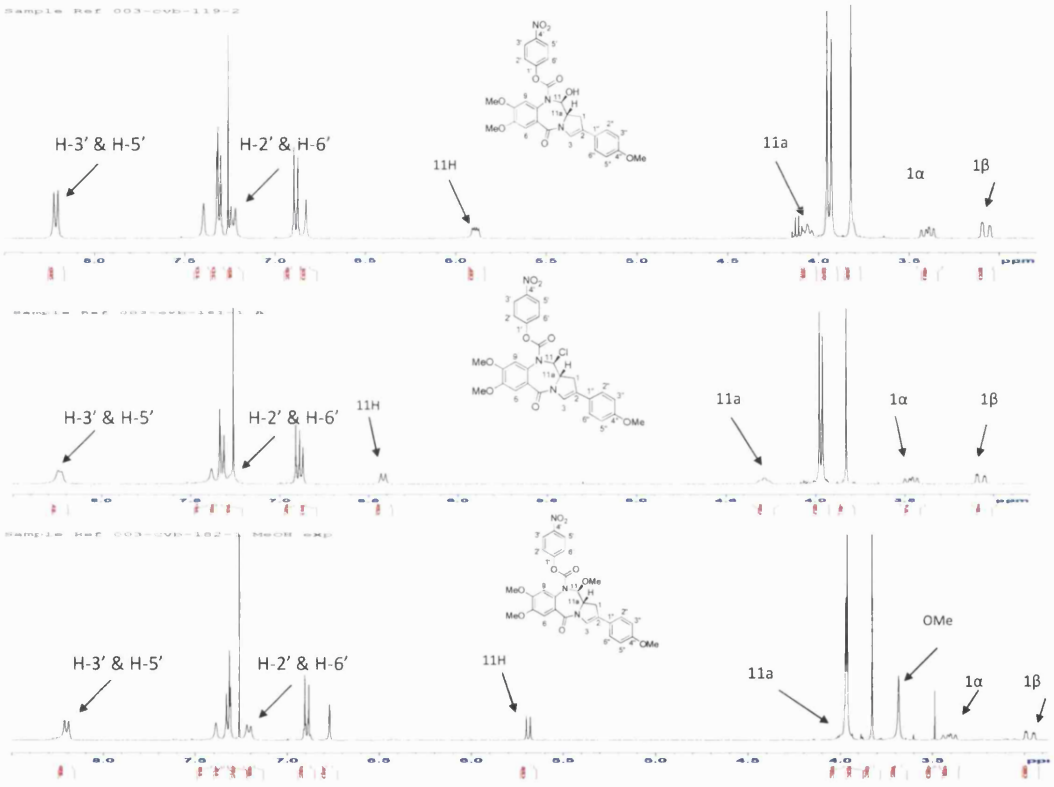

Figure 70: ^{1}H NMR comparison of 283, 284 and 287 in $CDCl_3$.

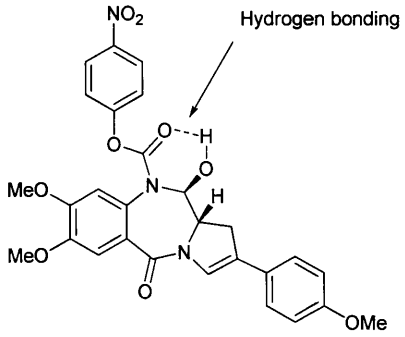

Figure 71: Hydrogen bonding between the N10-carbamate carbonyl oxygen and the 11-hydroxy group.

4.7.9 Displacement of Nitrophenyl with p-Methoxy Benzyl Alkoxide

In order to investigate the scope of the displacement reaction, the nitrophenyl was replaced with *p*-methoxy benzyl alcohol. The substrate represents a simplified (and in principle more stable) version of the self-immolative prodrug. As well as extending the scope of the synthesis, the resulting carbamate was considered useful for biological and biophysical comparison with the prodrug.

The alkoxide of 4-methoxybenzyl alcohol was prepared overnight and added to p-nitrophenyl carbamate **287**. As expected, the *p*-nitrophenyl group was replaced by a 4-methoxybenzyl alkoxide but in low yield (8%), suggesting an alternative reaction route should be considered (**Scheme 57**).

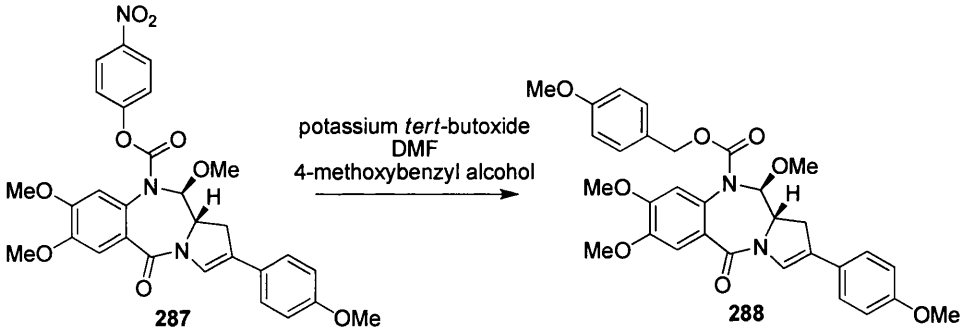

Scheme 57

The ^{1}H NMR of **288** (**Figure 72**) revealed five singlets between 3.4 and 3.9 ppm corresponding to the five methoxy groups. The characteristic two non-equivalent benzylic doublets were observed at 4.8 ppm and 5.3 ppm. Two peaks corresponding to the H1 protons (*i.e.* H-1 α and H-1 β) were recorded at 3.4 ppm and 3.0 ppm, and the 9-H signal was observed at a relatively upfield position (6.5 ppm) consistent with the presence of the electron-donating carbamate group.

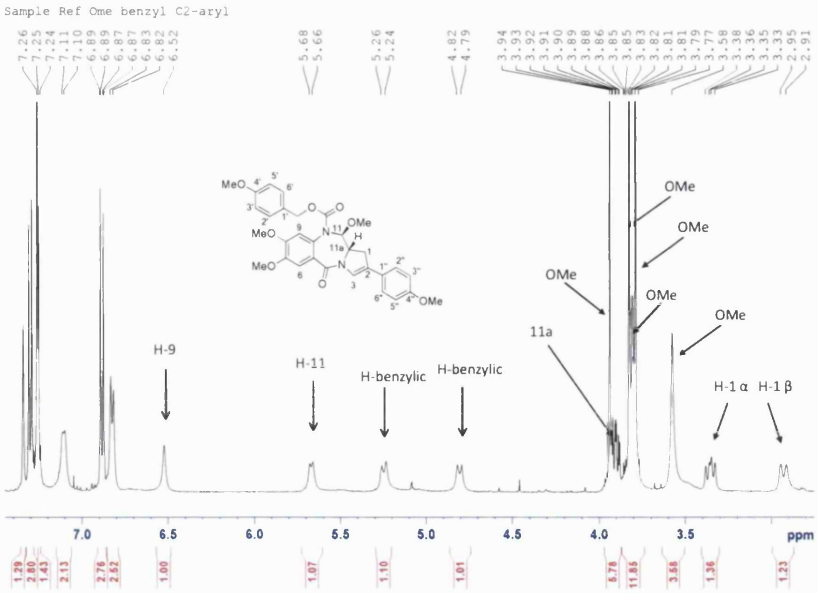

Figure 72: ^{1}H NMR spectrum of 288 in $CDCl_3$

The MS/MS mass spectrum showed the protonated $[M+H]^+$ ion at m/z 561 indicating a molecular weight of 560, the same as the expected mass **(Figure 73)**. The HRMS accurate mass $[M+H]^+$ ion was found at m/z 561.2226. The $[M+H^+]$ ion (m/z 561) of **288** was subjected to MS/MS, yielding a new fragment ion at m/z 529, a difference of 32, suggesting the presence of a methoxy ion.

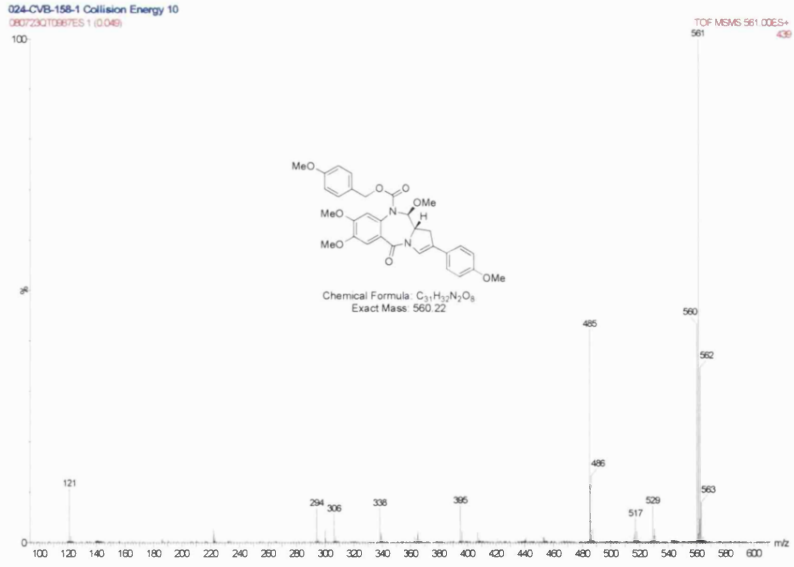

Figure 73: MS/MS fragmentation pattern of 288

4.7.10 Displacement of Nitrophenyl with the Progroup

The next goal was to introduce the actual progroup to the C2-aryl nitrophenyl carbinolamine intermediate. The alkoxide of progroup **288** should displace the nitrophenyl, thus forming the carbamate group.

The progroup alcohol **228** was deprotonated with potassium *tert*-butoxide in DMF and stirred overnight at room temperature, and the resulting alkoxide was treated with the C2-aryl nitrophenyl intermediate **284** in DMF (**Scheme 58**). One product was isolated, unfortunately NMR confirmed the product was recovered C2-aryl PBD imine **218**. The same reaction was repeated using the N10-protected carbinolamine methyl ether **287** as substrate, but unfortunately once again the C2-Aryl PBD imine (**218**) was recovered.

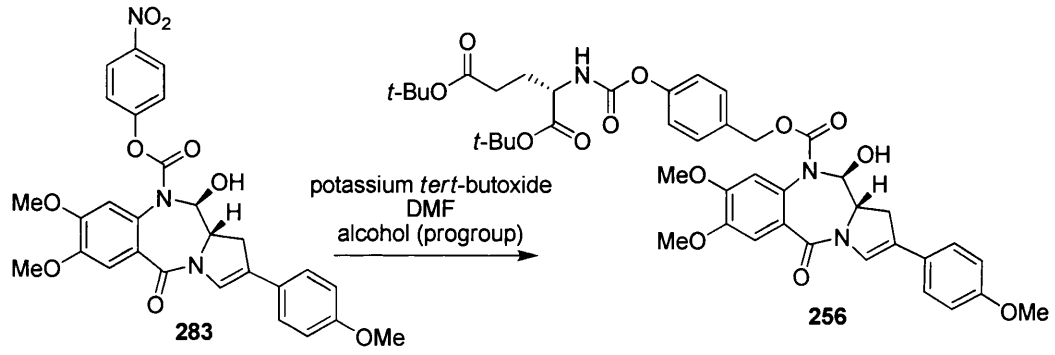

Scheme 58

4.8 Trichloromethyl Displacement Strategy

Bermudex *et al.* were able to prepare a number of derivatives **289** via the trichloromethyl carbamate intermediate **290.** Trichloromethyl chloroformate was added to a solution of the appropriate indoline in the presence of TEA to give intermediate **290**. The trichloromethyl group was then replaced by heating with a series of amines in toluene to afford a set of ureas **291**. [153]

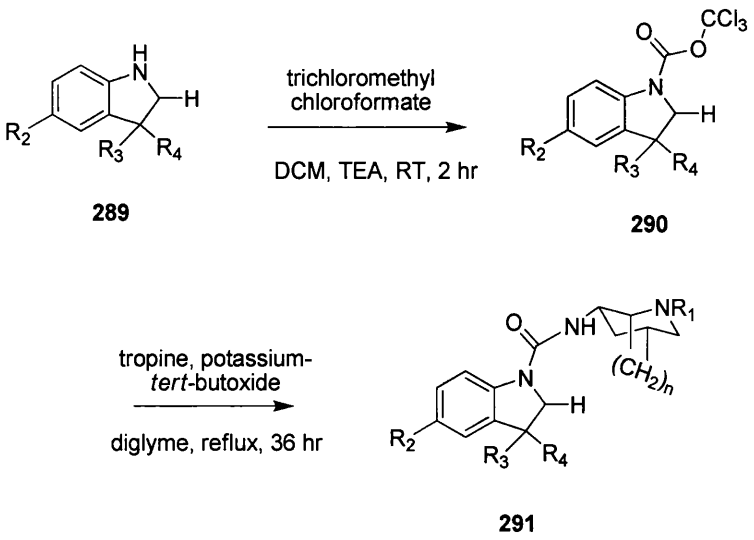

Scheme 59: Various R groups

	R_1	R_2	R_3	n
a	Me	H	H	3
b	Me	H	H	2
c	Et	H	H	2
d	Me	H	H	2
e	Me	MeO	H	2
f	Me	NO_2	Me	2
g	Me	H	Et	2

Table 15

4.8.1 Trichloromethyl Displacement Strategy Model Study

A similar approach could be applied to the synthesis of the N10 PBD carbamate. A model study with the unsubstituted imine **212,** demonstrated that it was possible to make a trichloromethyl carbamate intermediate on treatment with trichloromethyl chloroformate, aqueous sodium carbonate in DCM which gave one product **293** in 48% yield. [154]

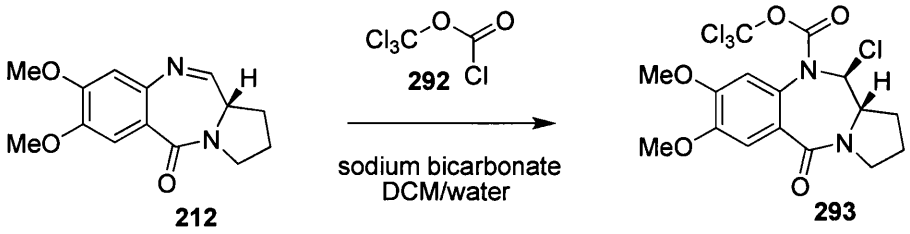

Scheme 60

The ^{1}H NMR spectrum in **Figure 74** revealed the N10 protected trichloromethyl carbamate intermediate **293**. The H-9 signal had a rotamer signature with two singlets at 6.7 ppm and 6.8 ppm, this effect being caused by the bulky CCl_3 group. The H-11 was a doublet which was relatively downfield at 6.1 ppm. This was in agreement with previously synthesised N10-protected molecules with chlorine at the C11 position, strongly suggesting the presence of a chloro group at the 11-position.

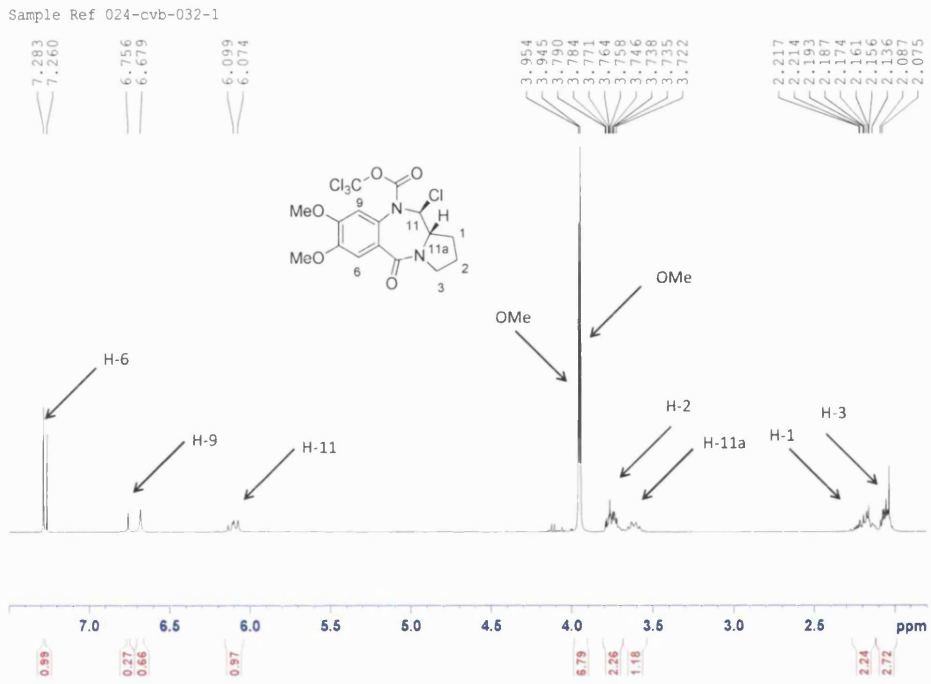

Figure 74: ^{1}H NMR spectrum of 293

The MS/MS mass spectrum of the model compound revealed protonated $[M+H]^+$ ions at m/z 457, 459 and 460 and sodiated $[M+H]^+$ ions at m/z 479, 481 and 482. These ions were consistent with the presence of a product with a mass of 458 (**Figure 75)**. Expansion of the mass spectrum around 458 revealed an isotopic pattern consistent with the presence of 4 chlorine atoms, which was identical to a theoretical mass spectrum generated for $C_{16}H_{16}Cl_4N_2O_5$ in (**Figure 76)**. Three chlorine atoms relating to the trichloromethyl carbamate were observed. The other chlorine was introduced at the C11 position, suggesting a similar reaction mechanism to the one proposed in **Scheme 54**.

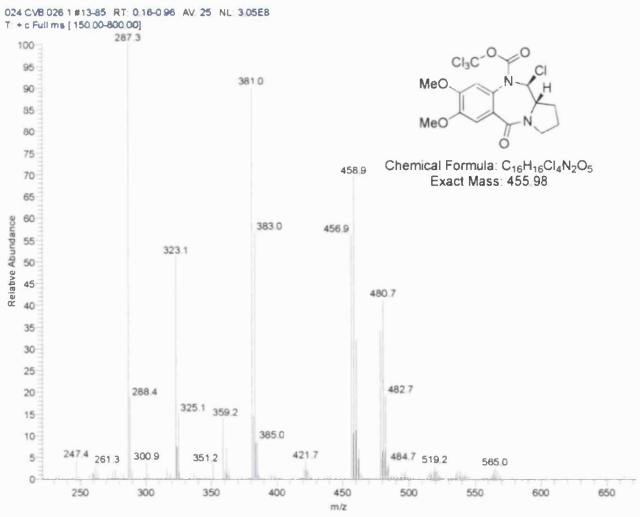

Figure 75: Full mass spectrum of compound $C_{16}H_{16}Cl_4N_2O_5$ (293).

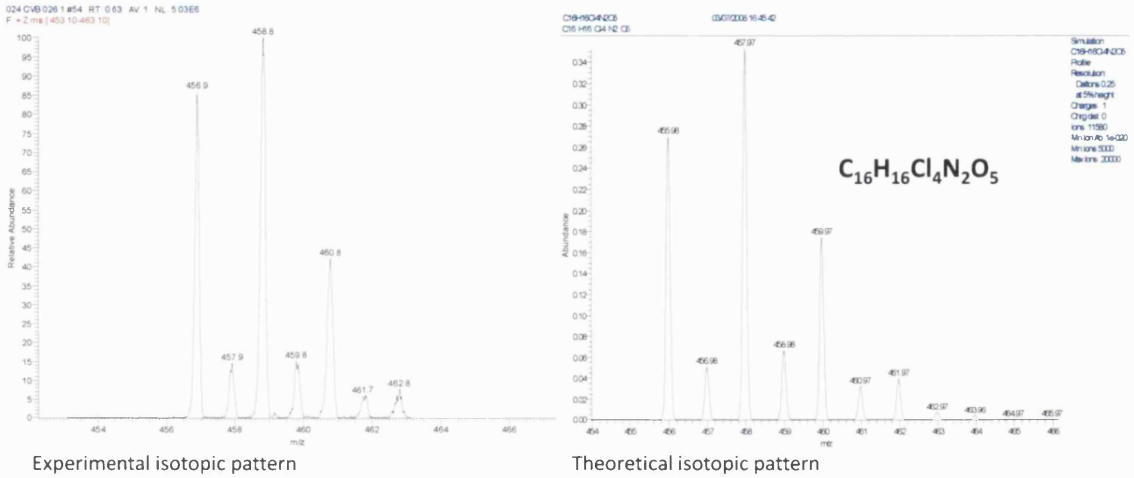

Figure 76: Comparison of the two isotopic patterns. Mass spectrum expansion of compound 294 and theoretical spectrum of $C_{16}H_{16}Cl_4N_2O_5$

4.8.2 Trichloromethyl Displacement Strategy with Methoxide Ion

The 11-chloro substituted compound **293** was treated with pyridine and methanol over 2 hours and, as expected, the trichloromethyl group was replaced by a methoxy moiety. However, NMR (**Figure 77**) (and MS data, **Figure 78**) revealed that the 11-chloro group was also displaced affording the MOC-protected carbinolamine methyl ether **294**.

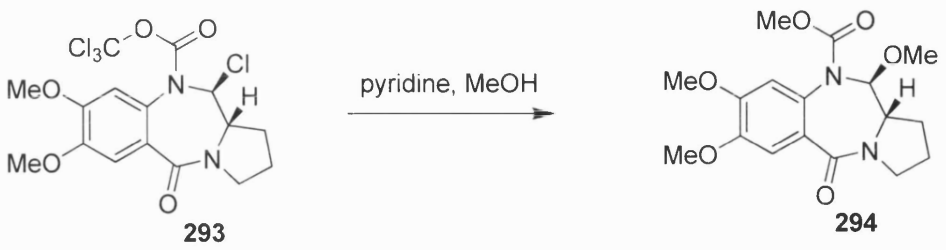

Scheme 61

The ^{1}H NMR revealed an upfield shift of the H-11 doublet (6.1 ppm to 5.4 ppm), suggesting displacement of the 11-chloro group by a methoxy moiety (**Figure 77**). Indeed, the shift and multiplicity of the 11-H signal was consistent with other 11-methoxy compounds synthesised during the course of the project. The H-9 proton was a singlet at 6.60 ppm, and the absence of rotamers indicated that the trichloromethyl group was no longer attached. There was also an appearance of two additional methoxy signals, singlets at 3.7 ppm and 3.5 ppm.

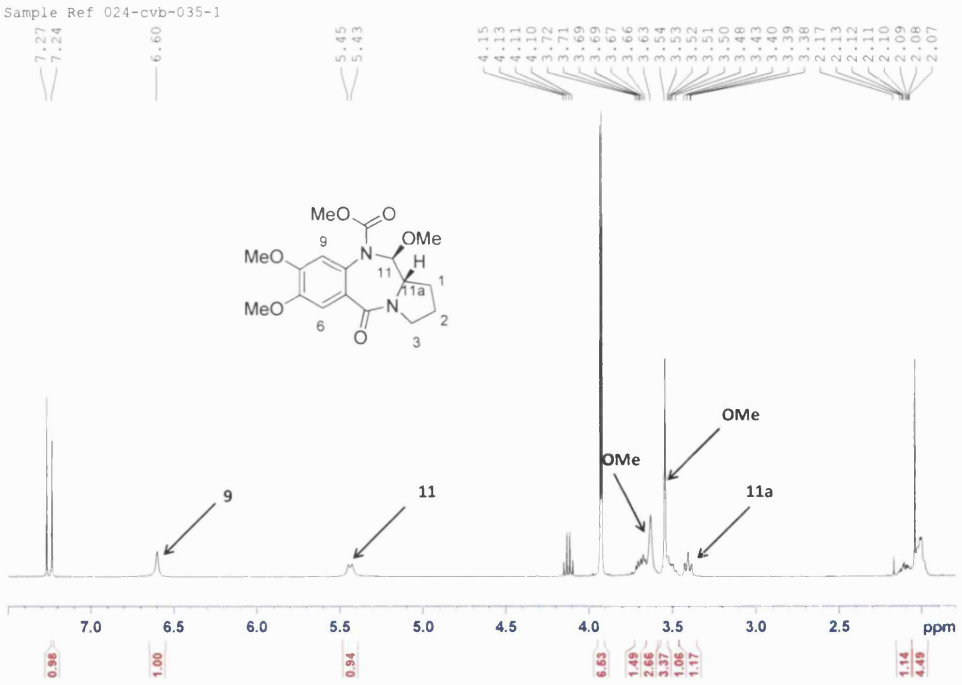

Figure 77: ^{1}H NMR spectrum of 294 in $CDCl_3$

The MS/MS data confirmed the presence of the 11-methoxy compound with a protonated molecular ion at 351 m/z (**Figure 78**).

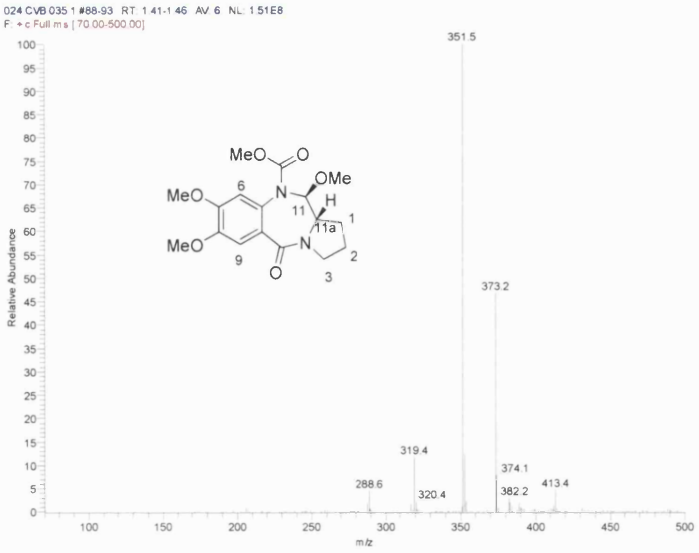

Figure 78: Full mass spectrum of compound 294.

4.8.3 Trichloromethyl Displacement Strategy with Progroup

The next step was to introduce the required progroup by replacing the trichloromethoxy moiety with alcohol **228**. This was achieved successfully by treating alcohol **228** with the N10-trichloromethyl carbamate intermediate in DCM at room temperature in the presence of pyridine to afford the desired unsubstituted prodrug **270** (**Scheme 270**).

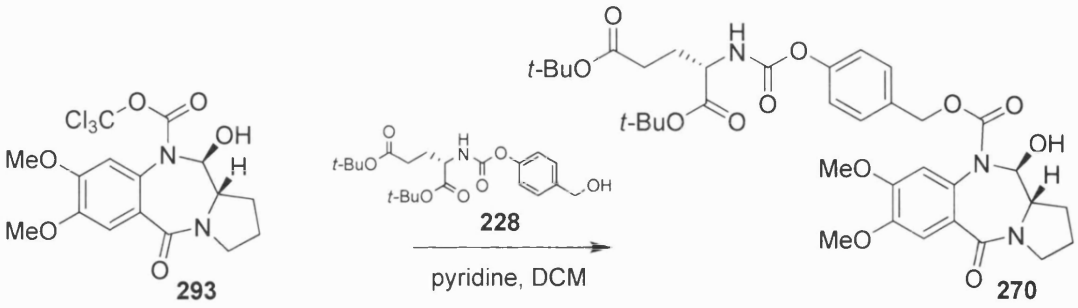

Scheme 62

The ^{1}H NMR (**Figure 79**) reveals that all the components of **270** are present. Signals which belong to the progroup are clearly visible; the diagnostic benzylic protons can be observed at 5.6 and 4.2 ppm, the N-H doublet at 5.5 ppm, the *tert*-butyl proton signals as two singlets at 1.5 ppm and the characteristic H-7', H-8' (H-8 α and H-8 β) and H-9' protons signals as multiplets between 1.8-2.4 ppm and at 4.3 ppm. Crucially, the correct integration ratio of PBD signals to carbamate progroup signals was observed. Finally, the 9-H signals were found at a relatively upfield

position (6.5 ppm) consistent with the presence of the electron-donating carbamate group.

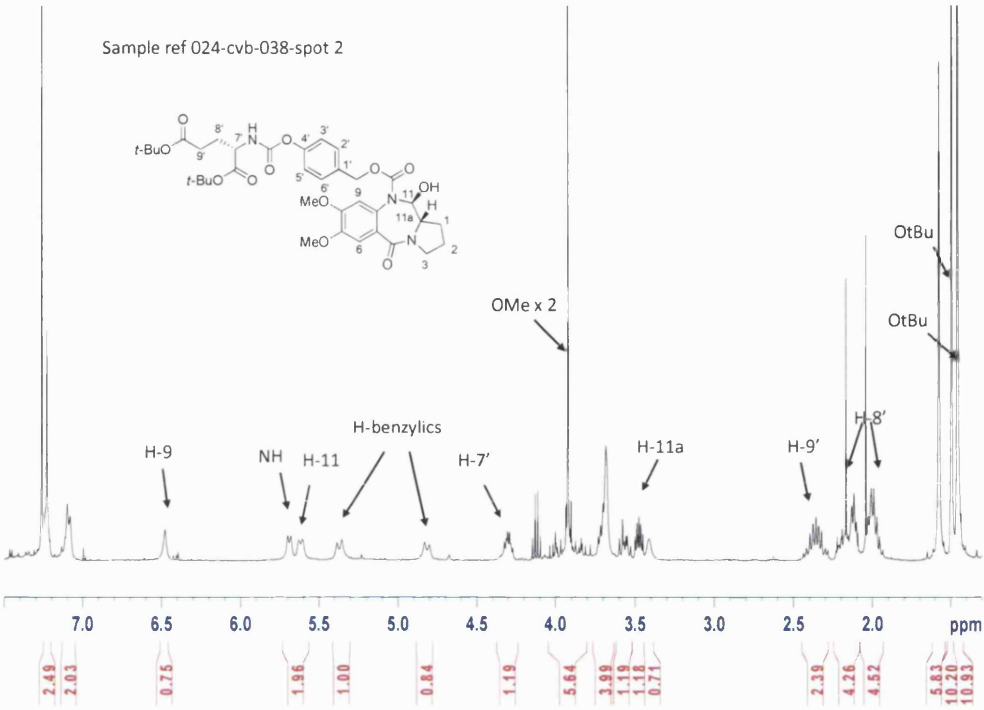

Figure 79: ^{1}H NMR spectrum of 270 in $CDCl_3$

The MS/MS mass spectrum confirmed the success of the reduction, revealing the protonated $[M+H]^+$ ion at m/z 714, indicating a molecular weight of 713 which is the same molecular mass as **270**. It had a HRMS accurate mass ion of m/z 714.3237 consistent with structure.

4.8.4 Trichloromethyl Displacement Strategy with the C2-aryl N10-C11 imine PBD

The next step was to investigate the possibility of synthesising the N10 trichloromethyl carbmate of a C2-aryl compound. The C2-aryl imine PBD **218** was treated with trichloromethyl chloroformate and aqueous sodium carbonate in DCM to afford the desired product **295** in 45% yield.

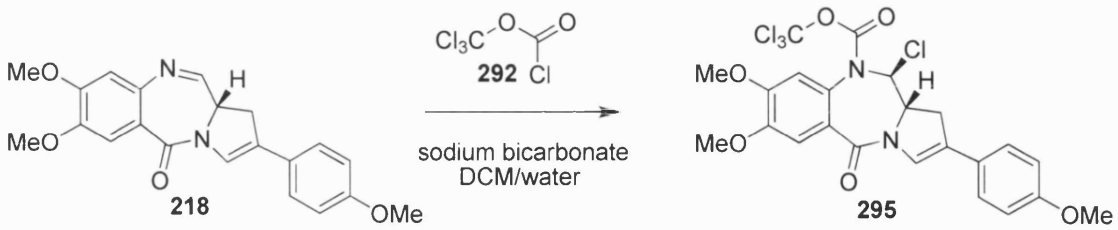

Scheme 63

The ^{1}H NMR (**Figure 80**) showed the characteristic signals of the trichloromethyl carbamate intermediate **295** with rotameric H-9 signals at 6.8 ppm and 6.7 ppm. The C-ring signals were observed as two spin systems corresponding to H-1 α and H-1 β at 3.4 ppm and 3.1 ppm. The H-11 signal was observed as an upfield doublet at 6.3 ppm, suggesting the presence of chlorine at the C11 position.

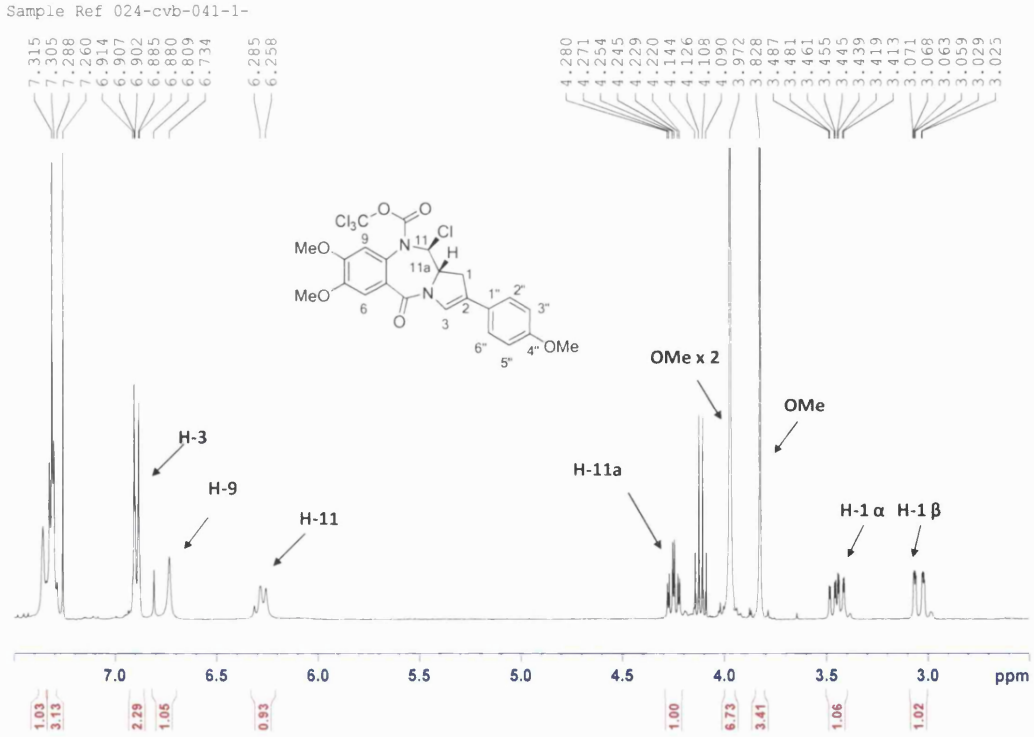

Figure 80: ^{1}H NMR spectrum of 295 in $CDCl_3$

The MS/MS mass spectrum showed a protonated $[M+H]^+$ ion at m/z 563, indicating a molecular weight of 562 (**Figure 81**). The fragmentation pattern was identical to a theoretical isotope pattern generated for the chloro compound $C_{23}H_{20}Cl_4N_2O_6$ (**Figure 82**). Thus, NMR and MS/MS fully supported the formation of the 11-chloro-10-trichloromethyl carbamate **295**.

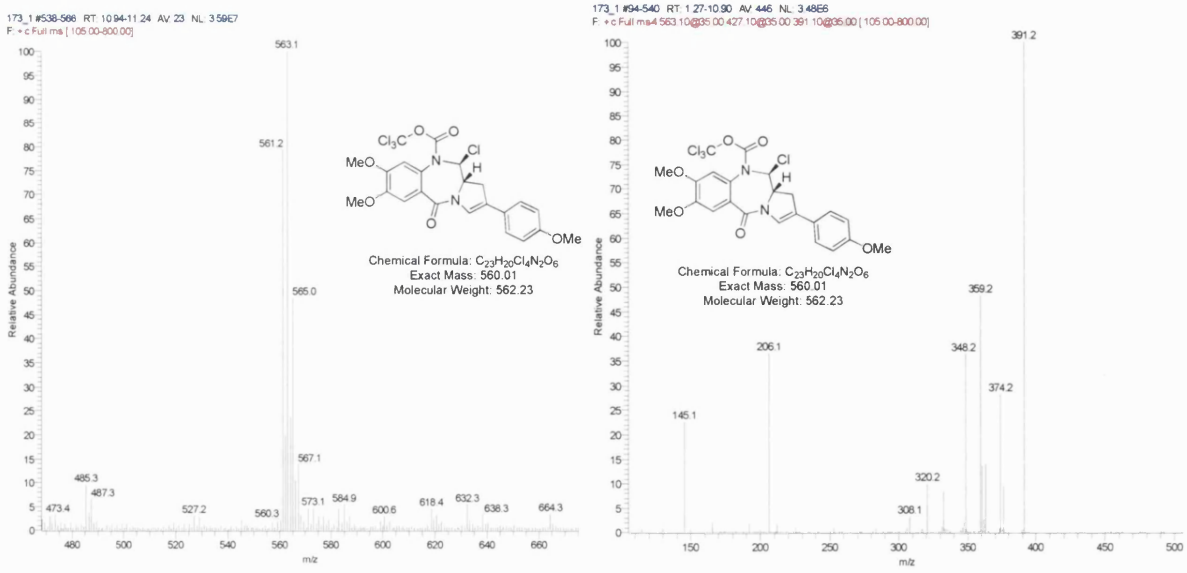

Figure 81: Full Mass Spectrum of compound 295 and MS/MS spectrum of m/z 563.

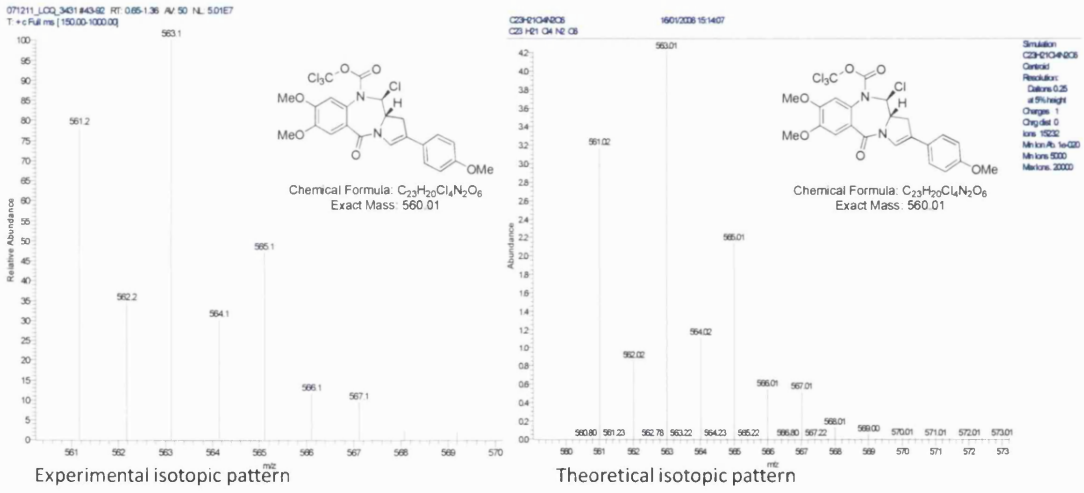

Figure 82: Experimental isotopic pattern for 295 and theoretical isotopic pattern for $C_{23}H_{20}Cl_4N_2O_6$

4.8.5 Trichloromethyl Displacement Strategy with Methoxide

The 11-chloro substituted compound **295** was treated with pyridine and methanol over 2 hours. As expected the trichloromethyl group was replaced by a methoxy group in an analogous fashion. However, NMR and MS/MS analyse indicated that the 11-chloro group had also been displaced, thus affording the MOC-protected carbinolamine methyl ether **286**.

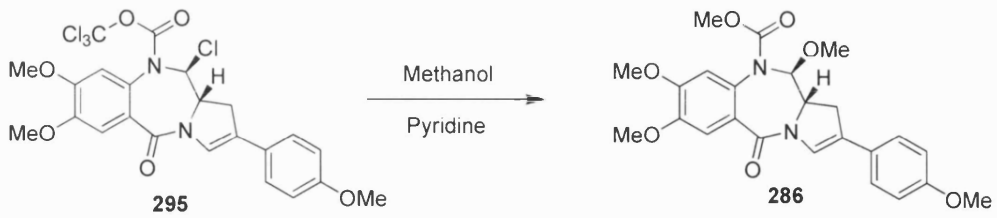

Scheme 64

The ^{1}H NMR (**Figure 83**) shows a relatively upfield shift of the H-11 proton at 5.6 ppm, indicating a change at the H-11 position. The ppm value is consistent with previously synthesized molecules with a methoxy group at the C11-position. The H-9 proton is observed as a singlet at 6.65 ppm; the absence of rotamers indicates that the trichloromethyl group is no longer present. There was also the appearance of two additional methoxy singlets at 3.7 ppm and 3.6 ppm.

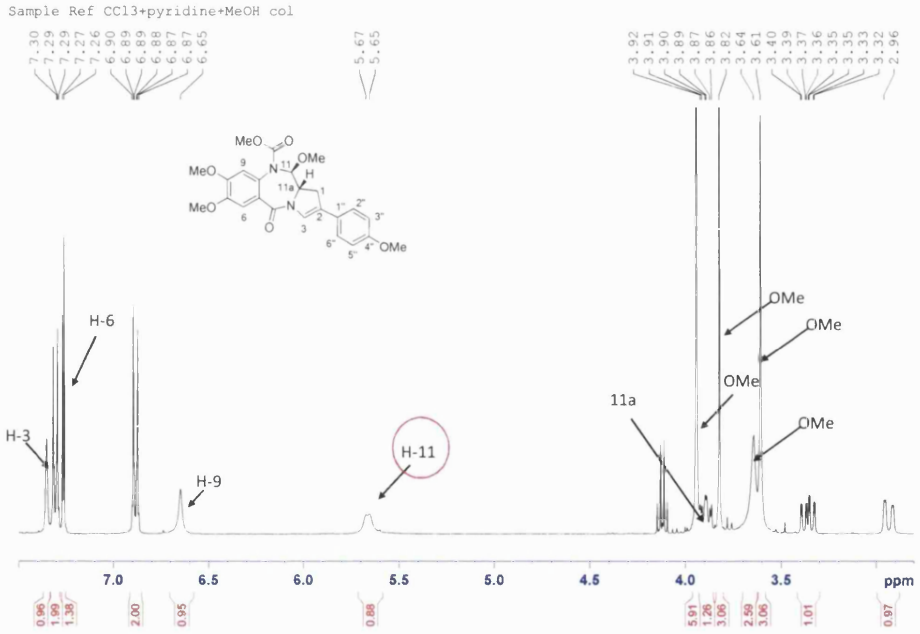

Figure 83: ^{1}H NMR spectrum of 286 in $CDCl_3$

The MS/MS mass spectrum revealed a protonated $[M+H]^+$ ion at m/z 455, indicating a molecular weight of 454, consistent with **286**, A HRMS accurate mass was measured $[M+H]^+$ ion at m/z 455.1805, also consistent with structure

The $[M+H^+]$ ion (m/z 455) of was subjected to MS/MS (**Figure 84**), yielding a new fragment ion at m/z 423, a difference of 32, suggesting the presence of a methoxy ion. Similarly, MS/MS of the fragment ion m/z 423 revealed a new mass at

m/z 391, a difference of 32 suggesting the presence of a second methoxy ion. This evidence supported the presence of two additional methoxy groups, one at the C11 postion while the other corresponded to the N10-methoxy carbamate.

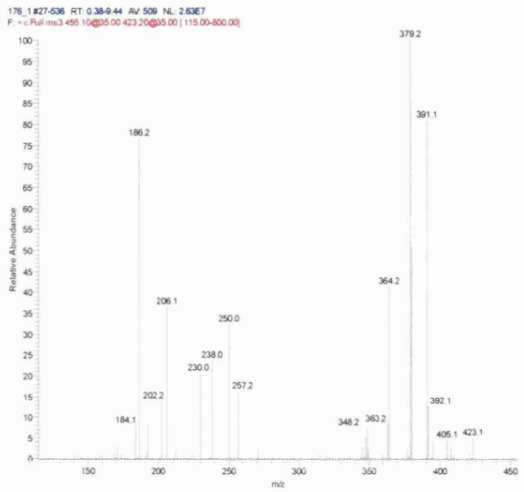

Figure 84: MS/MS of spectrum of m/z 455.2 of fragment ion m/z 423.

4.8.6 Selective Substitution of Chlorine with a Methoxy Group

Attempts to selectively displace the 11-chloro group in neat methanol were unsuccessful (**Scheme 65**), with the NMR revealing the formation of the 11-methoxy-10-methoxy carbamate compound **286** (**Figure 85**).

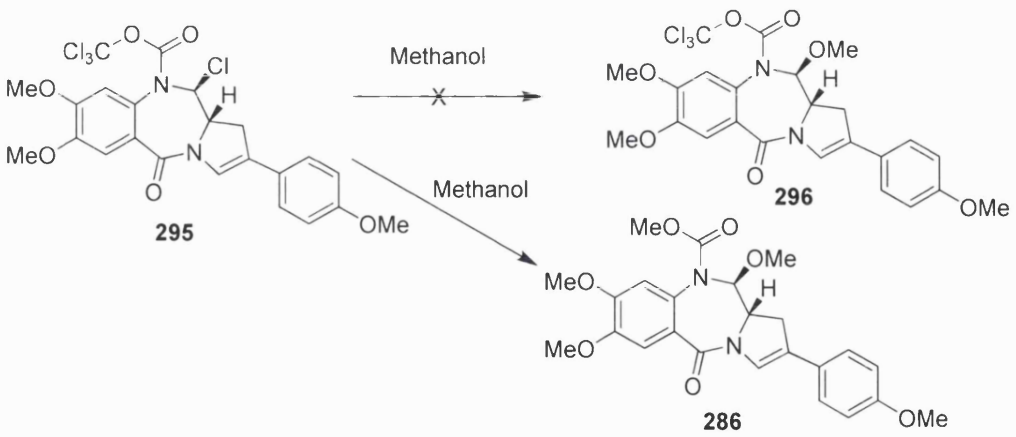

Scheme 65:

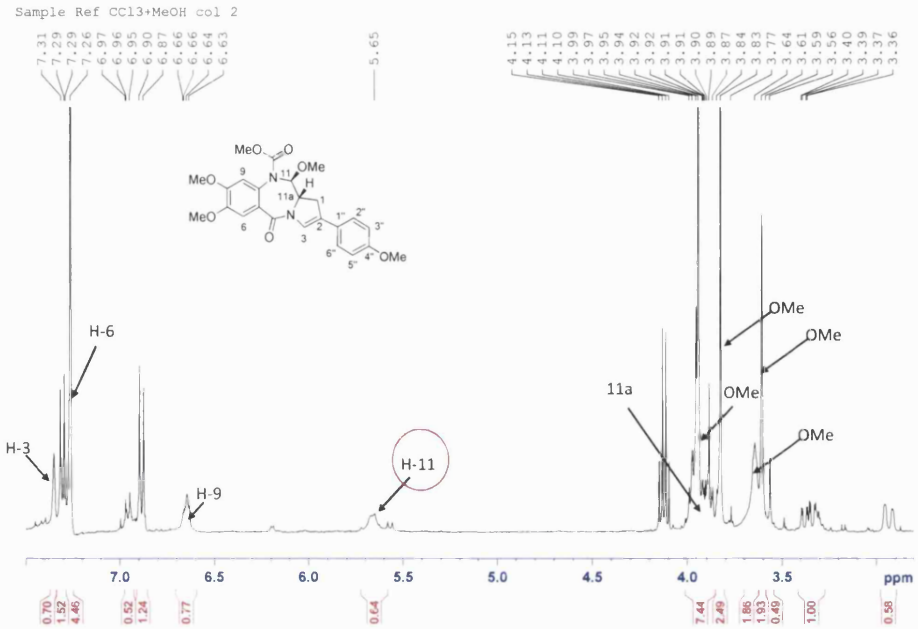

Figure 85: ^{1}H NMR spectrum of 286 in $CDCl_3$

4.8.7 Trichloromethyl Displacement Strategy with Progroup Alcohol

Following the model studies, the trichloromethyl carbamate strategy was applied to the synthesis of the C2-aryl substituted target prodrug. Treatment of the progroup alcohol **228** with the trichloromethyl carbamate **286** in DCM at room temperature afforded the parent imine (15%) and an unknown major product **256b**.

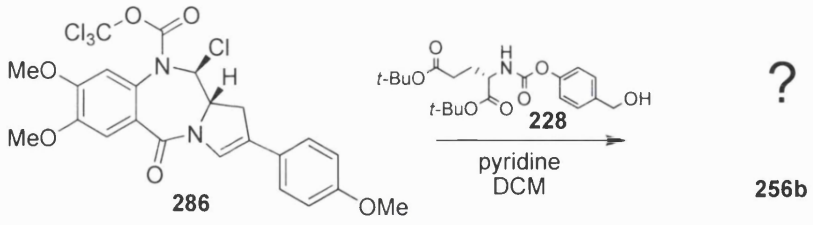

Scheme 66

The ^{1}H NMR (**Figure 86**) of the unknown product revealed signals arising from both the PBD system and the progroup, suggesting that coupling had successfully occurred. (see **Figure 86**). However, the diagnostic benzylic doublets were absent from the spectrum, being replaced by a singlet. In addition he H-11 doublet was observed downfield at approximately 6.2 ppm, a shift previously associated with the

presence of an electron withdrawing chloride group. The presence of an 11-chloro group may explain the change in the benzylic signals. The bulky group could lock the progroup in a conformation where both benzylic protons were equivalent. (Alternatively, the chloro group would not be able to hydrogen bond to the carbamate carbonyl, allowing free rotation and affording a time averaged singlet for the benzylic protons).

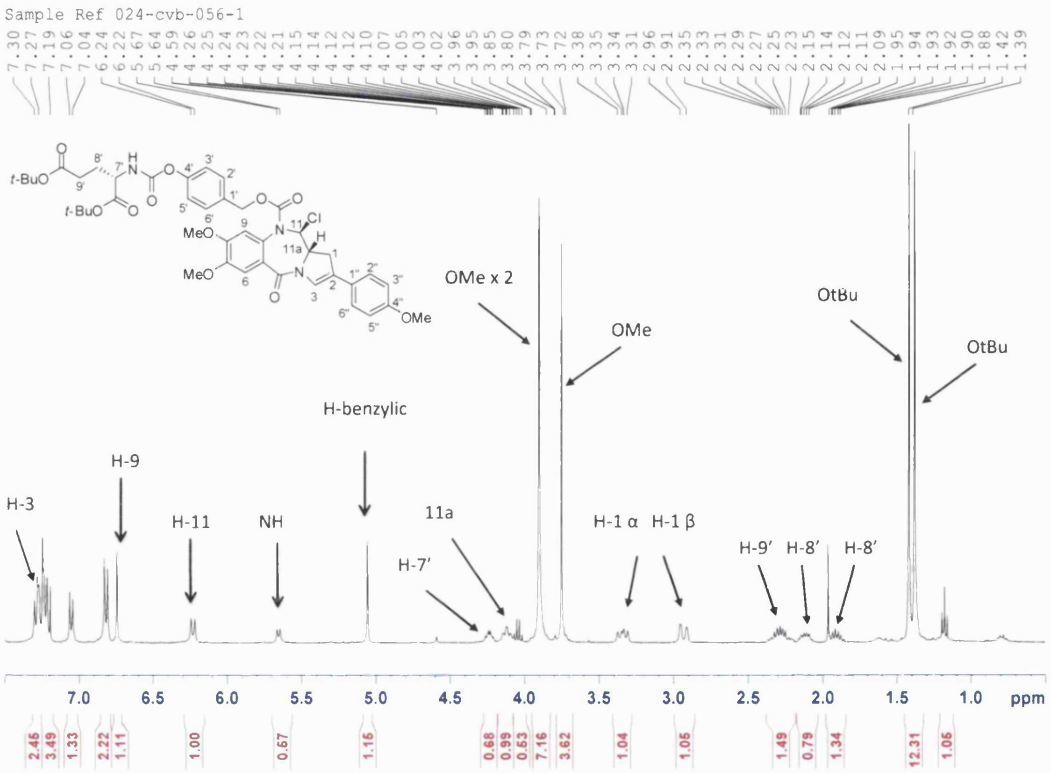

Figure 86: ^{1}H NMR spectrum of 256 b

MS/MS was employed to confirm the presence of the chloro group. The experimental isotope pattern closely resembled the theoretical for a compound of empirical formula $C_{43}H_{51}ClN_3O_{12}$ (**Figure 88)**.

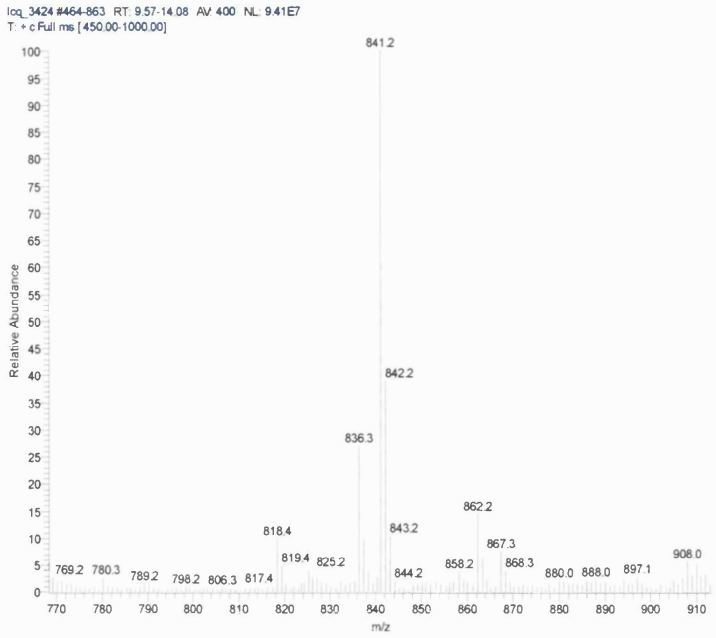

Figure 87: Mass Spectrum of compound 256 b

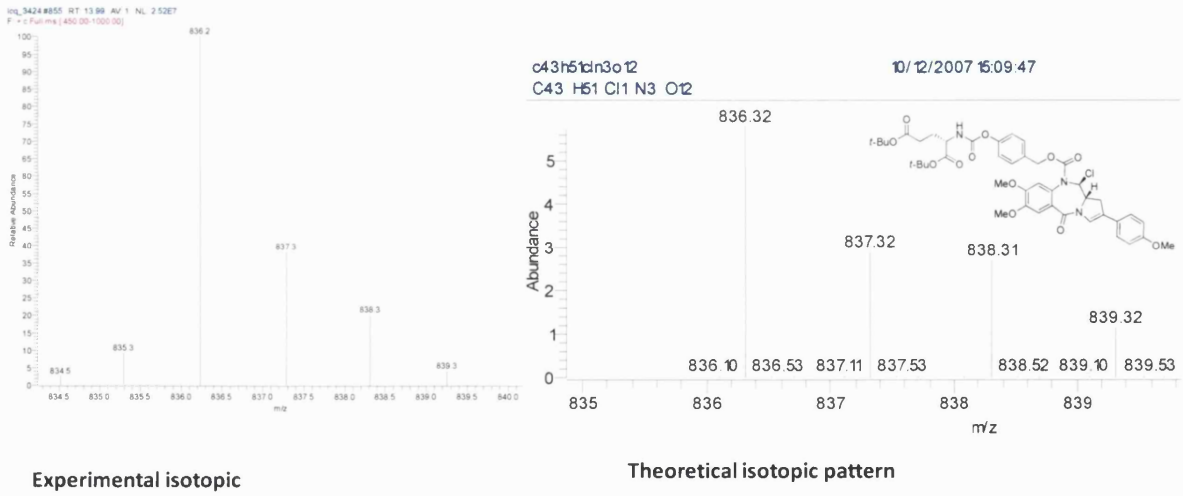

Experimental isotopic **Theoretical isotopic pattern**

Figure 88: Experimental isotopic pattern for 256 b and theoretical isotopic pattern for $C_{43}H_{51}ClN_3O_{12}$

Based on the MS/MS and ^1H NMR data the most probable structure for the major component from the displacement reaction is the chloro substituted progroup precursor **256b**.

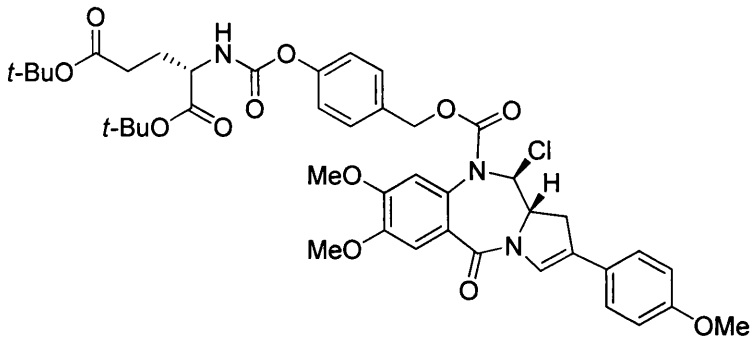

Figure 89: Mass Spectrum of compound 256

Unfortunately attempts to remove the butyl groups from this compound **256b** with formic acid lead to its degradation.

Chapter 5

Conclusions and Future Work: Chemistry

5.1 Conclusions and Future Work: Chemistry

The prodrug target molecule was successfully synthesised in sufficient quantity to allow preliminary biological evaluation *in vitro*. A robust 13 step synthesis was devised and performed to afford the N10-protected C2-ketone PBD intermediate. However, the critical triflation reaction, a prerequisite for the Suzuki coupling to introduce the C2-aryl group, produced a mixture of isomers which could only be separated by preparative LC/MS (**Scheme 67**). The separated triflate isomers were subjected to a Suzuki coupling, followed by a final deprotection to remove the butyl and acetate protecting groups. The crude product was purified again by preparative LC/MS to yield the target molecules for biological testing (6.80 mg of 1,2-isomer and 4.05 mg of 2,3-isomer).

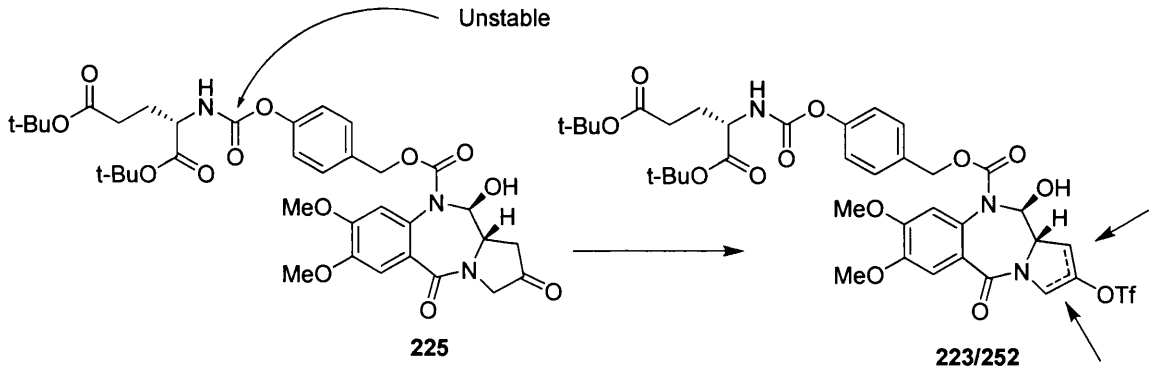

Scheme 67: The N10 progroup is necessarily fragile and is not robust enough to survive the conditions required to unambiguously afford the 2,3-enol triflate.

Although the initial synthetic campaign was successful, a number of synthetic challenges have been identified. The self-immolative N10 progroup is necessarily fragile and is not robust enough to survive the conditions required to unambiguously afford the 2,3-enol triflate. It is inefficient to make a mixture of isomers and purify them twice by preparative LC/MS (both at the triflate stage and the final purification of the diacid prodrug) as it significantly reduces the quantity of prodrug available for further work.

It might be possible to overcome this problem by installing the N10 progroup at the end of the synthesis, after the triflation and Suzuki coupling or by performing triflation and Suzuki coupling on a C-ring ketone prior to joining to A-ring.

5.1 Late Stage Introduction of Progroup

The late introduction of the progroup to the imine at the N10 position is a strategically attractive approach as a wide range of pre-existing imine PBDs (naturally occurring or synthetic imine PBDs) could be converted to their prodrug form (**Scheme 68**).

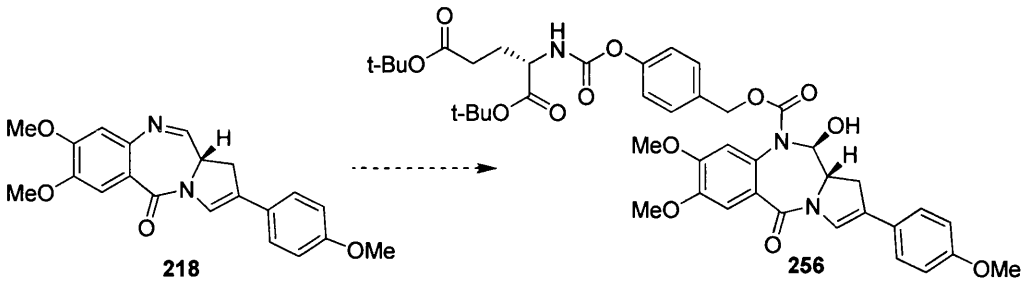

218 **256**

Scheme 68

The imine PBDs **212** and **218** was successfully protected with different chloroformates to synthesise a range of N10-protected PBDs (**Scheme 69**). The benzylic chloroformates (**262, 263**) had long reactions times, up to 5 days when compared to the more reactive *p*-nitrophenoxy and trichloromethoxy chloroformate (e.g. 15 minutes for the formation of the N10-trichloromethoxy carbamate).

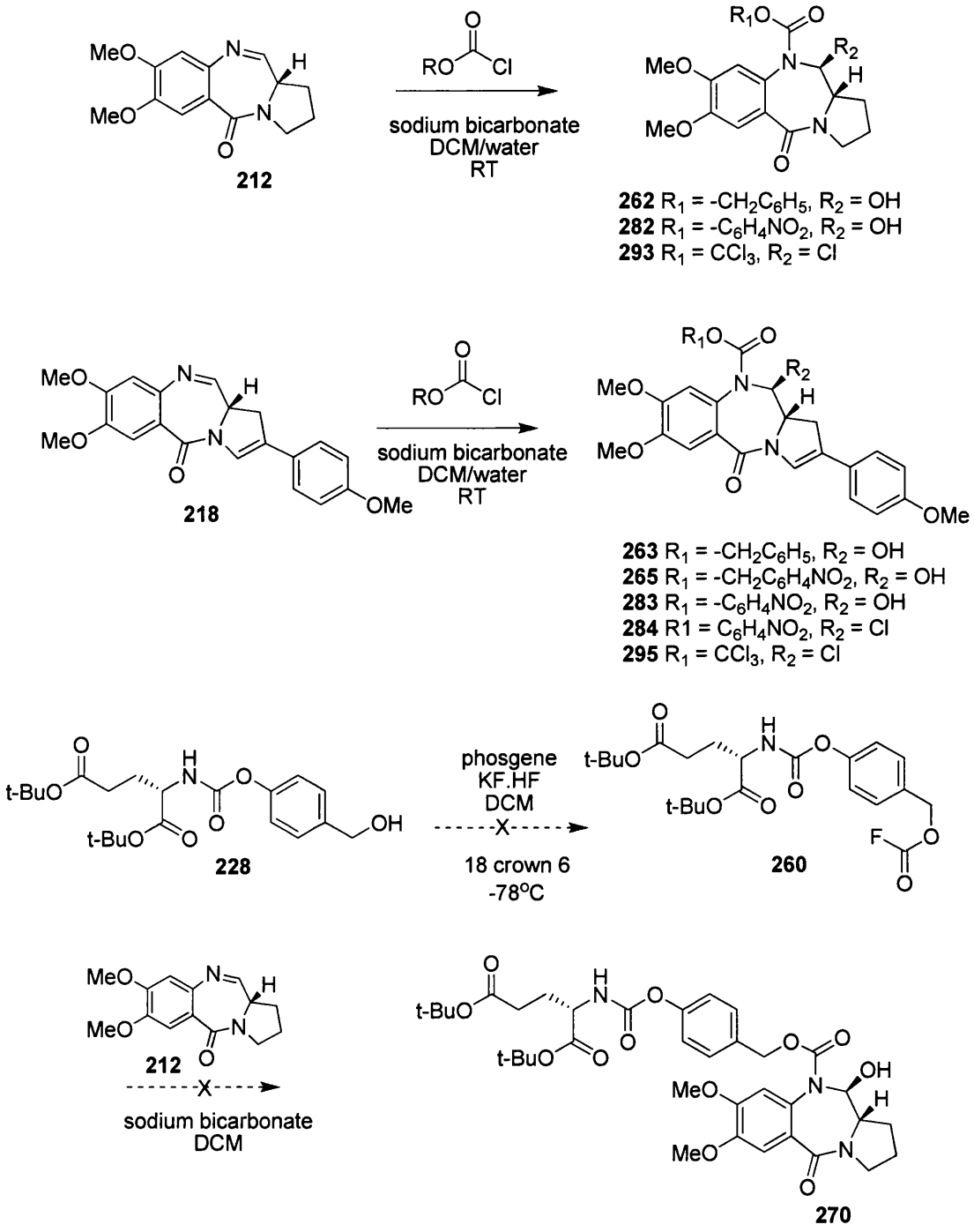

Scheme 69: Model studies

Unfortunately, it proved impossible to synthesis the chloroformate/fluorformate derivatives of the progroup (**228**). However, the *p*-nitrophenoxy and trichloromethoxy carbamates (**282, 265, 284,** and **287**) could be exploited as intermediates for the formation of other types of N10 derivatives. The displacement of the *p*-nitrophenyl

group with an alkoxide was investigated in a number of model systems. In model studies involving the simple PBD **293**, the results appeared promising but the reactions were low yielding and there was formation of the undesired parent compound **212**. It was also possible to displace the *p*-nitrophenyl carbamate C2-aryl of intermediate **212** with sodium methoxide. Displacements with the alkoxide of *p*-methoxybenzyl alcohol were less successful (2% yield) and attempts to introduce the progroup were unsuccessful.

An interesting feature of the *p*-nitrophenoxy carbamate displacement strategy was the formation of the 11-chloro substituted PBDs. It was found that the chlorine group could be selectively displaced in the presence of the N10 nitrophenyl carbamate by using the parent alcohol rather than the alkoxide.

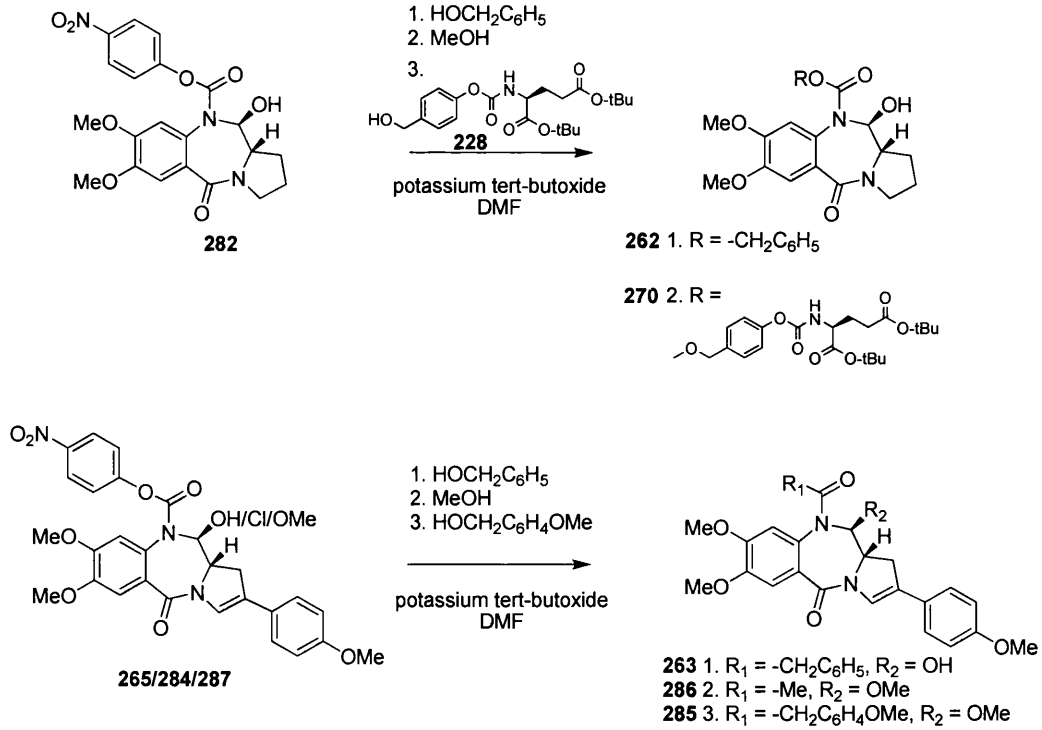

Scheme 70

A variant of the N10-displacement strategy employing a trichloromethyl carbamate was also invstigated. Once again the formation of C-11 chlorinated species was observed. Due to the inherent reactivity of the trichloromethyl carbamate the 11-Cl group could not be selectively displaced without affecting the N10 moiety. However, it proved possible to successfully displace the trichloromethyl carbamate,

forming the prodrug of the unsubstituted PBD **270**. Application of the approach to the more complex C2-aryl substituted system yielded the 11-Cl substituted progroup on a small scale.

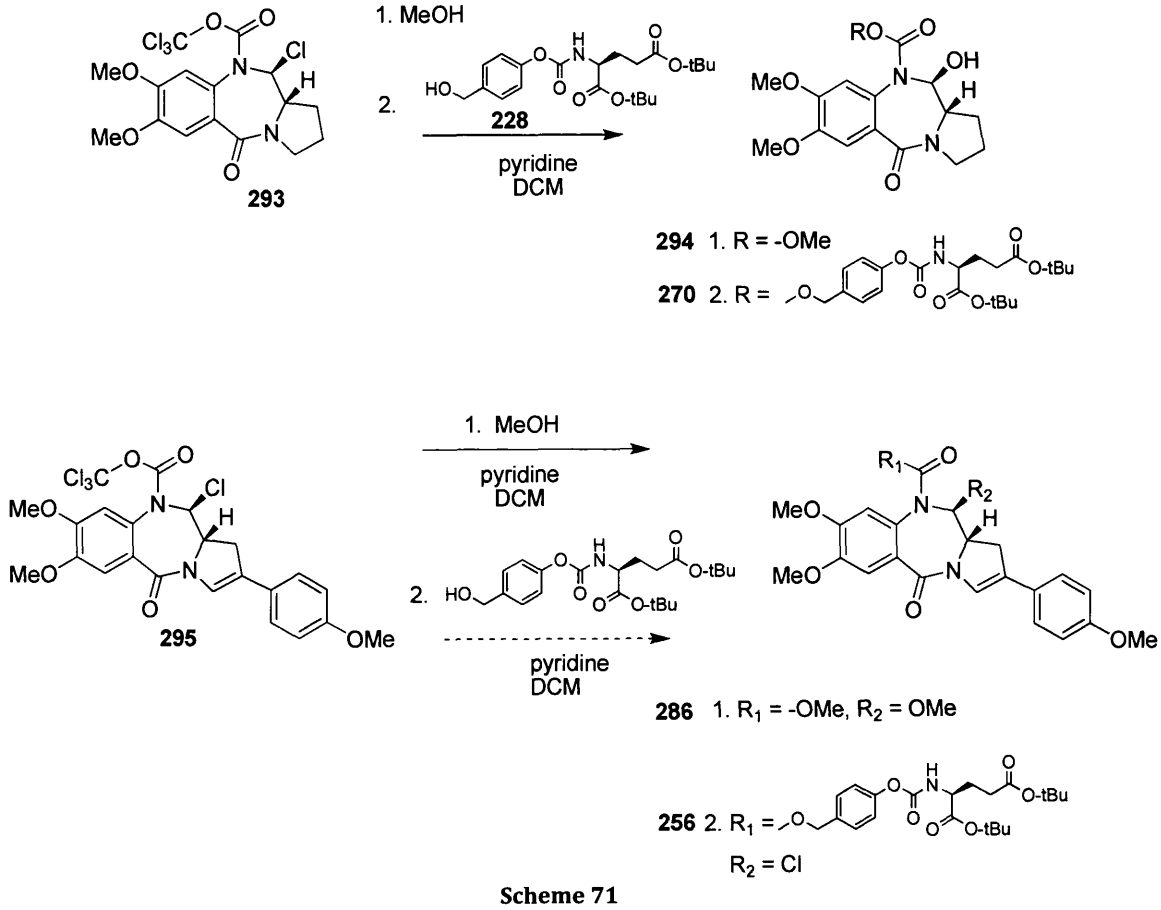

Scheme 71

5.2 Future work: Chemistry

5.2.1 Alternative Synthetic Route: Triflation and Suzuki Reactions on the PBD C-Ring

The main problem encountered in the first generation synthesis of the C2-aryl prodrug was the instability of the N10-progroup to conditions that unambiguously afforded the 2,3-enol triflate. Attempts to overcome this hurdle by introducing the progroup via a reactive N10-carbmate were only partially successful. An alterative strategy of performing the triflation and Suzuki coupling reactions on a C-ring ketone fragment prior to joining to an A-ring (**Scheme 72**), may umambiguously yield the 1,2-product. In principle, the 1,2-product can be isomerised to the 2,3-product.[145, 155]

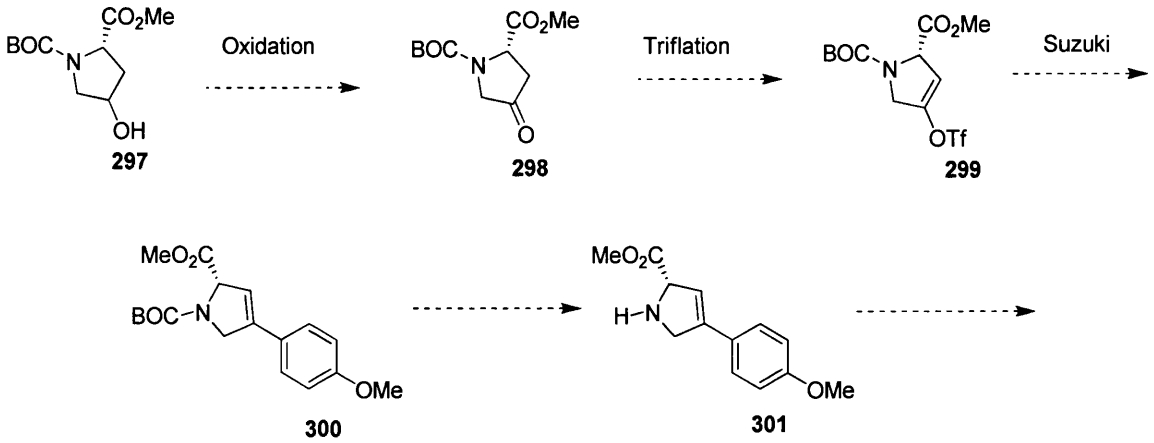

Scheme 72 Alternative Synthetic Route

Mori *et al.* (**Scheme 73**) reported a synthetic study aimed towards anthramycin in 2004.[156] Although the C-ring building block was prone to undesirable C2/C1 *endo*-unsaturation, they overcame this problem by isomerisation of the double bond in the pyrrolidine ring with $RhCl_3.3H_2O$. The resulting isomerisation product **303** was reported to posses the correct *S* stereochemistry at C11a ($[\alpha]^{24.1}_D$ = + 244 (c = 0.58 $CHCl_3$). Thus, their results demonstrated the ability of $RhCl_3.3H_2O$ to exchange the double bond position in the C-ring of PBDs.

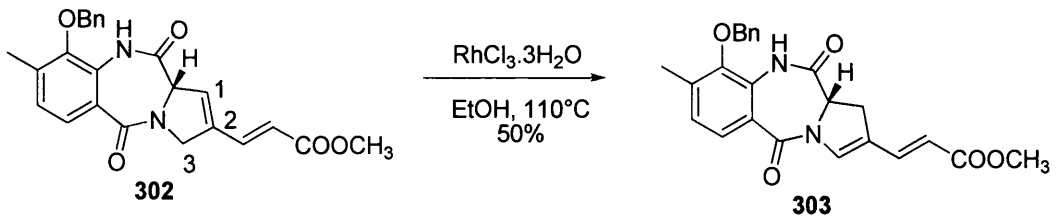

Scheme 73: Mori's isomerization of the C1-C2 double bond

Scheme 74 illlustrates the potential of applying the Mori approach to isomerising the C1/C2-*endo* unsaturation obtained from kinetic triflation to the C2/C3-*endo* unsaturation.

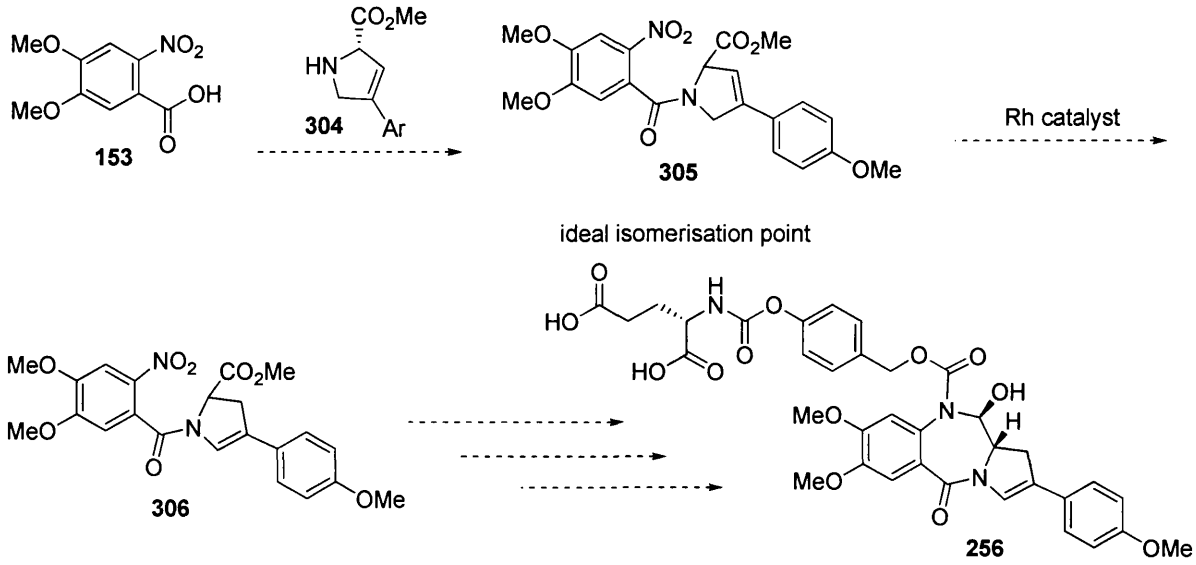

Scheme 74: Initial isomerisation of the double bond in the pyrrolidine ring with $RhCl_3.3H_2O$ prior to PBD formation.

Even if this isomerisation was unsuccessful, it should not be forgotten that C1-C2 PBD unsaturated isomers still retain biological activity (**Table 16**).[156] However, a disadvantage lies in the early commitment to a specific C2-aryl substituent, making the approach unsuitable for library synthesis.

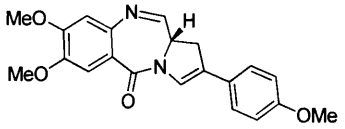 **218**	**IC_{50} 0.28 (nM) K562**
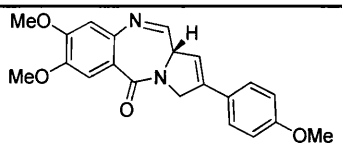 **307**	**IC_{50} 0. 94 (μM) K562**

Table 16: Cytotoxicity of 1,2-isomer (307) and 2,3-isomer (218) PBD imines (parent compounds).

Chapter 6

Biological Evaluation

6. Biological Evaluation

Dr Victoria Spanswick, Professor John Hartley, Dr Surinder Sharma, Dr Hassan Shahbakhti, Professor Nicol Keith, and Katrina Stevenson are acknowledged for providing the biological data presented in this chapter.

6.1 ADEPT

6.1.1 Background

As mentioned previously, Masterson *et al.*[126] synthesized two novel sets of PBD prodrugs (**214, 215** and **216, 217**; **Figure 31, Section 3.1**) based on existing PBD dimers and monomers, which were potentially suitable for use in CPG2-based ADEPT therapy. These molecules have a potential advantage over existing prodrugs such as the mustard-based prodrugs because their adducts may be more resistant to repair,[157, 158] thus reducing the probability of clinical resistance developing.

Stability studies on these compounds were performed using high-performance liquid chromatography. Both prodrug/parent pairs (**214, 215** and **212; 216, 217** and **213**) could be readily separated and detected using a Phenomenex™ column (C18 5 μM, 25 cm, 0.46 cm) with a mobile phase of H_2O (with 0.1% trifluoroacetic acid)/acetonitrile 70:30 (1 mL/min) and detection at 254 nM. Stability was assessed over a 24 h period in distilled water at both room temperature and 37 °C. Differences in the rate of conversion of prodrugs to parent PBDs were observed between the carbamate and urea series. The urea prodrugs **215** and **217** were unstable at both room temperature and 37 °C, and were almost completely converted into the parent PBDs within 24 h. In constrast, the carbamate prodrugs **214** and **216** were reasonably stable at room temperature undergoing only 7% and 3% conversion, respectively, after exposure to water at 37 ^{0}C for 24 hours. **Figures 91** and **92** show stability profiles for both monomers at 37 °C.

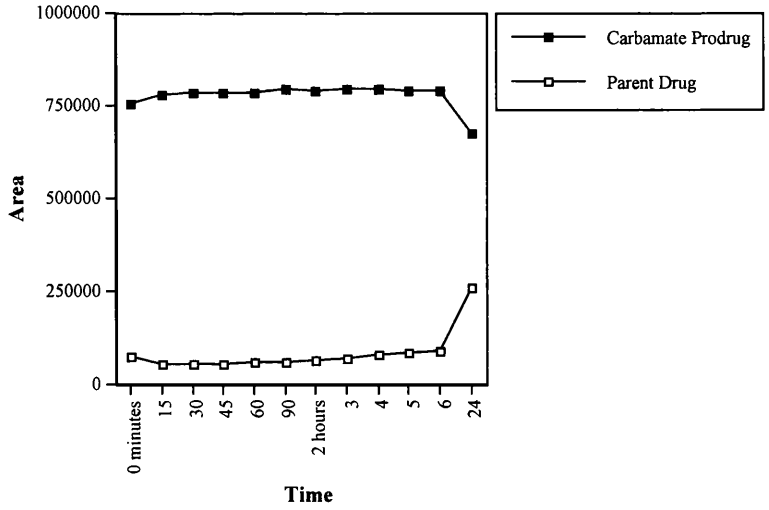

Figure 91: Stability of the Carbamate Prodrug 214 at 37°C in water

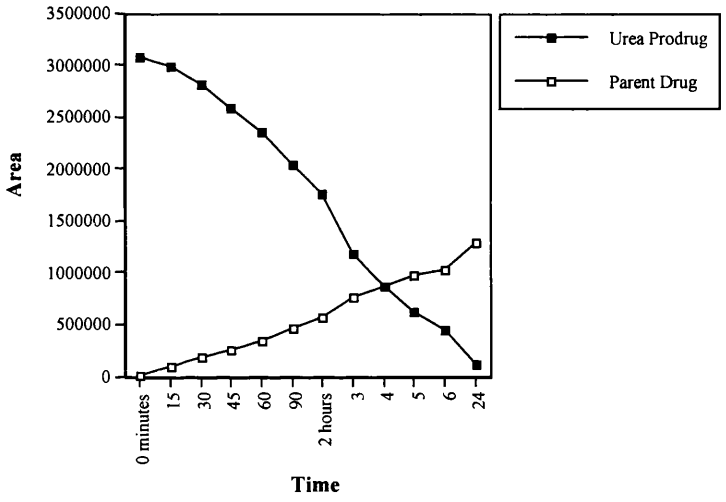

Figure 92: Stability of the Urea Prodrug 215 at 37°C in water

The *in vitro* cytotoxicity of the prodrugs was assessed in the LS174T human colon cell line (**Table 7, Section 3.1**). The results reflected the stability of the prodrugs, with the unstable urea compounds (**215** and **217**) giving relatively poor cytotoxicity differentials between prodrugs and parents (i.e., approximately 2:1 for both after 1 h exposure). However, the carbamate prodrugs afforded improved cytotoxicity differentials between the parent PBDs and prodrugs of >7.1 and >15.4, respectively, for 1 h exposure to enzymes rising to >14.3 and >44.7 for continuous exposure. All of the compounds examined were between 5- and 27-times more cytotoxic on

continuous exposure compared to 1 h incubation, presumably due to increased exposure time leading to greater hydrolysis of the prodrugs.

Finally, the carbamate monomer and dimer prodrugs **214** and **216** were incubated with 1 unit of CPG2 and both compounds were found to be good substrates (**Figure 93**). The monomer prodrug **214** was completely converted into the cytotoxic parent PBD **212** within 50 min with no apparent chemical degradation observed in the assay buffer (100 mM Tris–HCl/260 lM ZnCl, pH 7.3) in the absence of CPG2 over the same time period. Similarly, the dimer prodrug **216** was completely converted into the cytotoxic PBD dimer **213** in 75 min with no chemical degradation in the absence of CPG2. To confirm the potential value of these prodrugs in ADEPT therapy, the monomer (**214**) and dimer (**216**) prodrugs were incubated with CPG2 in the presence of LS174T cells for 1 h. This reduced the IC_{50} values for **214** and **216** by 7.6- and 9.0-fold, respectively, thus confirming their transformation into cytotoxic species.

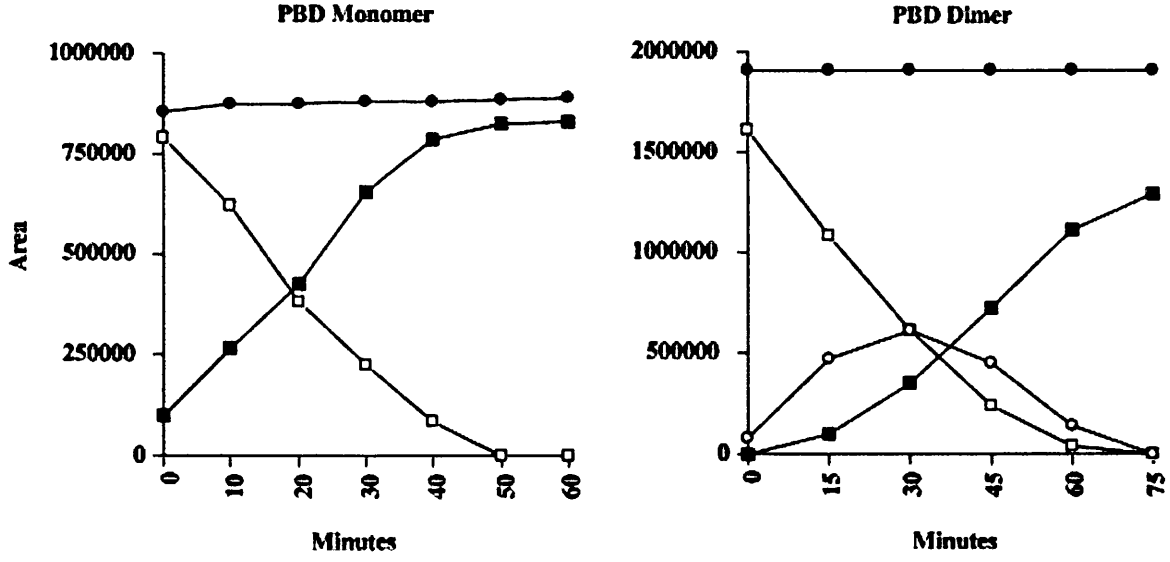

Figure 93: Conversion of the carbamate PBD monomer (214) and PBD dimer (216) prodrugs into parent PBDs (212 and 213, respectively) by CPG2 at 37 °C. Left-hand panel: empty square = 214, filled square = 212, filled circle = control; Right-hand panel: empty square= 216, filled square = 213, filled square = control; empty circle = mono-protected PBD dimer intermediate. Note: control = incubation of prodrugs in the absence of CPG2; Y axis = relative areas under HPLC peaks.

These results demonstrated that it was possible to synthesize N10-protected PBD prodrugs suitable for CPG2-based ADEPT therapy and was the stimulus for this PhD project. The prodrugs were more stable as the carbamate derivatives **214** and **216**, and significantly less cytotoxic than the parent compounds. They were good substrates for

CPG2, being rapidly converted into the cytotoxic monomer and dimer parent PBDs upon exposure to enzyme.

6.1.2 Hypothesis

The introduction of a C2-aryl group should significantly increase the differential between prodrug and parent. The presence of a protecting group at the N10 position should switch off PBD activity. In order to achieve the intial goals of the project the N10 protecting group should be stable and a good substrate for CPG2 to release the parent compound and to switch on activity.

6.1.3 Stability of Novel ADEPT Prodrugs

The aqueous stability of the new prodrugs synthesised in this PhD project was measured both at room temperature and 37°C by HPLC using the same conditions as previously used for prodrugs **214** and **215**. Degradation of the prodrugs and subsequent formation of the parent PBD were measured at each time point. Results were expressed as percentage of peak area (see **Figure 94**).

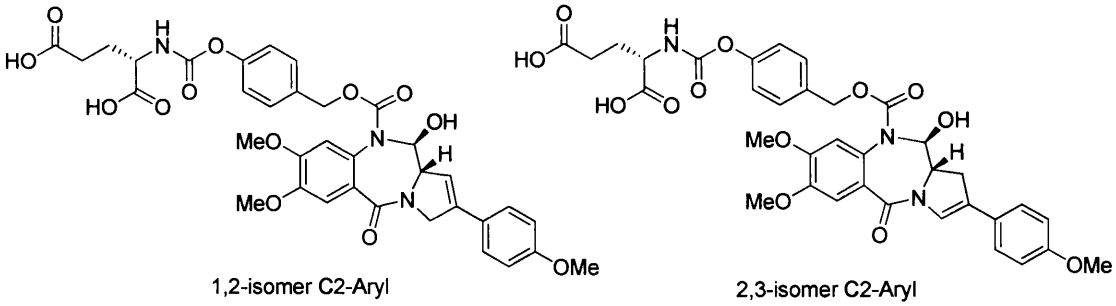

Figure 94: Structures of 1,2-isomer 255 and 2,3-isomer 222

Figure 95 illustrates the stability of 1,2-isomer **255** over a 24 hour period. Percentage area is plotted against time and taken to be proportional to drug concentration. Less than 1% degradation was observed over the first 6 hours increasing to 2 % over a 24 hour period.

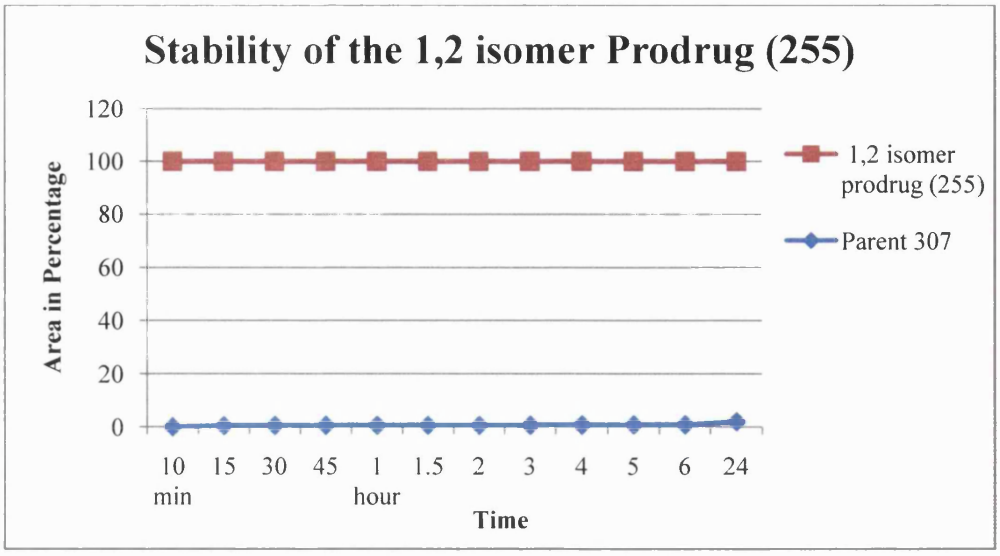

Figure 95: Stability of the 1,2- isomer (255), at 37°C by HPLC.

A similar pattern was observed for the 2,3-isomer (**222**) with no degradation for the first 6 hours, but slightly more degradation over a 24 hour period of 3.9%.

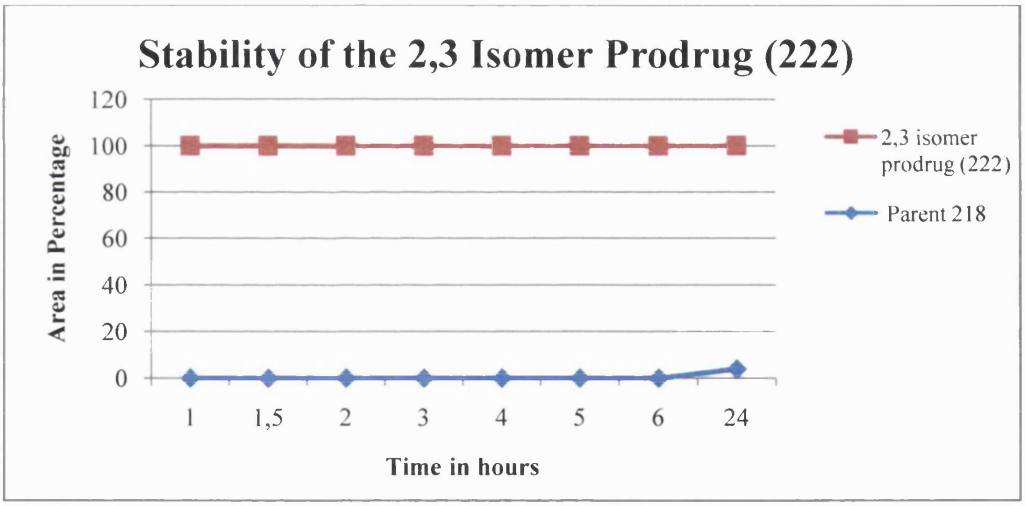

Figure 96: Stability of the 2,3- isomer (222) at 37°C by HPLC.

6.1.4 In Vitro Cytotoxicity of Compounds 255 and 222 in LS174T Cells

The cytotoxicities of prodrugs **255** (1,2-isomer) and **222** (2,3-isomer) was evaluated in the human colon adenocarcinoma LS174T cell line. In addition, the 1,2-isomer (**255**) was evaluated in the human erythromyeloblastoid leukemia K562 cell line.

An IC_{50} value of 2.5 μM was recorded for the 1,2-isomer **255** in LS174T cells after 1 hour exposure. On continuous exposure for 96 hours the IC_{50} value decreased to 0.19 μM. The parent drug **307** was evaluated under identical conditions and was found to have IC_{50} values of 1.4 μM and 0.14 μM after 1 hour exposure or continuous exposure, respectively. This revealed differential cytotoxicity values of 1.8 and 1.4 for the 1 hour and continuous exposure experiments, respectively.

A similar investigation of the 2,3-isomer **222** and its parent **218** gave IC_{50} values of 0.18 μM and 0.016 μM for 1 hour exposure or continuous exposure, respectively. This gave differential cytotoxicity values of 12 and 3 after 1 hour or continuous exposure, respectively.

Compound	A	B	C	Mean ±SE (μM)	Differential
255	1.5	2.2	3.9	2.5±0.7	1.8
307	1.2	1.5	1.6	1.4±0.1	-

Table 18: Cytotoxic values for 255 and 307 at 1 hour incubation

Compound	A	B	C	Mean ±SE (μM)	Differential
255	0.19	0.18	0.19	0.19±0.03	1.4
307	0.12	0.17	0.12	0.14±0.02	-

Table 19: Cytotoxic values for 255 and 307 on Continuous incubation (96 hours)

2,3-isomer 222

Compound	A	Differential
222	0.18 μM	12
218	0.015 μM	-

Table 20: Cytotoxicity values for 222 and 218 at 1 hour incubation

Compound	A	Differential
222	0.016 μM	3
218	0.006 μM	-

Table 21: Cytotoxicity values for 222 and 218 on Continuous incubation (96 hours)

6.1.5 In Vitro Cytotoxicity of 255 in K562 Cells

The 1,2-isomer prodrug **255** was also evaluated in the K562 cell line giving IC_{50} values of 0.7 μM after one hour and 0.015 μM on continuous exposure. This result demonstrated that the activity of the prodrugs was not specific to the LS175T cell type.

Compound	A	Differential
255	0.7 μM	1.4
307	0.5 μM	-

Table 22: Cytotoxicity values for 255 and 307 at 1 hour incubation

Compound	A	Differential
255	0.015 μM	0
307	0.015 μM	-

Table 23: Cytotoxicity values for 255 and 307 on Continuous incubation (96 hours)

The results above were unexpected and raised the question as to why the C2-aryl carbamate prodrugs showed such high cytotoxicity *in vitro*.

6.2.1 Prodrug Analogs

A series of prodrug analogs were synthesised and evaluated (**308, 218, 307, 263, 265, 288, 287, 255,** and **222**) to investigate the reason for the high cytotoxicity of the candidate prodrugs.

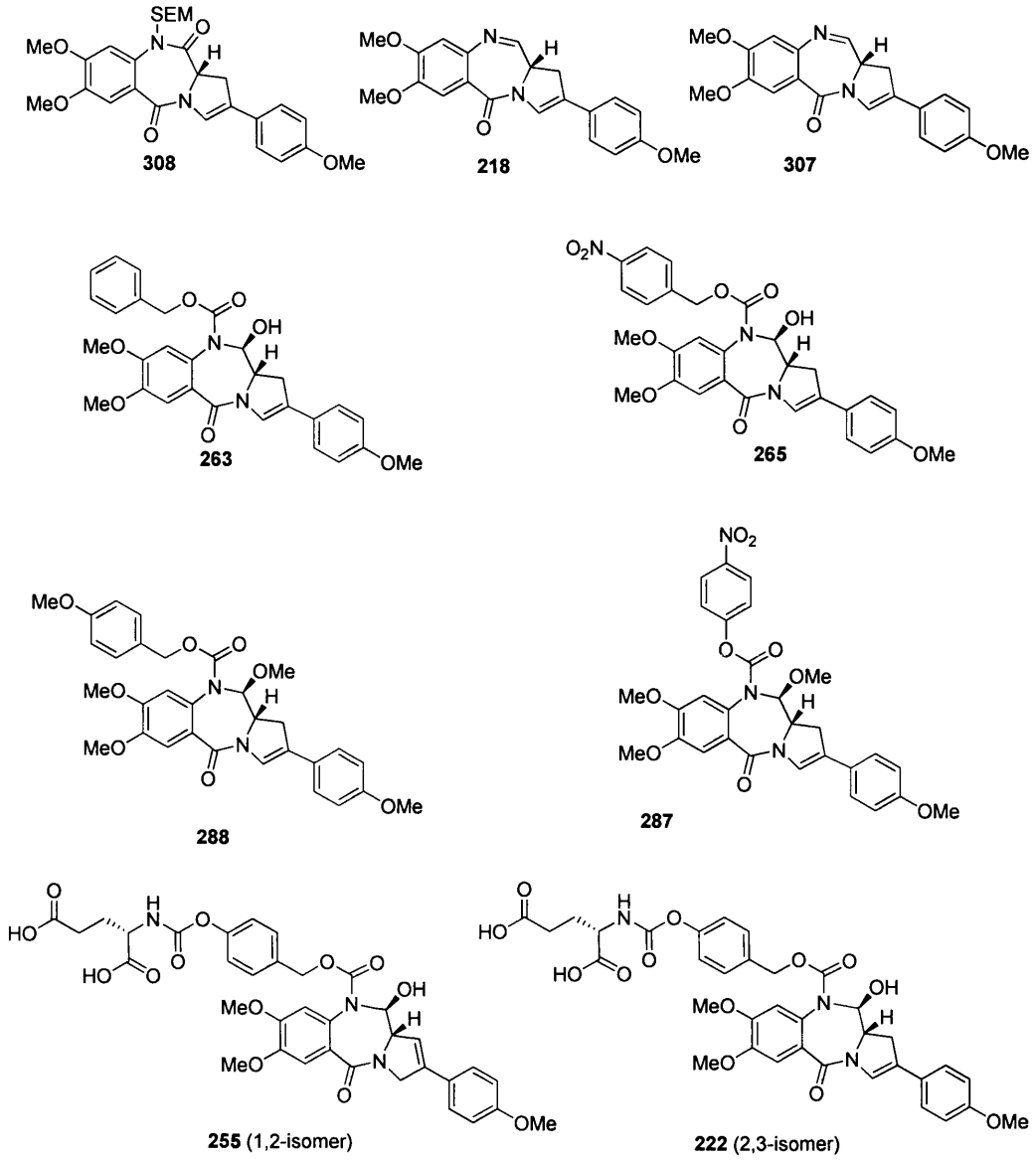

Figure 97: Structures of prodrug analogues synthesised in this project.

The cytotoxicity data for compounds **308, 218, 307, 263, 265, 288, 287, 255,** and **222** were surprising in that the N10-protected PBDs were not expected to exhibit low to sub-micromolar IC_{50} values. The potency of the ADEPT prodrugs **255** and **222** led to poor differential cytotoxicities, especially when compared with the values obtained by Masterson *et al.* for their C2-unsubstituted PBD prodrugs. Two possibilities were apparent: either the candidate prodrugs were inherently cytotoxic, or the free PBD was being released in the absence of carboxypeptidase enzyme. The SEM dilactam (**308**) was synthesised as a control, as it does not have an imine group at the N10-C11 position and should not covalently bind in the minor groove of DNA. If this molecule had been active, it would have suggested that the C2-aryl compounds could exert

cytotoxicity via an alternative mechanism. If the carbamate prodrugs undergo hydrolysis in the absence of carboxypeptidase, this would suggest an intrinsic instability within the N10-progroup. In order to investigate this possibility, three N10-benzyl carbamates were synthesised: **263, 288** and **265**. The unsubstituted benzyl carbamate **263** was intended to act as a bench mark, with the *p*-methoxy (**288**) and *p*-nitrobenzyl (**265**) carbamates probing the effect of the different electronic properties of these functional groups on hydrolysis. The *p*-methoxybenzyl compound (**288**) was of special interest, as its structure shares many of the features of the self-immolative group used in the candidate prodrugs **255** and **222**. Finally, the *p*-nitrophenyl carbamate (**287**) was structurally different to the other carbamates, lacking the self-immolative benzyl function while still maintaining a carbamate structure.

Table 24: below summarises the biological evaluation of two parent drugs (**307** and **218** (positive controls)), one N10-SEM dilactam (**308** (negative control)), four N10-carbamates (**263, 265, 288** and **287**) and the two ADEPT prodrugs (**255** and **222**).

Compound	Structure	Mean 1 hour IC_{50} (μM)	Mean Continuous IC_{50} (μM)	Differential 1 hour IC_{50} (μM)
307	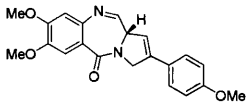	1.4±0.01	0.14±0.02	N/A
218	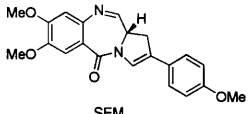	0.04±0.02	0.003±0	N/A
308	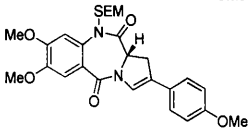	>100	11±2	>2308[a]
263	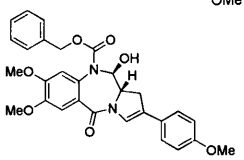	56±8	7.2±4	1300[a]
265	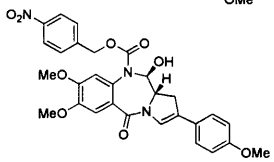	6±0.1	1.4±0.5	137[a]
287	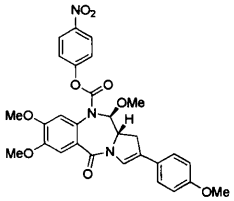	4.1±1.9	1.4±0.6	95[a]
288	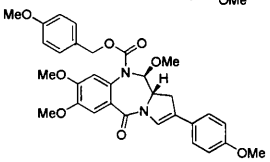	1.1±0.5	0.24±0.15	26[a]
255 (1,2 isomer)	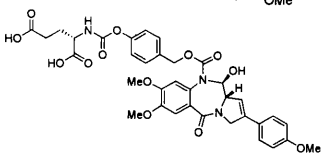	2.5±0.7	0.19±0.03	1.8[b]
222 (2,3 isomer)	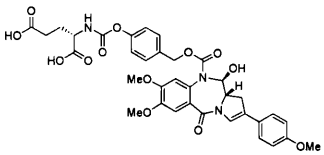	0.17±0.03	0.015±0.008	4[a]
214	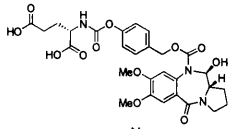	>100	20±1.2	4.7[c]
212	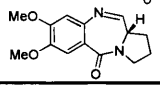	14±1.5	1.4±0.1	N/A

Table 24: *In vitro* cytotoxicity of C2-aryl PBD in LS174T cells. mean values are ±s.e.

The *in vitro* results shown in **Table 24** reveal that, as expected, the SEM dilactam **308** has a low activity (>100 μM) after 1 hour exposure. The positive controls, 1,2-isomer **255** and the 2,3-isomer **222** were predictably potent. The 1,2-isomer was cytotoxic with an IC_{50} value of 1.4 μM at 1 hour exposure. However, the 2,3-isomer had a significantly higher activity with an IC_{50} value of 0.04 μM at 1 hour.

The cytotoxicity values of the six N10-protected C2-aryl PBD carbamates were compared with the activities of the parent compounds to provide differential activities. A large differential suggested that the carbamate is not easily converted to imine under the conditions of the biological assay. Conversely a low differential indicated that the carbamate is readily converted. In the case of the two prodrugs **255** and **222**, their differentials suggested their potential as prodrugs. The largest differential observed was >2308 between the negative and positive control molecules; i.e. imine PBD **218** and SEM dilactam **308**. The second largest differential was 1300 between the benzyl carbamate **263** and the parent imine **218**. The next largest differential was 137 observed between the *p*-nitrobenzyl carbamate **265** and the parent imine **218**. This was followed by a differential of 95 between the *p*-nitrophenyl carbamate **287** and parent imine **218**. The differential between the *p*-methoxybenzyl carbamate **288** and its parent **218** was considerably lower with a value of 26. Disappointingly, the differentials between the candidate ADEPT prodrugs and their corresponding parent PBD were very low, with a value of 1.8 between the 1,2-isomer **255** and the corresponding parent imine **307**, and a value of 4 between the 2,3-isomer prodrug **222** and **218**.

6.2.2 Discussion

The aqueous stability of the new prodrugs **255** and **222** was assessed at 37°C by HPLC in order to ascertain their suitability as prodrugs in antibody-directed enzyme prodrug therapy (ADEPT). The 2,3-isomer prodrug appeared to be the more stable of the two prodrugs. An overall degradation of 4% for the 1,2-isomer (**255**) and 2% for the 2,3-isomer (**222**) was observed after 24 hours. Comparison with earlier PBD prodrugs synthesised by Masterson *et al.* revealed that the C2-aryl prodrugs **255** and **222** are significantly more stable than the **214, 215, 216 and 217** prodrugs.

The candidate prodrugs **255** and **222** have the bulkiest protecting group at the N10 position. In theory they should have a high IC_{50} value and a similar differential to the SEM dilactam **308**. However, this was not the case. Even though the stability studies demonstrated that the 1,2-isomer (**255**) and 2,3-isomer (**222**) prodrugs are stable in water, they were unexpectedly cytotoxic in LS174T cells. Mammalian cells contain a variety of esterase and carbamase enzymes that presumably hydrolyse the N10-carbamate in a non-specific fashion. The results from the K562 cells gave similar IC_{50} values to these from LS174T, suggesting that whatever mechanism is responsible for degradation is not specific to one cell-type. Significantly, previously prepared prodrugs **214** and **216** were not cytotoxic in the absence of carboxypeptidase. However, these compounds lack a C2-aryl substituent which may be responsible for making the new prodrugs sensitive to esterases. The data indicate that the N10-progroup carbamates are more labile than their simple benzylic counterparts. The progroup contains two potential hydrolysis sites corresponding to carbamate functionalities (**Scheme 75**). One carbamate functionality is adjacent to the glutamate residue and may be partially vulnerable to enzymes naturally present in tumour cells.

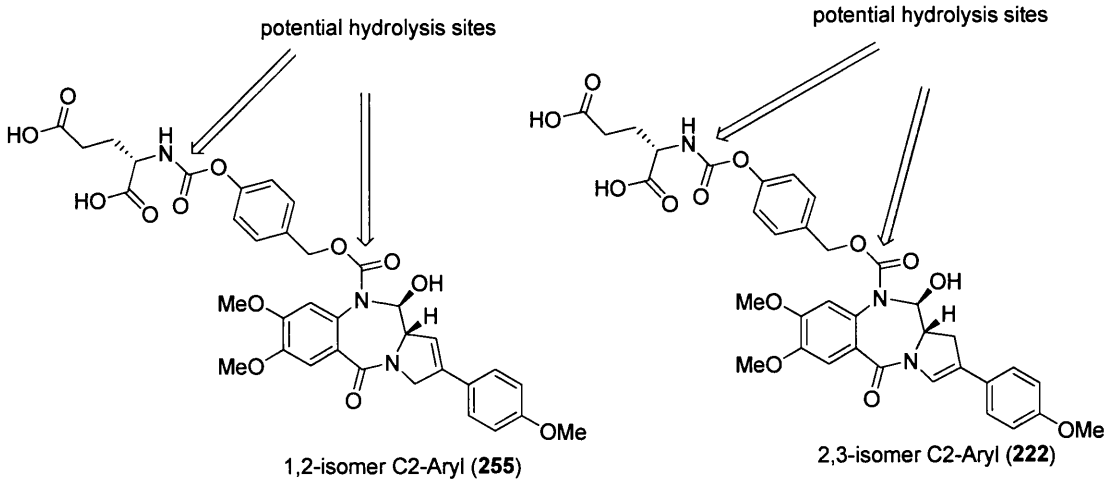

Scheme 75

The second largest differential was 1300 between the N-10-benzyl carbamate **263** and the parent drug **218**. This was be interpreted as the benzyl carbamate **263** being relatively stable under cellular conditions. The N10-C11 functionality remains protected and therefore the molecule cannot covalently bind in the minor groove of DNA. The high IC_{50} value of 56 μM at 1 hour indicates little or no degradation to the

parent compound. On continuous exposure the IC_{50} value increased to 7.2 μM suggesting there is some release to parent **218** over time.

The *p*-methoxybenzyl compound **288** on the other hand had an electron donating group in the *para* position thus increasing the tendency to self-immolation. As a result, compound **288** should release the parent imine (**218**) more readily, hence the comparatively low IC_{50} value of 4.1 μM at 1 hour exposure and a small differential of 26 compared to the benzyl carbamate **263** (**Scheme 76**).

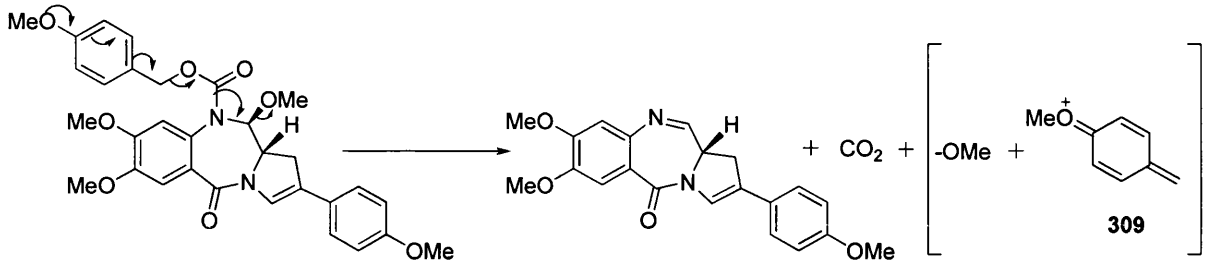

288 **218**

Scheme 76: Self-immolation of the N10-*p*-methoxybenzyl compound 288

The *p*-nitrophenyl carbamate **X** does not contain an obvious self-immolative feature but could be sensitive to hydrolysis due to the potential for the *p*-nitrophenoxy moiety to act as a good leaving group (**Scheme 77**).

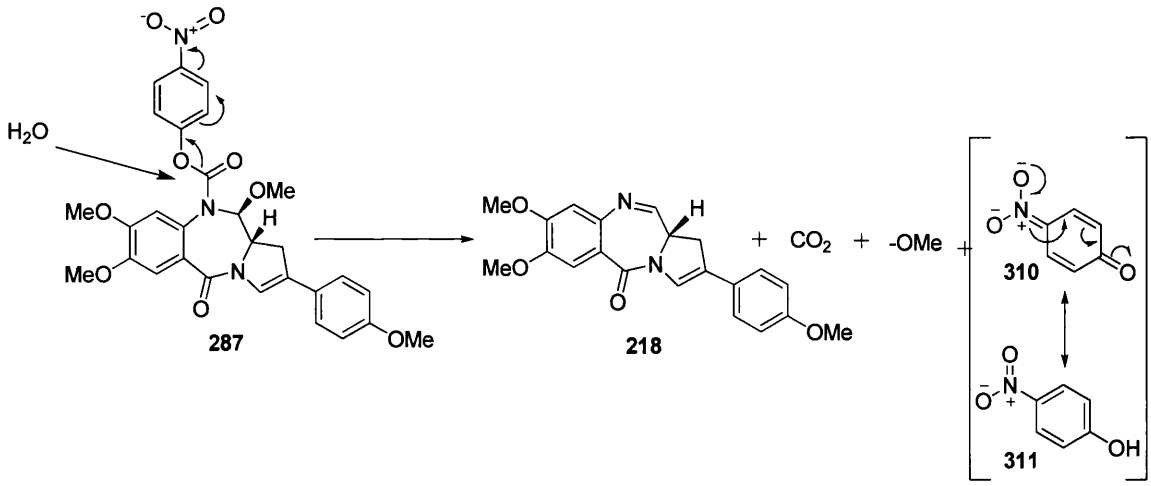

287 **218**

Scheme 77: Hydrolysis of the N1-*p*-nitrophenyl carbamate 287

The unexpected activity of the N10-*p*-nitrobenzyl PBD **287** (IC_{50} = 6 μM) is interesting. Following the explanation for the activity of **288**, the nitrobenzyl compound might be expected to be resistant to hydrolysis because the nitro group (in the para position) is electron withdrawing and so not conducive to self-immolation.

However, the IC_{50} value is much lower than expected suggesting that its activity may be due to an alternative mechanism. According to the literature the *p*-nitrobenzyl functionality can be used as a protecting group and is stable at physiological pH, as well as under oxidative, nucleophilic and organometalic conditions. It only becomes labile at pH values below 1 or greater than 12, and under reducing conditions. The general robustness of the *p*-nitrobenzyl group combined with its vulnerability to reducing conditions suggests that a nitroreductase enzyme could be implicated in the unexpected activity of **265** (see **Scheme 78**). Alternatively, the nitro group may enhance hydrolysis of the carbamate (see **Scheme 79**), by stabilising the alkoxide through the σ-framework

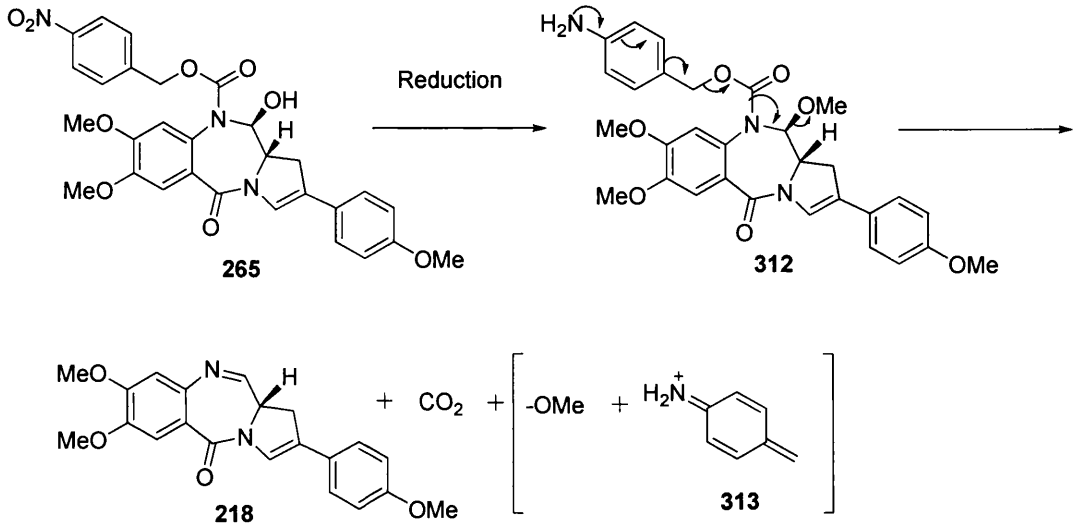

Scheme 78: Reduction and self-immolation of the *p*-nitrobenzyl prodrug 265

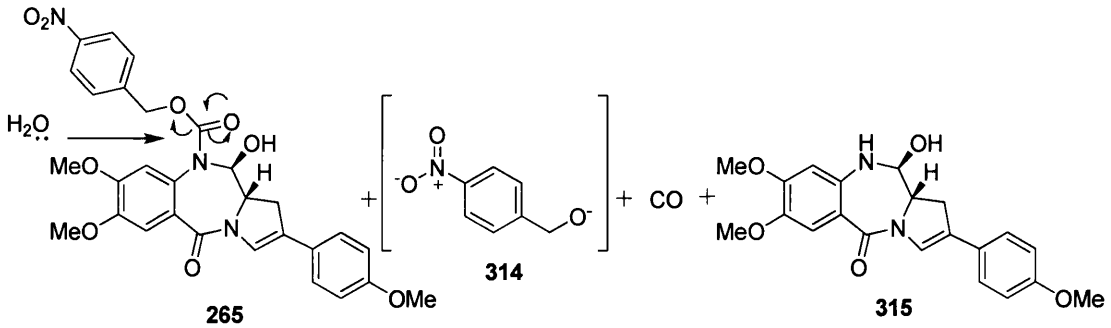

Scheme 79: Hydrolysis of the *p*-nitrobenzyl prodrug 265

6.3 Results of MTT Assay for ADEPT

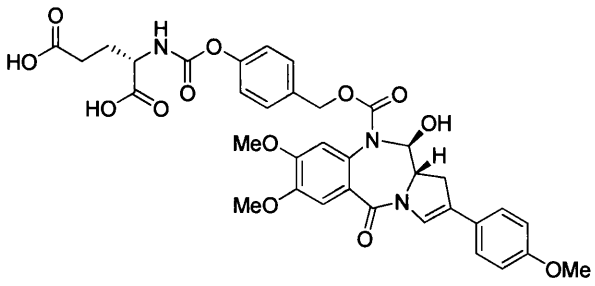

222 2,3-isomer

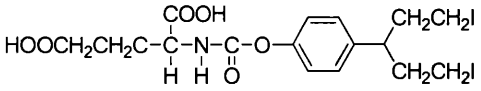

49 Bis-iodo prodrug

Figure 98: Structures of the PBD prodrug 222 (2,3-isomer) and 49 (mustard prodrug).

The initial target molecule **222** (2,3-isomer) was designed as a second generation PBD prodrug for use in ADEPT. Currently the bis-iodo prodrug **49** is being used in Phase I ADEPT clinical trials. However, the DNA lesions generated by the parent mustard are readily repaired thus reducing the impact of the ADEPT approach. PBDs are thought to be superior alkylating agents to nitrogen mustards because they bind covalently in the minor groove of DNA without distorting the helix and are more resistant to DNA repair mechanisms. The 2,3-isomer **222** was evaluated *in vitro* in combination with the carboxypeptidase enzyme conjugate (MFECP, as used in ADEPT) to investigate its potential as a prodrug. The results were similar to the previous studies, revealing the 2,3-isomer **222** to be significantly cytotoxic even in the absence of the carboxypeptidase conjugate. Six experiments were performed in total, three with the LS174T cell line (the same cell line used previously), and three experiments with a human colorectal carcinoma SW1222 cell line. The results for the LS174T cell line study provided data on percentage cell survival at time intervals of 24, 48 and 96 hours and four different concentrations (0.25, 0.5, 1 and 2 μM).

A carboxpeptidase-labile prodrug would not be expected to be cytotoxic in the absence of enzyme conjugate. However, in the presence of enzyme cell death should increase with time as prodrug is converted to drug. This process can be clearly observed for the bis-iodo mustard prodrug (**Figure 99-102**). However, in the case of the candidate prodrug (**222**), both cell lines are killed in a time and dose-dependent fashion even in the absence of enzyme conjugate. Introduction of conjugate resulted in only a slight increase in cell death.

These results were consistent with the earlier (UCL) study, and supported the idea that another enzyme (or enzymes) present in both cell lines is responsible for activation of the prodrug.

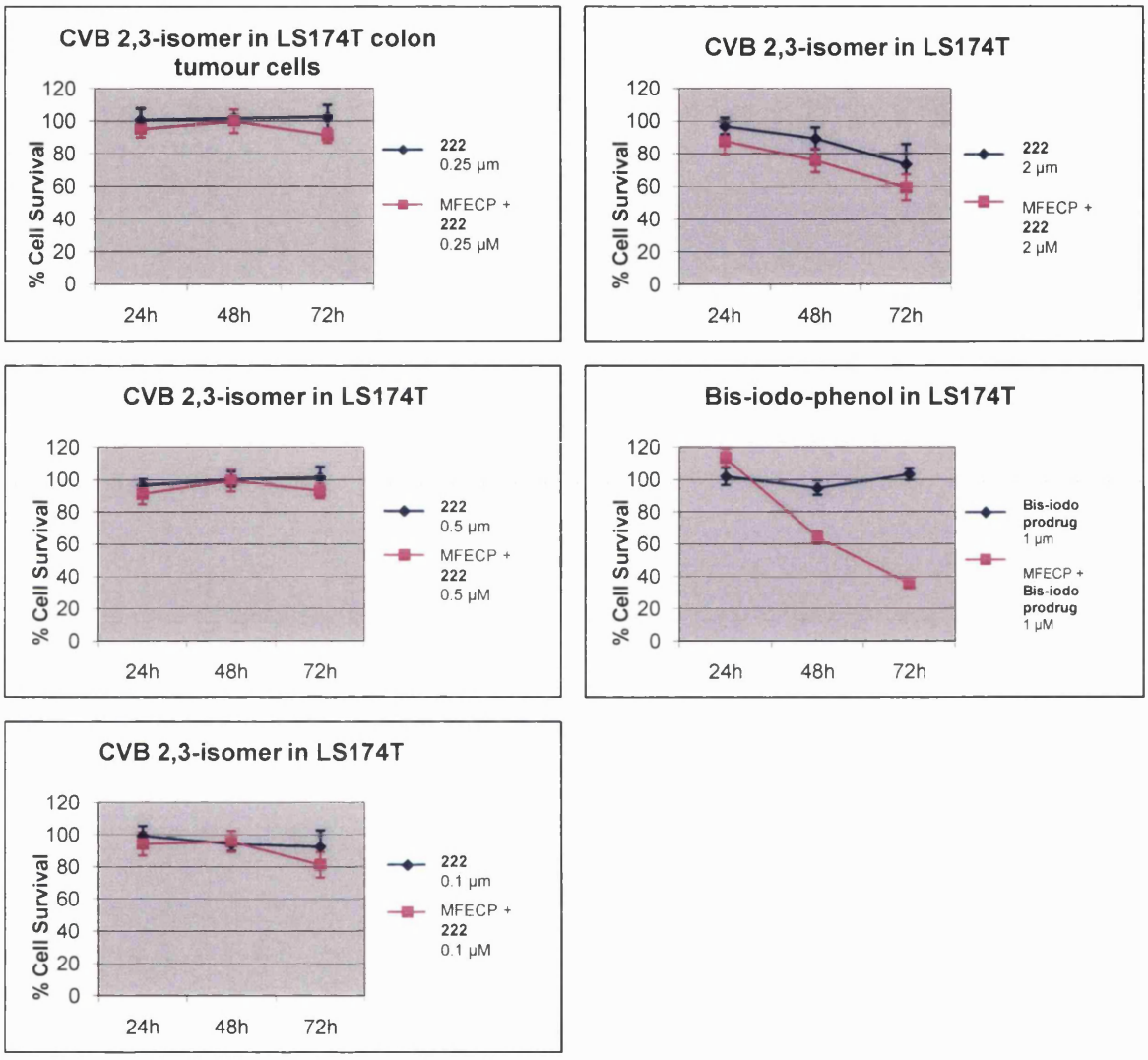

Figure 99: Cell survival in the LS174T cell line after treatment with the PBD and mustard prodrug in the presence and absence of MFECP (at concentrations 0.25, 0.5, 1, and 2 µM for PBD and 1 µM for mustard prodrug).

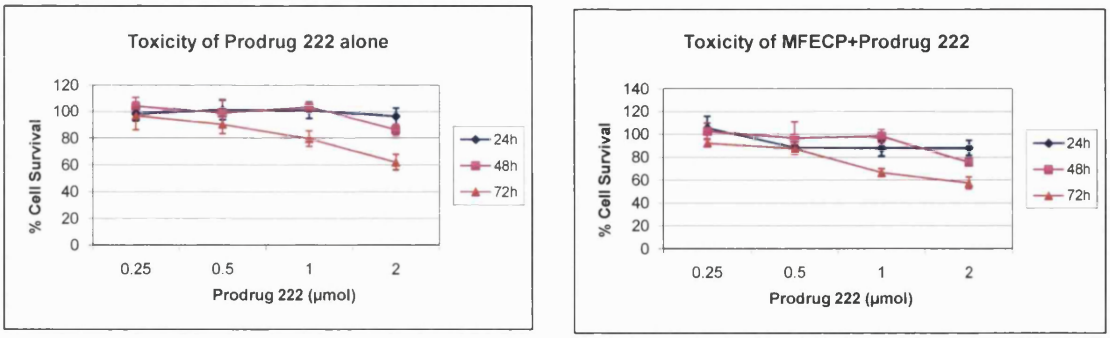

Figure 100: Cell survival in the LS174T cell line after treatment with the PBD and mustard prodrug in the presence and absence of MFECP (Comparrison of concentrations 0.25, 0.5, 1, and 2 µM for PBD and mustard prodrug).

The evaluation of the candidate prodrug **222** and the bis-iodo prodrug in the SW1222 cells was carried out in the same fashion as LS174T cell line but at five different concentrations: 0.25, 0.5, 1, 2 and 5 µM (**Figure 101** and **102**). The results were similar, revealing that the degree of cell survival for the 2,3-prodrug alone was low, and as exposure time and concentration increased, so did cytotoxicity. There was a small difference in the rate of cell survival between the 2,3-isomer prodrug alone and in combination with the MFECP conjugate, (i.e., marginal decrease in cell survival when MFECP was present). However, with the bis-iodo prodrug, addition of the MFECP conjugate gave a significant increase in cytotoxcitity.

It is not understood why the 2,3-isomer prodrug (**222**) does not release a significant amount of parent PBD imine (**218**) on exposure to MFECP enzyme. One possible explanation is that prodrug **222** is much larger than the mustard (**49**) and may not interact so well at the active site of the enzyme. Also, it should be noted that these experiments used the recombinant fusion protein MFECP rather than CPG2 alone which was used in the earlier experiments of Masterson *et al.*[126] Time and resources did not permit comparison of the activity of both CPG2 and MFECP towards the 1,2- (**255**) and 2,3- isomers (**222**).

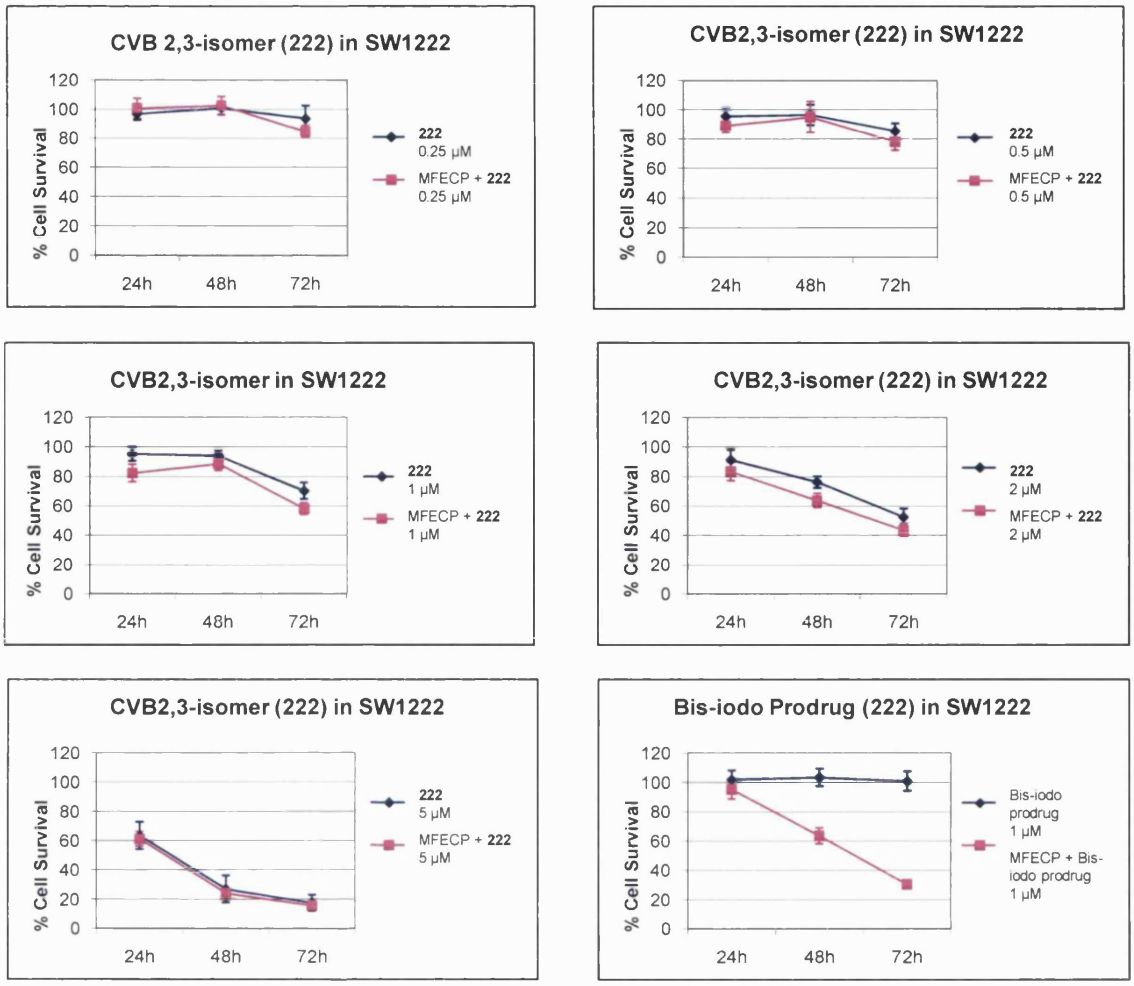

Figure 101: Cell survival in the SW1222 cell line after treatment with the PBD (222) and mustard prodrug (in the presence and absence of MFECP (at concentrations 0.25, 0.5, 1, 2 and 5 µM for PBD and 1 µM for mustard prodrug).

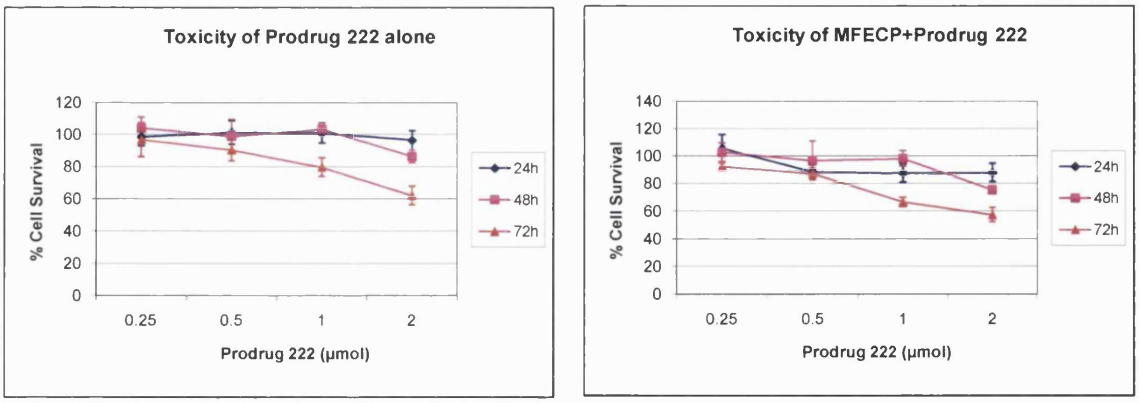

Figure 102: Cell survival in the SW1222 cell line after treatment with the PBD (222) and mustard prodrug (49) in the presence and absence of MFECP (Comparison of concentrations 0.25, 0.5, 1 and 2 µM for PBD and mustard prodrug).

6.4 GDEPT

The candidate prodrug **222** could not be considered any further as an ADEPT prodrug due to its cytotoxicity in three different cancer cell lines (i.e., average 0.16±0.02 μM and 0.015±0.001 μM at 1 hour exposure and continuous exposure, retrospectively). This was thought to be due to instability of the prodrug *in vitro*, with release of the parent drug in the absence of carboxypeptidase.

However, results for the N10-*p*-nitrobenzyl carbamate **265** in the *in vitro* studies were encouraging and suggested further investigations of its potential as a nitroreductase sensitive prodrug. In particular, it was decided to evaluate this agent as a potential prodrug for use in experimental GDEPT therapies presently based on CB (1954).

6.4.1 Background

Human telomeres are located at the end of eukaryotic chromosomes and are comprised of repeating TTAGGG sequences. Most telomeric DNA is double stranded except for the end which is 3'-single-stranded and more than 200 nucleotides in length. Telomeres are thought to prevent aberrant chromosome fusion and exonucleolytic degradation. They also control the correct mitotic and meiotic separations of sister chromatids. During cell division there is incomplete replication of the telomeres resulting in the loss of telomeric repeats (attrition). This causes the life span of normal somatic cells to be limited to 50-70 divisions, and thus telomere attrition acts as a 'mitotic clock'. However, activation of human telomerase prevents attrition.

Telomerase is a multi-subunit ribonucleoprotein transcriptase that extends human telomeres through a terminal transferase activity of RNA hTR and hTERT. It is thought that hTR acts as a scaffold for recruiting accessory proteins and hTERT acts as a catalytic component containing several motifs characteristic of reverse transcriptase but with a different spacing. hTERT has a unique N-terminal T motif, which is well-conserved amongst telomerases which provides the polymerisation activity of the enzyme. When hTR and hTERT are combined under acellular conditions, they are able to reproduce telomerase activity towards oligonucelotide

substrates.[159, 160] There have been many attempts to inhibit telomerase enzyme activity but so far these studies have been restricted to cell culture. However, there has been some success in preclinical studies, exploiting the selectivity of telomerase gene expression within cancer cells to develop gene therapy strategies.[161-164]

One approach to exploiting differential telomerase expression in tumour cells involves the use of telomerase promoters to control the expression of nitroreductase enzyme capable of activating reduction-sensitive prodrugs.

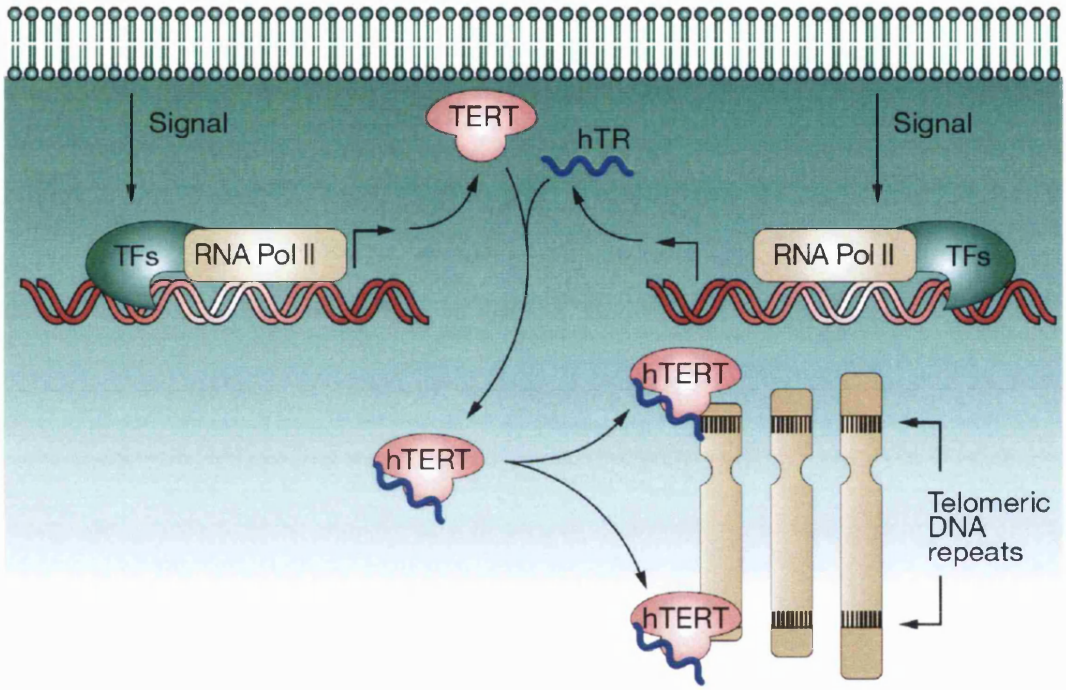

Figure 103: The products of two genes are required to reconstitute basic telomerase activity; the RNA component, hTR, which includes the template for synthesis of telomere DNA, and the protein catalytic component, hTERT, which has reverse transcriptase activity. Additional molecules are necessary for full regulation *in vivo*. Telomerase is absent from most normal somatic cells. Every time a normal cell divides a telomere repeat sequence is lost from the end of the chromosome. Eventually, after many cell divisions, the gradual erosion of the telomere is sensed by the cell once ultimately telomeres reach a critically short length and cell signaling pathways initiate the senescence program resulting in a cessation of cellular proliferation. In cancer cells, the senescence program is bypassed through the activation of telomerase. Once activated in the cancer cell, telomerase maintains telomeres at a length compatible with cell proliferation through the addition of telomere repeat sequences and the cancer cell becomes immortal.[161]

Bilsland *et al.*[104] employed an "Adeasy" system to construct E1/E3-deleted adenovirus constructs harbouring the NRT coding sequence under the transcriptional control of hTR and hTERT promoters, affording the first generation of adenoviral (Ad) vectors Ad-hTR-NRT and Ad-hTERT-NRT. These vectors were used to infect a

panel of 7 tumour and 4 normal cells lines, which were exposed to the nitroreductase sensitive prodrug CB 1954 (see **Figure 104** and **Table 25**).[165]

The subsequent MTT cytotoxicity assay revealed that the tumour cell lines, unlike the normal cells, were selectively sensitised (up to 18-fold) to CB 1954 due to their ability to activate under the control of the hTR and hTERT promoters.

The study also demonstrated that hTR was a stronger promoter than hTERT. It was observed that sensitisation also occurred in poorly infected cells, perhaps due to the 'bystander effect'.

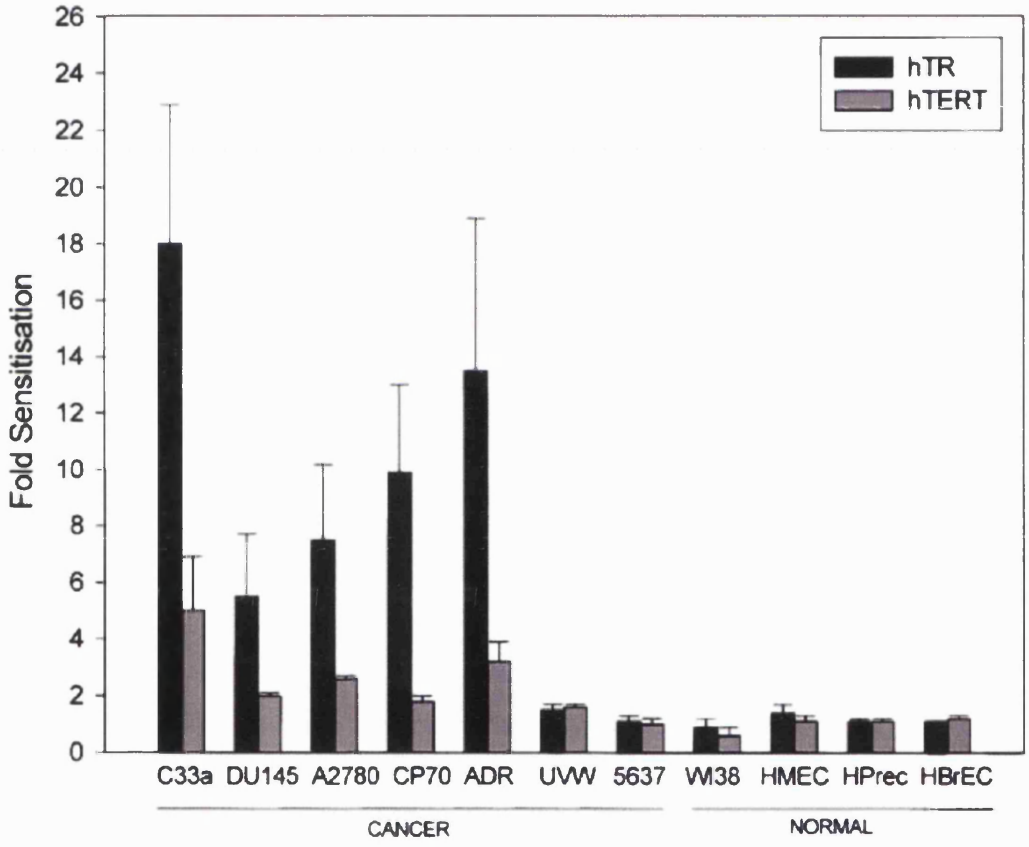

Figure 104: Mean sensitization to CB1954 and infectivity in adenovirus-infected cancer and normal cell lines. Cell lines were infected with 50 PFU per cell Ad-hTR-NTR or Ad-hTERT-NTR and subjected to CB1954 challenge and MTT assay. IC_{50} values for individual experiments in each cell line were taken to be the concentration of CB1954 required to reduce cell densities in MTT assays to 50% of those of untreated controls. Sensitization values were the fold-difference between the IC_{50} of the mock-infected cells and those of cells infected with the gene therapy vectors. Black bars correspond to Ad-hTR-NTR-infected cells and grey bars to Ad-hTERTNTR infected cells. Data are means, and s.e.'s are calculated from three experiments.[104]

Cell line	Mock IC_{50} μM (s.e)	hTR 10 PFU IC_{50} (s.e) μM	hTR 50 PFU IC_{50} (s.e) μM	hTERT 10 PFU IC_{50} (s.e) μM	hTERT 50 PFU IC_{50} (s.e) μM	% Infectivity (s.e) 10 PFU	% Infectivity (s.e) 10 PFU
C33a	176.1 (10.0)	33.4 (14.6)	9.8 (2.7)	63.1 (17.1)	35.9 (13.3)	59.2 (0.2)	80.3 (2.7)
DU145	39.4 (2.7)	25.9 (4.8)	7.1 (2.9)	41.6 (5.6)	20.2 (1.4)	64.2 (10.0)	92.4 (4.8)
A2780	28.5 (13.9)	10.7 (3.7)	3.8 (1.4)	17.7 (4.4)	10.9 (0.6)	16.3 (1.8)	33.6 (6.6)
A2780-CP70	59.6 (12,1)	25.9 (2.9)	6.0 (1.9)	48.3 (9.6)	33.9 (3.1)	20.1 (5.8)	47.5 (2.9)
A270-ADR	238 (45.1)	54.2 (11)	17.6 (7)	112.7 (30.5)	74.4 (15.5)	58.4 (2.7)	71.7 (2)
UVW	214.4 (15.7)	144.6 (9.8)	77.7 (15.9)	180.8 (26.0)	136.2 (11.4)	56.9 (19.3)	74.5 (12.6)
5637	102.9 (14.2)	93.5 (16.0)	73.4 (14.6)	112.6 (20.0)	103.2 (22.4)	72.3 (11.0)	94.5 (1.2)
W138	153.6 (48.5)	178.1 (68.0)	164.7 (55.2)	148.6 (54.8)	174.1 (74.1)	65.0 (2.6)	97.8 (0.1)
HMEC	31.7 (11.2)	45.4 (20.5)	36.0 (11.3)	27.8 (6.3)	29.6 (4.5)	34.4 (1.1)	66.2 (0.7)
HPr EC	266.3 (49.8)	238.7 (13.0)	190.5 (25.3)	297.3 (32.0)	235.3 (13.5)	8.0 (2.9)	36.8 (10.9)
HBrEC	188.1 (22.3)	169.2 (26.8)	148.9 (3.2)	196.1 (27.8)	156.8 (8.0)	24.4 (1.1)	68.3 (2.4)

Table 25: IC_{50} values for CB1954 cytotoxicity in cell lines infected with Ad-hTR-NTR and Ad-hTERT-NTR gene therapy viruses. Abbrivations: PFU (plaque forming units), adult mammary (HMEC), prostate (HPrEC) and bronchial (HBrEC) epithelial cell strains.[104]

The *in vitro* investigation was followed up by a xenograft study with the A2780 and C33a cell types which had shown 8- and 18-fold sensitisation *in vitro*. The animals received a single intra-tumoural injection of either Ad-hTR-NRT and Ad-hTERT-NRT or "mock virus", Ad-CMV-LACZ vectors, followed after 24 hours by a single injection of 80 mg/kg of CB 1954. The C33a tumours revealed a 43% and 40% reduction in relative tumour volume for the Ad-hTR-NRT and Ad-hTERT-NRT viruses, retrospectively. Similarly, A2780 xenograft-bearing mice revealed a reduction of tumour volume of 54% and 57% for the Ad-hTR-NRT and Ad-hTERT-NRT viruses, respectively.

These results clearly demonstrated the use of telomerase-specific molecular therapy to selectivity produce high intracellular concentrations of an active alkyating

agent. However, cell lines with lower promoter activity were not sensitised to CB 1954 even when all the cells were infected. [162]

6.4.2 CB 1954 and CB 1954 Alternatives

N10-*p*-nitrobenzyloxy-substituted PBDs were considered to have potential as second-generation nitroreductase-labile prodrugs for GDEPT therapies. Reduction of the nitro group should produce the *p*-aminobenzyl carbamate moiety required for self-immolation. Previous studies indicated that N10 *p*-nitrobenzyloxy substituted PBDs were significantly less cytotoxic than their parent N10-C11 imines.[105]

The *p*-nitrobenzyl carbamate **265**, together with a set of similarly related PBDs and CB 1954 as a positive control were evaluated against a panel of human tumour cells transfected with the NTR gene. As levels of telomerase expression vary between tumour cell lines, the initial studies focussing on the sensitivity of prodrugs to nitroreductase activity, were performed using the CMV promoter. This promoter efficiently transduces NRT expression regardless of cell line type.

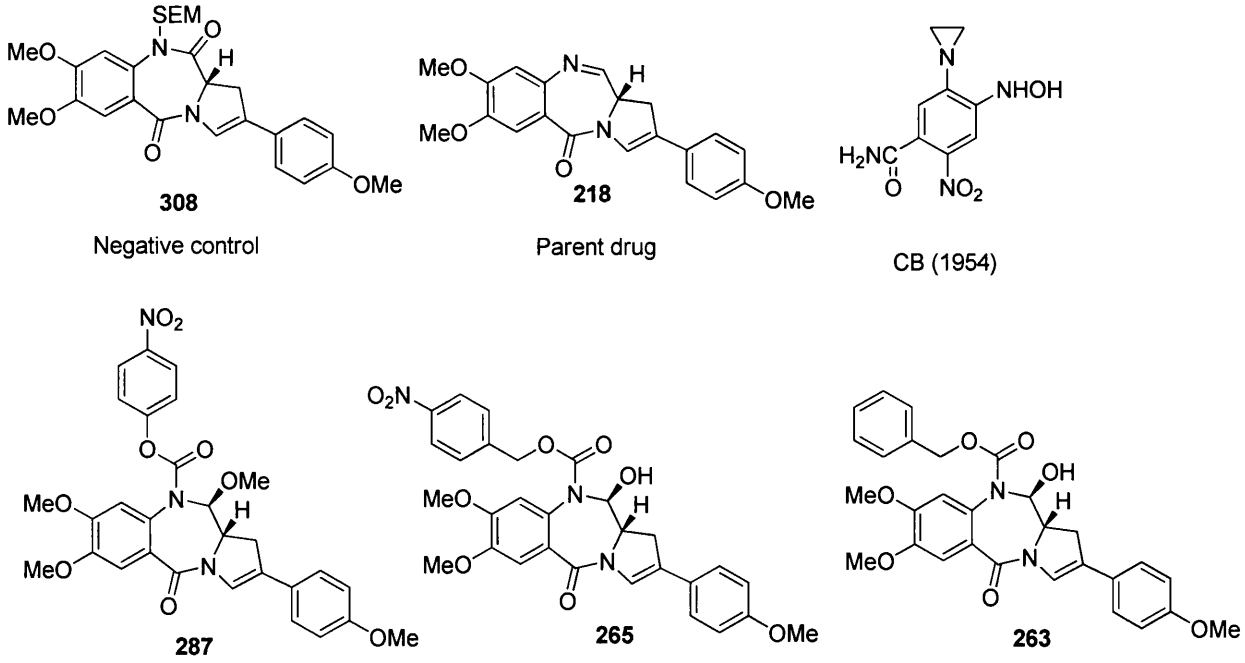

Figure 105: Structures of prodrugs and control molecules evaluated in the parent and CMV NTR cell lines.

The cell lines used were:

Parent line	NTR Exressing
A2780 Basic	A2780 CMV NTR
C33a Basic	C33a CMV NTR
A549 Basic	A549 CMV NTR
5637 Basic	5637 CMV NTR

6.4.3 Results

The MTT experiments were repeated twice for all cell lines (apart from C33a where it was only carried out once). Due to the low amounts of **308** available, the second MTT assays with A2780 and 5637 cells were carried out at the lower starting concentration of 20 μM. IC_{50} (μM) values were determined using Softmax Pro 4.6 software to analyse plates.

IC_{50} (μM)								
Drug	**A2780 basic**	**A2780 CMV NTR**	**A549 Basic**	**A549 CMV NTR**	**C33a Basic**	**C33a CMV NTR**	**5637 Basic**	**5637 CMV NTR**
308	3.162	2.038	25.89225	18.0935	7.7185	15.355	14.4925	16.824
218	0.000151	0.00028	0.001355	0.000594	0.001319	0.00052	0.000126	0.000109
287	0.000307	2.12E-05	0.246073	0.378625	0.004875	0.04785	0.181175	0.0778
265	0.2903	0.01576	5.1735	0.6395	0.47205	0.18673	0.594592	0.40599
263	3.3935	1.9125	7.96675	5.76925	0.7425	0.6695	2.7785	2.2775
CB1954	0.1502	0.253	30.583	36.5125	13.526	1.7365	49.015	22.85

Table 26: Showing IC_{50} (μM) values determined by SoftMax software. Average of two experiments (apart from C33a which was only carried out once).

Sensitisation of the cells to each of the drugs was calculated by dividing the IC_{50} (μM) for the basic cells by the IC_{50} (μM) for the CMV NTR transfected cells.

Sensitisation				
Drug	**A2780**	**A549**	**C33a**	**5637**
308	1.551521	1.431025	0.50267	0.861418
218	0.461189	2.81328	2.575816	1.156188
287	14.50012	0.649911	0.101881	2.328728
265	18.42005	8.089914	2.58049	1.464536
263	1.774379	1.380899	1.109037	1.219978
CB1954	0.593676	0.837604	7.789231	2.145077

Table 27: Sensitisation of the cell lines to each of the compounds.

The parent imine (**218**) was found to be extremely cytotoxic across the entire cell line panel. The SEM-protected dilactam (**308**) exhibited moderate micromolar activity in the A2780 cell line and lower levels of activity in the A549, C33a and 5637 cell lines. The *p*-nitrophenyl carbamate (**287**) was active across the panel with sub-micromolar levels of activity in the A2780 cell lines. The *p*-nitrobenzyl carbamate (**265**), had sub-micromolar activity across the panel but revealed significant differences between the basic and CMV cell lines. The benzyl carbamate (**263**) exhibited lower levels of activity against the A2780, A549, C33a and 5637 cell lines. CB 1954 had sub-micromolar activity in the A2780 cell lines but gave an approximately 8-fold sensitisation in the C33a CMV cells.

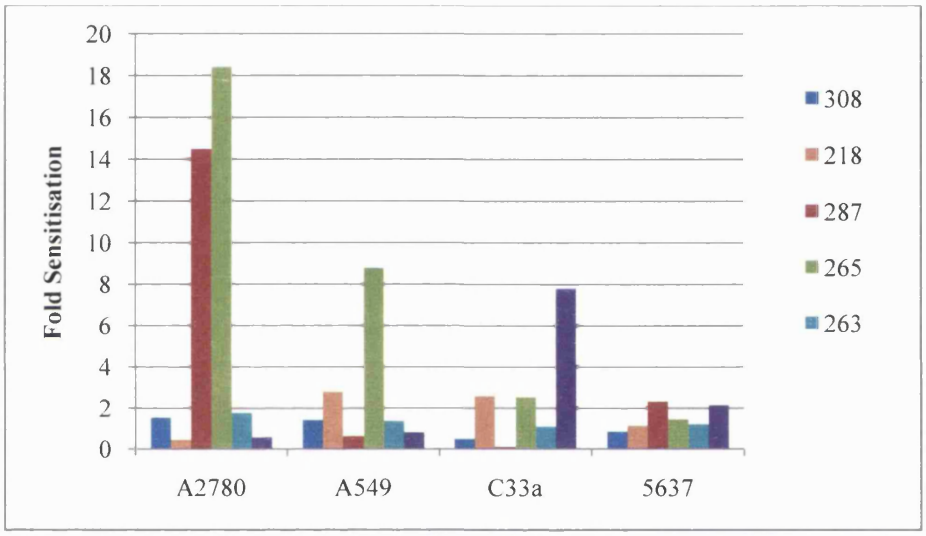

Figure 106: Sensitisation of the cell line pairs to compounds 308, 287, 265, 263 and CB 1954.

Drug	A2780 basic	A549 Basic	C33a Basic	5637 basic
265	1922.517	602.583	50.4928	2231.254
263	22473.510	5879.542	562.9265	22051.59

Table 28: Differential cytotoxicity values between parent compound 218 and compounds 256 and 263 in the basic A2780, A549 C33a and 5637 cell lines.

Drug	A2780 CMV NTR	A549 CMV NTR	C33a CMV NTR	5637 NTR
265	56.28571	366.5825	29.71154	1621.468
263	6836.357	9712.542	1287.5	20894.5

Table 29: Differential cytotoxicity values between parent compound 218 and compounds 256 and 263 in the CMV NTR A2780, A549, C33a and 5637 cell lines

6.4.4 Discussion

As anticipated, the parent PBD imine **218** was highly cytotoxic across the whole panel. These results were consistent with the well-documented *in vitro* cytotoxicity of this compound. Conversely, the PBD-dilactam (**308**), which lacks a N10-C11 electrophilic moiety was significantly less active, reflecting its inability to bind to DNA.

For compound **287**, although the *p*-nitrophenoxy moiety is a good leaving group, it is not generally recognised as being part of a self-immolative benzyloxy system. Instead, it is more likely that the N10-carbamate is vulnerable to non-specific hydrolysis thus releasing the potent parent PBD imine (**218**) and explaining its cytotoxcity.

As expected, the benzyl carbamate (**263**) showed no differential between basic and NRT cell lines because it does not possess a reductable nitro group. However, it does show some cytotoxicity in the C33 cell line, presumably due to hydrolysis of the N10- progroup by cellular carbamases or esterases.

The *p*-nitrobenzyl carbamate (**265)** was surprisingly cytotoxic across the panel, especially in the context of earlier data obtained in LS147T cell lines where it gave values of 6 μM and 1.4 μM after 1 hour exposure or continuous exposure, respectively. Sub-micromolar activities were observed in both the basic and transfected cell lines ranging from 1.47-fold to 18.4-fold (see **Table 27**). As **265** is realitively stable in aqueous conditions its inherent cytotoxcity must again be due to celllar esterases and carbamases.

However, critically the *p*-nitrobenzyl carbamate (**265**) is significantly less cytotoxic than the parent imine (**218**), with a 2231-fold differential in the basic 5637 cell line (**Table 28**). Interestingly **265** is also significantly less toxic in the CMV NTR transduced cell lines, indicating that reduction of the nitro group is not proceeding with optimum efficiency.

Similary, benzyl carbamate **263** has a 22473-fold differential compared to its parent **218** in the basic A2780 cell line, confirming the assertion that blocking the N10-position is preventing DNA interaction and thus acting as an "on/off" switch.

6.4.4.1 Comparison with CB 1954

Compound **265** was significantly more cytotoxic than CB 1954 in all the cell lines studied except the A2780 parent cell line. In the two cell lines with a strong sensitisation (A2780 and C33a), **265** was 200- and 17-times more active than CB 1954. The major significance of these results is that there is sensitisation in all of the cell line pairs ranging from 1.46 to 18.4, indicating that **265** is definitely behaving as a nitroreductase-activated prodrug. It is interesting to note that compound **287**, which contains a non-self-immolative N10-protecting group, shows sensitisation in two cell-line pairs (14.5- and 2.32-fold for A2780 and 5637 cell lines), suggesting that this molecule is also working as a nitroreductase sensitive prodrug despite not having a traditionally-reconized self-immolative N10-progoup.

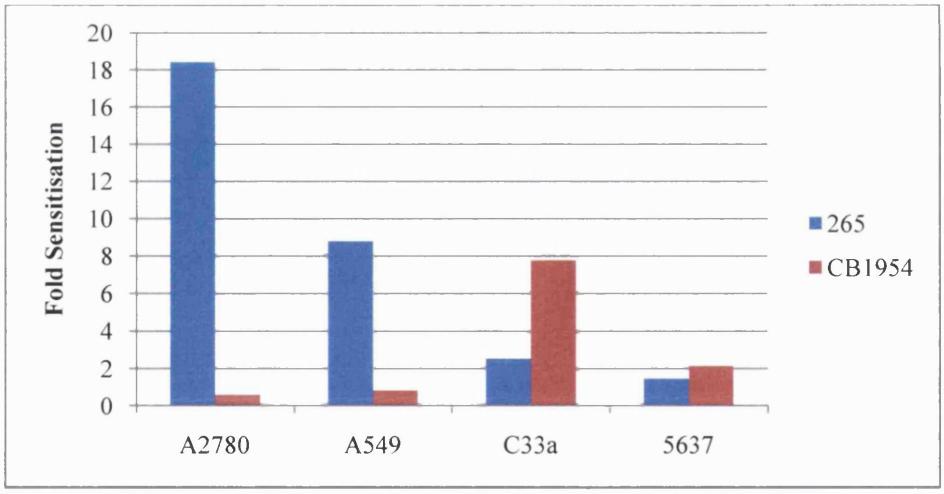

Figure 107: Sensitisation of the cell lines to CB 1954 and compound 256.

6.5 Future Work: Biology

Due to the encouraging results obtained in the CMV transfected cell lines, further *in vitro* and *in vivo* studies are planned.

6.5.1 In Vitro Studies

The initial *in vitro* studies were performed using an efficient but exogenous CMV promoter. Future work will focus on systems exploiting endogenous telomerase activity to activate the nirtoreductase gene. In the subsequent *in vitro* assays, the activity of compound **265** will be compared to CB 1954 in A2780, and C33a cell lines infected with hTERT-NTR and hTR-NRT viruses.

6.5.2 In Vivo Studies

Prodrug **265** is undergoing evaluation in a human tumour xenograft study, using an NTR transfected A2780 xenograft model in the hope that a greater therapeutic index (TI) can be obtained compared to CB 1954. The SEM dilactam **308** will be used as a reduction insensitive control.

Chapter 7

Final Conclusions

7. Final Conclusions

- The target ADEPT prodrug was successfully synthesised in sufficient quantity to allow preliminary *in vitro* biological evaluation.
- A 16-step synthesis was devised and performed affording a mixture of 1,2- (**255**) and 2,3-isomers (**222**), which were separated and purified by preparative LC/MS.
- An alternative strategy of installing the N10-progroup at a later stage of the synthesis was explored which had the advantage that the progroup could be introduced to a N10-C11 imine-containing PBD of any structure. Unfortunately, the more-complex glutamate N10-protecting group was unstable to the conditions required to introduce it to the N10-position of the PBD. This alternative strategy did, however, enable a range of molecules to be synthesised and evaluated thus affording important SAR data.
- HPLC studies demonstrated that the 1,2- (**255**) and 2,3-isomeric (**222**) prodrugs were stable in water but were unexpectedly cytotoxic in LS174T, K562 and SW1222 cells.
- Prodrug **222** could not be developed any further due to its high cytotoxicity in three different cancer cell lines (*i.e.*, average 0.16±0.02 μM and 0.015±0.001 μM at 1 hour exposure and continuous exposure, respectively). This cytotoxicity was thought to be due to release of the parent drug in cells by non-specific esterase and/or carbamase enzymes in the absence of carboxypeptidase.
- A number of N10-carbamate analogues were also synthesized as potential nitroreductase-sensitive prodrugs for use in GDEPT therapies. A lead molecule, the N10-*p*-nitrobenzyl carbamate **265**, was identified that provided sensitization ratios of up to 18.4-fold (in A2780) in CMV NRT transfected cell lines compared to the parent cell line. These studies also demonstrated that for the parent PBD (**218**) in some cell lines (*e.g.*, CMV NTR A549), protecting the N10-position can provide a differential of up to 22473-fold (i.e. for **263**). Based on the encouraging *in vitro* results for prodrug **265**, *in vivo* studies are presently underway.

In summary, these studies have clearly demonstrated that the glutamate progroup used in the present generation of mustard-based ADEPT prodrugs cannot be adapted for use with PBDs, as the prodrugs are unstable in the cellular environment in the absence of carboxypeptidase enzyme. However, it has been shown that nitro-reductase sensitive progroups attached at the N10-position of PBDs can produce prodrugs suitable for GDEPT therapies.

Chapter 8:

Experimental Section

8. Experimental Section

8.1 General Synthetic Methods

Optical rotations were measured on an ADP 220 polarimeter (Bellingham Stanley Ltd.) and concentrations (*c*) are given in g/100mL.

Melting points were measured using a digital melting point apparatus (Electrothermal).

IR spectra were recorded on a Perkin-Elmer Spectrum 1000 FT IR Spectrometer.

^{1}H NMR and **^{13}C NMR** spectra were acquired at 300 K using a Bruker Avance NMR spectrometer at 400 and 100 MHz, respectively. Chemical shifts are reported relative to TMS (δ= 0.0 ppm), and signals are designated as s (singlet), d (doublet), t (triplet), dt (double triplet), dd (doublet of doublets), ddd (double doublet of doublets) or m (multiplet), with coupling constants given in Hertz (Hz).

Mass spectroscopy data were collected using a Waters Micromass ZQ instrument coupled to a Waters 2695 HPLC with a Waters 2996 PDA. Waters Micromass ZQ parameters used were: Capillary (kV), 3.38; Cone (V), 35; Extractor (V), 3.0; Source temperature (°C), 100; Desolvation Temperature (°C), 200; Cone flow rate (L/h), 50; De-solvation flow rate (L/h), 250. High-resolution mass spectroscopy data were recorded on a Waters Micromass QTOF Global in positive W-mode using metal-coated borosilicate glass tips to introduce the samples into the instrument.

Accurate Mass measurements were performed on a Micromass Q-TOF Ultima Global (Waters, Manchster, UK) mass spectrometer. For the acquisition of ESI spectra, analyte was dissolved in acetonitrile (1-10 ng/μL), and loaded into a metal-coated capillary with a spraying orifice of 1-10 μm (Proxeon, Odense, Denmark). ESI was initiated by applying a potential of approximately 1.7 kV to the capillary. All other parameters were as follows:- cone voltage, 100 V; RF lens voltage, 35 and 0.1 V; source temperature, 800; desolvation temperature, 1500; LM resolution 10; RM resolution 10; cone gas 50 L/hr. The TOF analyser was operated in W-mode (17,500 resolution, full width at half maximum height definition).

Nano-ESI-MSn spectra were recorded on an LCQduo ion-trap mass spectrometer (Finnigan, now Thermo Fisher Scientific, San Jose, CA, USA) fitted with a nano-ESI source. ESI was from a metal-coated capillary (Proxeon, Odense, Denmark) raised to 1.1 kV. The heated-capillary temperature was 2000 and no sheath or auxiliary gas was used. For acquisition of mass spectra the m/z range scanned was 50 - 600 Da. MS2 spectra were recorded on a selected precursor ion, and MS3 spectra were recorded on the most abundant fragment ion from MS2 spectrum. MS and MSn scans consisted of three averaged "microscans" each with a maximum injection time of 200 ms, and the isolation width for parent-ion selection was set 2.0. The normalized collision energy was 35%.

Thin Layer Chromatography (TLC) was performed on silica gel aluminium plates (Merck 60, F_{254}), and flash chromatography utilised silica gel (Merck 60, 230-400 mesh ASTM), all other chemicals and solvents were purchased from Sigma-Aldrich.

8.2 Experimental Methods

8.2.1 Constructing the PBD Skeleton, Joining the A + C-Ring PBD Precursor

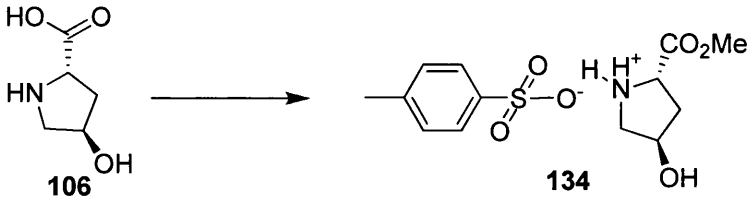

Synthesis of toluene-4-sulphonate-4-hydroxy-2-methoxycarbonyl pyrrolidinium[128]

Para-toluenesulphonic acid (159.6 g, 839 mmol, 1.1 eq.) was added to a stirred solution of *trans*-4-hydroxy-L-proline **106** (100 g, 763 mmol, 1 eq.) in methanol (333 mL) and benzene (667 mL **Caution!**) and heated at reflux for 4.5 hours (water liberated during the reaction was removed azeotropically using a Dean-Stark trap). The reaction mixture was allowed to cool to room temperature and diethyl ether was added slowly (1 L). The resulting crystals were collected by filtration, washed with diethyl ether (300 mL). The crude product was recrystallized (ethanol/diethyl ether),

washed with diethyl ether and dried in a vacuum oven to give pearl white crystals **134** (83 g, 48%). **^{1}H NMR** (400 MHz, CD_3OD) δ 7.19-7.15 (m, 2H, (CH x 2)), 6.71-6.68 (m, 2H, (CH x 2)), 4.28 (s, 3H, CH_3), 4.08-4.03, (m, 2H), 2.89 (dd, 1H, *J*= 12.2, 3.7 Hz,), 2.78-2.74 (m, 2H), 1.87 (ddt, 1H, *J* = 13.8, 7.6, 1.7 Hz,), 1.8 (s, 3H, CH_3), 1.65 (ddd, 1H, *J* = 13.7, 10.6, 4.2 Hz). **^{13}C NMR** (100 MHz, CD_3OD) δ 143.6, 141.7, 129.8 (CH x 2), 127.0 (CH x 2), 70.63, 59.5 (CH_2), 55.1 (CH), 54.0 (CH_3), 38.6 (CH), 21.3 (CH_2). Data is in agreement with literature[117, 128].

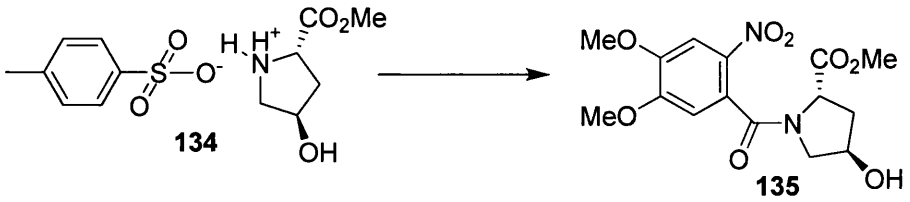

Synthesis of 1-(4,5-Dimethoxy-2-nitro-benzoyl)-4-hydroxy-pyrrolidine-2-carboxylic acid methyl ester.

Oxalyl chloride (15.38 g, 121 mmol, 1.1 eq.) was added in a single portion to 2-nitro-4,5 dimethoxybenzoic acid (25 g, 110 mmol, 1 eq.) in DCM (500 mL), followed by a catalytic amount of DMF (2-5 drops). **Caution! Gas production**. The reaction vessel was fitted with a drying tube and the reaction mixture was allowed to stir at room temperature for 18 hours to give the acid chloride. The newly formed acid chloride solution was added dropwise to a vigorously stirred solution of amine **62** (34.90 g, 110 mmol, 1 eq.) in anhydrous DCM (1L) and TEA (46 mL, 33.4 g, 330 mmol, 3 eq.) at –20°C, and the reaction mixture was allowed to warm to room temperature and stir for 16 hours. The reaction mixture was washed with saturated $NaHCO_3$ (2 x 300 mL), water (2 x 200 mL) and brine (2 x 20 mL). The DCM layer was dried over $MgSO_4$, filtered and excess solvent was removed by rotary evaporation under reduced pressure, to afford **135** a yellow glass (37.41 g, 96%). **m.p** 80 °C. **$[\alpha]^{22}_D$** = -90 ° (c = 0.2, $CHCl_3$). **^{1}H NMR** (400 MHz, $CDCl_3$). Mixture of rotamers δ 7.70 (s, 1H, CH), rotamers 6.86 (s, 1H, CH), 4.85-4.89 (t, 1H, *J* = 8.1 Hz, CH). rotamers 4.49-4.47 (m, 1H), 4.01-3.95 (m, 1H), 3.99 (s, 3H), 3.98 (s, 3H), 3.82 (s, 3H), 3.57-3.53 (dd, 1H, *J* = 11.2, 4.3 Hz), 3.20-3.16 (m, 1H), 2.47-2.41 (m, 1H), 2.23–2.14 (m, 1H). **^{13}C NMR** (100 MHz, $CDCl_3$) δ 143.6, 141.7, 129.8, 127.0, 70.6, 59.5 (CH_3), 55.1 (CH_3), 54.0, (CH_2), 38.6 (CH_2), 21.3. **IR** (ATR ν_{max}/cm^{-1}) 3404, 2952, 1740, 1621, 1578, 1522, 1455, 1430, 1335, 1275, 1222, 1178, 1074, 1050,

1024, 870, 787, 761, 646, 615, 563 cm^{-1}. **HRMS** theoretical mass $[M + H]^+$ ion at 355.1141 $[M + H]^+$, measured mass $[M + H]^+$ ion at 355.1152 $[M + H]^+$.

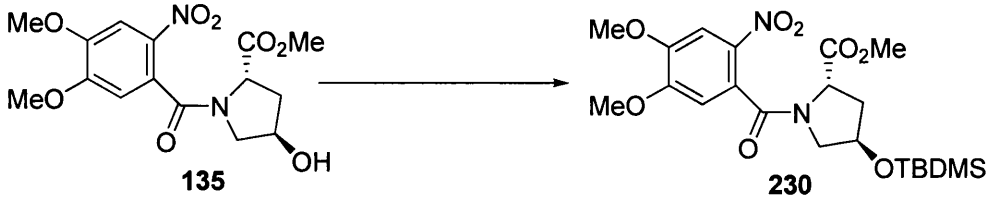

4-(*tert*-Butyl-dimethyl-silanyloxy)-1-(4,5-dimethoxy-2-nitro-benzoyl)-pyrrolidine-2-carboxylic acid methyl ester

TBDMSCl (3.45 g, 22.8 mmol, 1.3 eq.) was added to a solution of alcohol **135** (6.25 g, 17.54 mmol, 1 eq.) and imidazole (2.99 g, 43.9 mmol, 2.5 eq.) in anhydrous DMF (20 mL). The reaction mixture was allowed stir at room temperature for 18 hours under an atmosphere of nitrogen at which time TLC (1:1 EtOAc:hexane) revealed the complete consumption of starting material. The reaction mixture was diluted with water and extracted with ethyl acetate (3 x 300 mL). The combined organic phases were washed with water (2 x 200 mL), brine (2 x 200 mL), dried over $MgSO_4$ and solvent was removed by rotary evaporation under reduced pressure. The crude product was purified by flash column chromatography, eluting with 1:1 hexane:EtOAc, followed by 1:4 hexane:EtOAC. Excess eluent was removed by rotary evaporation under reduced pressure to give **230** a yellow oil (4.5 g, 55%). $[\alpha]^{23}_D$ = +15 ° (c = 0.2, $CHCl_3$). **^{1}H NMR** (400 MHz, $CDCl_3$) Mixture of rotamers (δ 7.73 (s, 1H, H9), rotamers 6.84 (s, 1H, H6), 4.79-4.83 (t, 1H, *J* = 7.6, H11a), rotamers 4.44-4.47 (m, 1H,), rotamers 4.00 (s, 3H, OMe), rotamers 3.99 (s, 3H, OMe), rotmers 3.84 (s, 3H, OMe), 3.45 (dd, *J* = 4.7, 10.4 Hz, 1H), 3.06 (dd, *J* = 4.7, 10.4 Hz, 1H), 2.29-2.31 (m, 1H, H1), 2.14–2.19 (m, 1H, H1), rotamers 0.86 (s, 9H, $C(CH_3)_3$), rotamers 0.06 (s, 3H, $Si(CH_3)$), rotamers 0.00 (s, 3H, $Si(CH_3)$). **^{13}C NMR** (100 MHz, $CDCl_3$) δ 166.4, 154.2, 149.3, 137.7, 127.11, 109.4, 107.1, 70.2(CH), 69.2 (CH), 59.2, 57.6 (CH_3), 56.5 (CH_3), 56.2 (CH_2), 54.3 (CH_2), 52.4, 39.9 (CH_2), 38.5 (CH_2), 25.7 (CH_3), 25.6 (CH_3), 17.9, -4.71 (CH_3), -4.91 (CH_3). **IR** (ATR ν_{max}/cm^{-1}) 2951, 1746, 1650, 1577, 1523, 1457, 1426, 1336, 1279, 1225, 1202, 1181, 1090, 1026, 838, 790, 670, 637, 612, 582, 563 cm^{-1}. **HRMS** theoretical mass $[M + H]^+$ ion at 469.2006 *m/z*, measured mass $[M + H]^+$ ion at 469.2000 *m/z*, δ 1 ppm.

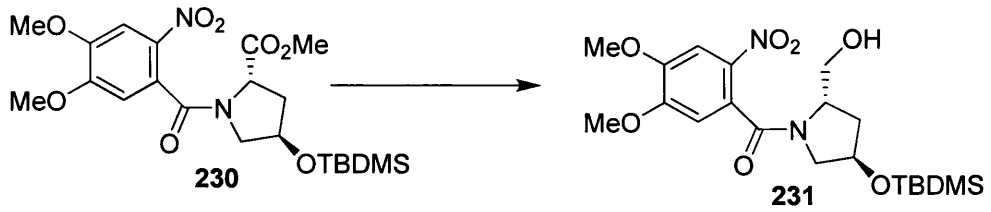

[4-(*tert*-Butyl-dimethyl-silanyloxy)-2-hydroxymethyl-pyrrolidin-1-yl]-(4,5-dimethoxy-2-nitro-phenyl)-methanone

Lithium borohydride (2.45 g, 112.31 mmol, 3 eq.) was added portion wise to a solution of **230** (17.52 g, 37.44 mol, 1eq.) in THF (500 mL) at 0°C with an ice bath. The reaction mixture was stirred at 0°C for 30 minutes, then allowed to warm to room temperature and stirred for another 2 hours, at what time TLC (ethyl acetate) revealed complete consumption of starting material. The reaction mixture was cooled to 0°C and water (250 mL) was added slowly **Caution! Gas production**. 1 M HCl was added dropwise until no more gas evolved. Solvent was removed by rotary evaporation under reduced pressure. The remaining aqueous layer was extracted with EtOAc (3 x 300 mL). The combined organic phases were washed with brine (2 x 150 mL), dried over $MgSO_4$ and excess solvent was removed by rotary evaporation under reduced pressure to give **231** as a yellow solid (14.96 g, 91%) which was taken to the next step without further purification. **m.p** 107 °C. $[\alpha]^{28}_D$ = -68 ° (c = 0.2, $CHCl_3$) **^{1}H NMR** (400 MHz, $CDCl_3$) δ 7.71 (s, 1H, H9), 6.80 (s, 1H, H6), 4.53-4.47 (m, 1H), 4.32-4.29 (m, 1H), 4.08-4.03 (m, 1H), 4.01-3.97 (m, 1H), 3.99 (s, 3H, CH_3), 3.95 (s, 3H, CH_3), 3.27 (dd, 1H, *J* = 10.8, 3.8 Hz), 3.03 (d, 1H, *J* = 11.0) 2.11-2.08 (m, 1H, H1) and 1.90-1.89 (m, 1H, H1), 0.86 (s, 9H, $C(CH_3)_3$), (0.04 (s, 3H, $Si(CH_3)$) and -0.02 (s, 3H, $Si(CH_3)$). **^{13}C NMR** (100 MHz, $CDCl_3$) δ 154.5, 149.3, 137.6, 127.8, 108.9 (CH), 107.2 (CH), 69.9 (CH), 60.3 (CH), 60.3, 57.8 (CH_2), 56.5 ((CH_3) x 2), 37.6 (CH_2), 25.7 ((CH_3) x 3), 21.0, -4.71 (CH_3), -4.91 (CH_3). **IR** (ATR ν_{max}/cm) 3369, 2932, 2854, 1619, 1578, 1522, 1461, 1430, 1334, 1275, 1222, 1107, 1077, 1056, 1028, 834, 776, 754 cm^{-1}. **Exact mass measurement** (HRMS-ES$^+$) *m/z*: theoretical mass: 441.2057 $[M + H]^+$; measured mass: 441.2053 $[M + H]^+$.

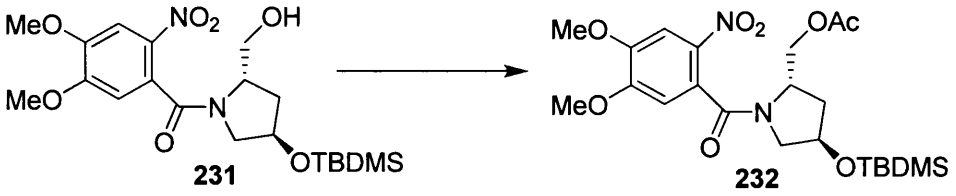

Acetic acid 4-(*tert*-butyl-dimethyl-silanyloxy)-1-(4,5-dimethoxy-2-nitro-benzoyl)-pyrrolidin-2-ylmethyl ester

A solution of acetyl chloride (0.63 mL, 0.69 g, 8.83 mmol, 1.5 eq.) in anhydrous DCM (30 mL) was added dropwise to a solution of alcohol **231** (2.59 g, 5.89 mmol, 1 eq.), in DCM (30 mL) and TEA (1.06 mL, 0.77 g, 1.3 eq.) at 0°C (ice bath). The reaction was allowed to warm to room temperature and stirred for 18 hours under an atmosphere of nitrogen, at what time TLC (ethyl acetate) revealed complete consumption of starting material. The reaction mixture was diluted with DCM (100 mL) and washed with brine (3 x 50 mL). The DCM layer was dried over $MgSO_4$, and excess solvent was removed by rotary evaporation under reduced pressure. The crude product was purified by flash chromatography (1:1 EtOAc:Hexane), eluent was removed by rotary evaporation under reduced pressure to give **232** as a pale solid (2.58 g, 91%). **m.p** 115 °C. $[\alpha]^{22}_{D}$ = -190 ° (c = 0.2, $CHCl_3$). **^{1}H NMR** (400 MHz, $CDCl_3$) δ 7.69 (s, 1H, H9), 6.81 (s, 1H, H6), 4.67-4.64 (m, 2H, CH_2), 4.43-4.38 (m, 1H), (4.32-4.27, m), 3.96 (s, 3H, CH_3), 3.96 (s, 3H, CH_3), 3.27 (dd, 1H, *J*= 10.6, 4.8 Hz, CH_2), 2.98 (dd, 1H, *J* = 10.5, 3.1 Hz, CH_2), 2.11 (s, 3H, OAc), 2.10-2.04 (m, 2H, CH_2), rotamer 0.84 (s, 9H, $C(CH_3)_3$), rotamer (0.04 (s, 3H, $Si(CH_3)$), -0.02 (s, 3H, $Si(CH_3)$). **^{13}C NMR** (100 MHz, $CDCl_3$) δ 154.2, 149.1, 127.8, 109.3 (CH), 107.1 (CH), 70.2 (CH), 63.4 (CH_2), 56.6 (CH_2), 56.5 (CH_3), 54.8 (CH_3), 37.3 (CH_2), 25.7 ((CH_3) x 3), 17.9, -4.8 (CH_3), -5.0 (CH_3). **IR** (ATR ν_{max}/cm^{-1}) 2946, 2861, 1742, 1645, 1578, 1523, 1463, 1425, 1337, 1278, 1249, 1225, 1120, 1057, 1030, 839, 776, 638, 613, 584, 563 cm^{-1} **Exact mass measurement** (HRMS-ES$^+$) *m/z*: theoretical mass: 483.2163 $[M + H]^+$; measured mass: 483.2169 $[M + H]^+$.

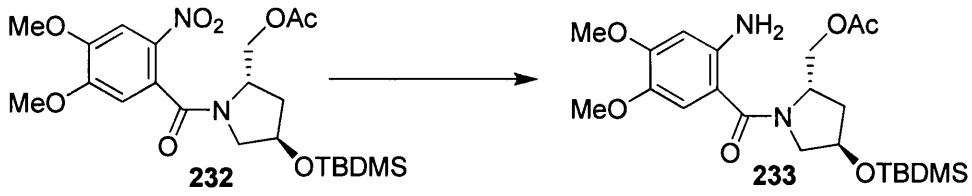

Acetic acid 1-(2-amino-4,5-dimethoxy-benzoyl)-4-(*tert*-butyl-dimethyl-silanyloxy)-pyrrolidin-2-ylmethyl ester

A slurry of 10% Pd/C (1.631 g, 3.384 mmol) in EtOAc (~6 mL) was added to a solution of the nitro compound **232** (16.31 g, 33.84 mL) in ethanol (60 mL). The reaction mixture was subjected to hydrogeneration at 50 psi for 2.5 hours on a Parr apparatus. LC-MS revealed one peak with a mass corresponding to desired product. The catalyst was removed by filtration, washed with ethanol **[CAUTION!]** and excess solvent was removed by rotary evaporation under reduced pressure. The crude product was purified by flash chromatography on silica gel (1:1 EtOAc:Hexane). Excess solvent was removed by rotary evaporation under reduced pressure to give the pale orange solid **233** (13.13 g, 84% over 3 steps). **m.p** 86 °C. $[\alpha]^{24}_{D}$ = -95 ° (c = 0.2, $CHCl_3$). **^{1}H NMR** (400 MHz, $CDCl_3$) δ 6.71 (s, 1H, H9), 6.21 (s, 1H, H9), 4.69 (s, 1H, NH) 4.34 (s, 4H), 4.27-4.20 (m, 1H, CH), 3.84 (s, 3H, CH_3), 3.78 (s, 3H, CH_3), 3.55 (dd, 1H, *J*= 11.5, 3.5 Hz), 3.45-3.43 (m, 1H), 2.10-2.06 (m, 4H), 1.94-1.89 (m, 1H), 0.87 (s, 9H, $C(CH_3)_3$), 0.03 (s, 3H, $Si(CH_3)$), -0.03 (s, 3H, $Si(CH_3)$). **^{13}C NMR** (100 MHz, $CDCl_3$) δ 151.8, 140.8, 112.5 (CH), 100.5 (CH), 70.5 (CH), 64.8 (CH_2), 60.4 (CH_2), 55.7 ((CH_3) x2), 54.3, 37.5 (CH_2), 25.6 ((CH_3) x 3), 17.86, -4.7 (CH_3), -4.9 (CH_3). **IR** (ATR ν_{max}/cm^{-1}) 2952, 2861, 1742, 1633, 1597, 1515, 1457, 1426, 1396, 1234, 1165, 1107, 1059, 1029, 831, 775, 638, 581, 563 cm^{-1}. **Exact mass measurement** (HRMS-ES$^+$) *m/z*: theoretical mass: 483.2163 $[M + H]^+$; measured mass: 483.2169 $[M + H]^+$.

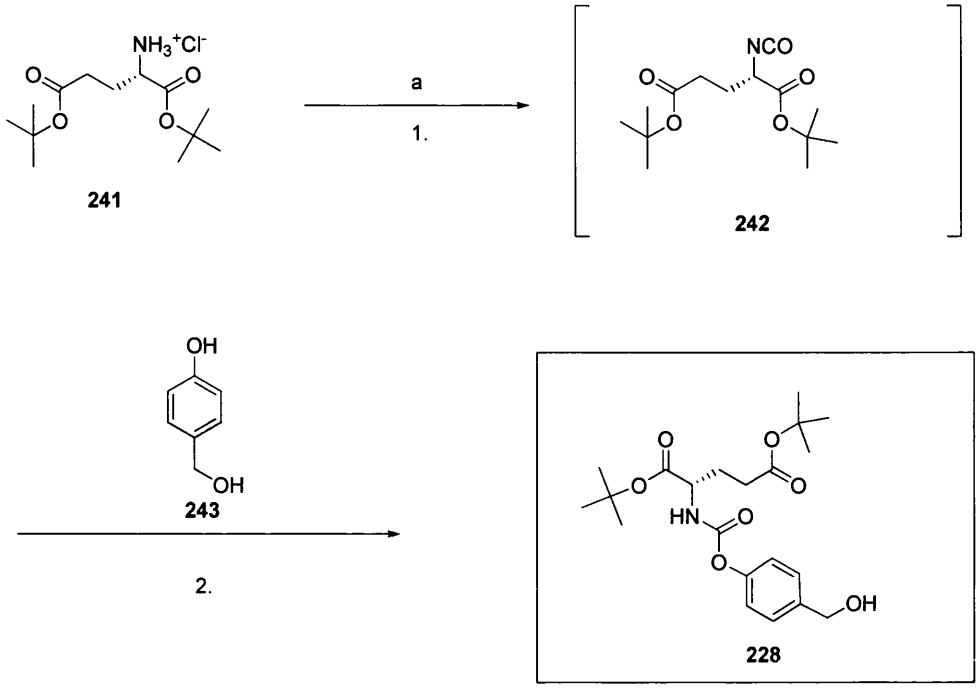

a) 1. Triphosgene, TEA, DCM, -78°C, 2. TEA, DCM, 0°C, 2Hr, 67%.

2-(4-Hydroxymethyl-phenoxycarbonylamino)-pentanedioic acid di-*tert*-butyl ester

A solution of TEA (1.705 g, 2.33 mL, 16.9 mmol) in anhydrous DCM was added at a slow rate to a solution H-Glu(OtBu):OtBu:HCl **241** (2.5 g, 8.45 mmol, 1 eq.) and triphosgene (0.825 g, 2.74 mmol, 0.33 eq.) in anhydrous DCM (150 ml) at –78°C (acetone/card ice bath) under an atmosphere of nitrogen. The reaction mixture was gradually allowed to warm to –10°C over 2 hours, at which point IR showed a sharp strong band at 2248 cm^{-1} indicating the presence of isocyanate. The Isocyanate solution was kept below 0°C and added dropwise to a solution of 4-hydroxybenzyalcohol (1.05 g, 8.45 mmol, 1 eq.), TEA (1.705 g, 2.33 mL, 16.9 mmol) in anhydrous DCM at 0°C (ice bath). The reaction was allowed to warm to room temperature and stir under a nitrogen atmosphere for 2.5 hours, at which point IR revealed the complete consumption of isocyanate. The excess solvent was removed by rotary evaporation under reduced pressure and the resulting solid was purified by flash chromatography using the Jones Flash Master (hexane/EtOAc 100:0 gradient 80:20 in 60 min) to give **228** as a colourless oil (2.31 g, 67%). $[\alpha]^{22}_{D}$ = +18.2 ° (c = 0.2, $CHCl_3$). **^{1}H NMR** (400 MHz), $(CD_3)_2SO$ δ 7.35 (d, *J* = 8.5 Hz, 2H, (CH x 2)), 7.13 (d, *J* = 8.5 Hz, 2H, (CH x 2)), 5.68 (d, *J* = 79 Hz, 1H, NH), 4.67 (d, *J* = 5.7 Hz,

2H, CH_2), 4.34-4.29 (m, 1H, CH), 2.44-2.28 (m, 2H, CH_2), 2.22-2.16 (m, 1H, CH_2), 2.04-1.93 (m, 1H, CH_2), 1.66 (t, J = 5.8 Hz, OH) 1.50 (s, 9H, $-OC(CH_3)_3$) 1.46 (s, 9H, $-OC(CH_3)_3$). **^{13}C NMR** (100 MHz, $(CD_3)_2SO$) δ 127.3 (CH), 121.1 (CH), 80.8, 62.4 (CH_2), 31.1, 30.7 (CH_2), 27.7 ($CH_3)_3$, 27.6 ($CH_3)_3$, 25.0 (CH_2). **IR** (ATR ν_{max}/cm) 3334, 2977, 2933, 2363, 1715, 1535, 1503, 1455, 1393, 1367, 1251, 1210, 1148, 1013, 845, 752, 651, 628 cm^{-1}; **Exact mass measurement** (HRMS-ES$^+$) *m/z*: theoretical mass: 410.2179 $[M + H]^+$; measured mass: 410.2166 $[M + H]^+$.

8.2.2 Attachment of Progroup and Cyclisation of B Ring

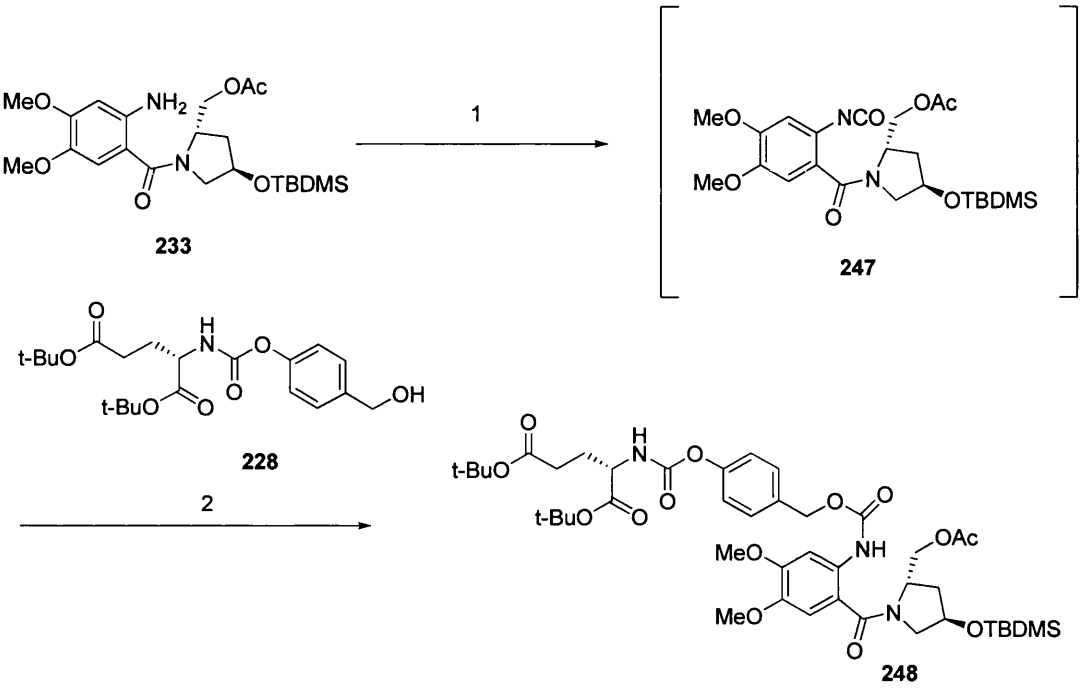

1. triphosgene, TEA, tolune, RT, 3 hr, 2. TEA, RT, toluene, 70%.

2*S*-(4-phenoxycarbonylamino)-pentanedioic acid di-*tert*-butyl ester.

Triphosgene (0.54 g, 1.83 mmol) was added to a solution of amine **233** (2.5 g, 5.58 mmol) in anhydrous toluene (120 mL) under an atmosphere of nitrogen at room temperature. The reaction mixture was cooled to 0°C (ice bath) and treated with a solution of TEA (1.15 mL, 0.84 g, 8.30 mmol) in anhydrous toluene (25 mL) at a steady rate. The reaction mixture was allowed to stir at 0°C for 2 hours at which time the IR spectrum of the reaction mixture revealed an isocyanate peak at 2264.87 cm^{-1}. The isocyanate was then added dropwise to solution of alcohol **7** (2.26 g, 5.53 mmol)

in anhydrous toluene (60 mL) and TEA (1.15 mL, 0.84 g, 8.30 mmol) at 0 °C. The reaction mixture was allowed to warm to room temperature and stirred for two hours, at which point the IR spectrum revealed the complete consumption of isocyanate. The reaction solvent was removed by rotary evaporation under reduced pressure and the residue was purified by flash chromatography using a Jones Flash Master with hexane/EtOAc, gradient 100:0 to 50:50 in 70 min, to give **248**, as a colourless oil (5.48 g, 83%). $[\alpha]^{22}_{D}$ = -20 ° (c = 0.2, $CHCl_3$). **^{1}H NMR** (400 MHz, DMSO) δ 9.14 (s, 1H, NH), 8.167 (d, 1H, *J* = 7.9 Hz), 7.38 (d, 2H, *J* = 8.6 Hz), 7.07 (d, 2H, *J* = 8.5 Hz), 6.79 (s, 1H), 5.07 (s, 2H, CH_2), 4.46-4.44 (m, 1H), 4.29 (s, 1H), 4.17-4.13 (m, 2H), 3.98-3.93 (m, 1H), 3.75 (s, 3H, OCH_3), 3.71 (s, 3H, OCH_3), 3.48-3.43 (m, 1H), 3.08-3.04 (m, 1H), 2.34-2.29 (m, 2H), 1.99 (s, 3H, OAc), 1.97-1.90 (m, 2H, CH_2), 1.85-1.79 (m, 2H, CH_2), 1.40 ((2 x s), 18H, (-$OC(CH_3)_3$) x 2), 0.67 (s, 9H, $C(CH_3)_3$), 0.068 (s, 3H, $Si(CH_3)$), -0.188 (s, 3H, $Si(CH_3)$). **^{13}C NMR** (100 MHz, DMSO) δ 129.3 (CH), 121.5 (CH), 82.9 (CH), 79.8 (CH), 55.7, 55.4, 30.7 (CH_2), 27.7 (CH_3), 27.6 (CH_3), 25.3 (CH_2), -4.7 (CH_3), -4.9 (CH_3). **IR** (ATR ν_{max}/cm) 3333, 2932, 2360, 1726, 1602, 1523, 1504, 1457, 1394, 1367, 1202, 1154, 1034, 839, 776, 754, 669; **Exact mass measurement** (HRMS-ES$^+$) *m/z*: theoretical mass: 888.4303 $[M + H]^+$; measured mass: 888.4282 $[M + H]^+$.

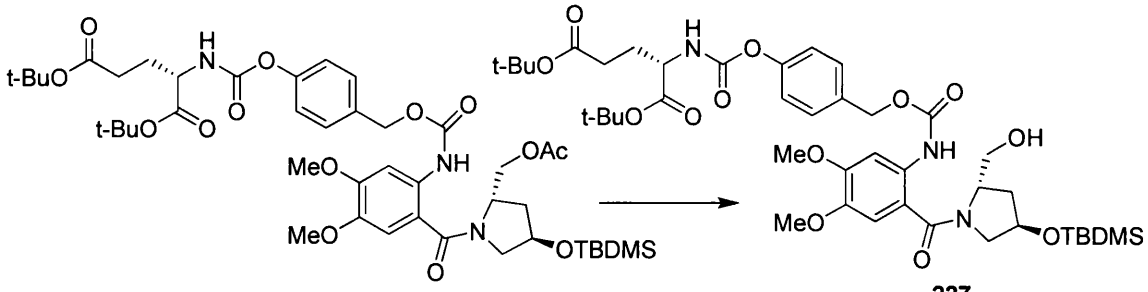

2S-(4-(2-[4-(*tert*-Butyl-dimethyl-silanyloxy)-2-hydroxymethyl-pyrrolidine-1-carbonyl]-4,5-dimethoxy-phenylcarbamoyloxymethyl)-phenoxycarbonylamino)-pentanedioic acid di-*tert*-butyl ester.

A 1M solution of 'Super Hydride' in THF (2.86 mL, 0.303 g, 2.86 mmol) was added dropwise to **248** (1.27 g, 1.43 mmol) in anhydrous THF (20 mL) at –78°C (acetone/card ice bath). The reaction mixture was allowed to stir at –78°C for 2 hours under a nitrogen atmosphere, and then quenched with acetic acid (0.164 mL, 0.171 g,

2.86 mmol). The reaction mixture was allowed to warm slowly to 0°C, diluted with EtOAc (100 mL) and washed with water (100 mL). The aqueous layer was extracted with EtOAc (2 x 100 mL). The combined organic phases were dried over $MgSO_4$ and excess solvent was removed by rotary evaporation under reduced pressure. The resulting yellow oil was purified by column chromatography (Hexane/EtOAc 1:1 to 1:4 MeOH/EtOAc) to give **227** as a colourless solid (0.92 g, 76%). **m.p** 77 °C. $[\alpha]^{23}_{D}$ = -48 ° (C = 0.2). **^{1}H NMR** (400 MHz, $CDCl_3$) δ 8.61 (s, 1H, NH), 7.77 (s, 1H, CH), 7.38 (d, 2H), 7.13 (d, 2H), 6.74 (s, 1H, CH), 5.71 (d, 1H J_1 = 7.5 Hz), 5.12 (q, 2H, J= 16.8 Hz, CH_2), 4.62-4.60 (m, 1H), 4.30 (td, 1H, J = 8.2, 4.8 Hz), 4.25 (s, 1H), 3.92 (s, 3H, OCH_3), 3.90-3.87 (m, 1H), 3.82 (s, 3H, OCH_3), 3.66-3.65 (m, 1H), 3.49 (dd, J = 11.3, 2.6, 1H, CH_2), 3.38 (d, J = 11.1, 1H, CH_2), 2.39-2.31 (m, 2H, CH_2), 2.21-2.15 (m, 1H, CH_2), 2.07-1.94 (m, 1H, CH_2), 1.75-1.74 (1, m), 1.48 (s, 9H, $-OC(CH_3)_3$), 1.45 (s, 9H, $-OC(CH_3)_3$), 0.76 (s, 9H, $C(CH_3)_3$), -0.01 (s, 3H, $Si(CH_3)$), -0.10 (s, 3H, $Si(CH_3)$). **^{13}C NMR** (100 MHz, $CDCl_3$) δ 207.1, 170.9, 154.1, 153.6, 151.0, 150.8, 133.3 (CH), 121.7 (CH), 100.7 (CH), 82.6, 80.9, 70.0, 66.2 (CH_2), 66.0 (CH_2), 59.8 (CH_2), 59.2 (CH_2), 56.4 (CH_3), 56.0 (CH_3), 54.1 (CH), 37.3(CH_2), 31.5 (CH_2), 28.1 (CH_3), 28.0 (CH_3), 27.8 (CH_2), 25.5 (CH_3), 17.86, -4.7 (CH_3), -4.9 (CH_3). **IR** (ATR ν_{max}/cm) 3348, 2932, 2856, 1728, 1599, 1523, 1504, 1462, 1395, 1368, 1255, 1199, 1154, 1117, 1032, 1006, 837, 776; **Exact mass measurement** (HRMS-ES$^+$) *m/z*: theoretical mass: $[M + H]^+$; 846.4203 measured mass: 846.4194 $[M + H]^+$.

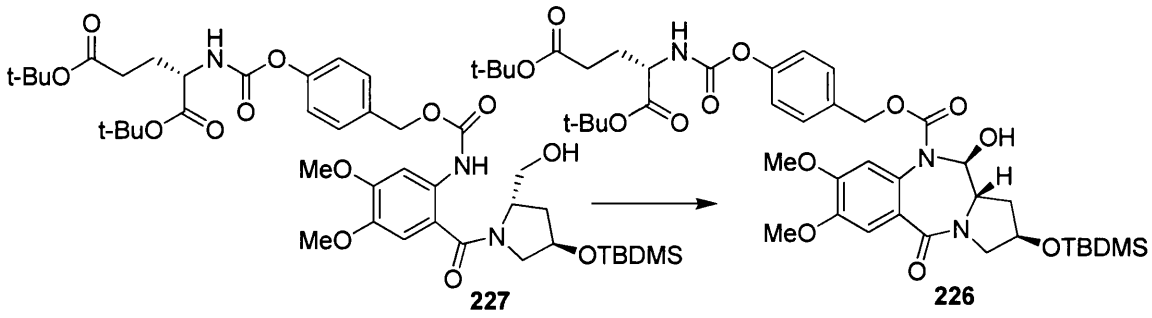

2*S*-(4-[2-(*tert*-Butyl-dimethyl-silanyloxy)-11*S*-hydroxy-7,8-dimethoxy-5-oxo-2,3,11*S*,11a*S*-tetrahydro-1H,5H-pyrrolo[2,1-*c*][1,4]benzodiazepine-10-carbonyl oxymethyl]-phenoxycarbonylamino)-pentanedioic acid di-*tert*-butyl ester

DAIB (0.53 g, 1.65 mmol), and TEMPO (0.023 g, 0.15 mmol) were added to alcohol **227** (1.27 g, 1.50 mmol), in anhydrous DCM (20 mL). The reaction mixture

was allowed to stir for 18 hours at room temperature under an atmosphere of nitrogen, at which time LC-MS revealed that the desired product had formed. The reaction mixture was diluted with DCM (100 mL) and washed with saturated sodium bisulphite. The aqueous layer was extracted with DCM. The organic layers were combined, washed with brine (100 mL), dried over $MgSO_4$ and solvent was removed by rotary evaporation under reduced pressure. The crude yellow oil was purified by flash column chromatography on silica gel, eluting with 1:1 EtOAc:Hexane. Product containing fractions were combined and excess eluent was removed by rotary evaporation at reduced pressure to afford **226** as a yellow solid (1.04 g, 83%). **m.p** 105 °C. $[\alpha]^{23}_{D}$ = +95 ° (c = 0.20) **^{1}H NMR** (400 MHz, $CDCl_3$) δ 7.23-7.20 (s, 3H), 7.08 (d, 2H, *J* = 8.1 Hz), 6.41 (s, 1H), 5.72 (d, *J*= 8.1 Hz, 1H), 5.60 (dd, *J* = 9.6, 3.4 Hz, 1H), 5.36 (d, *J* = 12.1 Hz, 1H) 4.80 (d, *J* = 12.4 Hz, 1H), 4.51-4.48 (m, 1H), 4.29 (td, *J* = 8.0, 4.9 Hz, 1H), 3.91 (s, 3H, OCH_3), 3.67-3.66 (m, 3H, OCH_3), 3.62-3.56 (m, 2H, CH_2), 2.41-2.31 (m, 1H, CH_2), 2.19-2.17 (m, 1H, CH_2), 1.49 (s, 9H, $-OC(CH_3)_3$), 1.45 (s, 9H, $-OC(CH_3)_3$), 0.84 (s, 9H, $C(CH_3)_3$), 0.07 (s, 3H, $Si(CH_3)$), 0.06 (s, 3H, $Si(CH_3)$). **^{13}C NMR** (100 MHz, $CDCl_3$) δ 207.1, 172.1, 170.8, 150.8, 148.4, 129.3 (CH), 121.8 (CH), 112.2 (CH), 110.5, 87.0 (CH), 82.7, 80.90, 69.3, 67.2 (CH_2), 60.4 (CH_2), 58.4, 56.2 (CH_3), 56.1 (CH_3), 54.1, 53.7 (CH_2), 38.6 (CH_2), 31.5 (CH_2), 31.0, 28.1 (CH_3), 28.0 (CH_2), 27.8 (CH_3), 25.7 (CH_3), 21.1, 18.0, -4.8 (CH_3), -4.9 (CH_3). **IR** (ATR ν_{max}/cm) 3337, 2933, 2360, 2158, 1725, 1628, 1605, 1506, 1456, 1432, 1393, 1368, 1303, 1255, 1216, 1153, 1062, 1019, 837, 777, 733, 669, 645; **Exact mass measurement** (HRMS-ES$^+$) *m/z*: theoretical mass: $[M + H]^+$; 441.2057 measured mass: 441.2053 $[M + H]^+$.

8.2.3 Synthesis of C2 Ketone

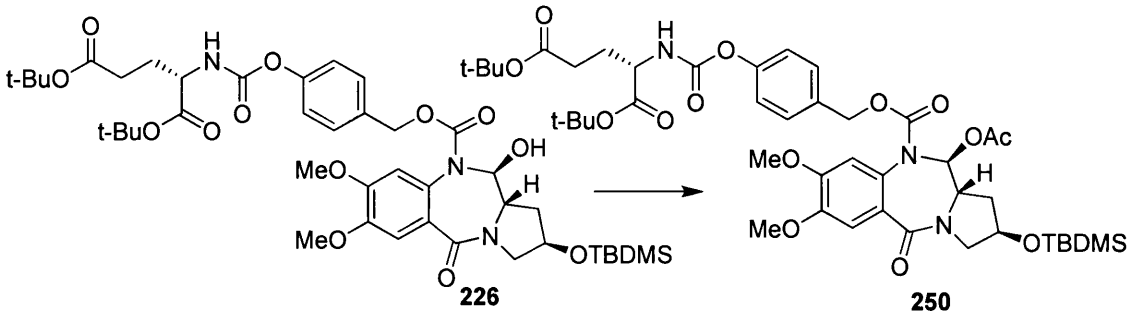

2*S*-(4-[11*S*-Acetoxy-2-(*tert*-butyl-dimethyl-silanyloxy)-7,8-dimethoxy-5-oxo-1,2,3,10,11,11a*S*-hexahydro-1H,5H-pyrrolo[2,1-*c*][1,4]benzodiazepine-10-carbonyloxymethyl]-phenoxycarbonylamino)-pentanedioic acid di-*tert*-butyl ester

Acetic anhydride (0.44 g, 0.41 mL, 0.36 mmol) and DMAP was added to a solution of alcohol **226** (3.03 g, 3.59 mmol), in anhydrous DCM (60 mL). The reaction mixture was allowed to stir at room temperature under an atmosphere of nitrogen for 2 hours. LC-MS revealed a single peak with ionising mass (M+H) 886 corresponding to the desired product. The reaction mixture was diluted with DCM and washed with saturated sodium bicarbonate (2 x 100 mL). The aqueous layer was washed with DCM (100 mL). The combined organic phases were washed with brine (100 mL), water (100 mL), dried over $MgSO_4$ and solvent was removed by rotary evaporation under reduced pressure to give **250** a yellow oil (2.97 g, 93%). **^{1}H NMR** (400 MHz, $CDCl_3$) δ 7.23-7.21 (m, 2H), 7.10-7.08 (d, J = 6.9 Hz, 2H), 6.90 (s, 1H,), 6.55 (s, 1H), 5.71 (d, J= 8.1 Hz, 1H), 5.34-5.29 (m, 1H), 4.83 (s, 1H), 4.65-4.52 (m, 1H,), 4.33-4.28 (m, 1H), 3.91 (s, 3H, OCH_3), 3.78-3.66 (m, 5H, OCH_3, CH_2), 2.42-2.30 (m, 2H, CH_2), 2.23-2.17 (m, 1H, CH_2), 2.10-2.01 (m, 3H, OAc), 2.02-1.95 (m, 1H, CH_2), 1.50 (s, 9H, -$OC(CH_3)_3$), 1.46 (s, 9H, -$OC(CH_3)_3$), 0.85 (s, 9H, $C(CH_3)_3$), 0.090 (s, 3H, $Si(CH_3)$), 0.66 (s, 3H $Si(CH_3)$). **^{13}C NMR** (100 MHz, $CDCl_3$) δ 167.7, 121.7, (CH), 112.4 (CH), 110.5 (CH), 85.0, 82.7, 80.9, 69.36, 60.42, 58.10, 56.2 (CH_3), 54.1 (CH_2), 37.5 (CH_2), 31.5 (CH_2), 28.1 (CH_3), 28.0 (CH_3), 27.8 (CH_2), 25.7, 21.2, 17.9, -4.8 (CH_3), -4.9 (CH_3). **IR** ATR ν_{max}/cm) 2936, 2366, 2355, 2027, 1730, 1641, 1501, 1370, 1259, 1209, 1156, 1009; **Exact mass measurement** (HRMS-ES$^+$) *m/z*: theoretical mass: 886.4152 $[M + H]^+$; measured mass: 886.4150 $[M + H]^+$.

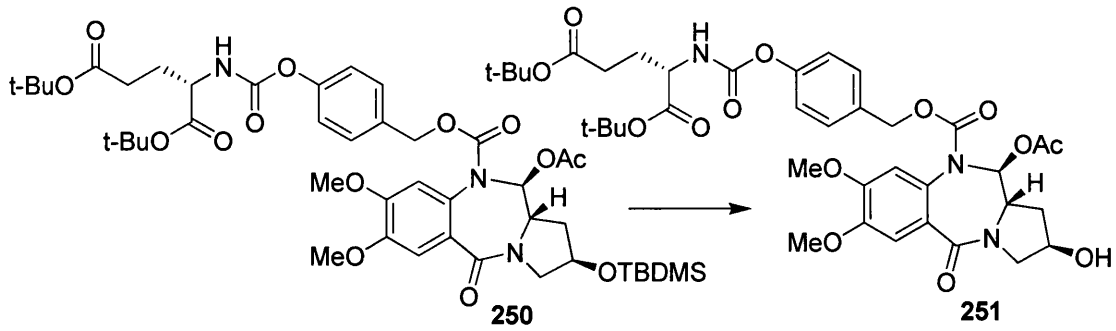

2*S*-[4-(11*S*-Acetoxy-2-hydroxy-7,8-dimethoxy-5-oxo-2,3,11*S*,11a*S*-hexahydro-1H,5H-pyrrolo[2,1-*c*][1,4]benzodiazepine-10-carbonyloxymethyl)-phenoxy carbonylamino]-pentanedioic acid di-*tert*-butyl ester

An excess of hydrogen-fluoride pyridine complex (4.4 mL) **(Caution! hydrogen fluoride-pyridine extremely toxic, Marigold gloves must be worn)** was added dropwise to a solution of the silyl ether **250** (2.24 g) in anhydrous THF (40 mL) in a dry polyethylene flask at 0°C (ice bath), under an atmosphere of nitrogen. The reaction mixture was allowed to stir at 0°C for 30 minutes and then allowed to warm to room temperature and stir for 1.5 hours. The reaction mixture was diluted with ether and neutralised with sodium hydrogen carbonate solution until no more carbon dioxide was liberated. The combined organic phases were washed with brine (3 x 100 mL), dried over $MgSO_4$ and excess solvent removed by rotary evaporation under reduced pressure, the residue was azeotroped with toluene and purified by flash column chromatography (1:1 EtOAc:hexane to EtOAC). Product containing fractions were combined and excess eluent was removed by rotary evaporation under reduced pressure to afford **251** as a yellow solid (1.60 g, 82%). **m.p** 96 °C. **^{1}H NMR** (400 MHz, $CDCl_3$) δ 7.21-7.20 (m, 3H), 7.08-7.07 (m, 2H), 6.89 (s, 1H,), 6.54 (s, 1H), 5.76 (d, J = 7.2 Hz, 1H), 5.27 (d, J = 11.5 Hz), 4.83 (s, 1H), 4.56 (s, 1H), 4.28 (td, J = 8.1, 4.8 Hz, 1H), 3.91-3.87 (m, 1H), 3.89 (s, 3H, OCH_3), 3.84-3.76 (m, 3H, OCH_3), 3.62-3.60 (m, 1H), 2.64-2.62 (m, 1H), 2.34-2.32 (m, 2H), 2.27-2.16 (m, 2H), 2.07 (s, 3H, OAc), 2.02-1.94 (m, 1H), 1.48 (s, 9H, $-OC(CH_3)_3$), 1.47 (s, 9H, $-OC(CH_3)_3$). **^{13}C NMR** (100 MHz, $CDCl_3$) δ 132.5, 123.9, 121.7(CH), 84.8, 82.7, 80.9, 56.5 (CH_3), 56.3 (CH_3), 54.1, 52.7 (CH_2), 38.7 (CH_2), 31.5 (CH_2), 28.1 (CH_3), 28.0 (CH_3), 27.8 (CH_2). **IR** ATR ν_{max}/cm) 2978, 2364, 2015, 1726, 1636, 1516, 1456, 1369, 1207,

1156, 1015, 844, 762, 642; **Exact mass measurement** (HRMS-ES$^+$) *m/z*: theoretical mass: 772.3287 $[M + H]^+$; measured mass: 772.3274 $[M + H]^+$.

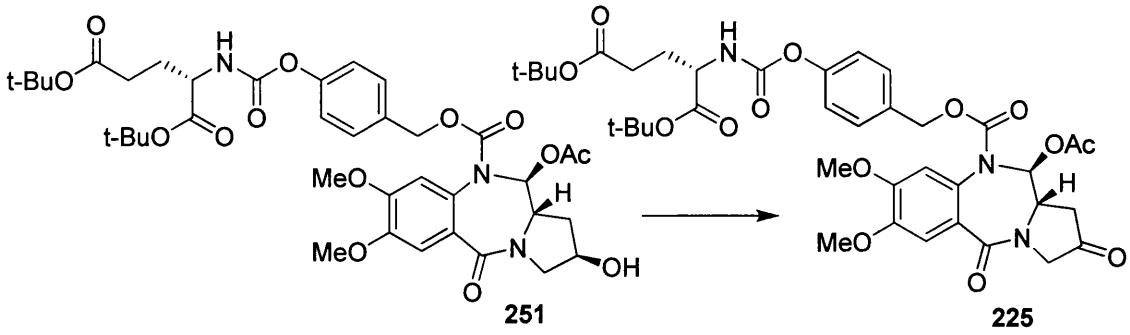

2*S*-[4-(11*S*-Acetoxy-7,8-dimethoxy-2,5-dioxo-2,3,11S,11a*S*-hexahydro-1H,5H-pyrrolo[2,1-*c*][1,4]benzodiazepine-10-carbonyloxymethyl)-phenoxycarbonyl amino]-pentanedioic acid di-*tert*-butyl ester.

A 15 % solution of Dess-Martin periodinane (2.27 mL, 0.413 g, 0.97 mmol) in DCM was added slowly to a solution of alcohol **251** (0.5 g, 0.65 mmol) in anhydrous DCM (40 mL). The reaction mixture was allowed to stir at room temperature under a nitrogen atmosphere for 1 hour, at which point TLC (1:3 hexane:EtOAc) revealed a single product. The reaction mixture was diluted with DCM (50mL), filtered and excess solvent was removed by rotary evaporation under reduced pressure. The residue was purified by flash column chromatography on silica gel, eluting with 1:3 hexane:EtOAc. Product fractions were combined and excess eluent was removed by rotary evaporation under reduced pressure to afford **225** as a white solid (0.46 g, 92%). **m.p** 102 °C. $[\alpha]^{23}_D$ = +225 ° (c = 0.2, $CHCl_3$). **^{1}H NMR** (400 MHz, $CDCl_3$) δ 7.29-7.23 (m, 2H), 7.17-7.05 (m, 3H), 6.62 (s, 1H,), 5.76-5.74 (d, *J* = 8.1 Hz, 1H), 5.36-5.26 (m, 1H), 4.92-4.82 (m, 1H), 4.38 (s, 1H, CH_2), 4.35-4.30 (m, 2H, CH_2), 4.17-4.10 (m, 1H), 4.01 (s, 1H, CH_2), 3.97-3.96 (m, 3H, OCH_3), 3.83 (s, 3H, OCH_3), 2.84 (d, 7.8 Hz, 2H, CH_2), 2.46-2.31 (m, 2H, CH_2), 2.26-2.16 (m, 1H, CH_2) 2.12 (s, 3H, OAc), 2.16-2.1.96 (m, 1H, CH_2), 1.52 (s, 9H, -$OC(CH_3)_3$), 1.48 (s, 9H, -$OC(CH_3)_3$). **^{13}C NMR** (100 MHz, $CDCl_3$) δ 206.7, 172.1, 170.8, 169.3, 167.7, 154.0, 151.6, 151.0, 149.1, 132.5, 129.4, 128.4, 123.9, 121.7, 112.5, 110.5 (CH), 84.8, 82.7, 80.9, 67.7 (CH), 60.4 (CH_3), 56.5 (CH_3), 54.1, 52.7 (CH_2), 38.7 (CH_2), 31.5, 28.1 (CH_3), 28.0 (CH_3), 27.8 (CH_2). **IR** ATR ν_{max}/cm) 2365, 2337, 2002, 1968, 1728,

1636, 1608, 1512, 1461, 1430, 1368, 1293, 1218, 1156, 1014, 949 846, 761. **HRMS** theoretical mass $[M + H]^+$ ion at 770.3136 *m/z*, measured mass $[M + H]^+$ ion at 770.3157 *m/z*, δ 3 ppm.

8.2.4 Triflation and Suzuki Coupling

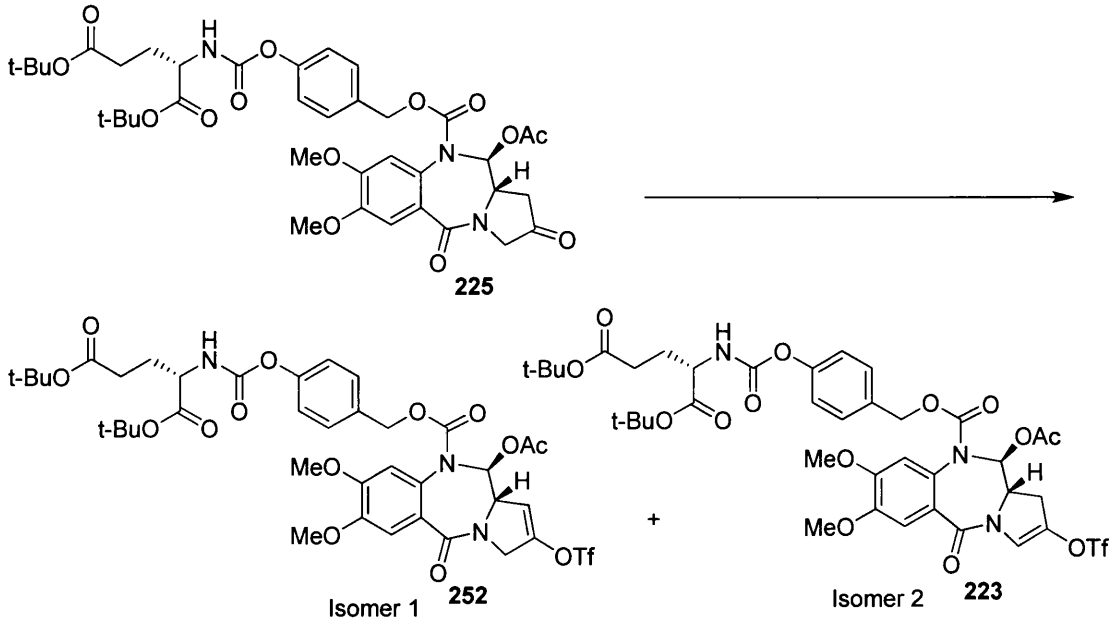

5-chloro-*N,N*-(trifluromethanesulphonyl) aminopyridine, LHMDS, THF, -78°C to RT, 47%

A 1M solution of lithium hexamethyldisilylamide in THF (0.03 g, 0.18 ml, 0.182 mmol) at –78oC (acetone/card ice bath) under N2 atmosphere was added dropwise to a solution of ketone 225 (0.127 g, 0.165 mmol) in anhydrous THF (1 mL). The reaction mixture was allowed to stir at –78oC for 40 minutes, when a solution 5-chloro-N-N-(trifluromethanesulphonyl) aminopyridine (0.071 g, 0.182 mmol) in anhydrous THF (1 mL) at –78oC was added dropwise. The resulting reaction mixture was allowed to warm to room temperature and stir for 2 hours, at which point TLC (1:1 EtOAc:hexane) revealed one product. The reaction mixture was diluted with DCM, washed with brine (2 x 3 mL), water (2 x 3 mL) and the combined organic phase was dried over MgSO4 and solvent was removed by rotary evaporation under reduced pressure. The crude product was purified by preparative LC-MS. Using a C8 phenomenex column 150 mm x 21 mm, 5μ, mobile phase solvent A water with 1%

formic acid, solvent B acetronitrile 1% formic acid and inlet file (table below) over a 25 minutes gradient.

Time (min)	Flow rate (mL/min)	Solvent A (water with 1% formic acid)	Solvent B (acetronitrile 1% formic acid)
0	25	70	30
1	25	70	30
2	25	50	50
10	25	38	62
22	25	38	62
23	25	05	95
24	25	05	95
25	25	70	30

Excess solvent was removed by freeze drying to afford 1,2-enol triflate isomer **252** (11 mg, 22%) and 2,3-enol triflate isomer **223**

(9 mg, 18%).

2-[4-(11-Acetoxy-7,8-dimethoxy-5-oxo-2-trifluoromethanesulfonyloxy-3,10,11,11a-tetrahydro-3H,5H-pyrrolo[2,1-c][1,4]benzodiazepine-10-carbonyl oxymethyl)-phenoxycarbonylamino]-pentanedioic acid di-tert-butyl ester

1,2-enol triflate somer **252** **^{1}H NMR** (400 MHz, CD_3OD) δ 7.19 (s, 2H, (CH x 2)), 7.13 (s, 1H, CH) 6.99-7.01 (d, 2H, J = 8.0 Hz, (CH x 2)), 6.83-6.86 (d, 1H, J = 9.4 Hz, CH), 6.74 (s, 1H, CH), 5.87 (s, 1H, CH), 5.11-5.14 (d, 1H, J = 12.1 Hz, CH_2), 4.84-4.89 (m, 1H, CH_2), 4.52-4.56 (d, 1H, J = 15.6 Hz, CH_2), 4.27-4.32 (m, 1H, CH_2), 4.38-4.42 (m, 1H, CH), 4.02-4.24 (m, 1H, CH), 3.79 (s, 3H, OCH_3), 3.69 (s, 3H, CH_3), 2.27-2.31 (m, 2H, CH_2), 2.06 (s, 3H, OAc), 2.00-2.05 (m, 1H, CH_2), 1.55-1.86 (m, 1H, CH_2), 1.40 (s, 9H, $-OC(CH_3)_3$), 1.37 (s, 9H, $-OC(CH_3)_3$). **^{13}C NMR** (400 MHz, CD_3OD) δ 122.9, 56.6 (CH_3), 28.4 (CH_3), 28.3 (CH_3), 27.9 (CH_2). **IR** (ATR

ν_{max}/cm^{-1}) 2927, 2358, 1725, 1679, 1651, 1605, 1517, 1426, 1368, 1257, 1205, 1135, 1013, 952, 912, 838, 764, 730, 696, 643, 609 cm^{-1}. **Exact mass measurement** (HRMS-ES^+) *m/z*: theoretical mass: 902.2627 $[M + H]^+$; measured mass: 902.2627 $[M + H]^+$.

2-[4-(11-Acetoxy-7,8-dimethoxy-5-oxo-2-trifluoromethanesulfonyloxy-1,10,11,11a-tetrahydro-1H,5H-pyrrolo[2,1-*c*][1,4]benzodiazepine-10-carbonyl oxymethyl)-phenoxycarbonylamino]-pentanedioic acid di-tert-butyl ester.

2,3-enol triflate isomer **223** **^{1}H NMR** (400 MHz, CD_3OD). δ 7.16 (s, 2H, (CH x 2)), 7.11 (s, 1H, CH), 6.99-7.02 (d, 2H, *J* = 9.6 Hz, (CH x 2)), 6.97 (s, 1H, CH), 6.72 (s, 1H, CH), 5.09-5.13 (d, 1H, *J* = 12.2 Hz, CH_2) 4.83-5.05 (m, 1H, CH_2), 4.10-4.15 (m, 1H, CH), 3.95-4.09 (m, 1H) CH, 3.78 (s, 3H, OCH_3), 3.70 (s, 3H, OCH_3), (3.19-3.20 (m, 1H) and 2.89-2.93 (d, 1H, *J* = 16.8 Hz) CH_2, 2.26-2.30 (d, 2H, *J* = 7.6 Hz, CH_2), 1.99 (s, 3H, OAc), (2.01-2.07 (m, 1H, CH_2), 1.76-1.92 (m, 1H, CH_2), 1.38 (s, 9H, $-OC(CH_3)_3$) 1.36 (s, 9H, $-OC(CH_3)_3$). **^{13}C NMR** (100 MHz, CD_3OD) δ 173.7, 138.6, 130.6, 122.9, 83.08, 59.8, 56.9, 56.7 (CH_3), 55.6, 32.6, 30.7, 28.4 (CH_3), 28.3 (CH_3), 27.9 (CH_2). **IR** (ATR ν_{max}/cm^{-1}) 2927, 2362, 1729, 1651, 1605, 1517, 1452, 1424, 1370, 1212, 1149, 1139, 1014, 957, 912, 823, 764, 733, 695, 643, 611, 575 cm^{-1}. **Exact mass measurement** (HRMS-ES^+) *m/z*: theoretical mass: 902.2629 $[M + H]^+$; measured mass: 902.2672 $[M + H]^+$.

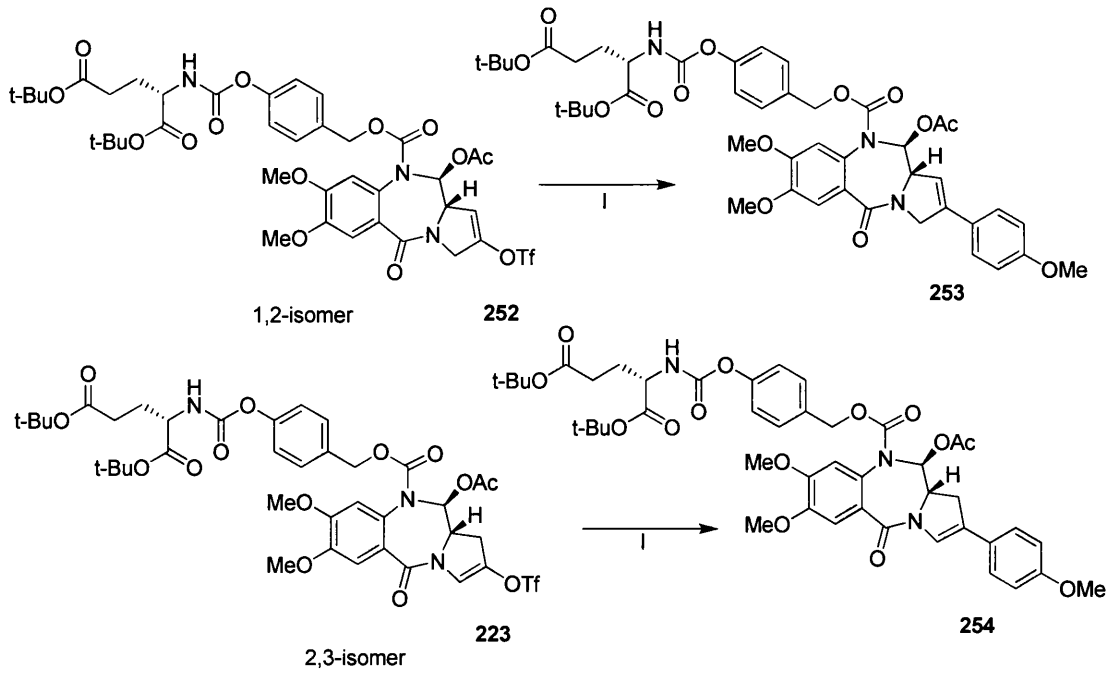

I. TEA, Water, ethanol, toluene, $Pd(PPh_3)_4$, 4-methoxyphenylboronic acid, RT

2-(4-[11-Acetoxy-7,8-dimethoxy-2-(4-methoxy-phenyl)-5-oxo-3,10,11,11a-tetrahydro-3H,5H-pyrrolo[2,1-*c*][1,4]benzodiazepine-10-carbonyloxymethyl]-phenoxycarbonylamino)-pentanedioic acid di-tert-butyl ester

A catalytic amount of $Pd(Ph_3)_4$ (8.8 mg, 0.07 mmol) was added to a solution of 4-methoxyphenylboronic acid (0.072 g, 0.476 mmol), TEA (9.3 μ, 0.007 g, 0.011 mmol) and enol triflate **252** (0.11 g, 0.15 mL, 1.10 mol) in toluene (5 mL), water (0.75 mL), ethanol (5 mL). The reaction mixture was allowed to stir at room temperature for 1.5 hours under a N_2 atmosphere, at which point TLC (1:1 EtOAC:hexane) revealed the absence of starting material. The reaction mixture was filtered through Pd catalyst filter paper and excess solvent was removed by rotary evaporation under reduced pressure. The residue was dissolved in EtOAc (25 mL), washed with brine (15 mL), water (15 mL). The organic phase was dried over $MgSO_4$ and excess solvent was removed by rotary evaporation under reduced pressure to afford as a dark orange oil **253**, the product was taken forward without further purification. 1,2-enol triflate isomer **^{1}H NMR** (400 MHz, CD_3OD). δ 7.43 (d, 2H, J = 8.80 Hz, (CH x 2)), (s, 2H, (CH x 2)), 7.26 (s, 1H, CH), 7.08 (d, 2H, J = 8.32 Hz (CH x 2)), 6.94 (d, 1H, J = 8.88 Hz, CH), 6.90 (d, 1H, 9.36 Hz, CH), 6.84 (s, 1H, CH), 5.21 (d, 1H, J =12.36 Hz, CH), 5.05 (s, 1H), 4.84-4.85 (m, 1H, CH_2), 4.55-4.60 (m,

1H, CH), 4.47-4.51 (m, 1H, CH_2), 3.90 (s, 3H, OCH_3), 3.80 (s, 6H, (OCH_3 x 2)), 2.10-2.18 (m, 1H, CH_2), 2.13 (s, 3H, OAc), 1.87-1.96 (m, 1H, CH_2), 1.49 (s, 9H, -$OC(CH_3)_3$), 1.47 (s, 9H, -$OC(CH_3)_3$). **Exact mass measurement** (HRMS-ES^+) *m/z*: theoretical mass: 860.3606 $[M + H]^+$; measured mass: 860.3583 $[M + H]^+$.

2-(4-[11-Acetoxy-7,8-dimethoxy-2-(4-methoxy-phenyl)-5-oxo-1,10,11,11a-tetrahydro-1H,5H-pyrrolo[2,1-*c*][1,4]benzodiazepine-10-carbonyloxymethyl]-phenoxycarbonylamino)-pentanedioic acid di-tert-butyl ester

Identical conditions were applied to the 2,3-triflate **223** to afford the 2,3-C2 aryl product **254** as a dark orange oil. The product was taken to the next step without further purification. 2,3-enol triflate isomer **^{1}H NMR** (400 MHz, CD_3OD). δ 7.36 (d, 2H, *J* = 8.84 Hz, (CH x 2)), 7.33 (s, 1H, CH), 7.27 (s, 2H, (CH x 2)), 7.25 (s, 1H, CH), 7.08 (d, *J* = 9.44 Hz, 2H, (CH x 2)), 7.06 (d, *J* = 9.76 Hz, 1H, CH), 6.92 (d, *J* = 8.84 Hz, 2H, (CH x 2)), 6.85 (s, 1H, CH), 5.20 (d, *J* = 12.28 Hz, 1H, CH_2), 5.05 (s, 1H, CH_2), 4.19-4.22 (m, 1H, CH), 4.13-4.18 (m, 1H, CH), 3.90 (s, 3H, OCH_3), 3.81 (s, 6H, (OCH_3 x 2)), 3.20-3.28 (m, 1H, CH_2), 3.02 (d, *J* = 15.53 Hz, 1H, CH_2), 2.37-2.41 (m, 2H, CH_2) 2.10-2.18 (m, 1H, CH_2), 2.13 (s, 3H, OAc), 1.87-1.95 (m, 1H, CH_2), 1.49 (s, 9H, -$OC(CH_3)_3$), 1.47 (s, 9H, -$OC(CH_3)_3$). **Exact mass measurement** (HRMS-ES^+) *m/z*: theoretical mass: 860.3606 $[M + H]^+$; measured mass: 860.3616 $[M + H]^+$.

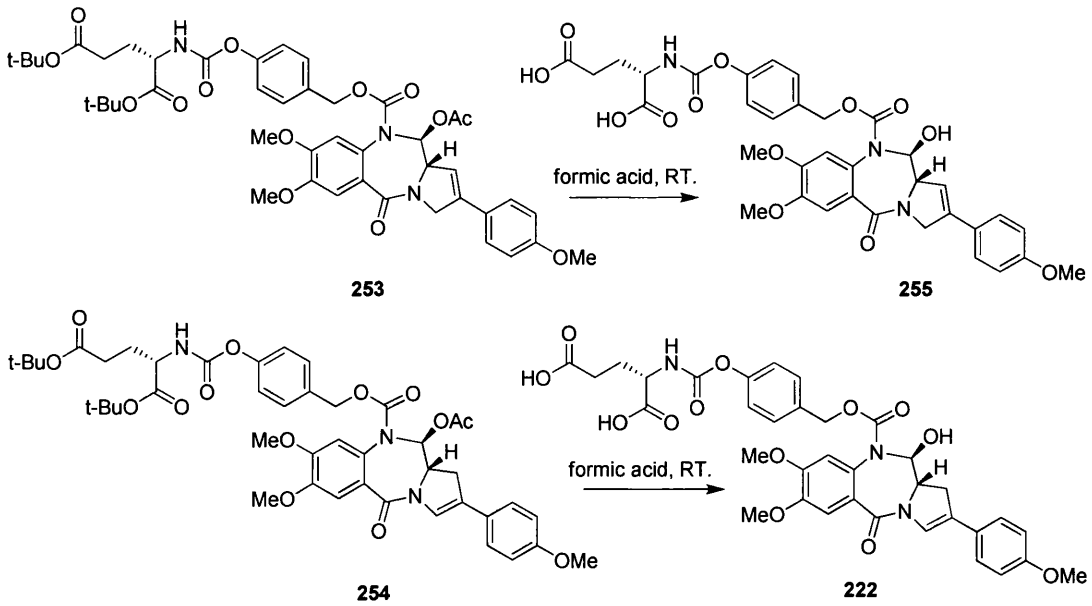

2-(4-[11-Hydroxy-7,8-dimethoxy-2-(4-methoxy-phenyl)-5-oxo-3,10,11,11a-tetrahydro-3H,5H-pyrrolo[2,1-*c*][1,4]benzodiazepine-10-carbonyloxymethyl]-phenoxycarbonylamino)-pentanedioic acid

Formic acid (0.5 mL) was added to the product **253** from the previous step and allowed to stir at room temperature for 18 hours. Excess solvent was removed by rotary evaporation under reduced pressure, the residue was azeotroped with toluene and purified by preperative LC-MS, products containing fractions were combined and excess eluent was removed by freeze drying to afford final compound **255** ready for biological testing.

^{1}H NMR (400 MHz, CD_3OD) 1,2-isomer δ 7.45 (d, 2H, J = 8.76 Hz, (CH x 2)), 7.30 (s, 1H, CH), 7.23 (s, 1H, CH), 7.10 (d, J = 8.32 Hz, 2H, (CH x 2)), 6.94 (d, J = 8.84 Hz, 2H, (CH x 2)), 6.75 (s, 1H, CH), 6.19 (s, 1H, CH), 5.74 (d, J = 9.08 Hz, 1H, CH_2), 5.27 (d, J = 12.12 Hz, 1H, CH_2), 4.93 (under solvent peak, 1H, CH_2), 4.85 (under solvent peak, 1H, CH_2), 4.56 (d, J = 15.16, 1H, CH_2), 4.23-4.29 (m, 2H, CH), 3.89 (s, 3H, OCH_3), 3.82 (s, 3H, OCH_3), 3.75 (s, 2H, OH), 2.46-2.49 (m, 2H, CH_2), 2.20-2.28 (m, 1H, CH_2), 1.98-2.05 (m, 1H, CH_2) **Exact mass measurement** (HRMS-ES$^+$) *m/z*: theoretical mass: 706.2242 $[M + H]^+$; measured mass: 706.2224 $[M + H]^+$.

2-(4-[11-Hydroxy-7,8-dimethoxy-2-(4-methoxy-phenyl)-5-oxo-1,10,11,11a-tetrahydro-1H,5H-pyrrolo[2,1-*c*][1,4]benzodiazepine-10-carbonyloxymethyl] phenoxycarbonylamino)-pentanedioic acid

Identical treatment of the **254** afforded the 2,3 product **222**. **^{1}H NMR** (400 MHz, CD_3OD) 2,3-isomer δ 7.40 (d, J = 8.84 Hz, 2H, (CH x 2)), 7.32 (s, 1H, CH), 7.25 (s, 1H, CH), 7.22 (s, 2H, (CH x 2)), 7.10 (d, J = 8.36 Hz, 2H, (CH x 2)), 6.92 (d, J = 8.88 Hz, 2H, (CH x 2)), 6.77 (s, 1H, CH), 5.82 (d, J = 9.08 Hz, 1H, CH), 5.28 (d, J = 12.12 Hz, 1H, CH_2), 4.93 (under solvent peak, 1H, CH_2), 4.21-4.25 (m, 1H, CH), 3.91-3.97 (m, 1H, CH), 3.89 (s, 3H, OCH_3), 3.81 (s, 3H, OCH_3), 3.75 (s, 2H, OH), 3.37-3.44 (m, 1H, CH_2), 3.01 (d, J = 16.41 Hz, 1H, CH_2), 2.45-2.48 (m, 2H, CH_2), 2.19-2.28 (m, 1H, CH_2), 2.00-2.05 (m, 1H, CH_2) **Exact mass measurement** (HRMS-ES$^+$) *m/z*: theoretical mass: 706.2242 $[M + H]^+$; measured mass: 706.2224 $[M + H]^+$.

8.3 Alternative Synthesis of C2-Aryl PBD Prodrugs

8.3.1 Model Study Part 1

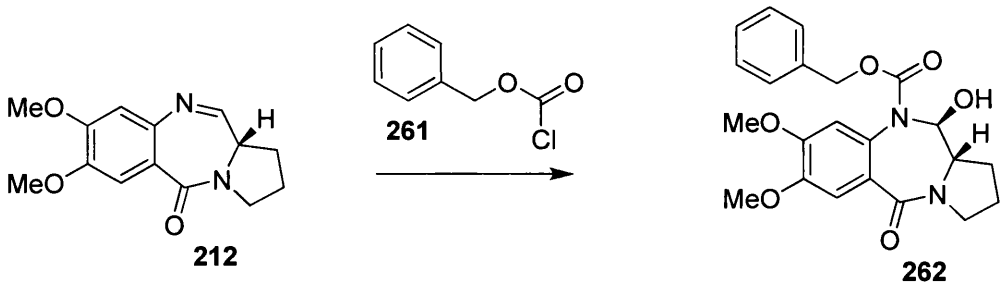

(11S,11aS)-benzyl-11-hydroxy-7,8-dimethoxy-5-oxo-2,3,11,11a-hexahydro-1H, 5H-pyrrolo[2,1-*c*][1,4]benzodiazepine-10-carboxylate

Benzyl chloroformate (0.019 mL, 0.023 g, 0.133 mmol) in DCM was added to a solution if PBD **212** (imine form) (0.03 g, 0.115 mmol) in toluene (0.5 mL) and sodium bicarbonate (0.024 g, 0.288 mmol) in water (1.5 mL). After 5 days of stirring at room temperature, under an atmosphere of nitrogen there was complete consumption of starting material. The reaction mixture was diluted with ethyl acetate (10 mL) and washed with water (3 x 10 mL). The organic phase was dried over $MgSO_4$ and excess solvent was removed by rotary evaporation under reduced pressure. The resulting residue was purified by column chromatography to give **262**

as a white solid (0.014 g, 29%). The structure was confirmed by NMR, MS/MS and HRMS. **^{1}H NMR** (400 MHz, $CDCl_3$) δ 7.35-7.28 (m, 3H), 7.25-7.21 (m, 3H), 6.53 (s, 1H), 5.65 (dd, *J* = 3.7, 9.4, 1H), 5.40 (d, *J* = 12.3, 1H), 4.87 (d, *J* = 12.1, 1H), 3.93 (s, 3H), 3.78-3.64 (m, 5H), 3.61-3.54 (m, 1H), 3.52-3.44 (m, 1H), 2.15-2.09 (m, 2H), 2.04-1.97 (m, 2H). **IR** (ATR ν_{max}/cm) 2960, 2360, 1708, 1618, 1604, 1515, 1452, 1433, 1405, 1312, 1294, 1279, 1217, 1133, 1104, 1051, 967, 875, 700, 645, 587 cm^{-1}. **MS/MS** $[M+H]^+$ ion at *m/z* 413.1: fragment ions 351.1 (RA 100%), 313.9 (RA 13%), 270.2 (RA 13%), 261.3 (RA 7%). **HRMS** theoretical mass $[M+H]^+$ ion at *m/z* 413.1707, measured mass $[M+H]^+$ ion at *m/z* 413.1703, δ 1 ppm.

8.3.2 Model Study Part 2

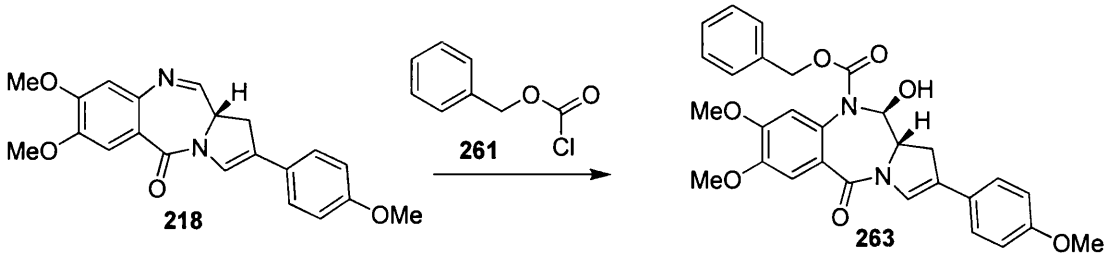

(11S,11aS)-benzyl 11-hydroxy-7,8-dimethoxy-2-(4-methoxyphenyl)-5-oxo-11,11a-tetrahydro-1H- pyrrolo[2,1-*c*][1,4]benzodiazepine-10(5H)-carboxylate

Benzyl chloroformate (0.020 mL, 0.024 g, 0.126 mmol) in DCM (3 mL) was added to a solution of C2-aryl PBD **218** (imine form) (0.045 g, 0.124 mmol) in DCM (2 mL) and sodium bicarbonate (0.026 g, 0.310 mmol) in water (2 mL). The reaction mixture was allowed to stir at room temperature for 22 hours under an atmosphere of nitrogen, then was diluted with DCM (20 mL) and washed with water (3 x 20 mL). The organic phase was dried over $MgSO_4$ and excess solvent was removed by rotary evaporation under reduced pressure. The resulting residue was purified by column chromatography to give **263** as a white solid (0.019g, 30%). The structure was confirmed by NMR, MS/MS and HRMS. **^{1}H NMR** (400 MHz, $CDCl_3$) δ 7.37 (s, 1H), 7.34-7.29 (m, 5H), 7.28-7,21 (m, 3H), 6.89 (d, *J* = 8.5 Hz, 2H), 6.56 (s, 1H), 5.85 (d, *J* = 6.7 Hz, 1H), 5.41 (d, *J* = 12.3 Hz, 1H), 4.88 (d, *J* = 11.9 Hz, 1H), 4.01 (td, *J* = 3.0, 10.0 Hz, 1H), 3.94 (s, 3H), 3.83 (s, 3H), 3.78-3.67 (m, 4H), 3.36 (dd, *J* = 10.3, 16.5

Hz, 1H), 3.06 (d, J = 16.2 Hz, 1H). **IR** (ATR ν_{max}/cm^{-1}) 3378, 2361, 1707, 1604, 1515, 1455, 1432, 1405, 1305, 1281, 1255, 1218, 1180, 1122, 1032, 856, 825, 757, 689, 650, 589 cm^{-1}. **MS/MS** $[M+H]^+$ ion at *m/z* 517.1: fragment ions 499.1 (RA 11%), 455.1 (RA 30%), 426.0 (RA 16%), 313.8 (RA 7%), 294.1 (RA 100%), 270.2, (RA 10%), 203.0 (RA 6%), 174.2 (RA 7%). **HRMS** theoretical mass $[M+H]^+$ ion at *m/z* 517.1969, measured mass $[M+H]^+$ ion at *m/z* 517.1962, δ 1 ppm.

8.3.3 Molecules for Biological Evaluation with Nitroreductase

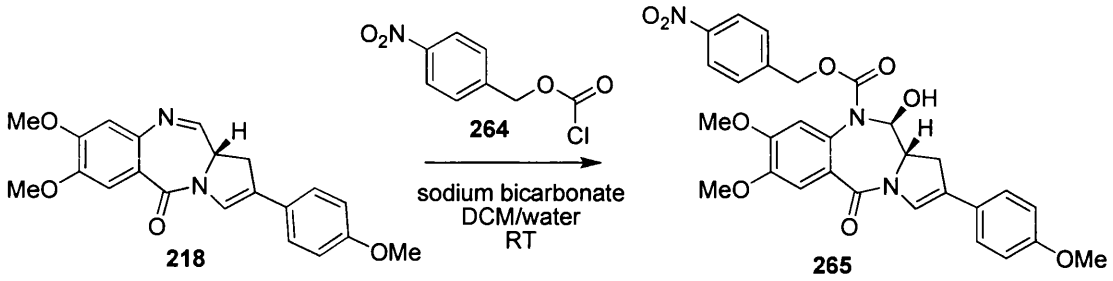

(11S,11aS)-4-nitrobenzyl-11-hydroxy-7,8-dimethoxy-2-(4-methoxyphenyl)-5-oxo-11,11a-tetrahydro-1H-pyrrolo[2,1-*c*][1,4]benzodiazepine-10(5H)-carboxylate

C2-aryl imine PBD **218** (0.1 g, 0.27 mmol) was treated with sodium bicarbonate (0.058 g, 0.69 mmol) in water (2 mL), *p*-nitrophenyl chloroformate (0.065 g, 0.30 mmol) in DCM (2 ml) and allowed to stir at room temperature for 24 hours under an atmosphere of nitrogen. The reaction mixture was diluted with DCM (30 mL) and washed with water (3 x 30 mL). The organic phase was dried over $MgSO_4$ and excess solvent was removed by rotary evaporation under reduced pressure. The resulting residue was purified by column chromatography (Hexane/EtOAc 1:1 then neat EtOAc) to give **265** a yellow solid (20 mg, 15%). **^{1}H NMR** (400 MHz, $CDCl_3$) δ 8.18 (d, J = 8.4 Hz, 2H), 7.38-7.32 (m, 3H), 7.30 (d, J = 8.8 Hz, 2H), 7.28 (s, 1H), 6.88 (d, J = 8.8 Hz, 2H), 6.66 (s, 1H), 5.85 (dd, J = 3.3, 9.1 Hz, 1H), 5.32 (d, J = 13.5 Hz, 1H), 5.09 (d, J = 13.1 Hz, 1H), 4.05-3.97 (m, 1H), 3.95 (s, 3H), 3.82 (s, 6H), 3.56 (s, 1H), 3.44-3.29 (m, 1H), 3.05 (d, J = 15.5 Hz, 1H). **^{13}C NMR** (100 MHz, $CDCl_3$) δ 163.00, 159.22, 151.29, 148.94, 127.93, 126.19, 126.08, 125.14, 123.85, 121.59, 114.24, 112.36, 110.88, 86.35, 66.44, 59.37, 56.24, 56.21, 55.34, 41.73, 35.12. **MS/MS** $[M+H]^+$ ion at 562.2 *m/z*: fragment ions 544.0 (RA 15%), 500.1 (RA 5%),

426.0 (RA 9%), 358.9 (RA 100%), 315.1 (RA 72%), 206.1 (RA 5%), 204.0 (RA 53%), 186.2 (RA 5%). **HRMS** theoretical mass $[M+H]^+$ ion at 562.1827 *m/z*, measured mass $[M+H]^+$ ion at 562.1818 *m/z*, δ 2 ppm.

8.4.1 p-Nitrophenyl Carbamate Displacement Strategy Model Study

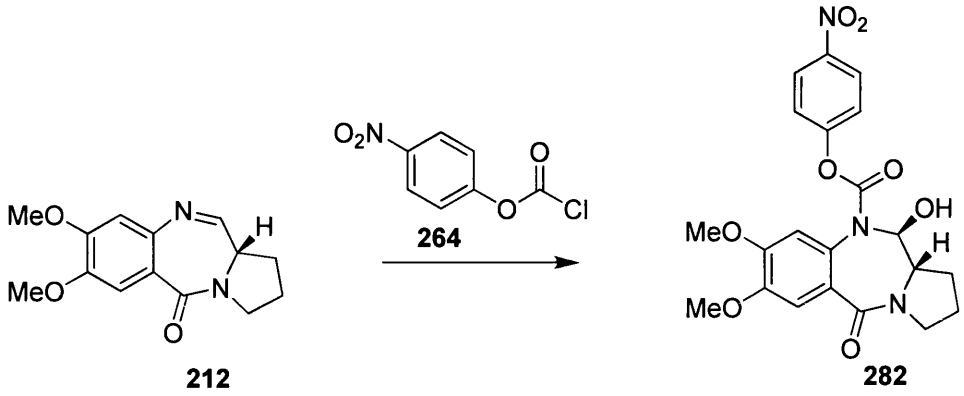

(11S,11aS)-4-nitrophenyl-11-hydroxy-7,8-dimethoxy-5-oxo-2,3,11,11a-hexahydro-1H-pyrrolo[2,1-*c*][1,4]benzodiazepine-10(5H)-carboxylate

4-nitrophenyl chloroformate (0.48 g, 2.38 mmol) in DCM (8 mL) was added to a solution of C-ring unsubstituted PBD **212** (imine form) (0.41 g, 1.58 mmol) in DCM (8 mL) and sodium bicarbonate (0.33 g, 3.96 mmol) in water (4 mL). After stirring at room temperature for 1 hour under an atmosphere of nitrogen, complete consumption of starting materials was observed. The reaction mixture was diluted with DCM (100 mL) and washed with water (3 x 100 mL). The organic phase was dried over $MgSO_4$ and excess solvent was removed by rotary evaporation under reduced pressure. The resulting residue was purified by column chromatography (hexane/EtOAc 1:2), to afford *p*-nitrophenyl carbamate **282,** as a yellow solid (0.15 g, 21 %). The structure was confirmed by NMR, MS/MS and HRMS. **^{1}H NMR** (400 MHz, $CDCl_3$) δ 8.17 (d, J = 9.0 Hz, 2H), 7.28 (s, 1H), 7.20 (d, J = 8.9 Hz, 2H), 6.80 (s, 1H), 5.68 (dd, J = 4.6, 9.6 Hz, 1H), 4.14-4.11 (m, 1H), 3.91 (s, 3H), 3.89 (s, 3H), 3.76-3.69 (m, 1H), 3.61-3.49 (m, 2H), 2.16-2.06 (m, 2H), 2.14-1.96 (m, 2H). **^{13}C NMR** (100 MHz, $CDCl_3$) δ 166.90, 155.41, 151.16, 149.04, 145.19, 127.66, 126.04, 125.12, 121.97, 112.21, 110.78, 86.64, 60.40, 60.11, 56.32, 56.22, 46.51, 28.64, 23.07, 21.02, 14.17. **IR** (ATR ν_{max}/cm^{-1}) 2355, 1731, 1616, 1604, 1520, 1456, 1434, 1399, 1338, 1318, 1280, 1212,

1164, 1096, 1017, 962, 861, 651, 602 cm^{-1}. **MS/MS** $[M+H]^+$ ion at *m/z* 444.2: fragment ions 426.1 (RA 7%), 344.9 (RA 100%), 304.9 (RA 8%), 206.0 (RA 39%). **HRMS** theoretical mass $[M+H]^+$ ion at *m/z* 444.1401, measured mass $[M+H]^+$ ion at *m/z* 444.1410, δ 2 ppm.

8.4.2 Displacement of Nitrophenyl with Benzyl Group

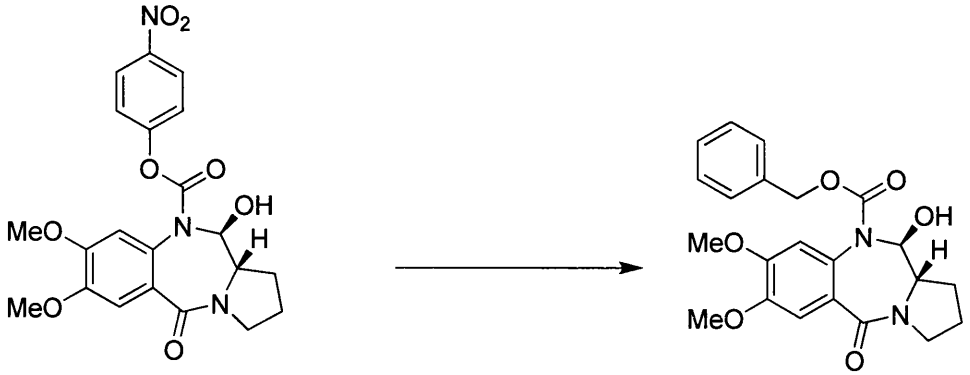

282 **262**

(11S,11aS)-benzyl-11-hydroxy-7,8-dimethoxy-5-oxo-2,3,11,11a-tetrahydro-1H-pyrrolo[2,1-*c*][1,4]benzodiazepine-10(5H)-carboxylate

A solution unsubstituted nitrophenyl intermediate **262** (0.05 g, 0.11 mmol) in anhydrous DMF (1 mL) was added to the freshly prepared alkoxide solutioin (Commercially available benzyl alcohol (0.018 mL, 0.018 g, 0.17 mmol) anhydrous DMF (1 mL) was converted to the alkoxide with potassium *tert*-butoxide (0.011 mL, 0.013 g, 0.11 mmol) under an atmosphere of nitrogen and was allowed to stir at room temperature overnight) and allowed to stir at room temperature for 5 minutes. LC-MS of the reaction mixture revealed two products, one corresponding to parent PBD imine and the other to the desired product **262**. The desired product was confirmed by LC-MS, the retention time and mass spectrum trace was identical to previously prepared material **262** (**Section 8.3.2**). LC/MS revealed the Retention Time at 5.05 minutes and $[M+H]^+$ ion at 466.32 *m/z*.

8.4.3 Displacement of Nitrophenyl with Alcohol Progroup

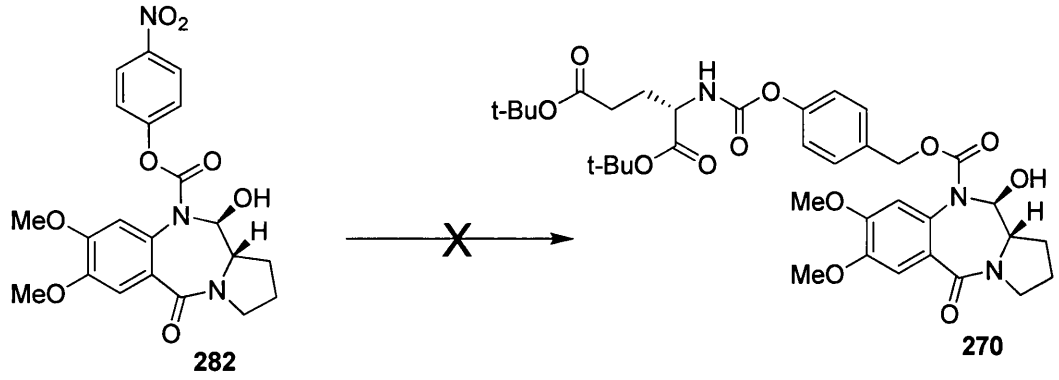

(S)-di-tert-butyl-2-((4-(((11S,11aS)-11-hydroxy-7,8-dimethoxy-5-oxo-2,3,5,10,11,11a-hexahydro-1H-pyrrolo[2,1-*c*][1,4]benzodiazepine-10-carbonyloxy)methyl)phenoxy)carbonylamino)pentanedioate

A solution of unsubstituted nitrophenyl intermediate **282** (0.2 g, 0.45 mmol), in anhydrous DMF (2 mL) was added to the freshly prepared alkoxide solution (Alcohol XX (0.185 g, 0.45 mmol) in anhydrous DMF (4 mL) was converted to the alkoxide with potassium *tert*-butoxide (0.051 g, 0.045 mmol) under an atmosphere of nitrogen and was allowed to stir at room temperature overnight) and allowed to stir at room temperature for 20 minutes. The reaction mixture was diluted with ethyl acetate (50 mL) and washed with 1N NaOH (3 x 50 mL), then with water (50 ml). The organic phase was dried over $MgSO_4$ and excess solvent was removed by rotary evaporation under reduced pressure. The resulting residue was purified by column chromatography (chloroform/methanol 99:1) to give product **270** a solid (0.085 g, 26%). Analytical evidence failed to confirm the product to be desired product. **^{1}H NMR** (400 MHz, $CDCl_3$) δ 7.27 (s, 1H), 6.95 (s, 1H), 5.57 (dd, J = 3.5, 10.0 Hz, 1H), 5.18 (d, J = 8.4 Hz, 1H), 5.02-4.92 (m, 1H), 4.38 (td, J = 4.6, 8.6 Hz, 1H), 4.30 (td, J = 5.0, 7.9 Hz, 1H), 3.95-3.88 (m, 7H), 3.75-3.64 (m, 1H), 3.61 (d, J = 3.5 Hz, 1H), 3.58-3.50 (m, 1H), 3.48-3.39 (m, 1H), 2.94-2.84 (m, 1H), 2.38-2.22 (m, 2H), 2.21-2.15 (m, 2H), 2.15-2.07 (m, 2H), 2.07-1.92 (m, 4H), 1.91-1.76 (m, 1H), 1.74-1.63 (m, 1H), 1.44 (s, 7H), 1.42 (s, 9H), 1.41 (s, 7H), 1.37 (s, 8H). **IR** (ATR ν_{max}/cm) 2372, 2331, 1636, 1517, 1467, 1394, 1278, 1256, 1153, 1062, 978, 846, 796, 761, 664, 574 cm^{-1}. **MS/MS** $[M+H]^+$ ion at *m/z* 567.3: fragment ions 511.1 (RA 100%), 455.1 (RA 59%), 399.1 (RA 16%), 343.1 (RA 3%).

8.4.4 p-Nitrophenyl Carbamate Displacement Strategy

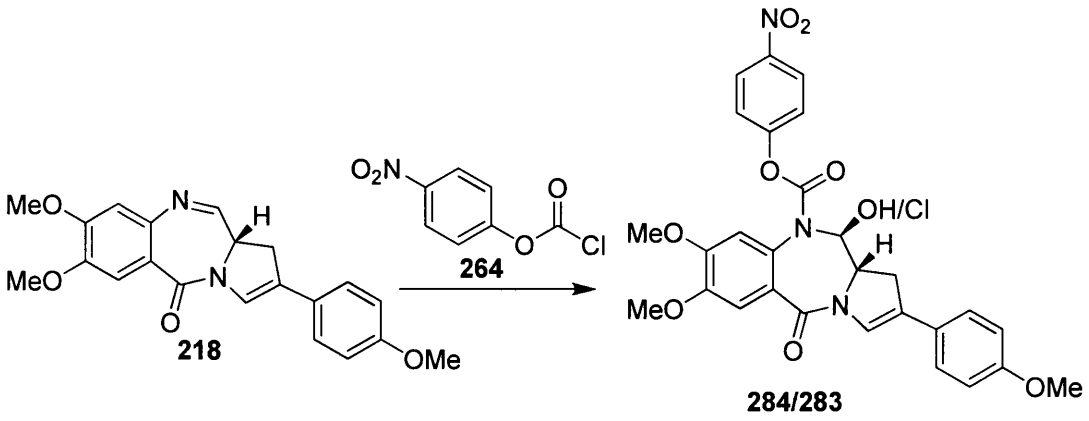

p-nitrophenyl chloroformate (0.057 g, 0.28 mmol) in DCM (2 ml) was added to a solution of C2-aryl PBD **218** (imine form) (0.10 g, 0.28 mmol) in DCM (2 mL) and sodium bicarbonate (0.059 g, 0.71 mmol) in water (2 ml) and allowed to stir at room temperature for 30 minutes under an atmosphere of nitrogen. The reaction mixture was diluted with DCM (30 mL) and washed with water (3 x 30 mL). The organic phase was dried over $MgSO_4$ and excess solvent was removed by rotary evaporation under reduced pressure. The resulting residue was purified by column chromatography (hexane/EtOAc 1:1 then neat EtOAc) to give two products **284** as a yellow solid (0.023 g, 15%) and product **283** as a yellow solid (0.076 g, 49 %).

(11S,11aS)-4-nitrophenyl-11-chloro-7,8-dimethoxy-2-(4-methoxyphenyl)-5-oxo-11,11a-tetrahydro-1H-pyrrolo[2,1-*c*][1,4]benzodiazepine-10(5H)-carboxylate

284 Major Product

^{1}H NMR (400 MHz, $CDCl_3$) δ 8.24 (d, J = 7.5 Hz, 2H), 7.38 (s, 1H), 7.35-7.27 (m, 4H), 6.90 (d, J = 8.8 Hz, 2H), 6.87 (s, 1H), 6.42 (d, J = 10.2 Hz, 1H), 4.29 (t, J = 8.5 Hz, 1H), 4.02-3.92 (m, 7H), 3.83 (s, 3H), 3.47 (ddd, J = 2.0, 10.2, 16.7 Hz, 1H), 3.10-3.04 (m, 1H). **^{13}C NMR** (100 MHz, $CDCl_3$) δ 162.93, 159.28, 159.28, 151.46, 149.26, 145.30, 126.22, 126.22, 125.96, 125.20, 125.20, 125.11, 121.94, 121.94, 121.55, 114.25, 114.25, 112.12, 110.99, 110.99, 86.65, 59.39, 56.29, 56.29, 55.35, 55.35, 35.10, 29.69, 14.19. **IR** ATR (ν_{max}/cm) 1742.8, 1849.8, 1604.8, 1516.7, 1453.8, 1425.8, 1395.8, 1346.9, 1282.8, 1254.8, 1208.7, 1180.8, 1109.9 1033.9, 825.9. **MS/MS** $[M+H]^+$ ion at *m/z* 566.2: fragment ions 530.1 (RA 100%), 487.1 (RA

28%), 391.1 (RA 49%), 206.0 (RA 43%), 186.1 (RA 41%). **HRMS** theoretical mass $[M+H]^+$ ion at *m/z* 566.1324, measured mass $[M+H]^+$ ion at *m/z* 566.1330, δ 1.1 ppm.

(11S,11aS)-4-nitrophenyl-11-hydroxy-7,8-dimethoxy-2-(4-methoxyphenyl)-5-oxo-11,11a-tetrahydro-1H-pyrrolo[2,1-*c*][1,4]benzodiazepine-10(5H)-carboxylate

283 Minor Product

^{1}H NMR (400 MHz, $CDCl_3$) δ 8.22 (d, *J* = 9.0 Hz, 2H), 7.40 (s, 1H), 7.34-7.29 (m, 3H), 7.23 (d, *J* = 9.0 Hz, 2H), 6.88 (d, *J* = 8.8 Hz, 2H), 6.83 (s, 1H), 5.89 (dd, *J* = 4.5, 9.5 Hz, 1H), 4.10-4.01 (m, 1H), 3.94 (d, *J* = 9.5 Hz, 6H), 3.82 (s, 4H), 3.40 (ddd, *J* = 1.9, 10.2, 16.6 Hz, 1H), 3.10-3.04 (m, 1H). **^{13}C NMR** (100 MHz, $CDCl_3$) δ 162.99, 162.29, 159.46, 154.98, 151.80, 126.31, 126.16, 125.50, 125.40, 125.22, 121.94, 121.25, 115.63, 114.31, 112.05, 111.03, 78.53, 64.40, 62.10, 56.53, 56.34, 55.36, 35.28, 30.64, 21.00, 19.11, 14.18, 13.68. **IR** (ATR ν_{max}/cm^{-1}) 2360, 1743, 1647, 1606, 1517, 1454, 1426, 1397, 1347, 1284, 1256, 1209, 1181, 1109, 1033, 861, 667, 643, 589 cm^{-1}. **MS/MS** $[M+H]^+$ ion at *m/z* 548.1: fragment ions 530.0 (RA 19%), 344.8 (RA 62%), 204.0 (RA 100%). **HRMS** theoretical mass $[M+H]^+$ ion at *m/z* 548.1664, measured mass $[M+H]^+$ ion at *m/z* 548.1669, δ 1 ppm.

8.4.5 Displacement of Nitrophenyl with Methoxy Group

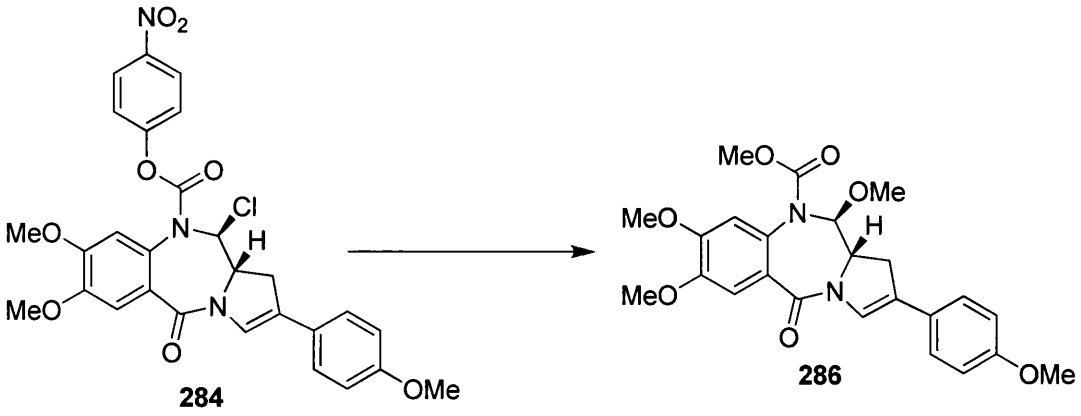

(11S,11aS)-methyl-7,8,11-trimethoxy-2-(4-methoxyphenyl)-5-oxo-11,11a-tetrahydro-1H-pyrrolo[2,1-*c*][1,4]benzodiazepine-10(5H)-carboxylate

Sodium metal (0.126 g, 0.055 mmol) was added to anhydrous methanol (10 mL) under an atmosphere of nitrogen at room temperature. After the sodium had all been

completely consumed, 0.1 mL of the sodium methoxide solution was added to an already stirring solution of nitrophenyl intermediate **284** (0.02 g, 0.037 mmol) in 1 mL of anhydrous methanol. The reaction mixture was allowed at room temperature for 2 hours. Excess solvent was removed by rotary evaporation under reduced pressure. The resulting residue was purified by column chromatography (EtOAc/hexane 1:1) to give product **286** a yellow solid (10 mg, 63 %). **^{1}H NMR** (400 MHz, $CDCl_3$) δ 7.35 (s, 1H), 7.31 (d, J = 8.8 Hz, 2H), 7.26 (s, 1H), 6.92-6.86 (m, 2H), 6.65 (s, 1H), 5.67 (d, J = 8.5 Hz, 1H), 3.94 (d, J = 4.5, 6H), 3.89 (dd, J = 3.0, 9.7 Hz, 1H), 3.83 (s, 3H), 3.64 (s, 3H), 3.61 (s, 3H), 3.37 (ddd, J = 2.2, 10.4, 16.5 Hz, 1H), 2.94 (dd, J = 2.0, 16.6 Hz, 1H). **IR** (ATR ν_{max}/cm^{-1}) 2957, 1711, 1640, 1604, 1515, 1428, 1401, 1318, 1275, 1254, 1216, 1179, 1123, 1099, 1076, 1032, 977, 850, 825, 723, 647, 605 cm^{-1}. **MS/MS** $[M+H]^+$ ion at *m/z* 455.19: fragment ions 423.2 (RA 92%), 391.1 (RA 25%), 380.2 (RA 22%), 364.2 (RA 12%), 321.1 (RA 10%) 250.1 (RA 48%), 244.1 (RA 43%), 238.1 (RA 35%), 218.1 (RA 21%), 206 (RA 88%), 186.1 (RA 100%). **HRMS** theoretical mass $[M+H]^+$ ion at 455.1818 m/z, measured mass $[M+H]^+$ ion at 455.1805 m/z, δ 3 ppm.

8.4.6 Displacement of Nitrophenyl with para-methoxy benzyl alkoxide

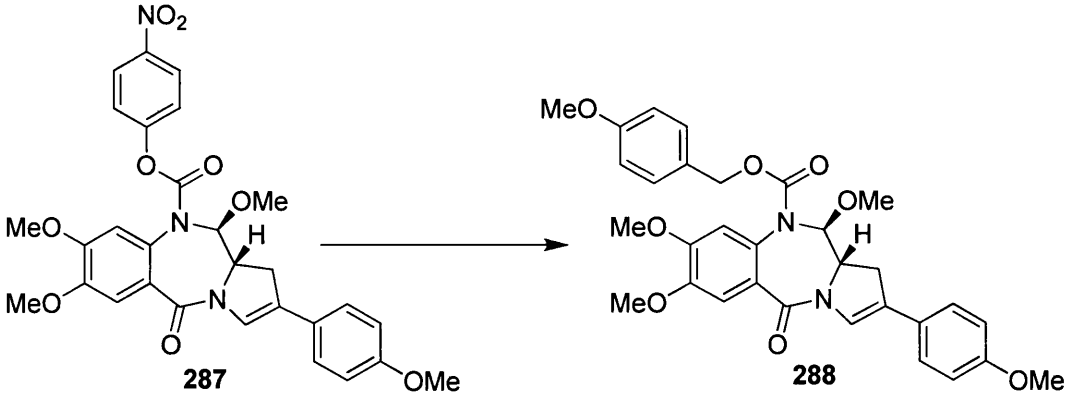

(11S,11aS)-4-methoxybenzyl-7,8,11-trimethoxy-2-(4-methoxyphenyl)-5-oxo-11,11a-tetrahydro-1H-pyrrolo[2,1-*c*][1,4]benzodiazepine-10(5H)-carboxylate

A solution of *p*-nitrophenyl intermediate **287** (50 mg, 0.089 mmol) in DMF (2 mL) was added to the freshly prepared alkoxide solution. (4-methoxybenzyl alcohol (17 µl, 18 mg, 0.134 mmol) was converted to the alkoxide with potassium *tert*-butoxide (89 µl, 0.01 g, 0.089 mmol) in DMF (2 mL) and allowed to stir overnight).

The reaction mixture was allowed at room temperature for 2 hours. Excess reaction mixture solvent was removed by rotary evaporation under reduced pressure. The resulting residue was purified by preparative LC-MS to give product **288** a yellow solid (2.8 mg, 6%) and side product corresponding to imine. **^{1}H NMR** (500 MHz, $CDCl_3$) δ 7.34 (s, 1H), 7.30 (d, J = 8.8 Hz, 2H), 7.25 (s, 1H), 7.11 (d, J = 6.4 Hz, 2H), 6.88 (d, J = 8.8 Hz, 2H), 6.82 (d, J = 8.1 Hz, 2H), 6.52 (s, 1H), 5.67 (d, J = 7.1 Hz, 1H), 5.25 (d, J = 11.8 Hz, 1H), 4.80 (d, J = 12.8 Hz, 1H), 3.97-3.87 (m, 4H), 3.87-3.74 (m, 9H), 3.58 (s, 3H), 3.41-3.30 (m, 1H), 2.93 (d, J = 16.2 Hz, 1H). **MS/MS** $[M+H]^+$ ion at *m/z* 561.3: fragment ions 529.2 (RA 8%), 485.2 (RA 44%), 395.2 (RA 5%), 338.2 (RA 8%), 294.2 (RA 5%), 121 (RA 10%). **HRMS** theoretical mass $[M+H]^+$ ion at 561.2237 m/z, measured mass $[M+H]^+$ ion at 561.2226 m/z, δ 2 ppm.

8.4.7 Selective Substitution of Chlorine for a Methoxy Group

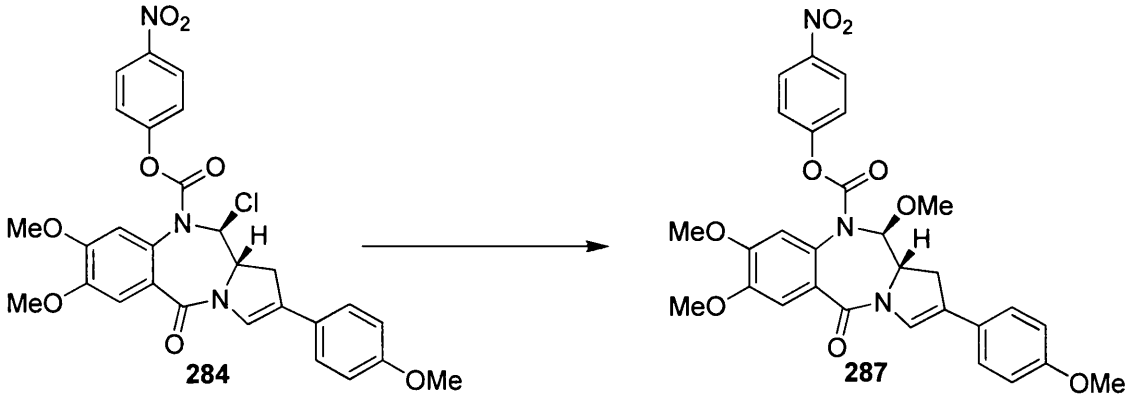

(11S,11aS)-4-nitrophenyl-7,8,11-trimethoxy-2-(4-methoxyphenyl)-5-oxo-11,11a-tetrahydro-1H-pyrrolo[2,1-*c*][1,4]benzodiazepine-10(5H)-carboxylate

A methanolic (4 mL) solution of intermediate **284** (0.02 g, 0.037 mmol) was allowed to stir at room temperature for 48 hours. Excess solvent was removed by rotary evaporation under reduced pressure. The resulting residue did not required further purification, affording **287** a solid (0.019 g, 95%). **^{1}H NMR** (400 MHz, $CDCl_3$) δ 8.20 (d, J = 8.9 Hz, 2H), 7.39 (s, 1H), 7.34-7.30 (m, 3H), 7.21 (d, J = 9.1 Hz, 2H), 6.92-6.86 (m, 2H), 6.77 (s, 1H), 5.69 (d, J = 9.1 Hz, 1H), 4.03-3.91 (m, 7H), 3.83 (s, 3H), 3.68 (s, 3H), 3.41 (ddd, J = 2.0, 10.4, 16.3 Hz, 1H), 2.97 (ddd, J = 1.2, 3.4, 16.5 Hz, 1H). **IR** (ATR ν_{max}/cm^{-1}) 2359, 1734, 1637, 1606, 1517, 1453, 1428, 1403, 1347, 1316, 1277, 1256, 1214, 1180, 1137, 1088, 1034, 969, 861, 804,643, 568

cm^{-1}. **MS/MS** $[M+H]^+$ ion at *m/z* 562.3: fragment ions 530.1 (RA 100%), 487.2 (RA 26%), 428.2 (RA 12%), 391.1 (RA 22%), 351.1 (RA 19%), 206.1 (RA 24%), 186.2 (RA 43%). **HRMS** theoretical mass $[M+H]^+$ ion at *m/z* 562.1820, measured mass $[M+H]^+$ ion at *m/z* 562.1837, δ 4 ppm.

8.5 Trichloromethyl Displacement Strategy

8.5.1 Trichloromethyl Displacement Strategy Model Study

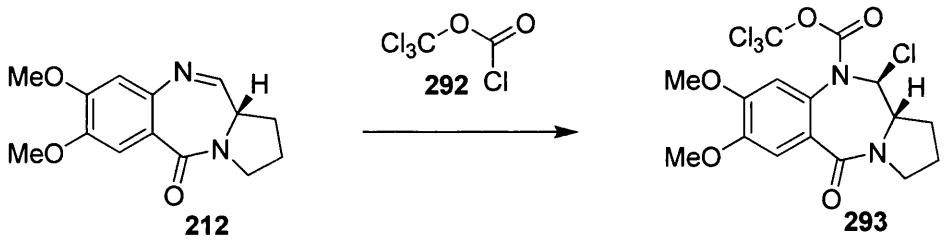

(11S,11aS)-trichloromethyl-11-chloro-7,8-dimethoxy-5-oxo-2,3,11,11a-hexahydro-1H-pyrrolo[2,1-*c*][1,4]benzodiazepine-10(5H)-carboxylate

Trichloromethyl chloroformate (0.38 g, 0.23 mL, 1.92 mmol) in DCM (3 ml) was added to a solution of unsubstituted PBD **212** (imine form) (0.50 g, 1.92 mmol) in DCM (3 mL) and sodium bicarbonate (0.40 g, 4.81 mmol) in water (3 mL). The reaction was allowed to stir at room temperature for 3 hours under an atmosphere of nitrogen. LC-MS showed starting material had been consumed and revealed a major new product. The reaction mixture was diluted with DCM (50 mL) and washed with water (3 x 50 mL). The organic phase was dried over $MgSO_4$ and excess solvent was removed by rotary evaporation under reduced pressure. The resulting residue was purified by column chromatography (EtOAc/Hexane 1:3) to give product **293** a pale brown solid (0.40 g, 48%). **^{1}H NMR** (400 MHz, $CDCl_3$) δ 7.28 (s, 1H), rotamers ((6.76, s and 6.68, s,) 1H), 6.10 (d, J = 10.4 Hz, 1H), 3.95 (s, 3H), 3.95 (s, 3H), 3.80-3.68 (m, 2H), 3.67-3.54 (m, 1H), 2.28-2.10 (m, 2H), 2.10-1.98 (m, 2H). **^{13}C NMR** (100 MHz, $CDCl_3$) δ 166.6, 151.4, 149.7, 126.1, 113.1, 111.9, 110.9, 63.0, 62.6, 56.5 (CH_3), 56.4, (CH_3), 46.9, 46.8 (CH_2), 30.9, 28.8, (CH_2), 23.0 (CH_2). **^{13}C NMR** (100 MHz, $CDCl_3$) δ 166.55, 151.42, 149.72, 111.85, 110.87, 63.04, 62.56, 56.45, 56.31, 56.25, 46.88, 46.79, 30.90, 28.76, 23.04. **IR** (ATR ν_{max}/cm^{-1}) 3746, 2359, 1772, 1646, 1517, 1456, 1425, 1392, 1281, 1222, 1088, 1022, 978, 906, 643, 598 cm^{-1}. **MS/MS**

$[M+H]^+$ ion at 458.9 *m/z*: fragment ions 323.9 (RA 35%), 288.2 (RA 100%), 262.1 (RA 6%). **HRMS** theoretical mass $[M+H]^+$ ion at *m/z* 439.0225, measured mass $[M+H]^+$ ion at *m/z* 439.0244, δ 4 ppm.

8.5.2 Trichloromethyl Displacement Strategy with Methoxy Group

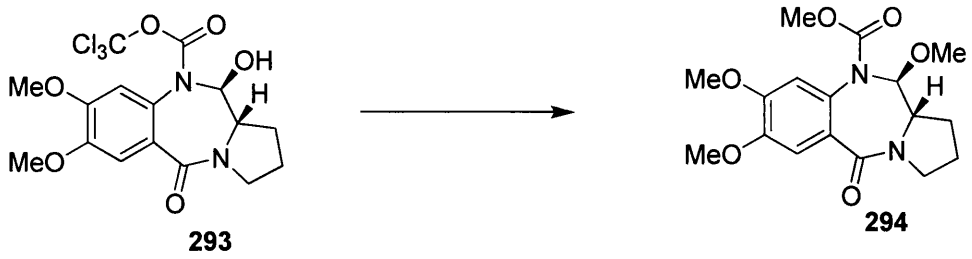

(11S,11aS)-methyl-7,8,11-trimethoxy-5-oxo-2,3,11,11a-hexahydro-1H-pyrrolo[2,1-*c*][1,4]benzodiazepine-10(5H)-carboxylate

A methanolic solution (anhydrous methanol (2 mL)) of **293** (0.066 g, 0.15 mmol) was allowed to stir for 2 hrs under a nitrogen atmosphere in the presence of anhydrous pyridine (0.061 mL, 0.059 g, 0.75 mmol). Excess solvent was removed by rotary evaporation under reduced pressure. The resulting residue was purified by column chromatography (EtOAc/hexane 1:1) to give product **294** a solid (0.35 g, 66%). **^{1}H NMR** (400 MHz, $CDCl_3$) δ 7.24 (s, 1H), 6.60 (s, 1H), 5.44 (d, *J* = 8.8 Hz, 1H), 3.92 (d, *J* = 3.5 Hz, 6H), 3.72-3.59 (m, 4H), 3.56-3.46 (m, 4H), 3.40 (t, *J* = 8.7 Hz, 1H), 2.14-2.07 (m, 1H), 2.03-1.97 (m, 3H). **IR** (ATR ν_{max}/cm^{-1}) 2949, 2362, 2342, 1706, 1637, 1640, 1514, 1428, 1399, 1318, 1296, 1271, 1216, 1136, 1109, 1084, 1053, 1019, 969, 935, 861, 827, 774, 720, 688, 645, 592 cm^{-1}. **MS/MS** $[M+Na]^+$ ion at 373.2 *m/z* and $[M+H]^+$ ion at 351.5 *m/z*: fragment ions 319.1 (RA 100%), 287.2 (RA 9%). **HRMS** theoretical mass $[M+H]^+$ ion at 351.1551 *m/z*, measured mass $[M+H]^+$ ion at 351.1559 *m/z*, δ 2 ppm.

8.5.3 Trichloromethyl Displacement Strategy with Progroup

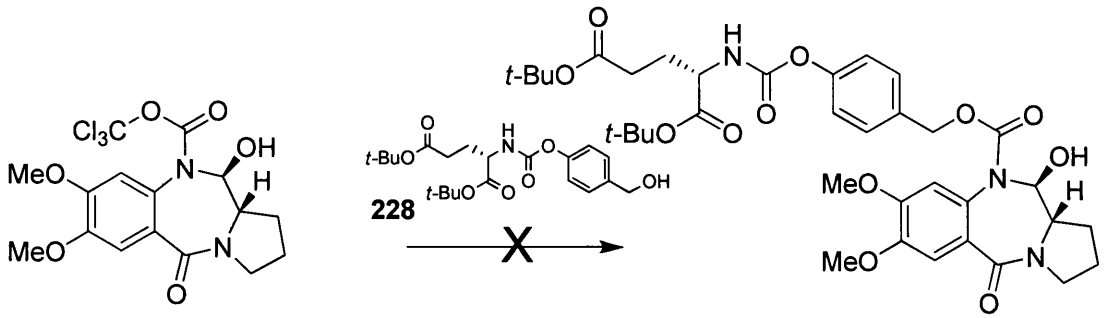

293 **228** **270**

(S)-di-tert-butyl-2-((4-(((11S,11aS)-11-hydroxy-7,8-dimethoxy-5-oxo-2,3,5,10,11,11a-hexahydro-1H-pyrrolo[2,1-*c*][1,4]benzodiazepine-10-carbonyloxy)methyl)phenoxy)carbonylamino)pentanedioate

Progroup alcohol **228** (0.070 g, 0.17 mmol) in anhydrous DMF (1 mL) was converted to the alkoxide on treatment nwith potassium *tert*-butoxide (0.009 mL, 0.009 g, 0.11 mmol) under an atmosphere of nitrogen and was allowed to stir at room temperature overnight, then was added to a solution of trichloromethy carbamate **293** (0.050 g, 0.11 mmol) in anhydrous DMF (1 mL) and allowed to stir at room temperature for 1 hour. LC-MS of the reaction mixture showed two products had been formed, one corresponding to parent PBD imine **212** and an unidentified product **270**. **^{1}H NMR** (400 MHz, $CDCl_3$) δ 7.25-7.21 (m, 2H), 7.09 (d, J = 7.7 Hz, 2H), 6.48 (s, 1H), 5.69 (d, J = 7.7 Hz, 1H), 5.62 (d, J = 7.8 Hz, 1H), 5.37 (d, J = 11.9 Hz, 1H), 4.82 (d, J = 12.7 Hz, 1H), 4.30 (td, J = 4.9, 8.0 Hz, 1H), 4.04-3.93 (m, 1H), 3.92 (s, 3H), 3.91-3.80 (m, 1H), 3.74-3.65 (m, 4H), 3.61-3.52 (m, 1H), 3.51-3.45 (m, 1H), 3.41 (s, 1H), 2.44-2.28 (m, 2H), 2.16-2.08 (m, 2H), 2.04-1.91 (m, 3H), 1.50 (s, 9H), 1.45 (s, 9H). **IR** (ATR ν_{max}/cm^{-1}) 3325, 2974, 2360, 2341, 1716, 1625, 1605, 1506, 1456, 1433, 1368, 1315, 1278, 1216, 1154, 1103, 1012, 969, 840, 644, 586 cm^{-1}. **HRMS** theoretical mass $[M+H]^+$ ion at 714.3232 *m/z*, measured mass $[M+H]^+$ ion at 714.3237 *m/z*, δ 1 ppm.

8.5.4 Trichloromethyl Intermediate

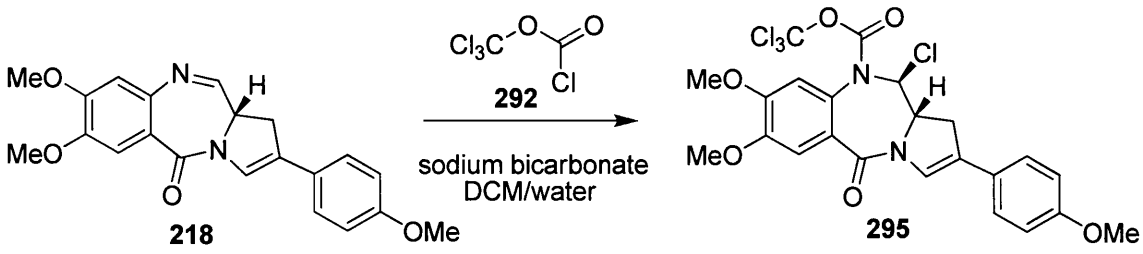

(11S,11aS)-trichloromethyl 11-chloro-7,8-dimethoxy-2-(4-methoxyphenyl)-5-oxo-11,11a-tetrahydro-1H-pyrrolo[2,1-*c*][1,4]benzodiazepine-10(5H)-carboxylate

Trichloromethyl chloroformate (0.066 mL, 0.11 g, 0.55 mmol) in DCM (3 ml) was added to a solution of C2-aryl PBD **218** (imine form) (0.20 g, 0.55 mmol) in DCM (3 mL) and sodium bicarbonate (0.12 g, 1.37 mmol) in water (3 ml). After allowing the reaction mixture to stir at room temperature for 10 minutes under an atmosphere of nitrogen, the reaction was diluted with DCM (50 mL) and washed with water (3 x 50 mL). The organic phase was dried over $MgSO_4$ and excess solvent was removed by rotary evaporation under reduced pressure. The resulting residue was purified by column chromatography (EtOAc/Hexane 1:3) to give product **295** a pale orange solid (0.14 g, 46%) and some recovered starting material **218** (0.38 g, 19 %). **^{1}H NMR** (400 MHz, $CDCl_3$) δ 7.36 (s, 1H), 7.33-7.30 (m, 3H), 6.90 (d, J = 8.8 Hz, 2H), rotamers ((6.81, s and 6.73, s,) 1H), 6.33-6.21 (m, 1H), 4.25 (td, J = 3.5, 10.3 Hz, 1H), 3.97 (s, 6H), 3.83 (s, 3H), 3.45 (ddd, J = 2.2, 10.3, 16.8 Hz, 1H), 3.09-3.00 (m, 1H). **^{13}C NMR** (100 MHz, $CDCl_3$) δ 162.68, 159.43, 151.75, 149.96, 126.30, 125.52, 121.40, 114.30, 111.91, 111.08, 77.78, 61.85, 60.37, 56.52, 56.32, 55.35, 35.28, 21.03, 14.19. IR (ATR ν_{max}/cm^{-1}) 1765, 1648, 1605, 1516, 1452, 1426, 1393, 1280, 1223, 1090, 1020, 669, 587 cm-1. **MS/MS** $[M+H]^+$ ion at 563 *m/z*: fragment ions 429.0 (RA 37%), 427.0 (RA 100%), 391.2 (RA, 67%). $[M+H]^+$ ion at 427 *m/z*: fragment ions 391.2 (RA 100%), 374.2 (RA 28%), 359.2 (RA 49%), 348.2 (RA 35%), 320.2 (RA 10%), 206.1 (RA 37%), 145.1 (RA 22%). **HRMS** theoretical mass $[M+H]^+$ ion at 561.0154 *m/z*, measured mass $[M+H]^+$ ion at 561.0167*m/z*, δ 2 ppm.

8.5.5 Trichloromethyl Displacement Strategy with Methoxide

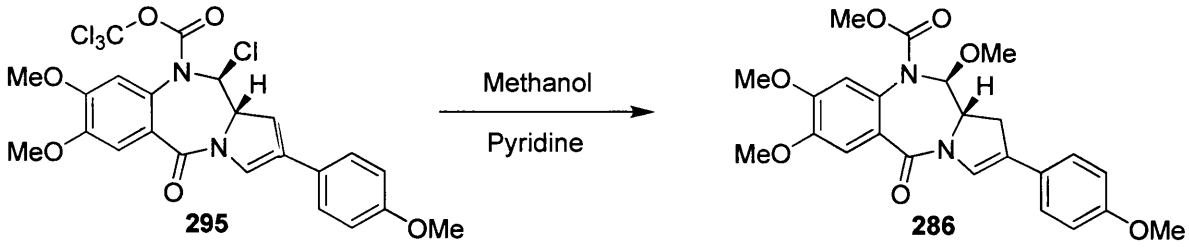

(11S,11aS)-methyl-7,8,11-trimethoxy-2-(4-methoxyphenyl)-5-oxo-11,11a-tetrahydro-1H- pyrrolo[2,1-*c*][1,4]benzodiazepine-10(5H)-carboxylate

A methanolic solution (anhydrous methanol (2 mL)) of **295** (0.3 g, 0.053 mmol) was allowed to stir for 2 hrs under a nitrogen atmosphere in the presence of anhydrous pyridine (0.0048 mL, 0.0047 g, 0.058 mmol). Excess solvent was removed by rotary evaporation under reduced pressure. The resulting residue was purified by column chromatography (EtOAc/Hexane 1:1) to give product **286** a solid (0.18 g, 75%). **^{1}H NMR** (400 MHz, $CDCl_3$) δ 7.35 (s, 1H), 7.31 (d, J = 8.8 Hz, 2H), 7.26 (s, 1H), 6.92-6.86 (m, 2H), 6.65 (s, 1H), 5.67 (d, J = 8.5 Hz, 1H), 3.94 (d, J = 4.5, 6H), 3.89 (dd, J = 3.0, 9.7 Hz, 1H), 3.83 (s, 3H), 3.64 (s, 3H), 3.61 (s, 3H), 3.37 (ddd, J = 2.2, 10.4, 16.5 Hz, 1H), 2.94 (dd, J = 2.0, 16.6 Hz, 1H). **IR** (ATR ν_{max}/cm^{-1}) 2957, 1711, 1640, 1604, 1515, 1428, 1401, 1318, 1275, 1254, 1216, 1179, 1123, 1099, 1076, 1032, 977, 850, 825, 723, 647, 605 cm^{-1}. **MS/MS** $[M+H]^+$ ion at 455.6 *m/z*: fragment ions 423.0 (RA 100%), 380.2 (RA 10%), 244.1 (RA 7%), 280.0 (RA 5%), 206.1 (RA 5%), 186.2 (RA 24%). **HRMS** theoretical mass $[M+H]^+$ ion at 455.1818 *m/z*, measured mass $[M+H]^+$ ion at 455.1794 *m/z*, δ 5 ppm.

8.5.6 Trichloromethyl Displacement Strategy with Progroup

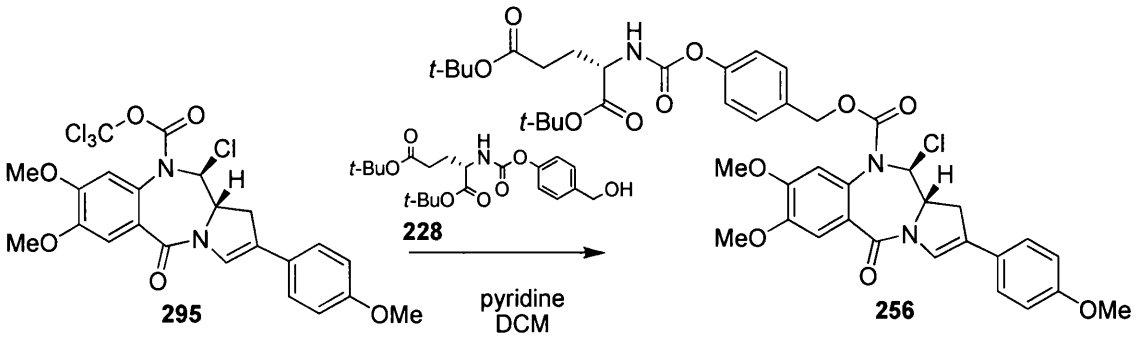

(S)-di-tert-butyl-2-((4-(((11S,11aS)-11-hydroxy-7,8-dimethoxy-2-(4-methoxyphenyl)-5-oxo-5,10,11,11a-tetrahydro-1H-pyrrolo[2,1-*c*][1,4]benzodiazepine-10-carbonyloxy)methyl)phenoxy)carbonylamino) pentanedioate

295 (0.1 g, 0.20 mmol) and progroup **228** (0.089 g, 0.22 mmol) in anhydrous DCM (6 mL) was treated with anhydrous pyridine (0.032 mL, 0.031 g, 0.40 mmol). The reaction mixture was allowed to stir at room temperature for 2 hours under an atmosphere of nitrogen. Excess solvent was removed by rotary evaporation under reduced pressure. The resulting residue was purified by column chromatography to give unknown product **256.** **^{1}H NMR** (400 MHz, $CDCl_3$) δ 7.34 (td, J = 8.7, 11.5 Hz, 5H), 7.14 (d, J = 8.5 Hz, 1H), 6.90 (d, J = 8.7 Hz, 2H), 6.83 (s, 1H), 6.32 (d, J = 10.1 Hz 1H), 5.74 (d, J = 8.1 Hz, OH), 5.14 (s, 1H), 4.32 (dd, J = 8.1, 12.9 Hz, 1H), 4.21 (t, J = 8.6 Hz, 1H), 3.98 (s, 7H), 3.83 (s, 3H), 3.43 (dd, J = 11.0, 16.0 Hz, 1H), 3.02 (d, J = 16.9 Hz, 1H), 2.36 (qd, J = 7.7, 16.4 Hz, 1H), 2.20 (dd, J = 6.8, 13.6 Hz, 1H), 2.05-1.93 (m, 1H), 1.49 (d, J = 15.1 Hz, 11H). **^{13}C NMR** (100 MHz, $CDCl_3$) δ 170.75, 169.49, 161.12, 158.07, 153.60, 152.63, 150.38, 149.74, 149.10, 149.01, 130.88, 128.19, 125.43, 124.94, 124.49, 124.13, 121.51, 120.33, 119.96, 112.95, 111.80, 109.73, 81.24, 79.48, 67.77, 60.99, 59.02, 55.22, 55.03, 53.99, 52.78, 33.77, 30.16, 26.73, 26.66, 26.46, 19.67, 12.84. **IR** (ATR ν_{max}/cm^{-1}) 2971, 2360, 1734, 1647, 1602, 1517, 1456, 1425, 1395, 1365, 1283, 1254, 1218, 1170, 1032, 824, 648, 592 cm^{-1}.

8.5 Biological Methods

8.5.1 Compound Structures

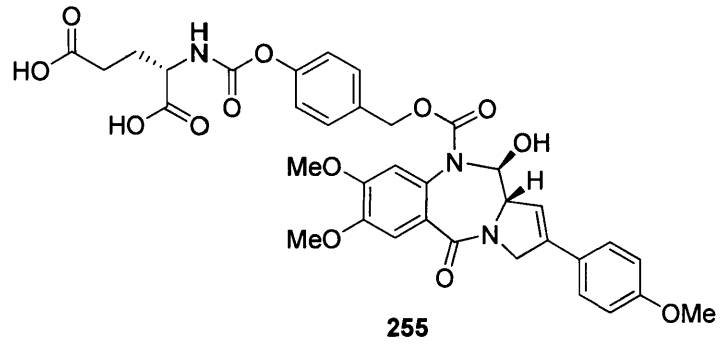

255

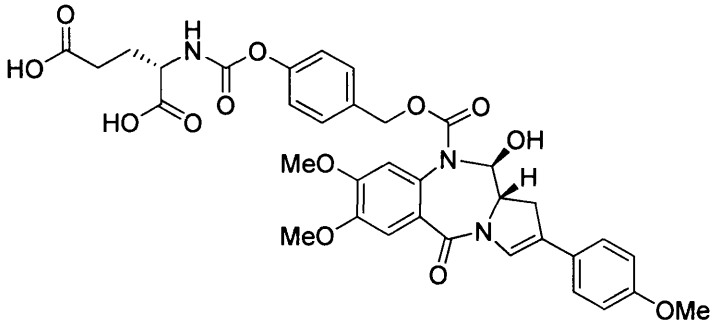

222

Parent compound = **307** for **255** (1,2-isomer)

Parent compound = **218** for **222** (2,3-isomer)

8.5.2Drug Dilutions and Incubations

The parent compounds **307** and **218** and the prodrugs **255** and **222** was diluted in methanol to give a 1 mM stock solution, this was stored at -20°C. All drug dilutions performed throughout originated from this stock.

For *in vivo* cytotoxicity, all drugs were then further diluted in the appropriate tissue culture medium prior to use and used at the following final concentrations 0.003, 0.01, 0.03, 0.1, 0.3, 1, 3 and 10 μM

For HPLC stability all drugs were further diluted in HPLC grade water immediately before incubation. Drug incubations were performed in water at room temperature and 37°C at a final concentration of 100 μM. 20 μl of the relevant drug was injected at the following time points: -0, 15, 30, 45, 60 and 90 minutes and 2,3,4,5, 6 and 24 hours

8.5.3 High-Performance Liquid Chromatography

All chromatographic analyses were carried out using a Waters 2690 separation module with a Waters 2487 dual λ absorbance detector. Results were acquired and process using the Millenium[32] chromatography manager. The stationary phase consisted of a Luna C18 (2) column 5 μm particle size, column 25 cm, 4.6 mm internal diameter (Phenomenex). The mobile phase consisted of water containing 0.1% formic acid and acetonitrile, 60:40. Elution was isocratic at a flow rate of 1 mL/minute and the column maintained at room temperature. Absorbance was monitored at 254 nm. An injection volume of 20 μL was used throughout.

8.5.4 Separation of Compounds

The 4 compounds were separated using the above conditions and could easily be detected at 1, 10 and 100 μM. Compounds were distinguished by retention time as shown in **Table 30.**

Compound	Group	Retention Time (min)
307	Parent molecule	8.0
255	1,2 isomer	10.4
218	Parent molecule	7.9
222	2,3 isomer	10.4

Table 30 Retention Times of CVB ADEPT Compounds

Purity of **255** was excellent but for **222** there was an additional impurity peak being detected at retention time 9.90.

8.5.5 Cell Line

The human colon adenocarcinoma LS174T was used. Cells were grown as a monolayer in Eagles Minimum Essential Medium (EMEM) containing 2 mM glutamine, 10% foetal calf serum and 1% non-essential amino acids. Cells were maintained at 37°C and 5% carbon dioxide. All experiments used exponentially growing cells.

8.6 MTT Assay Protocal

Exponentially growing cells were plated in 96 flat bottom plates at a final concentration of 5 x 10^4/mL with 200 µL/well. Cells were incubated overnight at 37°C and 5% carbon dioxide. The media was removed and 200 µL of the appropriate drug concentration added to the appropriate wells. Cells were incubated in the presence of drug at 37°C and 5% carbon dioxide for either 1 hour or continuously for 96 hours. Following the 1 hour exposure, the media was removed and replaced by drug-free media (200 µL/well). Cells were incubated at 37°C and 5% carbon dioxide for a further 96 hours.

At the end of the incubation period 20 µL 5 mg/mL MTT was added to each well and the plate incubated at 37°C and 5% carbon dioxide for a further 4 hours. The media was then removed and resultant crystals resuspended in 200 µL DMSO. Absorbance was then measured at 540 nm.Results were expressed as percentage cell survival and the dose giving 50% growth inhibition, IC_{50} was calculated for each experiment. The mean IC_{50} ± standard error was calculated based on 3 independent experiments.

8.6.1 MTT Assay Protocol for ADEPT

1. Seed the cells 24 hour prior to the exposure at 3500 cells per well (100 µl)
2. Treat the cells as followed for 1h or continuous exposure
    a. Remove the medium
    b. Prepare MFECP1 in the medium before adding 100 µl to all the wells
    c. Prepare 1 µM PD in medium and add 10 µl to the treatment wells
    d. Add 10 µl DMSO in the medium to the control
3. Wash the well once with 100 µl medium/ for continue exposure no wash
4. Incubate the cells in 100 µl medium for 72 hr
5. Add 11 µl 5mg/ml MTT from Sigma (M5666) prepare in PBS
6. Incubate the plate for father 2 hours at 37°C
7. Remove the solution gently

8. Add 150 µl DMSO:Ethanol
9. Leave for 20 minutes at room temperature

All prodrug and enzyme (MFECP) plus prodrug exposures are for 1 hr only. Cells were then washed and kept in drug free medium for either 24, 48 or 72 hours for MTT assay at these time points.

8.7 CB1954 alternatives

8.7.1 Drugs to be tested:

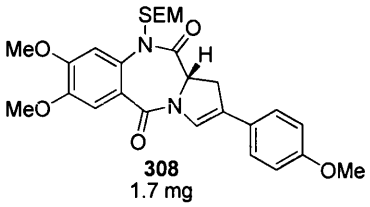

308
1.7 mg
negative control

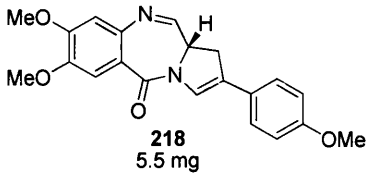

218
5.5 mg
parent drug

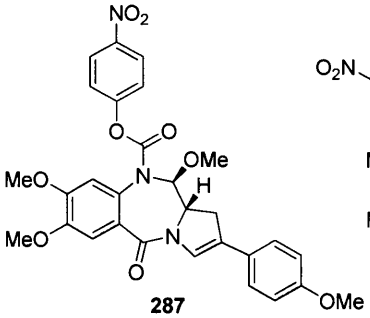

287
5.3 mg

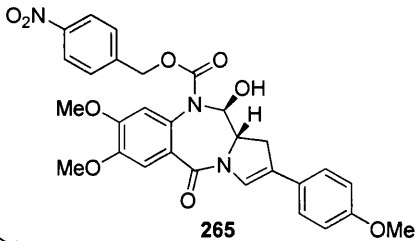

265
5.1 mg

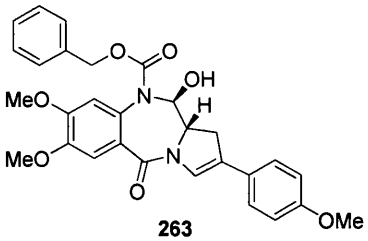

263
1.6 mg

8.7.2 Stable cell lines would be used:

A2780 Basic	A2780 CMV NTR
C33a Basic	C33a CMV NTR
A549 Basic	A549 CMV NTR
5637 Basic	5637 CMV NTR

The basic stable cell lines were used as a control in comparison to the CMV-NTR cells lines.

MTT assay was set up as follows for each cell line - a plate for each drug (in duplicate):

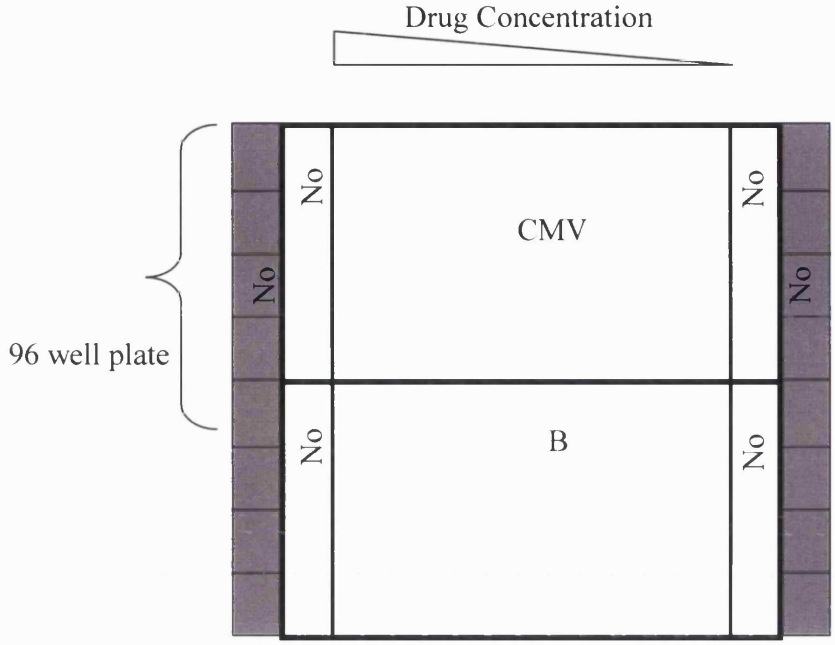

For each cell line half a plate was plated with the CMV-NTR stable cell line and the other half was plated with the Basic stable cell line at a low density (~1000 cells/well). After 2 days titration of eight concentrations of the drugs will then be added to the cells (4 fold titration from 100 μM) overnight. The following day the media was replaced and the cells were allowed to grow for a further 3 days before adding MTT reagent and measuring the cells that remain viable and capable of proliferation.

A total of - 10 plates for each cell line, 40 plates in total, followed by repeats.

Cytotoxicities of CB1954, **308, 218, 287, 265** and **263** in cell lines, each stably transfected with one of the nitroreductase gene therapy vectors, were quantified by MTT assay and IC_{50} values (mM) were determined using the Softmax 2.32 package (Molecular Devices),[165, 166] For each experiment, IC_{50} values for each compound were determined using the mean 50% y-intercept value of triplicate cytotoxity curves. The data shown in **Table 26** are the means derived from three independent experiments for each cell line.

V. Appendix 1

Cytotoxicity in basic and CMV NTR transduced cell lines.

Compound 308

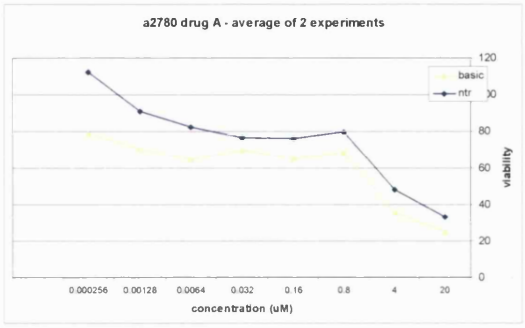

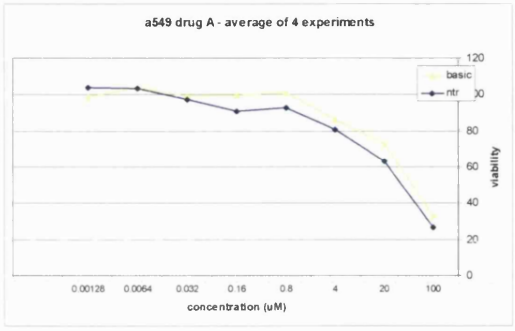

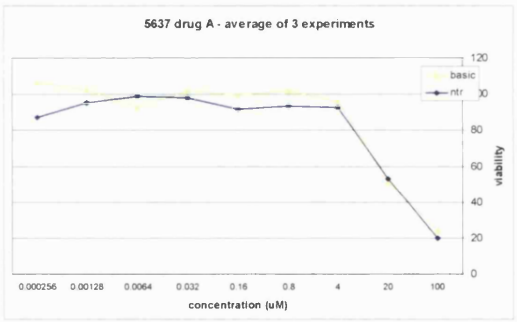

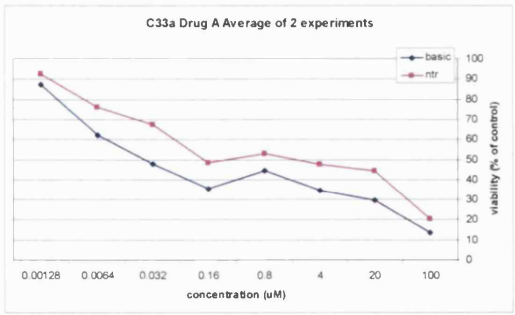

Compound **308** can be seen to be toxic to all cell lines at the higher concentrations, both A2780 and A549 cells show some sensitization to this prodrug.

Compound 218

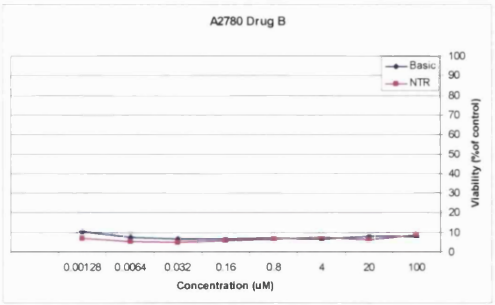

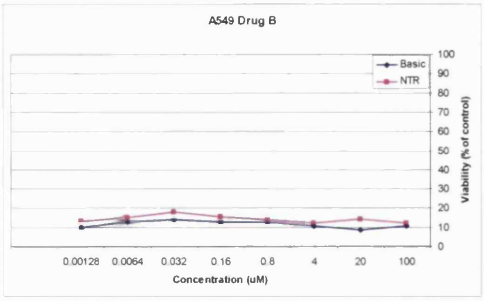

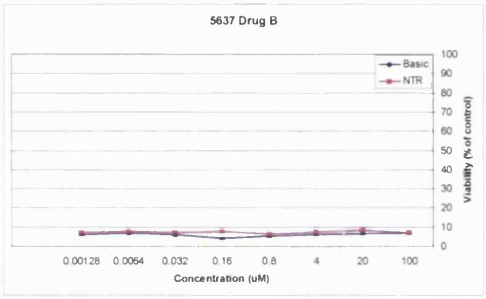

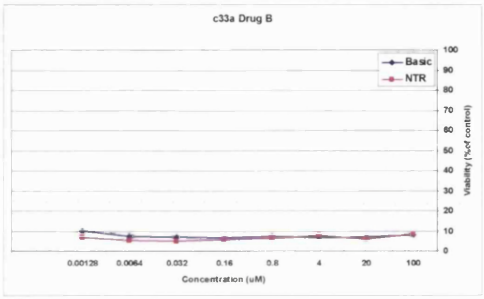

Compound **218** can be seen to be highly toxic at the concentrations 100 – 0.000256 μM in all cell lines, so it was therefore titrated out further to find the IC_{50}. This was carried out in the A2780, A549 and C33a cell lines. From there an IC_{50} was attainable.

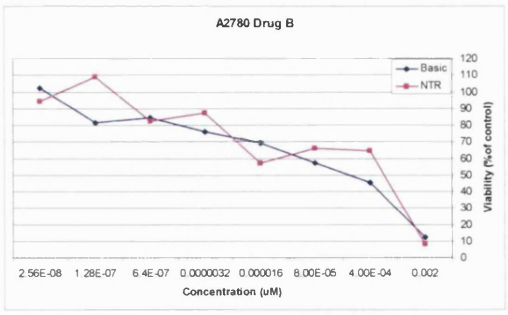

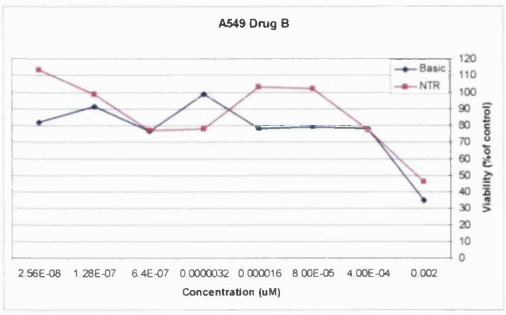

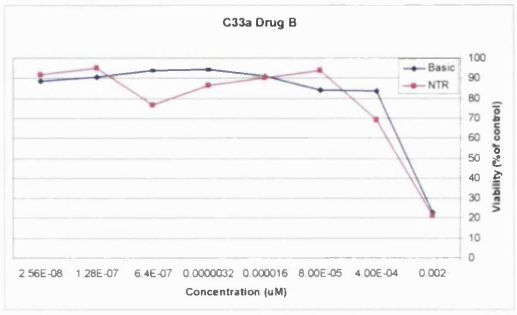

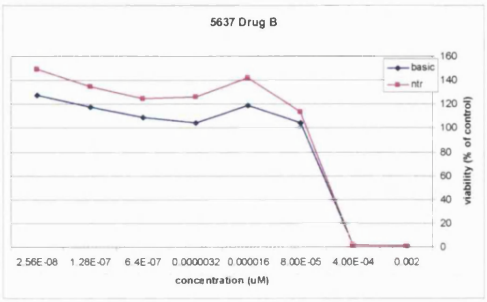

Compound 287

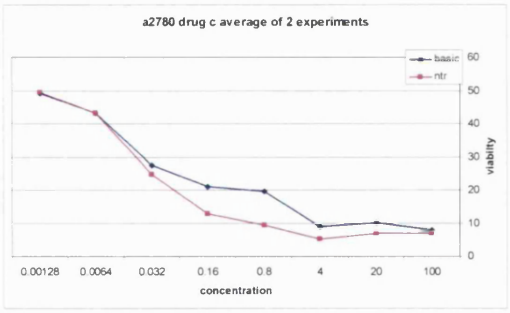

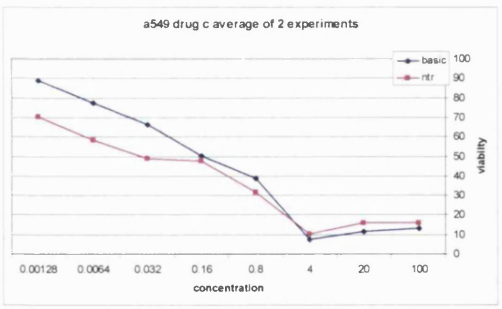

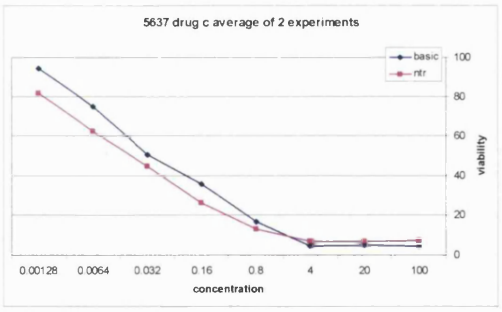

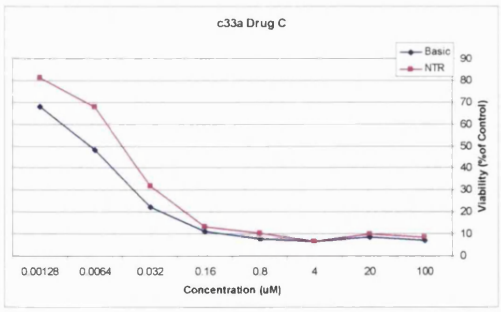

Compound **287** can be seen to be toxic to at least 4μM in all cell lines. A2780 and 5637 cells show sensitization to this prodrug, with the A2780 cells showing a 14.5 fold sensitization to the prodrug.

Compound 265

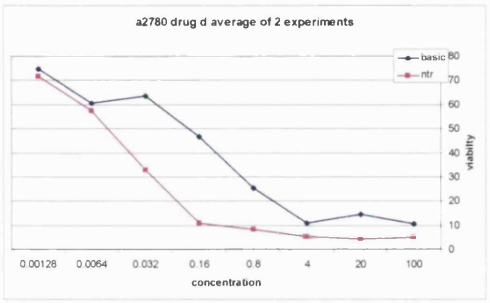

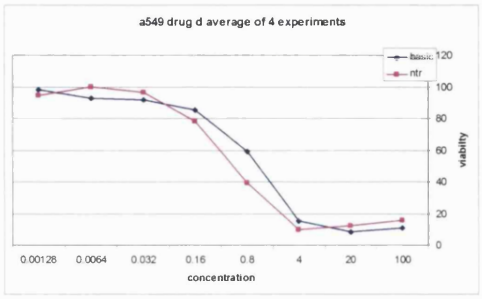

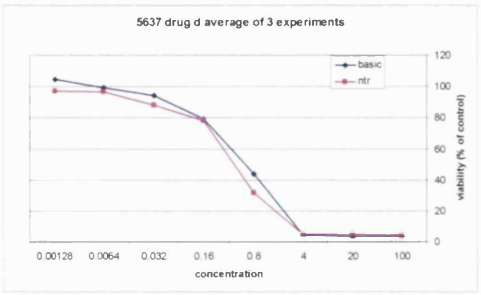

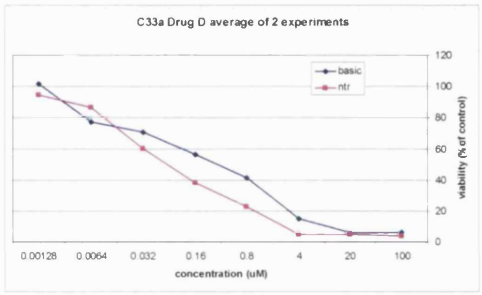

Compound **265** can be seen to be quite toxic in all cell lines to at least 4μM. All of the cell lines show sensitization to this prodrug, with A2780 being the most sensitive to this drug with an 18 fold sensitizaion.

CB 1954

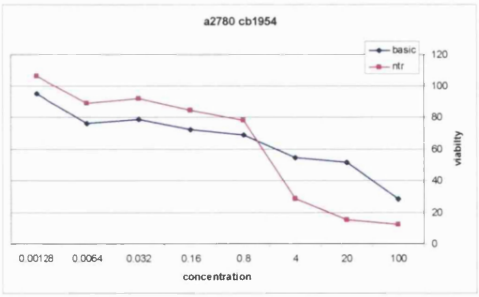

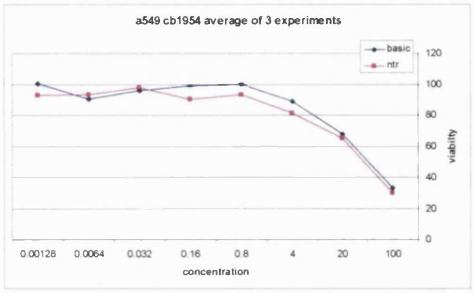

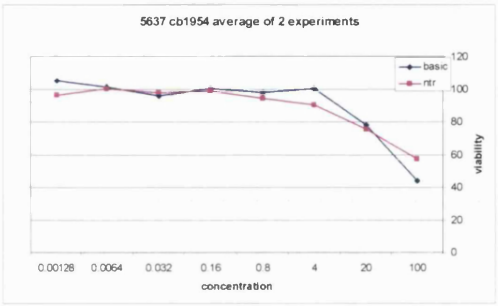

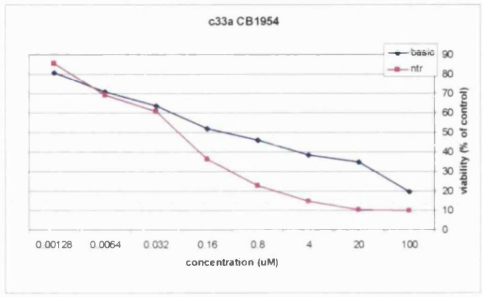

These graphs show the effects of CB 1954 as a prodrug, as has been documented before the cell lines show differing sensitivity to the prodrug.

Compound 263

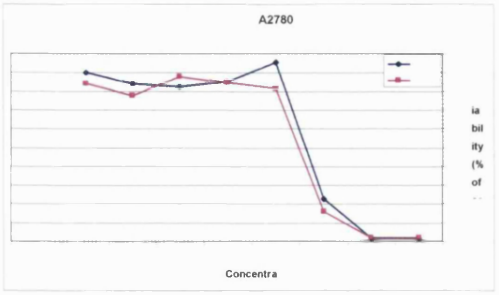

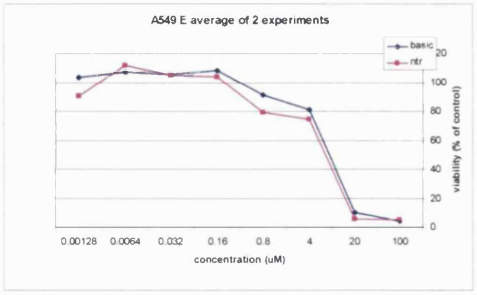

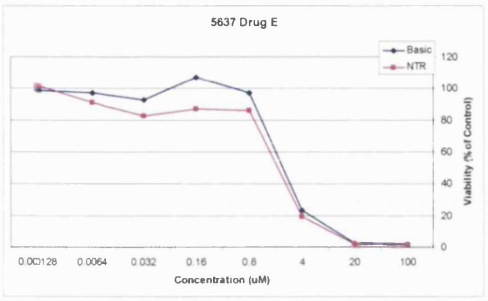

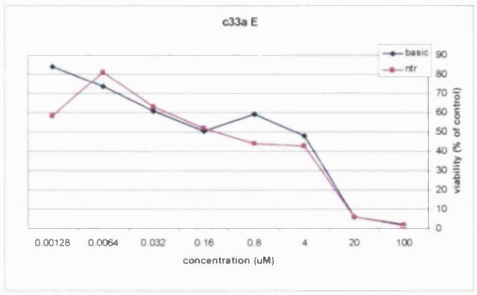

These graphs summarize the results gained so far using compound **263**. Little sensitivity is shown to this compound.

VI. References

1. www.rare-cancer.org/history-of-cancer.
2. www.training.seer.cancer.gov.
3. World-Health-Organisation, Cancer Fact Sheet. In World Health Organisation: 2007.
4. Thurston, D. E., The Chemotherapy of Cancer. In *Introduction to the Principles of Drug Design and Action* 4th ed.; Smith, H. J., Ed. CRC Press: 2006; pp 411-522.
5. http://encyclopedia.laborlawtalk.com/Cancer.
6. Pratt, W. B.; Ruddon, R. W.; Ensminger, W. D.; Maybaum, J., *The Anticancer Drugs*. second edition ed.; Oxford University Press: 1994; p 13-14.
7. Hanahan, D.; Weinberg, R. A., The Hallmarks of Cancer. *Cell* **2000,** 100, (1), 57-70.
8. Slamon, D. J.; Clark, G. M.; Wong, S. G.; Levin, W. J.; Ullrich, A.; McGuire, W. L., Human Breast Cancer: Correlation of Relapse and Survival with Amplification of the HER-2/neu Oncogene. *Science* **1987**, 177-82.
9. Yarden, Y.; Ullrich, A., EGF and erbB2 Receptor Overexpression in Human Tumors. Growth Factor Recepor Tyrosine Kinases. *Biochemistry* **1988,** 57, 443-478.
10. Fedi, P.; Tronick, S. R.; Aaronson, S. A., Growth Factors. In Cancer Medicine. **1997**, 41-64.
11. Werb, Z., ECM and Cell Surface Proteolysis: Regulating Cellular Ecology. *Cell* **1997,** 91, 439–442.
12. Weinberg, R. A., The Retinoblastoma Protein and Cell Cycle Control. *Cell* **1995,** 81, 323-330.
13. Harris, C. C., p53 Tumor Suppressor Gene: From the Basic Research Laboratory to the Clinic- An Abridged Historical Perspective. *Carcinogenesis* **1996,** 17, 1187-1198.
14. Hayflick, L., Mortality and Immortality at the Cellular Level. *Biochemistry* **1997,** 62, 1180-1190.
15. Counter, C. M.; Hahn, W. C.; Wei, W.; Dickinson Caddle, S.; Beijers-bergen, R. L.; Lansdorp, P. M.; Sedivy, J. M.; Weinberg, R. A., Dissociation Between

Telomerase Activity, Telomere Maintenance and Cellular Immortalization. *Proceedings of the National Academy of Sciences* **1998,** 95, 14723-14728.

16. Wright, W. E.; Pereira-Smith, O. M.; Shay, J. W., Reversible Cellular Senescence: Implications for Immortalization of Normal Human Diploid Fibroblasts. *Molecular Cell Biology* **1989,** 9, 3088-3092.
17. Bryan, T. M.; Englezou, A.; Gupta, J.; Bacchetti, S.; Reddel, R. R., Telomere Elongation in Immortal Human Cells Without Detectable Telomerase Activity. *EMBO* **1995,** 14, 4240-4248.
18. Stetler-Stevenson, W. G., Matrix Metalloproteinases in Angiogenesis: a Moving Target for Therapeutic Intervention. *Journal of Clinical Investigtion* **1999,** 103, 1237-1241.
19. Bouck, N.; Stellmach, V.; Hsu, S. C., How Tumours Become Angiogenic. *Advanced Drug Delivery Reviews* **1996,** (69), 135-174.
20. Hanahan, D.; Folkman, J., Patterns and Emerging Mechanisms of the Angiogenic Switch During Tumorigenesis. *Cell* **1996,** 86, 353-364.
21. Folkman, J., Tumor angiogenesis. In Cancer Medicine,. In *The Experimental Study of Tumor Progression*, London: Academic Press: 1997; Vol. I-III, pp 181-204.
22. Sporn, M. B., The War on Cancer. *Lancet* **1996,** 347, 1377-1381.
23. Aplin, A. E.; Howe, A.; Alahari, S. K.; Juliano, R. L., Signal Transduction and Signal Modulation by Cell Adhesion Receptors: the role of Integrins, Cadherins, Immunoglobulin-cell Adhesion Molecules, and Selectins. *Pharmacol. Rev.* **1998,** 50, 197-263.
24. Coussens, L. M.; Werb, Z., Matrix Metalloproteinases and the Development of Cancer. *Chem. Biol.* **1996,** 3, 895-904.
25. Chambers, A. F.; Matrisian, L. M., Changing Views of the Role of Matrix Metalloproteinases in Metastasis. *Journal of National Cancer Institute* **1997,** 89, 1260-1270.
26. Dubowchik, G. M.; Walker, M. A., Receptor-Mediated and Enzyme-dependent Targeting of Cytotoxic Anticancer Drugs. *Pharmacology & Therapeutics* **1999,** 83, (2), 67-123.

27. Edward Kerns, L. D., *Drug-like Properties: Concepts, Structure Design and Methods: from ADME to Toxicity Optimization.* 1 ed.; Academic Press: 2008; p 552.

28. Melton, R. G.; Knox, R. J., *Enzyme-Prodrug Strategies for Cancer Therapy.* Kluwer Academic/Plenum Publishers: New York, 1999.

29. Denny, W. A., Tumor-activated Prodrugs - A New Approach to Cancer Therapy. *Cancer Investigation* **2004,** 22, (4), 604-619.

30. Connors, T., Prodrugs in Cancer. In *Enzyme-Prodrug Strategies for Cancer therapy*, Melton, R. G.; Knox, R. J., Eds. Kluwer Academic/Plenum Publishers: New York, 1999.

31. Pesenti, E.; Franzetti, C.; Biasoli, G.; Ciomei, M.; Pastori, W.; Marsiglio, A., Synthesis and Biological Activity of Water Soluble Polymer-bound Derivatives. *Proceedings of the American Association for Cancer Research* **1995,** 36, 1824.

32. Rapoport, S. I., The blood Brain Barrier in Physiology and Medicine. *Raven, New York* **1976**.

33. Bodor, N.; Venkatraghavan, V.; Winwood, D.; Estes, K.; Brewster, M. E., Improved Delivery Through Biological Membranes. XLI. Brain-enhanced Delivery of Chlorambucil. *International Journal of Pharmaceutics* **1989,** 53, 195-208.

34. Vincent (F.M.H.) de Groot, Targeting - Cancer – Small Molecules. In *Prodrugs-Challenges and Rewards 1*, Valentino Stella, R. B., Michael Hageman, ; Reza Oliyai, H. M., Jefferson Tilley,, Eds. Springer: 2007; Vol. 1, pp 445-504.

35. Hamann, P. R., Monoclonal Antibody-drug Conjugates. *Expert Opinion* **2005,** 15, (9), 1087-1103.

36. Roger Rajewski, M. M., Theoretical and Computational Models. In *Prodrugs-Challenges and Rewards 1*, Valentino Stella, R. B., Michael Hageman, ; Reza Oliyai, H. M., Jefferson Tilley,, Eds. Springer: 2007; Vol. 1, p 431.

37. Chakravarty, P. K.; Carl, P. L.; Weber, M. J.; Katzenellenbogen, J. A., Plasmin-activated Prodrugs for Cancer Chemotherapy. 1. Synthesis and

Biological Activity of Peptidylacivicin and Peptidylphenylenediamine Mustard. *Journal of Medicinal Chemistry* **1983,** 26, (5), 633-638.

38. Chari, R. V. J., Targeted Cancer Therapy: Conferring Specificity to Cytotoxic Drugs. *American Chemical Society* **2007,** 41, (1), 98-107.
39. Kovtun, Y. V.; Goldmacher, V. S., Cell Killing by Antibody-Drug Conjugates. *Cancer Letters* **2007,** 225, 232-240.
40. Xu, G.; McLeod, H. L., Strategies for Enzyme/Prodrug Cancer Therapy. In 2001; Vol. 7, pp 3314-3324.
41. Stella, V. J. Prodrugs challenges and rewards. http://dx.doi.org/10.1007/978-0-387-49785-3
42. Bagshawe, K. D.; Burke, P. J.; Knox, R. J.; Melton, R. G.; Sharma, S. K., Targeting Enzymes to Cancer-New Developments. *Expert Option Investigational Drugs* **1999,** 8, (2), 161-171.
43. Bagshawe, K. D., Antibody Directed Enzymes Revive Anticancer Prodrugs Concept. *British Journal of Cancer* **1987,** 56, (5), 531-532.
44. Bagshawe, K. D.; Sharma, S. K.; Springer, C. J.; Antoniw, P., Antibody Directed Enzyme Prodrug Therapy: a Pilot Scale Clinical Trial. *Tumour Targeting* **1995,** 1, 17-30.
45. Senter, P. D.; Saulnier, M. G.; Schreiber, G. J.; Hirschberg, D. L.; Brown, J. P., Anti-tumor Effects of antibody-alkaline Phosphatase Conjugates in Combination with Etoposide Phosphate. *Oncogene* **1988,** 85, (13), 4842-4846.
46. Niculescu-Duvaz, I.; Scanlon, I.; Niculescu-Duvaz, D.; Friedlos, F.; Martin, J.; Marais, R.; Springer, C. J., Significant Differences in Biological Parameters between Prodrugs Cleavable by Carboxypeptidase G2 That Generate 3,5-Difluoro-phenol and -aniline Nitrogen Mustards in Gene-Directed Enzyme Prodrug Therapy Systems. *Journal of Medicinal Chemistry* **2004,** 47, (10), 2651-2658.
47. Huber, B. E.; Richards, C. A.; Krenitsky, T. A., Retroviral-mediated Gene Therapy for the Treatment of Hepato cellular Carcinoma: An Innovative Approach for Cancer Therapy. *The Proceedings of the National Academy of Sciences* **1991,** 88, (18), 8039–8043. .

48. Leamon, C. P.; DePrince, R. B.; Hendren, R. W., Folate-mediated Drug Delivery: Effect of Alternative Conjugation Chemistry. *Journal of Drug Targeting* **1999,** 7, (3), 157-69.

49. Maeda, H.; Matsumura, Y., Tumoritropic and Lymphotropic Principles of Macromolecular Drugs. *Critical Reviews in Therapeutic Drug Carrier Systems* **1989,** 6, (3), 193-210.

50. Miyazaki, M.; Schally, A. V.; Nagy, A.; Lamharzi, N.; Halmos, G.; Szepeshazi, K.; Armatis, P., Targeted cytotoxic analog of luteinizing hormone-releasing hormone AN-207 inhibits growth of OV-1063 human epithelial ovarian cancers in nude mice. *American Journal of Obstetrics & Gynecology* **1999,** 180, (5), 1095-1103.

51. Miyashita, H.; Karaki, Y.; Kikuchi, M.; Fujii, I., Prodrug Activation Via Catalytic Antibodies. *Proceedings of the National Academy of Sciences* **1993,** 90, (11), 5337-5340.

52. Bosslet, K.; Czech, J.; Hoffmann, D., Tumor-selective Prodrug Activation by Fusion Protein-mediated Catalysis. *American Association for Cancer Research* **1994,** 54, (8), 2151-2159.

53. Rooseboom, M.; Commandeur, J. N. M.; Vermeulen, N. P. E., Enzyme-Catalyzed Activation of Anticancer Prodrugs. *Pharmacol Review* **2004,** 56, (1), 53-102.

54. Carl, P. L.; Chakravarty, P. K.; Katzenellenbogen, J. A., A novel connector linkage applicable in prodrug design. *Journal of Medicinal Chemistry* **1981,** 24, (5), 479-480.

55. Erez, R.; Shabat, D., The Azaquinone-Methide Elimination: Comparison Study of 1,6- and 1,4-Eliminations Under Physiological Conditions. *Organic and Biomolecular Chemistry* **2008,** 6, 2669-2672.

56. Saari, W.; Schwering, J.; Lyle, P.; Smith, S.; Engelhardt, E., Cyclization-activated Prodrugs. Basic Carbamates of 4-hydroxyanisole. *Journal of Medicinal Chemistry* **1990,** 33, (1), 97-101.

57. de Groot, F. M. H.; Albrecht, C.; Koekkoek, R.; Beusker, P. H.; Scheeren, H. W., "Cascade-Release Dendrimers" Liberate All End Groups upon a Single Triggering Event in the Dendritic Core. *Chem. Int. Ed* **2003,** 42, 4490-4494.

58. de Groot, F. M. H.; Loos, W. J.; Koekkoek, R.; van Berkom, L. W. A.; Busscher, G. F.; Seelen, A. E.; Albrecht, C.; de Bruijn, P.; Scheeren, H. W., Elongated Multiple Electronic Cascade and Cyclization Spacer Systems in Activatible Anticancer Prodrugs for Enhanced Drug Release. *Journal of Organic Chemistry* **2001,** 66, (26), 8815-8830.

59. Soyez, H.; Schacht, E.; Vanderkerken, S., The Crucial Role of Spacer Groups in Macromolecular Prodrug Design *Advanced Drug Delivery Reviews* **1996,** 21, 81-106.

60. Bagshawe, K. D.; Springer, C. J.; Searle, F.; Antoniw, P.; Sharma, S. K.; Melton, R. G.; Sherwood, R. F., A Cytotoxic Agent Can Be Generated Selectively at Cancer Sites. *British Journal of Cancer* **1988,** 58, (6), 700-703.

61. Antoniw, P.; Springer, C. J.; Bagshawe, K. D.; Searle, F.; Melton, R. G.; Rogers, G. T.; Burke, P. J.; Sherwood, R. F., Disposition of the Prodrug 4-(Bis (2-Chloroethyl) Amino) Benzoyl-L-Glutamic Acid and Its Active Parent Drug in Mice. *British Journal of Cancer* **1990,** 62, (6), 909-914.

62. Springer, C.; Antoniw, P.; Bagshawe, K. D.; Frances, S.; Bisset, G. M. F., Novel Prodrogs Which are Activated to Cytotoxic Alkylating Agents by Carboxpeptidase G2. *American Chemical Society* **1990,** 33, 677-681.

63. Niculescu-Duvaz, I.; Friedlos, F.; Niculescu-Duvaz, D.; Davies, L.; Springer, C. J., Prodrugs for Antibody- and Gene-directed Enzyme Prodrug Therapies (ADEPT and GDEPT). *Anti-Cancer Drug Design* **1999,** 14, (6), 517-538.

64. Bagshawe, K. D.; Sharma, S. K.; Springer, C. J.; Rogers, G. T., Antibody-Directed Enzyme Prodrug Therapy (Adept) - Review. *Annals of Oncology* **1994,** 5, (10), 879-891.

65. Shukla, G. S.; Krag, D. N., Selective Delivery of Therapeutic Agents for the Diagnosis and Treatment of Cancer. *Expert Opinion on Biological Therapy* **2006,** 6, (1), 39-54.

66. Carter, P. J.; Senter, P. D., Antibody-Drug Conjugates for Cancer Therapy. *The Cancer Journal* **2008,** 14, (3), 154.

67. *Expert Reviews in Molecular Medicine*. Cambridge University Press: 2000.

68. Chester, K.; Pedley, B.; Tolner, B.; Violet, J.; Mayer, A.; Sharma, S.; Boxer, G.; Green, A.; Nagl, S.; Begent, R., Engineering Antibodies for Clinical Applications in Cancer. *Tumor Biology* **2004,** 25, (1-2), 91-98.

69. Mayer, A.; Francis, R. J.; Sharma, S. K.; Tolner, B.; Springer, C. J.; Martin, J.; Boxer, G. M.; Bell, J.; Green, A. J.; Hartley, J. A.; Cruickshank, C.; Wren, J.; Chester, K. A.; Begent, R. H. J., A phase I study of Single Administration of Antibody-directed Enzyme Prodrug Therapy with the Recombinant Anti-carcinoembryonic Antigen Antibody-enzyme Fusion Protein MFECP1 and a Bis-iodo Phenol Mustard Prodrug. *Clinical Cancer Research* **2006,** 12, (21), 6509-6516.

70. Senter, P. D.; Springer, C. J., Selective Activation of Anticancer Prodrugs by Monoclonal Antibody-enzyme Conjugates. *Advanced Drug Delivery Reviews* **2001,** 53, (3), 247-264.

71. Allen, T. M., Ligand-Targeted Therapeutics in Anticancer Therapy. *Nature Reviews Cancer* **2002,** 2, (10), 750-763.

72. Sharma, S. K.; Bagshawe, K. D.; Melton, R. G.; Sherwood, R. F., Human Immune Response to Monoclonal Antibody-enzyme Conjugates in ADEPT Pilot Clinical Trial. *Cell Biosynthesis* **1992,** 21, (1-3), 109-120.

73. Bagshawe, K. D.; Sharma, S. K., Cyclosporine Delays Host Immune Response to Antibody Enzyme Conjugate in ADEPT. *Transplantation Proceedings* **1996,** 28, (6), 3156-3158.

74. Heinis, C.; Alessi, P.; Neri, D., Engineering a Thermostable Human Prolyl Endopeptidase for Antibody-directed Enzyme Prodrug Therapy. *Biochemistry* **2004,** 43, (20), 6293-6303.

75. Sherwood, R. F., Advanced Drug Delivery Reviews: Enzyme Prodrug Therapy. *Advanced Drug Delivery Reviews* **1996,** 22, (3), 269-288.

76. Melton, R. G.; Sherwood, R. F., Antibody-enzyme Conjugates for Cancer Therapy. *Journal of the National Cancer Institute* **1996, 88**, (3), 153.

77. Roffler SR, W. S., Chern JW, Yeh MY, Tung E., Anti-neoplastic Glucuronide Prodrug Treatment of Human Tumor Cells Targeted with a Monoclonal Antibody-enzyme Conjugate. *Biochemical Pharmacology* **1991,** 42, (10), 2062-2065.

78. Burke, P. J., Alkylating Agent Prodrugs for ADEPT. *Advanced Drug Delivery Reviews* **1996,** 22, (3), 331-340.

79. Vrudhula, V. M.; Svensson, H. P.; Kennedy, K. A.; Senter, P. D.; Wallace, P. M., Antitumor activities of a cephalosporin prodrug in combination with monoclonal antibody-.beta.-lactamase conjugates. *Bioconjugate Chemistry* **1993,** 4, (5), 334-340.

80. Sherwood, R. F.; Melton, R. G.; Alwan, S. M.; Hughes, P., Purification and Properties of Carboxypeptidase G2 from Pseudomonas Sp Strain Rs-16 - Use of a Novel Triazine Dye Affinity Method. *European Journal of Biochemistry* **1985,** 148, (3), 447-453.

81. Niculescu-Duvaz, I.; Niculescu-Duvaz, D.; Friedlos, F.; Spooner, R.; Martin, J.; Marais, R.; Springer, C. J., Self-immolative Anthracycline Prodrugs for Suicide Gene Therapy. *Journal of Medicinal Chemistry* **1999,** 42, (13), 2485-2489.

82. Niculescu-Duvaz, D.; Niculescu-Duvaz, I.; Friedlos, F.; Martin, J.; Lehouritis, P.; Marais, R.; Springer, C. J., Self-Immolative Nitrogen Mustards Prodrugs Cleavable by Carboxypeptidase G2 (CPG2) Showing Large Cytotoxicity Differentials in GDEPT. *Journal of Medicinal Chemistry* **2003,** 46, (9), 1690-1705.

83. Hedley, D.; Ogilvie, L.; Springer, C., Carboxypeptidase G2-based gene-directed Enzyme-prodrug Therapy: A New Weapon in the GDEPT Armoury. *Nature Reviews Cancer* **2007**.

84. Sharma, S. K.; Pedley, R. B.; Bhatia, J.; Boxer, G. M.; El-Emir, E.; Qureshi, U.; Tolner, B.; Lowe, H.; Michael, N. P.; Minton, N.; Begent, R. H. J.; Chester, K. A., Sustained Tumor Regression of Human Colorectal Cancer Xenografts Using a Multifunctional Mannosylated Fusion Protein in Antibody-directed Enzyme Prodrug Therapy. *Clinical Cancer Research* **2005,** 11, (2), 814-825.

85. Kogelberg, H.; Tolner, B.; Sharma, S. K.; Lowdell, M. W.; Qureshi, U.; Robson, M.; Hillyer, T.; Pedley, R. B.; Vervecken, W.; Contreras, R.; Begent, R. H. J.; Chester, K. A., Clearance Mechanism of a Mannosylated Antibody-

enzyme Fusion Protein Used in Experimental Cancer Therapy. *Glycobiology* **2007,** 17, (1), 36-45.

86. Michael, P. N.; Chester, K. A.; Melton, R. G.; Robson, L.; Nicholas, W.; Boden, J. A.; Pedley, R. B.; Begent, R. H. J.; Sherwood, R. F.; Minton, N. P., *In vitro* and *in vivo* characterisation of a recombinant carboxypeptidase G_2::anti-CEA scFv fusion protein. *Immunotechnology 2* **1996**, 47-57.

87. Knox, R. J., Gene-directed Enzyme Prodrug Therapy (GDEPT)- Recognizing the Present Limitations of Gene Therapy for Treatment of Cancer. *Current Opinion in Investigational Drugs* **2001,** 2, (6), 835-838.

88. Denny, W. A., Prodrugs for Gene-Directed Enzyme-Prodrug Therapy (Suicide Gene Therapy). *Journal of Biomedicine and Biotechnology* **2003**, (1), 48-70.

89. Schepelmann, S. S., C J;, Viral Vectors for Gene-Directed Enzyme Prodrug Therapy. *Current Gene Therapy* **2006,** 6, (6), 647-670.

90. Wikipedia http://en.wikipedia.org/wiki/Image:Gene_therapy.jpg.

91. Schepelmann, S.; Hallenbeck, P.; Ogilvie, L. M.; Hedley, D.; Friedlos, F.; Martin, J.; Scanlon, I.; Hay, C.; Hawkins, L. K.; Marais, R.; Springer, C. J., Systemic Gene-Directed Enzyme Prodrug Therapy of Hepatocellular Carcinoma Using a Targeted Adenovirus Armed with Carboxypeptidase G2. *American Association for Cancer Research* **2005,** 65, (12), 5003-5008.

92. Parkinson, G. N.; Skelly, J. V.; Neidle, S., Crystal Structure of FMN-Dependent Nitroreductase from Escherichia coli B: A Prodrug-Activating Enzyme. *Journal of Medicinal Chemistry* **2000,** 43, (20), 3624-3631.

93. Lee, M.; Simpson, J. E.; Woo, S.; Kaenziga, C.; Anlezarkc, G. M.; Eno-Amooquaye, E.; Burke, P. J., Synthesis of an Aminopropyl Analog of the Experimental Anticancer Drug Tallimustine, and Activation of its 4-nitrobenzylcarbamoyl Prodrug by Nitroreductase and NADH *Bioorganic & Medicinal Chemistry Letters* **1997,** 7, (8), 1065-1070.

94. Hay, M. P.; Wilson, W. R.; Denny, W. A., Nitrobenzyl Carbamate Prodrugs of Enediynes for Nitroreductase Gene-directed Enzyme Prodrug Therapy (GDEPT). *Bioorganic & Medicinal Chemistry Letters* **1999,** 9, (24), 3417-3422.

95. Boger, D. L.; Johnson, D. S., CC-1065 and the Duocarmycins: Unraveling the Keys to a New Class of Naturally Derived DNA Alkylating Agents. In 1995; Vol. 92, pp 3642-3649.

96. Knox, R. J.; Burke, P. J.; Chen, S.; Kerr, D. J., CB 1954: From the Walker Tumor to NQO2 and VDEPT. *Current Pharmaceutical Design* **2003,** 9, 2091-2104.

97. Workman, P.; Morgan, J. E.; Talbot, K.; Wright, K. A.; Donaldson, J.; Twentyman, P. R., CB 1954 revisited. *Cancer Chemotherapy and Pharmacology* **1986,** 16, (1), 9-14.

98. Bibby, M. C.; Double, J. A.; Loadman, P. M.; Duke, C. V., Reduction of Tumor Blood Flow by Flavone Acetic Acid: A Possible Component of Therapy. *Journal of National Cancer Institute* **1989,** 81, (3), 216-220.

99. Friedlos F; Biggs P.J; Abrahamson J.A; R.J., K., Potentiation of CB 1954 Cytotoxicity by Reduced Pyridine Nucleotides in Human Tumour Cells by Stimulation of DT Diaphorase Activity. *Biochemical Pharmacology* **1992,** 44, (9), 1739-1743

100. Knox, R. J.; Friedlos, F.; Lydall, D. A.; Roberts, J. J., Mechanism of Cytotoxicity of Anticancer Platinum Drugs: Evidence That *cis*-Diamminedichloroplatinum(II) and *cis*-Diammine-(1,1-cyclobutanedicarboxylato)platinum(II) Differ Only in the Kinetics of Their Interaction with DNA. *Cancer Research* **1986,** 46, (4 Part 2), 1972-1979.

101. AbuKhader, M.; Heap, J.; De Matteis, C.; Kellam, B.; Doughty, S. W.; Minton, N.; Paoli, M., Binding of the Anticancer Prodrug CB1954 to the Activating Enzyme NQO2 Revealed by the Crystal Structure of Their Complex. *Journal of Medicinal Chemistry* **2005,** 48, (24), 7714-7719.

102. Keith WN, B. A., Hardie M, Evans TR, Drug Insight: Cancer Cell Immortality-telomerase as a Target for Novel Cancer Gene Therapies. *Nature Clinical Practice Oncology* **2004,** 1, (2), 88-96.

103. Plumb JA, B. A., Kakani R, Zhao J, Glasspool RM, Knox RJ, Evans TR, Keith WN., Telomerase-specific Suicide Gene Therapy Vectors Expressing Bacterial Nitroreductase Sensitize Human Cancer Cells to the Pro-drug CB1954. *Oncogene* **2001,** 20, 7797 - 7803.

104. Bilsland, A. E.; Anderson, C. J.; Fletcher-Monaghan, A. J.; McGregor, F.; Jeffry Evans, T. R.; Ganly, I.; Knox, R. J.; Plumb, J. A.; Nicol Keith, W., Selective Ablation of Human Cancer Cells by Telomerase-Specific Adenoviral Suicide Gene Therapy Vectors Expressing Bacterial Nitroreductase. *Oncogene* **2003,** 22, (3), 370-380.

105. Sagnou, M. J.; Howard, P. W.; Gregson, S. J.; Eno-Amooquaye, E.; Burke, P. J.; Thurston, D. E., Design and Synthesis of Novel Pyrrolobenzodiazepine (PBD) Prodrugs for ADEPT and GDEPT. *Bioorganic & Medicinal Chemistry Letters* **2000,** 10, (18), 2083-2086.

106. http://www-micro.msb.le.ac.uk/Video/Streptomyces.html.

107. Tendler, M. D.; Korman, S., 'Refuin' : a Non-cytotoxic Carcinostatic Compound proliferated by a Thermophilic Actinomycete. *Nature* **1963,** 199, 501.

108. Leimgruber, W.; Batcho, A. D.; Czajkowski, R. C., Total Synthesis of Anthramycin. *Journal of the American Chemical Society* **1968,** 90, (20), 5641-5643.

109. Leimgruber, W.; Batcho, A. D.; Schenker, F., The Structure of Anthramycin. *Journal of the American Chemical Society* **1965,** 87, (24), 5793-5795.

110. Leimgruber, W.; Stefanovic, V.; Schenker, F.; Karr, A.; Berger, J., Isolation and Characterization of Anthramycin, A New Antitumor Antibiotic. *Journal of the American Chemical Society* **1965,** 87, (24), 5791-5793.

111. Thurston, D. E.; Bose, D. S., Synthesis of DNA-Interactive Pyrrolo[2,1-*c*][1,4]Benzodiazepines. *Chemical Reviews* **1994,** 94, (2), 433-465.

112. Bose, D. S.; Jones, G. B.; Thurston, D. E., New Approaches to Pyrrolo[2,1-*c*][1,4]Benzodiazepines - Synthesis, DNA-Binding and Cytotoxicity of DC-81. *Tetrahedron* **1992,** 48, (4), 751-758.

113. Thurston, D. E., Advances in the Study of Pyrrolo [2,1-*c*][1,4] benzodiazepine(PBD) Antitumour Antibiotics. In *Molecular Aspects of Anticancer Drug-DNA Interactions*, Neidle, S.; Waring, M. J., Eds. Macmillan Press: London, 1993; Vol. 1, pp 54-88.

114. Puvvada, M. S.; Forrow, S. A.; Hartley, J. A.; Stephenson, P.; Gibson, I.; Jenkins, T. C.; Thurston, D. E., Inhibition of Bacteriophage T7 RNA

Polymerase *In Vitro* Transcription by DNA-binding Pyrrolo[2,1-*c*][1,4]benzodiazepines. *Biochemistry* **1997,** 36, (9), 2478-2484.

115. Mori, M.; Uozumi, Y.; Kimura, M.; Ban, Y., Total Synthesis of Prothracarcin and Tomaymycin by Use of Palladium Catalyzed Carnonylation. *Tetrahedron* **1986,** 42, 3793-3806.

116. Peña, M. R.; Stille, J. K., A Total Synthesis of Anthramycin - Application of Palladium-Catalyzed Coupling Reactions for the Attachment of the Acrylic Side-Chain. *Journal of the American Chemical Society* **1989,** 111, (14), 5417-5424.

117. Cooper, N.; Hagan, D. R.; Tiberghien, A.; Ademefun, T.; Matthews, C. S.; Howard, P. W.; Thurston, D. E., Synthesis of Novel C2-aryl Pyrrolobenzodiazepines (PBDs) as Potential Antitumour Agents. *Chemical Communications* **2002**, (16), 1764-1765.

118. Fukuyama, T.; Lin, S. C.; Li, L. P., Facile Reduction of Ethyl Thiol Esters to Aldehydes - Application to a Total Synthesis of (+)-Neothramycin-a Methyl-Ether. *Journal of the American Chemical Society* **1990,** 112, (19), 7050-7051.

119. Fukuyama, T.; Liu, G.; Linton, S. D.; Lin, S. C.; Nishino, H., Total Synthesis of (+)-Porothramycin-B. *Tetrahedron Letters* **1993,** 34, (16), 2577-2580.

120. Langlois, N.; Favre, F.; Rojas, A., Enantioselective Synthesis of (+) Porothramycin-B and Its 9-Demethoxy Analog. *Tetrahedron Letters* **1993,** 34, (29), 4635-4638.

121. Thurston, D.; Murty, V.; Langley, D.; Jones, G., O-Debenzylation of a Pyrrolo[2,1-*c*][1,4]benzodiazepine in the Presence of a Carbinolamine Functionality: Synthesis of DC-81. *Synthesis* **1990**, (01), 81-84.

122. Eguchi, S.; Yamashita, K.; Matsushita, Y.; Kakehi, A., Facile Synthesis of 1,4-Benzodiazepin-5-One Derivatives via Intramolecular Aza-Wittig Reaction - Application to an Efficient Synthesis of O-Benzyl Dc-81. *Journal of Organic Chemistry* **1995,** 60, (13), 4006-4012.

123. Molina, P.; Diaz, I.; Tarraga, A., Synthesis of Pyrrolo[2,1-*c*][1,4]Benzodiazepines Via an Intramolecular Aza-Wittig Reaction - Synthesis of the Antibiotic DC-81. *Tetrahedron* **1995,** 51, (19), 5617-5630.

124. O'Neil, I. A.; Murray, C. L.; Hunter, R. C.; Kalindjian, S. B.; Jenkins, T. C., The Synthesis of Functionalized Pyrrolo-[2,1-*c*][1,4]-benzodiazepines. *Synlett* **1997**, (1), 75-&.

125. Hurley, L. H.; Reck, T.; Thurston, D. E.; Langley, D. R.; Holden, K. G.; Hertzberg, R. P.; Hoover, J. R. E.; Gallagher, G.; Faucette, L. F.; Mong, S. M.; Johnson, R. K., Pyrrolo[1,4]Benzodiazepine Antitumor Antibiotics - Relationship of DNA Alkylation and Sequence Specificity to the Biological-Activity of Natural and Synthetic Compounds. *Chemical Research in Toxicology* **1988,** 1, (5), 258-268.

126. Masterson, L. A.; Spanswick, V. J.; Hartley, J. A.; Begent, R. H.; Howard, P. W.; Thurston, D. E., Synthesis and Biological Evaluation of Novel Pyrrolo[2,1-*c*][1,4]benzodiazepine Prodrugs for Use in Antibody-directed Enzyme Prodrug Therapy. *Bioorganic & Medicinal Chemistry Letters* **2006,** 16, (2), 252-256.

127. Antonow, D.; Stephenson, M.; Zloh, M.; Jenkins, T. C.; Howard, P. W.; Thurston, D. E., Synthesis , DNA Binding Affinity and Cytotoxicity of Novel Sibiromycin-Aglycone Analogues. In School of Pharmacy: London, 2007; pp 1-5.

128. Williams, M. A.; Rapoport, H., Synthesis of Conformationally Constrained DTPA Analogues *Journal of Organic Chemistry* **1994,** 59, 3616-3625.

129. Mori, S.; Ohno, T.; Harada, H.; Aoyama, T.; Shioiri, T., New Methods and Reagents in Organic Synthesis. 92. A Stereoselective Synthesis of Tilivalline and its Analogs. *Tetrahedron* **1991,** 47, (27), 5051-5070.

130. Niculescu-Duvaz, D.; Niculescu-Duvaz, I.; Friedlos, F.; Martin, J.; Spooner, R.; Davies, L.; Marais, R.; Springer, C. J., Self-immolative Nitrogen Mustard Prodrugs for Suicide Gene Therapy. *Journal of Medicinal Chemistry* **1998,** 41, (26), 5297-5309.

131. Blay, G.; Cardona, M. L.; Garcia, M. B.; Pedro, J., A Selective Hydrolysis of Aryl Acetates. *Synthesis* **1989**, (06), 438-439.

132. Kunesch, N.; Miet, C.; Poisson, J., Mild, Rapid and Selective Deprotection of Acetylated Carbohydrates and Phenols with Guanidine. *Tetrahedron Letters* **1987,** 28, (31), 3569-3572.

133. Williams, R. R.; Lin, X. F., Studies on the Synthesis of Aureolic Acid Antibiotics: Highly Stereoselective Synthesis of Aryl 2-Deoxy-P-glycosides via the Mitsunobu Reaction and synthesis of the Oliviomycin A-B Disaccharide. *Journal of Am. Chem. Soc* **1995,** 117, 2036-2250.

134. Ley, S. V.; Armstrong, A.; Díez-Martín, D.; Ford, M. J.; Grice, P.; Knight, J. G.; Kolb, H. C.; Madin, A.; Marby, C. A.; Mukherjee, S.; Shaw, A. N.; Slawin, A. M. Z.; Vile, S.; White, A. D.; Williams, D. J.; Woods, M., Total Synthesis of the Anthelmintic Macrolide Avermectin B1a. *Journal of the Chemical Society Perkin Transactions 1.* **1991**, 667-673.

135. Thompson, E. J.; Williams, A. C., A Stereoselective Approach to the δ-lactone Fragment of the Lankacidin Antibiotics. *j. Chem. Soc., Chem. Commun* **1987**, 992-994.

136. Farras, J.; Serra, C.; Vilarrasa, J., Cleavage of *tert*-Butyldimethylsilyl Ethers by Chloride Ion. *Tetrahedron Letters* **1998,** 39, 327-330.

137. King, S. A.; Pipik, B.; Thompson, A. S.; DeCamp, A.; Verhoeven, T. R., Efficient Synthesis of Carbapenems via the Oxalimide Cyclization. Manipulation of Protecting Groups at the Oxalimide Stage. *Tetrahedron Letters* **1995,** 36, (26), 4563-4566.

138. Wilson, N. S.; Keay, B. A., A Mild Palladium(II) Catalyzed Desilylation of Phenolic t-butyldimethylsilyl Ethers. *Tetrahedron Letters* **1996,** 37, (2), 153-156.

139. Vaino, A. R.; Szarek, W. A., A Mild and Efficient Method for the Deprotection of tert-Butyldimethylsilyl Ethers Using Iodine in Methanol. *Chemical Communications* **1996**, 2351-2352.

140. Cirillo, P. F.; Panek, J. S., Diastereoselectivity in Nucleophilic Addition Reactions (alpha, Beta-Dialkoxyacy)silanes: an Operationally Useful Route to Optically Active 1,2,3-*syn*-Triols. *Journal of Organic Chemistry* **1990,** 55, 6071-6073.

141. Tandon, M.; Begley, T. P., Selective Deprotection of *tert*-butyldimethylsilyl Ether with Lithium Bromide and 18-crown-6. *Synthetic Communications* **1997,** 27, (17), 2953-2959.

142. Williams, D. R.; Clark, M. P.; Berliner, M. A., Synthetic Studies Toward Phorboxazole A. Stereoselective Synthesis of the C3-C19 C20-C32 Subunits. *Tetrahedron Letters* **1999,** 40, 2287-2290.

143. Antonow, D.; Jenkins, T. C.; Howard, P. W.; Thurston, D. E., Synthesis of a Novel C2-aryl pyrrolo[2,1-*c*][1,4]benzodiazepine-5,11-dione Library: Effect of C2-aryl Substitution on Cytotoxicity and Non-Covalent DNA binding. *Bioorganic & Medicinal Chemistry* **2007,** In Press, Corrected Proof.

144. Chen, Z. Z.; Gregson, S. J.; Howard, P. W.; Thurston, D. E., A Novel Approach to the Synthesis of Cytotoxic C2-C3 Unsaturated Pyrrolo[2,1-*c*][1,4]benzodiazepines (PBDs) with Conjugated Acrylyl C2-substituents. *Bioorganic & Medicinal Chemistry Letters* **2004,** 14, (6), 1547-1549.

145. Kang, G. D.; Howard, P. W.; Thurston, D. E., Synthesis of a Novel C2-aryl Substituted 1,2-unsaturated Pyrrolobenzodiazepine. *Chemical Communications* **2003**, (14), 1688-1689.

146. Dubowchik, G. M.; Dalton King, H.; Pham-Kaplita, K., Efficient Mitomycin C Coupling with Stable *p*-nitrophenyl-benzyl Carbonates Using *p*-Hydroxybenzotriazole as a Catalytic Additive. *Tetrahedron Letters* **1997,** 38, (30), 5261-5264.

147. Hudson, S.; Kiankarimi, M.; Rowbottom, M. W.; Vickers, T. D.; Wu, D.; Pontillo, J.; Ching, B., Synthesis and Structure-activity Relationships of Retro Bis-aminopyrrolidine Urea (rAPU) Derived Small-molecule Antagonists of the Melanin-concentrating Hormone Receptor-1 (MVH-R1). *Bioorganic & Medicinal Chemistry Letters* **2006,** 16, 4922-4930.

148. Reichard, G.; Grice, A.; Shih, N.; Spitler, J.; Majmundar, S.; Wang, S. D.; Palwal, S.; Anthes, J. C., Preparation of Oxime Dual NK_1/NK_2 Antagonists with Reduced NK_3 Affinity. *Bioorganic & Medicinal Chemistry Letters* **2002,** 12, 2355-2358.

149. Letsinger, R. L.; Ogilvie, K. K., Use of *p*-Nitrophenyl Chloroformate in Blocking Hydroxyl Groups in Nucleosides. **1966**, 296-300.

150. Atwal, K. S.; Rovnyak, G. C.; O'Reilly, B. C.; Schwartz, J., Substituted 1,4-dihydropyrimidines. 3. Synthesis of Selectively Functionalized 2-hetero-1,4-dihydropyrimidines. *Journal of Organic Chemistry* **1989,** 54, (25), 5898-5907.

151. Alexander, R. P.; Beeley, N. R. A.; O'Driscoll, M.; O'Neill, F. P.; Millican, T. A.; Pratt, A. J.; Willenbrock, F. W., Cephalosporin Nitrogen Mustard Carbamate prodrugs for "ADEPT". *Tetrahedron Letters* **1991,** 32, (27), 3269-3272.

152. Wanner, M. J.; Koch, M.; Koomen, G., Synthesis and Antitumor Activity of Methyltriazen Prodrugs Simultaneously Releasing DNA-Methylating Agents and the Antiresistance Drug. *Journal of Medicinal Chemistry* **2004,** 47, 6875-6883.

153. Bermudez, J.; Dabbs, S.; Joiner, K. A.; King, F. D., 5-Hydroxytryptamine (5-HT3) Receptor Antagonists. 2. 1-Indolinecarboxamides. *Journal of Medicinal Chemistry* **1990,** 33, (7), 1929-1932.

154. Rege, P. D.; Tain, Y.; Corey, E. J., Studies of New Indole Alkaloid Coupling Method for the Synthesis of Haplophytine. *American Chemical Society* **2006,** 8, (14), 3117-3120.

155. Roffey, J., Unpublished Work. In School of Pharmacy: **2007.**

156. Kitamura, T.; Sato, Y.; Mori, M., Synthetic Study of (+)-Anthramycin Using Ring-closing Enyne Metathesis and Cross-metathesis. *Tetrahedron* **2004,** 60, (43), 9649-9657.

157. Hartley, J. A.; Spanswick, V. J.; Brooks, N.; Clingen, P. H.; McHugh, P. J.; Hochhauser, D.; Pedley, R. B.; Kelland, L. R.; Alley, M. C.; Schultz, R.; Hollingshead, M. G.; Schweikart, K. M.; Tomaszewski, J. E.; Sausville, E. A.; Gregson, S. J.; Howard, P. W.; Thurston, D. E., SJG-136 (NSC 694501), A Novel Rationally Designed DNA Minor Groove Interstrand Cross-linking Agent with Potent and Broad Spectrum Antitumor Activity. Part 1: Cellular pharmacology, *In Vitro* and Initial *In Vivo* Antitumor Activity. *Cancer Research* **2004,** 64, (18), 6693-6699.

158. Clingen, P. H.; De Silva, I. U.; McHugh, P. J.; Ghadessy, F. J.; Tilby, M. J.; Thurston, D. E.; Hartley, J. A., The XPF-ERCC1 Endonuclease and Homologous Recombination Contribute to the Repair of Minor Groove DNA Interstrand Crosslinks in Mammalian Cells Produced by the Pyrrolo[2,1-*c*][1,4]benzodiazepine Dimer SJG-136. *Nucleic Acids Research* **2005,** 33.

159. Lavelle, F.; Riou, J. F.; Laoui, A.; Mailliet, P., Telomerase: a therapeutic target for the third millennium? *Critical Reviews in Oncology/Hematology* **2000,** 34, 111-126.

160. Bilsland, A. E.; Stevenson, K.; Atkinson, S.; Kolch, W.; Keith, W. N., Transcriptional Repression of Telomerase RNA Gene Expression by c-Jun-NH2-Kinase and Sp1/Sp3. *American Association for Cancer Research* **2006,** 66, (3), 1363-1370.

161. Keith, W. N.; Bilsland, A.; Hardie, M.; Evans, T. R., Drug Insight: Cancer Cell Immortality-telomerase as a Target for Novel Cancer Gene Therapies. *Nature Clinical Practice Oncology* **2004,** 1, (2), 88-96.

162. Bilsland, A. E.; Merron, A.; Vassaux, G.; Keith, W. N., Modulation of Telomerase Promoter Tumor Selectivity in the Context of Oncolytic Adenoviruses. *American Association for Cancer Research* **2007,** 67, (3), 1299-1307.

163. Bilsland, A.; Fletcher-Monaghan, A. J.; Keith, W. N., Properties of a Telomerase-Specific Cre/Lox Switch for Transcriptionally Targeted Cancer Gene Therapy. *Neoplasia* **2005,** 7, (11), 1020-1029.

164. Anderson, C. J.; Hoare, S. F.; Ashcroft, M.; Bilsland, A. E.; Keith, W. N., Hypoxic Regulation of Telomerase Gene Expression by Transcriptional and Post-Transcriptional Mechanisms. *Oncogene* **2005,** 25, (1), 61-69.

165. Plumb, J. A.; Bilsland, A.; Kakani, R.; Zhao, J.; Glasspool, R. M.; Knox, R. J.; Evans, T. R.; Keith, W. N., Telomerase-specific Suicide Gene Therapy Vectors Expressing Bacterial Nitroreductase Sensitize Human Cancer Cells to the Pro-drug CB1954. *Oncogene* **2001,** 20, 7797 - 7803.

166. Mistry, P.; Stewart, A. J.; Dangefield, W.; Okiji, S.; Liddle, C.; Bootle, D.; Plumb, J. A.; Templeton, D.; Charlton, P., In Vitro and in Vivo Reversal of P-Glycoprotein-mediated Multidrug Resistance by a Novel Potent Modulator, XR9576 *Cancer Research* **2001,** 61, 749 - 758.